ISSN 2307-8960 (online)

World Journal of *Clinical Cases*

World J Clin Cases 2019 March 6; 7(5): 548-690

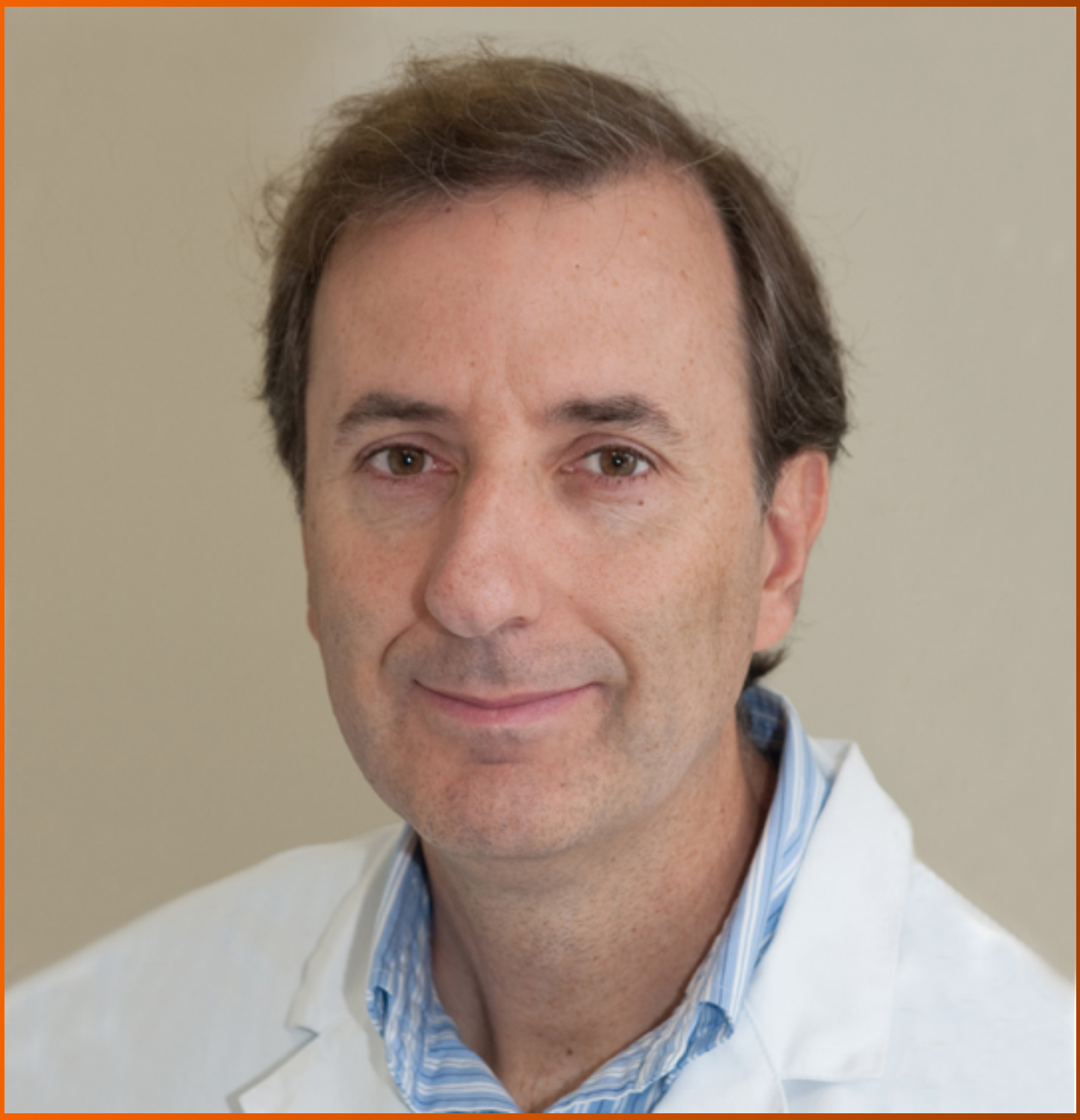

Published by Baishideng Publishing Group Inc

World Journal of Clinical Cases

Contents

Semimonthly Volume 7 Number 5 March 6, 2019

ORIGINAL ARTICLE

Retrospective Study

Observational Study

META-ANALYSIS

CASE REPORT

World Journal of Clinical Cases
Volume 7 Number 5 March 6, 2019

Contents

NAME OF JOURNAL
World Journal of Clinical Cases

ISSN
ISSN 2307-8960 (online)

LAUNCH DATE
April 16, 2013

FREQUENCY
Semimonthly

EDITORS-IN-CHIEF
Dennis A Bloomfield, Sandro Vento

EDITORIAL BOARD MEMBERS
https://www.wjgnet.com/2307-8960/editorialboard.htm

EDITORIAL OFFICE
Jin-Lei Wang, Director

PUBLICATION DATE
March 6, 2019

COPYRIGHT
© 2019 Baishideng Publishing Group Inc

INSTRUCTIONS TO AUTHORS
https://www.wjgnet.com/bpg/gerinfo/204

GUIDELINES FOR ETHICS DOCUMENTS
https://www.wjgnet.com/bpg/GerInfo/287

GUIDELINES FOR NON-NATIVE SPEAKERS OF ENGLISH
https://www.wjgnet.com/bpg/gerinfo/240

PUBLICATION MISCONDUCT
https://www.wjgnet.com/bpg/gerinfo/208

ARTICLE PROCESSING CHARGE
https://www.wjgnet.com/bpg/gerinfo/242

STEPS FOR SUBMITTING MANUSCRIPTS
https://www.wjgnet.com/bpg/GerInfo/239

ONLINE SUBMISSION
https://www.f6publishing.com

© 2019 Baishideng Publishing Group Inc. All rights reserved. 7041 Koll Center Parkway, Suite 160, Pleasanton, CA 94566, USA
E-mail: bpgoffice@wjgnet.com https://www.wjgnet.com

World Journal of Clinical Cases

Submit a Manuscript: https://www.f6publishing.com

World J Clin Cases 2019 March 6; 7(5): 548-561

DOI: 10.12998/wjcc.v7.i5.548

ISSN 2307-8960 (online)

ORIGINAL ARTICLE

Retrospective Study

Clinical presentation and early predictors for poor outcomes in pediatric myocarditis: A retrospective study

Moises Rodriguez-Gonzalez, Maria Isabel Sanchez-Codez, Manuel Lubian-Gutierrez, Ana Castellano-Martinez

ORCID number: Moises Rodriguez-Gonzalez (0000-0002-5587-435X); Maria Isabel Sánchez-Códez (0000-0003-0132-3015); Manuel Lubián-Gutiérrez (0000-0002-3970-3833); Ana Castellano-Martinez (0000-0001-7563-1235).

Author contributions: All authors helped to perform the research; Rodriguez-Gonzalez M contributed to the conception and design, performing procedures, manuscript writing, and data analysis; Sanchez-Codez MI contributed to the abstracted data, performing procedures, and manuscript writing; Castellano-Martinez A contributed to manuscript writing and data analysis; Lubian-Gutierrez M contributed to manuscript writing.

Institutional review board statement: This study was reviewed and approved by the Ethics Committee of the Puerta del Mar University Hospital.

Informed consent statement: Patients were not required to give informed consent to the study because the analysis used anonymous clinical data that were obtained after each patient agreed to treatment by written consent.

Conflict-of-interest statement: All authors declare no conflicts-of-interest related to this article.

Data sharing statement: No additional data are available.

STROBE statement: The authors have included all the items included in STROBE statement for

Moises Rodriguez-Gonzalez, Department of Pediatric Cardiology, Puerta del Mar University Hospital, Cadiz 11009, Spain

Maria Isabel Sanchez-Codez, Manuel Lubian-Gutierrez, Department of Pediatrics, Puerta del Mar University Hospital, Cadiz 11009, Spain

Ana Castellano-Martinez, Department of Pediatric Nephrology, Puerta del Mar University Hospital, Cadiz 11009, Spain

Corresponding author: Moises Rodriguez-Gonzalez, MD, Doctor, Department of Pediatric Cardiology, Puerta del Mar University Hospital, Ana de Viya Avenue 34, Cadiz 11009, Spain.
doctormoisesrodriguez@gmail.com
Telephone: +34-95-6002700

Abstract

BACKGROUND

Myocarditis is an important cause of morbidity and mortality in children, leading to long-term sequelae including chronic congestive heart failure, dilated cardiomyopathy, heart transplantation, and death. The initial diagnosis of myocarditis is usually based on clinical presentation, but this widely ranges from the severe sudden onset of a cardiogenic shock to asymptomatic patients. Early recognition is essential in order to monitor and start supportive treatment prior to the development of severe adverse events. Of note, many cases of fulminant myocarditis are usually misdiagnosed as otherwise minor conditions during the weeks before the unexpected deterioration.

AIM

To provide diagnostic clues to make an early recognition of pediatric myocarditis. To investigate early predictors for poor outcomes.

METHODS

We conducted a retrospective cross-sectional single-center study from January 2008 to November 2017 at the Pediatric Department of our institution, including children < 18-years-old diagnosed with myocarditis. Poor outcome was defined as the occurrence of any of the following facts: death, heart transplant, persistent left ventricular systolic dysfunction or dilation at hospital discharge (early poor outcome), or after 1 year of follow-up (late poor outcome). We analyzed different clinical features and diagnostic test findings in order to provide diagnostic clues for myocarditis in children. Multivariable stepwise logistic regression analysis was performed using all variables that had been selected by univariate analysis to

retrospective studies.

Open-Access: This article is an open-access article which was selected by an in-house editor and fully peer-reviewed by external reviewers. It is distributed in accordance with the Creative Commons Attribution Non Commercial (CC BY-NC 4.0) license, which permits others to distribute, remix, adapt, build upon this work non-commercially, and license their derivative works on different terms, provided the original work is properly cited and the use is non-commercial. See: http://creativecommons.org/licenses/by-nc/4.0/

Manuscript source: Invited manuscript

Received: November 22, 2018
Peer-review started: November 23, 2018
First decision: December 15, 2018
Revised: December 29, 2018
Accepted: January 30, 2019
Article in press: January 30, 2019
Published online: March 6, 2019

determine independent factors that predicted a poor early or late outcome in our study population.

RESULTS

A total of 42 patients [69% male; median age of 8 (1.5-12) years] met study inclusion criteria. Chest pain (40%) was the most common specific cardiac symptom. Respiratory tract symptoms (cough, apnea, rhinorrhea) (38%), shortness of breath (35%), gastrointestinal tract symptoms (vomiting, abdominal pain, diarrhea) (33%), and fever (31%) were the most common non-cardiac initial complaints. Tachycardia (57%) and tachypnea (52%) were the most common signs on the initial physical exam followed by nonspecific signs of respiratory tract infection (44%) and respiratory distress (35%). Specific abnormal signs of heart failure such as heart murmur (26%), systolic hypotension (24%), gallop rhythm (20%), or hepatomegaly (20%) were less prevalent. Up to 43% of patients presented an early poor outcome, and 16% presented a late poor outcome. In multivariate analysis, an initial left ventricular ejection fraction (LVEF) < 30% remained the only significant predictor for early [odds ratio (OR) (95%CI) = 21 (2-456), $P = 0.027$) and late [OR (95%CI) = 8 (0.56-135), $P = 0.047$) poor outcome in children with myocarditis. LVEF correlated well with age ($r = 0.51$, $P = 0.005$), days from the initiation of symptoms ($r = -0.31$, $P = 0.045$), and N-terminal pro-brain natriuretic peptide levels ($r = 0.66$, $P < 0.001$), but not with troponin T ($r = -0.05$, $P = 0.730$) or C-reactive protein levels ($r = -0.13$, $P = 0.391$). N-terminal pro-brain natriuretic peptide presented a high diagnostic accuracy for LVEF < 30% on echocardiography with an area under curve of 0.931 (95%CI: 0.858-0.995, $P < 0.001$). The best cut-off point was 2000 pg/mL with a sensitivity of 90%, specificity of 81%, positive predictive value of 60%, and negative predictive value of 96%.

CONCLUSION

The diagnosis of myocarditis in children is challenging due to the heterogeneous and unspecific clinical presentation. The presence of LVEF < 30% on echocardiography on admission was the major predictor for poor outcomes. Younger ages, a prolonged course of the disease, and N-terminal pro-brain natriuretic peptide levels could help to identify these high-risk patients.

Key words: Myocarditis; Children; Echocardiography; N-terminal pro-brain natriuretic peptide; Myocardial ischemia; Cardiac magnetic resonance imaging; Heart transplantation; Dilated cardiomyopathy

©The Author(s) 2019. Published by Baishideng Publishing Group Inc. All rights reserved.

Core tip: In this retrospective study involving 42 children with myocarditis, we delineated the heterogeneous and unspecific clinical presentation of this condition in order to provide clinical clues to improve its early recognition. We found that the presence of left ventricle ejection fraction < 30% on echocardiography on admission was the major predictor for poor early outcomes. Because echocardiography is not widely available at emergency departments, we found that younger ages (< 2-years-old), a prolonged course of the disease (> 7 d), and increased N-terminal pro-brain natriuretic peptide levels (> 5000 pg/mL) could help to identify these high-risk patients.

Citation: Rodriguez-Gonzalez M, Sanchez-Codez MI, Lubian-Gutierrez M, Castellano-Martinez A. Clinical presentation and early predictors for poor outcomes in pediatric myocarditis: A retrospective study. *World J Clin Cases* 2019; 7(5): 548-561
URL: https://www.wjgnet.com/2307-8960/full/v7/i5/548.htm
DOI: https://dx.doi.org/10.12998/wjcc.v7.i5.548

INTRODUCTION

Myocarditis is an inflammatory condition characterized by leukocyte infiltration and subsequent fibrosis and necrosis of the myocardium. Multiple causes can produce it,

but most cases are thought to be associated with viral infections[1,2]. The real prevalence of pediatric myocarditis is still unknown, but it is considered a rare disease that accounts for 0.05% of pediatric hospital discharges[3-5].

Despite its rarity, myocarditis is an important cause of morbidity and mortality in children. A high percentage of patients presents with congestive heart failure (CHF) and require hospitalization, intensive care admission, mechanical ventilation, cardiac medication, and inotropic or mechanical circulatory support[3-6]. Remarkably, the overall mortality rate in the acute phase is reported to be 7%-15%[3,5] with an increased likelihood of death early in the illness trajectory, and it has been found as the cause of up to 17% of cases of sudden cardiac death in children younger than 16-years-old[4]. Also, most patients with myocarditis develop a left ventricular (LV) dysfunction or dilation in the acute phase that does not recover completely leading to long-term sequelae including chronic CHF, dilated cardiomyopathy (DCM), and death[7,8]. Thus, myocarditis is one of the leading causes for DCM (27%) and for heart transplantation (80%) in children without congenital heart diseases[4,9].

The definitive diagnostic is made by established histological, immunological, and immunohistochemical findings in myocardial tissue samples obtained through endomyocardial biopsy (EMB)[10,11]. However, EMB has many inherent risks, is not widely available in most centers that initially treat patients with myocarditis, and is not routinely performed. Therefore, the initial diagnosis of myocarditis is usually based on clinical presentation, but it widely ranges from severe sudden onset of cardiogenic shock to asymptomatic patients[12-15]. Of note, many cases of fulminant myocarditis (FM) are usually misdiagnosed as otherwise minor conditions during the weeks prior to the unexpected and severe deterioration[13].

In this context, we sought to describe the clinical presentation and diagnostic tests´ findings of our cases of pediatric myocarditis in order to provide diagnostic clues that would help clinicians recognize these patients early. Also, we aimed to investigate the existence of early predictors for poor outcomes.

MATERIALS AND METHODS

Design, setting and study population

We conducted a retrospective cross-sectional single-center study from January 2008 to November 2017 at the Pediatric Department of our institution, a tertiary university-affiliated hospital with 25000 visits per year to our pediatric emergency department and 1200 admissions excluding the neonatal unit. The study was performed according to the requirements of our Institutional Review Board.

Patients were included if they were children up to 18-years-old, and they were diagnosed with myocarditis based on the International Classification of Diseases, Tenth Revision. In all cases, the final diagnosis was made by an expert pediatric cardiologist based on the context of possible myocardial injury with (probable acute myocarditis) or without (possible subclinical myocarditis) cardiovascular symptoms, and at least one of the following criteria[7]: (1) raised biomarkers of cardiac injury (troponin T); (2) ECG findings suggestive of cardiac injury[13,16-21]; (3) abnormal LV function or LV dilation on echocardiogram[22,23] or cardiac magnetic resonance imaging (cMRI); and (4) evidence of inflammation on cMRI (late gadolinium enhancement sequence)[24]. Because EMB was not available at our institution during the study period, no cases of definitive or confirmed myocarditis are presented. Patients were excluded if any etiology of DCM or CHF different from myocarditis (congenital heart diseases, Kawasaki disease, sepsis, cardiotoxic drugs, an inborn error of metabolism, neuromuscular disorders, malformation syndromes, or familial syndromes) was identified, and if there were incomplete medical records.

Data collection

A standardized data collection form was used to collect data from inpatient and outpatient medical records. Inpatient medical records were reviewed to obtain initial data at the time of evaluation at the emergency department when the patient was admitted with the clinical suspicion of myocarditis. Outpatient medical records were reviewed to obtain a follow-up data up to 1 yr following initial hospitalization. Data obtained from each patient included demographics, presenting symptoms, physical examination findings, diagnostic test results, treatment received, and outcomes.

Definitions

LV systolic dysfunction was defined as left ventricle ejection fraction (LVEF) < 50% and severe LV systolic dysfunction as LVEF < 30%. LV dilation was defined as left ventricle diastolic diameter > 2 Z score for body surface area[25]. Based on their clinical

presentation, patients were retrospectively classified under four different cardiac syndromes: (1) FM (abrupt cardiogenic shock or sudden cardiac death); (2) CHF without hemodynamic instability; (3) Dysrhythmia (palpitations associated to any abnormal rhythm documented on ECG)[18,19]; and (4) Acute coronary syndrome-like (ACS-like) (chest pain, ECG findings suggestive of myocardial ischemia, and raised troponin T)[17,26-29]. Increased CPR, troponin T, and N-terminal pro-brain natriuretic peptide (NT-proBNP) levels were defined as > 60 mg/L, > 10 ng/L, and > 600 pg/mL, respectively. Poor outcome was defined as the occurrence of any of the following facts: death, heart transplant, or persistent LV systolic dysfunction or dilation at hospital discharge (early poor outcome) or after 1 year of follow-up (late poor outcome).

Study strategy

We analyzed different variables in order to characterize the clinical presentation and to find diagnostic clues for myocarditis in children. Also, patients were divided into two groups based on the presence of poor early (at hospital discharge) and late (1 yr after admission) outcomes. Then, we looked for risk factors for poor outcomes at the presentation in our pediatric myocarditis cohort.

Statistical analysis

Data are presented descriptively using frequency and percentage for qualitative variables. Quantitative variables were expressed using the mean (± SD) or the median and interquartile range according to the variable's distribution (tested with Shapiro-Wilk normality test). For bivariate analysis, unpaired two-tailed Student's *t*-test or Mann-Whitney *U*-test was used depending on the distribution of the studied variables. Chi-squared test was used to compare categorical variables (Fisher's exact test was used when the expected frequency was less than 5). The relation among quantitative variables was explored through estimation of Pearson or Spearman correlation coefficients. Multivariable stepwise logistic regression analysis was performed using all variables that had been selected by univariate analysis to determine independent factors that predicted a poor early or late outcome in our population study, and the results were expressed as an odds ratio (OR) with a 95%CI. Significance level was considered as $P < 0.05$. A 95%CI that did not include 1.0 was interpreted to indicate statistical significance. Analyses were performed using the Stata 13.0. (StataCorp. 2013. Stata Statistical Software: Release 13. College Station, TX, United States: StataCorp LP).

RESULTS

A total of 42 patients (69% male) met study inclusion criteria. The median age was 8 (1.5-12) years with a bimodal age presentation: most cases were children < 2-years-old and > 12-year-old (35% for each group; Figure 1). Table 1 provides the baseline data of the patients enrolled.

Clinical presentation at the Emergency Department (ED)

The diagnosis of myocarditis was made after a median of 5 (2-10) d from the initial symptoms, and the patients consulted to the ED a median of 2 (1-2) times prior to their admission. The definitive diagnosis of myocarditis was made during the first visit at our ED in 41% of patients, 34% of cases were children > 10-years-old with the ACS-like presentation, and 7% were infants with FM. Most patients (59%) required two or more visits to the ED before the diagnosis of myocarditis. A previous diagnosis different from myocarditis was made in 52% of cases; 31% were categorized as respiratory infection (bronchiolitis, pneumonia, and upper respiratory tract infection), 17% as gastrointestinal infection, 2% as urinary tract infection, and 2% as infantile colic. The majority of patients (69%) presented a viral infection prior to the diagnosis, and a positive microbiologic study by serology or blood-PCR was observed in 47% of patients, with Coxsackie (30%) and Parvovirus B19 (20%) as the most prevalent agents.

Most patients had overlapping signs and symptoms at presentation. Chest pain (40%) was the most common specific cardiac symptom. Other specific cardiac symptoms such as palpitations (16%) or syncope (4%) were less prevalent. Respiratory tract symptoms (cough, apnea, rhinorrhea) (38%), shortness of breath (35%), gastrointestinal tract symptoms (vomiting, abdominal pain, diarrhea) (33%), and fever (31%) were the most common non-cardiac initial complaints. Tachycardia (57%) and tachypnea (52%) was the most common sign on the initial physical exam, followed by nonspecific signs of respiratory tract infection (44%) and respiratory distress (35%). Specific abnormal signs of heart failure such as heart murmur (26%), systolic

Table 1 Baseline characteristics at the time of hospital admission

Clinical and demographic data	*n* = 42
Age	Median (IQR) yr: 8 (1.5-12)
Male:Female gender	2.23
Evolution	Median (IQR) days from initial symptoms: 5 (2-10)
Visits to ED previously before diagnosis of myocarditis	Median (IQR) visits prior to admission: 2 (1-2); 1 visit (41), 2 visits (36), 3 visits (9), more than 3 visits (14)
Presenting symptoms (%)	Previous viral infection (69); Chest pain (40); Respiratory tract symptoms (cough, apnea, rhinorrhea) (38); Shortness of breath (35); Gastrointestinal tract symptoms (vomiting, abdominal pain, diarrhea) (33); Fever (31); Weakness, exercise or feeding intolerance (21); Palpitations (16); Lethargy (12); Syncope (4)
Physical exam (%)	Tachycardia (57); Tachypnea (52); Evidence of respiratory tract infection (44); Respiratory distress (35); Abnormal lung auscultation (31); Murmur (26); Systolic hypotension (24); Poor perfusion or diminished pulses (21); Gallop rhythm (20); Hepatomegaly (20); Edema (7); Cyanosis (2)
Cardiac syndrome (%)	ACS-like (34); Fulminant myocarditis (29); Congestive heart failure (23); Dysrhythmia (14)
Complementary exams	
Laboratory (%)	CRP > 60 mg/L (16); Troponin T > 10 ng/L (62); NT-proBNP > 600 pg/mL (40)
Chest X-Ray (%)	Cardiomegaly (35); Pulmonary edema (28); Pulmonary infiltrate (4%); Pleural effusion (2.5%)
ECG (%)	Abnormal ECG (93); Sinus tachycardia (61); Ischemic changes (57); Low voltage (50); SVT (2.5); VT (7); AVB (2.5); prolonged QT interval (2.5%)
Echocardiography (%)	Abnormal echocardiography (88): LV systolic dysfunction (50): severe (14), moderate (16), mild (20); Biventricular systolic dysfunction (10); Segmental wall motion abnormalities (38); LV dilation (43); Mitral regurgitation (69); Pericardial effusion (59)
Cardiac MRI (%)	MRI performed (50); Median days to realization from admission, 5 (3-9); Lake Louis criteria positive (86), equivocal (10), negative (4)
Microbiology (%)	Positive microbiology (47): Coxsakie (30); Parvovirus B19 (20); Adenovirus (15); EBV (15); CMV (10); Mycoplasma (10)
Treatment (%)	Any treatment (71): Diuretics (69); ACEI (69); Beta-blockers (64); Digoxin (14) Spironolactone (14); Antiarrhythmic (5); Inotropic support (35); Mechanical Ventilation (26); ECMO/VAD (2.5); Pacemaker (2.5)
Outcomes (%)	Hospitalization length of stay (d): Median 6 (IQR 3-13); Death (5), transplant (0)
	Poor early outcomes: Death, transplant, or LV systolic dysfunction/dilation at discharge (43)
	Poor late outcomes: Death, transplant or LV systolic dysfunction/dilation after 1 yr of follow-up (16); Spontaneous LV function recovery during first year after diagnosis (69)

IQR: Interquartile range; GI: Gastrointestinal; SCD: Sudden cardiac death; ACS: Acute coronary syndrome; CRP: C-reactive protein; NT-proBNP: N-terminal pro-brain natriuretic peptide; ECG: Electrocardiogram; SVT: Supraventricular tachycardia; VT: Ventricular tachycardia; AVB: Atrioventricular block; LV: Left ventricle; MRI: Magnetic resonance imaging; EBV: Epstein-Barr virus; CMV: cytomegalovirus; ACEI: Angiotensin-converting-enzyme inhibitors; ECMO: Extracorporeal membrane oxygenation; VAD: Ventricular assist device.

hypotension (24%), gallop rhythm (20%), or hepatomegaly (20%) were less prevalent. ACS-like was the most common cardiac syndrome (34%), followed by FM (29%), CHF (23%), and dysrhythmia (14%). Patients with ACS-like were older (median age 12.5 (11-13) years *vs* 2 (1.5-8) years; $P < 0.001$), presented earlier [median 2 (1-3) d *vs* 8.5 (4-12) d, $P = 0.005$], and with normal LV systolic function [median LVEF of 65% (62-77) *vs* 41% (30-53), $P < 0.001$] than patients with the rest of the cardiac syndromes. Conversely, patients with FM were younger [median age of 1.15 years [0.95-1.85 *vs* 11 years (6-13), $P < 0.001$], and presented later [median 9 (4.5-11) d *vs* 4 (2-10) d, $P = 0.017$] and with depressed LV systolic function [median LVEF of 32% (27-36) *vs* 62% (45-66), $P < 0.001$] compared to patients with other cardiac syndromes (Table 2).

Diagnostic tests

Troponin T plasma levels were assessed as a biomarker for myocardial damage in 90% of patients with median levels of 91 (5-550) pg/mL and were increased in 62% of cases. NT-proBNP as a biomarker for CHF was determined in 81% of patients with median levels of 482 (151-2500) pg/mL and was increased in 40% of cases. The

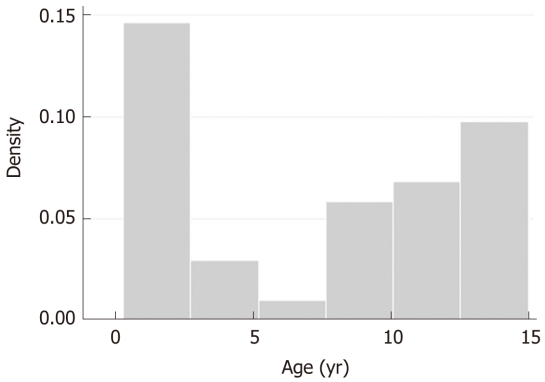

Figure 1 Histogram showing the age distribution of myocarditis pediatric population. Most patients (70%) were children younger than 2-years-old (35%), and older than 12-years-old (35%).

systemic inflammatory response was assessed by C-reactive protein (CPR) in all patients with median levels of 4 (2-144) mg/dL and was increased in 16% of cases. An abnormal ECG was observed in most patients (93%) with sinus tachycardia (61%) and signs suggestive of ischemia (57%) as the most common features. Life-threatening arrhythmias (ventricular tachycardia or acute complete atrioventricular block with cardiac arrest) were observed in 9.5% of patients. Chest X-ray revealed cardiomegaly in 35% and pulmonary edema in 28% of patients. Echocardiography was abnormal in 88% of patients. LV systolic dysfunction was observed in up to 50% of the entire cohort, 14% with severe LV dysfunction and 10% with biventricular dysfunction. Segmental wall motion abnormalities were observed in 38% of cases, most of them (76%) children with ACS-like and normal LVEF. cMRI was performed in 50% of the population study after a median of 4 (3-6) d of hospitalization, most of them (95%) children > 10-year-old without FM presentation confirming the presence of myocardial inflammation in 86% of cases.

Therapeutics and outcomes

Most patients (73%) received cardiac medications during the admission, mostly diuretics (69%), angiotensin-converting-enzyme inhibitors (69%), and beta-blockers (64%). No treatment with gammaglobulin or steroids was administered. Up to 35% of cases required inotropic support, whereas advanced circulatory support with extracorporeal membrane oxygenation or pacemaker implantation was required in 2.5% of cases. Up to 43% of patients were classified as having an early poor outcome and 16% as having a late poor outcome. The mortality rate secondary to cardiac causes was 5%, all cases during the first hospitalization with no cases of heart transplantation. The median length of hospitalization was 6 (3-13) d. LV dysfunction or dilation persisted in up to 38% and 12% of patients, respectively after the hospital discharge and after 1 year of follow-up. The spontaneous recovery rate of LV function was 69% during the first year of follow-up. Only one patient presented a permanent and significant non-cardiac complication, which was cerebral palsy due to prolonged cardiac arrest after acute atrioventricular block.

Risk factors for poor outcome at presentation

Upon univariate analysis (Table 2 and Table 3), age < 2 years, diagnosis > 7 d from initial symptoms, NT-proBNP admission levels > 5000 pg/mL, and LVEF < 30% predicted both early and late poor outcome. In multivariate analysis (Table 4 and Table 5), an initial LVEF < 30% remained the only significant predictor for early and late poor outcome in children with myocarditis.

Clinical and biochemical markers associated with LV systolic dysfunction on echocardiography at presentation

LVEF correlated well with age (r = 0.51, P = 0.005), days from initial symptoms (r = -0.31; P = 0.045), and NT-proBNP levels (r = 0.66, P = 0.001), but not with troponin T (r = -0.05, P = 0.730) or CRP levels (r = -0.13, P = 0.391) (Figure 2). NT-proBNP presented a high diagnostic accuracy for severe LV systolic dysfunction on echocardiography, with an area under the curve of 0.931 (95%CI: 0.858-0.995, P = 0.001) (Figure 3). The best cut-off point was 2000 pg/mL with a sensitivity of 90%, specificity of 81%, positive predictive value of 60%, and negative predictive value of 96%.

Table 2 Comparison between patients with acute coronary syndrome-like and fulminant myocarditis

Variable	ACS-like (*n* = 14; 33%)	No ACS-like (*n* = 28; 66%)	*P* value	FM (*n* = 12; 28%)	No FM (*n* = 30; 78%)	*P* value
Age (yr), median (IQR)	11 (5-12.5)	1.6 (1-8)	< 0.001	10 (2-13)	1.7 (0.9-3)	< 0.001
Male sex, *n* (%)	19 (71)	19 (67)	0.813	9 (75)	20 (66)	0.598
Days from initial symptoms, median (IQR)	2 (1-3)	8.5 (4-12)	0.005	9 (4.5-11)	4 (2-10)	0.017
Visits prior to admission, median (IQR)	1 (1-1)	2 (2-3)	< 0.001	2.5 (2-3)	1 (1-1)	< 0.001
Viral prodromal, *n* (%)	9 (31)	5 (38)	0.637	9 (31)	3 (23)	0.598
Altered ECG, *n* (%)	14 (100)	25 (89)	0.204	12 (100)	27 (90)	0.256
CPR (mg/dl), median (IQR)	5 (2.5-188)	3 (2-144)	0.179	29 (3-203)	3 (2-144)	0.095
Troponin T (ng/mL), median (IQR)	466 (89-800)	51 (4-353)	0.041	134 (71-431)	70 (4-160)	0.308
NT-proBNP (pg/mL), median (IQR)	137 (78-234)	1960 (272-3175)	< 0.001	2900 (2207-6125)	225 (105-561)	< 0.001
LVEF (%), median (IQR)	65 (62-67)	41 (30-53)	< 0.001	32 (27-36)	62 (45-66)	< 0.001
LGE in cMRI (*n* = 21), *n* (%)	10/14 (71)	5/7 (71)	1.000	0/1 (0)	15/20 (75)	0.105
Positive Microbiology, *n* (%)	9 (64)	18 (64)	1.000	8 (66)	19 (63)	0.839
Poor outcomes, *n* (%)	0 (0)	7 (25)	0.041	5 (41)	2 (7)	0.006

ACS-like: Acute coronary syndrome; FM: Fulminant myocarditis; IQR: Interquartile range; ECG: Electrocardiogram; CRP: C-reactive protein; NT-proBNP: N-terminal pro-brain natriuretic peptide; LVEF: Left ventricle ejection fraction; LGE: Late gadolinium enhancement; cMRI: Cardiac magnetic resonance imaging.

DISCUSSION

In this retrospective study, we described the clinical presentation and diagnostic method findings of 42 children with a clinical diagnosis of myocarditis. Also, we provided clues to improve the early recognition of myocarditis and define possible early predictors for poor outcome in these patients.

The challenges of diagnosing pediatric myocarditis

The identification of pediatric patients with myocarditis in the early phases of the disease is essential in order to start monitoring and supportive treatment in a timely manner. However, the diagnosis may be challenging at initial stages in milder cases before the development of severe adverse events. Our results showed a heterogeneous and unspecific clinical presentation of myocarditis in children. Most patients presented with a preceding viral illness involving the respiratory or gastrointestinal tracts that was not associated with myocarditis initially. Of note, the most common specific cardiac symptom (chest pain) was observed in a similar proportion with shortness of breath and nonspecific respiratory or gastrointestinal symptoms that could mimic the clinical presentation of benign viral infections[2,13-15]. Besides, the physical examination revealed specific cardiac signs only in a minority of cases, and the most common alterations found on physical examination (tachycardia, tachypnea, respiratory distress, and abnormal lung auscultation) were non-specific cardiac signs. Therefore, the early identification of pediatric myocarditis based on clinical presentation and physical examination is challenging. We characterized four specific cardiac presentations in our pediatric myocarditis cohort that included FM, ACS-like, dysrhythmia, and CHF. Remarkably, we observed that the clinical presentation was associated with the age and the time of evolution of symptoms. Thus, older children (> 10-years-old) with ACS-like were diagnosed early after the initial symptoms usually at the time of the first consultation. Conversely, infants (< 2-years-old) were diagnosed late usually after two or more consultations with FM or CHF. This may be explained by the capacity of the older children to describe their symptoms in detail leading to prompt medical consultation and diagnosis. Conversely, younger infants are not able to express their symptoms, and clinicians are more reliant on parents' observations. Therefore, they only seek medical attention when they observe late symptoms related to heart failure[6,24-26]. Also, the influence of the age on the immunologic response to viral infection of the myocardium might lead to different clinical courses and outcomes[7,29]. Our finding that most patients were consulted to the ED two or more times prior to the final diagnosis and that many patients had a previous diagnosis different from myocarditis, reinforces that a high index of suspicion is needed for infants with prolonged viral infections (overall with

Table 3 Comparison between patients with good and poor outcomes

Variable	Early outcome (hospital discharge)			Late outcome (1 yr after admission)		
	Good outcome(*n* = 24; 57%)	Poor outcome(*n* = 18; 43%)	*P* value	Good outcome (*n* = 35; 84%)	Poor outcome (*n* = 7; 16%)	*P* value
Age (years), median (IQR)	11 (5-12.5)	1.6 (1-8)	0.026	10 (2-13)	1.7 (0.9-3)	0.014
Male sex, *n* (%)	14 (78)	15 (62)	0.289	24 (68)	5 (71)	0.881
Evolution (days from initial symptoms), median (IQR)	2.5 (2-10)	7 (4-12)	0.036	4 (2-10)	7 (7-15)	0.043
Cardiac syndrome, *n* (%)						
FM	2 (8)	10 (55)	< 0.001	7 (20)	5 (71)	< 0.001
CHF	6 (25)	4 (22)	0.834	8 (23)	2 (28)	0.746
Dysrhythmia	3 (12)	3 (16)	0.793	6 (17)	0 (0)	0.237
ACS-like	13 (54)	1 (5)	0.001	14 (40)	0 (0)	0.041
Viral prodromal, *n* (%)	15 (62)	14 (68)	0.289	23 (65)	6 (85)	0.296
Altered ECG, *n* (%)	22 (91)	17 (94)	0.729	32 (91)	7 (100)	0.421
CPR (mg/dL), median (IQR)	4 (2-147)	4 (3-125)	0.443	4 (2-144)	33 (3-156)	0.415
Troponin T (ng/mL), median (IQR)	118 (5-580)	91 (32-196)	0.789	103 (5-610)	52 (32-177)	0.447
NT-proBNP (pg/mL), median (IQR)	291 (92-300)	2700 (1955-4320)	< 0.001	300 (123-1955)	5700 (2500-10321)	0.002
LVEF (%), median (IQR)	65 (58-66)	34 (28-41)	< 0.001	59 (41-66)	29 (27-31)	< 0.001
LVDD Z score > 2, *n* (%)	9 (37)	17 (94)	< 0.001	19 (54)	7 (100)	0.023
Dyskinesia, *n* (%)	11 (46)	5 (27)	0.233	15 (43)	1 (14)	0.155
LGE in cMRI (*n* =21), *n* (%)	12 (75)	3 (60)	0.517	14 (70)	1 (100)	0.517
Positive Microbiology, *n* (%)	12 (50)	8 (44)	0.307	16 (45)	4 (57)	0.666

IQR: Interquartile range; CHF: Congestive heart failure; SCD: Sudden cardiac death; ACS: Acute coronary syndrome; FM: Fulminant myocarditis; CRP: C-reactive protein; LVEF: Left ventricle ejection fraction; LVDD: Left ventricle diastolic dysfunction; LGE: Late gadolinium enhancement; cMRI: Cardiac magnetic resonance imaging.

respiratory signs or symptoms) that do not improve and lead to multiple medical consultations.

Another reason that diagnosing myocarditis is difficult is the limited diagnostic accuracy of most available noninvasive diagnostic tests. There are no accurate serum biomarkers for the diagnosis of myocarditis[1]. CPR can be elevated in the acute phase, but it is neither sensitive nor specific to determine the presence or absence of active myocardial inflammation. We observed elevated CRP levels only in 16% of our population, so normal values do not exclude a myocardial inflammatory process. Myocytes destruction also occurs in the acute phase of myocarditis; thus serum biomarkers of myocardial damage can be elevated in some cases. However, the sensitivity and negative predictive of elevated troponin I level in patients with biopsy-proven myocarditis were reported to be low[30-32]. We observed elevated troponin T levels in up to 65% of our population. Therefore, increased troponin T levels can reinforce the clinical suspicion of myocarditis in children, but a normal result does not exclude the diagnosis[1]. Natriuretic peptides are secreted by ventricular myocytes in response to volume or pressure overload to counteract the renin-angiotensin-aldosterone and sympathetic nervous system actions in the context of heart failure. Thus, natriuretic peptides can be elevated in myocarditis with LV dysfunction and heart failure[33]. We observed increased NT-proBNP levels only in 40% of patients, and therefore a normal value does not discard the diagnosis of myocarditis. Of note, increased NT-proBNP levels may aid in distinguishing a cardiac from a non-cardiac

Table 4 Predictors for poor outcome at hospital discharge

Variable	Univariate analysis		Multivariate logistic regression[1]	
	OR (95%CI)	*P* value	OR (95%CI)	*P* value
Age < 2 yr	8 (2-32)	0.005		
Evolution > 7 d	3 (0.9-11)	0.038		
NT-proBNP > 5000 pg/mL	15 (1.5-303)	0.037		
LVEF < 30%	60 (3-347)	0.006	21 (2-456)	0.027

[1]Multivariate logistic regression was performed only on risk factors in univariate analyses for early and late poor outcome (age < 2 yr, evolution > 7 d, N-terminal pro-brain natriuretic peptide > 5000, left ventricular ejection fraction < 30%). Odds ratios refer to the change in odds of poor early and late outcome when the predictor variables are presents. LVEF: Left ventricular ejection fraction; NT-proBNP: N-terminal pro-brain natriuretic peptide; OR: Odds ratio; CI: Confidence interval.

reason for respiratory symptoms in children[34,35]. This feature seems to be very useful to identify patients with a cardiac process in the context of nonspecific respiratory symptoms, as we observed in our young patients with myocarditis.

ECG and chest X-ray also have limited value for the diagnosis of myocarditis. Although ECG is virtually always abnormal in children with myocarditis[13], the abnormalities observed were widely variable, and there was not one specific abnormality that occurs with enough frequency to be a specific marker[16-19]. Also, chest X-ray revealed more specific cardiac findings such as cardiomegaly and pulmonary in a minority of patients.

Echocardiography remains the more useful diagnostic test in cases with clinical suspicion of myocarditis[22]. Most children had echocardiographic alterations on admission. The most typical findings associated with myocarditis were LV dilatation and reduced global LVEF. Another echocardiographic sign that can help make the diagnosis is the presence of segmental wall motion abnormalities mimicking ischemic cardiomyopathy[23], which were observed mostly in older children with ACS-like. This feature can be explained by the focal distribution of areas of inflammation frequently seen in myocarditis. Mitral regurgitation and pericardial effusion may also be observed and help make a diagnosis. Similar to the clinical presentation, echocardiographic findings depend on both the manner and timing of a patient's presentation. Thus, young patients with FM and more days of evolution presented the most depressed LVEF whereas older patients that were consulted early in the course of the disease with ACS-like usually presented a normal LVEF and segmental wall motion alterations.

cMRI is a promising diagnostic method for myocarditis. The major strength of cMRI is its capacity to detect inflammation, edema, necrosis, and fibrosis within myocardial tissue through several imaging sequences. The use of a mixed cMRI method (Lake Louis criteria) is preferred compared to EMB in clinically stable patients suspected of having myocarditis. Nevertheless, the presence of two of the three characteristics listed in the Lake Louise criteria leads to a low-moderate sensitivity (67%-78%) and negative predictive value (69%), and high specificity (91%) and positive predictive value (91%)[24]. Therefore, a negative test does not discard the clinical suspicion of myocarditis. The sensitivity of cMRI for the diagnosis of myocarditis is likely to be limited in patients with less inflammation and a prolonged duration of symptoms; thus cMRI may be more helpful in the diagnosis of acute myocarditis if performed within 14 d of the onset of symptoms[30]. Also, cMRI is not widely available in all centers, and it is difficult to carry out in non-stable patients and infants, which represent the most common clinical picture of myocarditis. Consistent with this, we performed cMRI early in the course of the disease (median of 4 d after admission) in 50% of our population, most of them teenagers with an ACS-like presentation, confirming the diagnosis of suspected myocarditis in 86%. The only cMRI in an infant with FM was performed after 14 d of diagnosis when the patient was stable and was negative. Although cMRI is a promising technology, its sensitivity for the diagnosis of myocarditis must be improved and used timely in the appropriate candidates.

Predictors for poor outcomes

Myocarditis is a significant etiology of CHF, often leading to DCM, need for heart transplantation, and death. Poor outcomes were observed in up to 43% of patients at the time of hospital discharge and 16% after 1 year of follow-up. The mortality rate

Table 5 Predictors for poor outcome at 1 yr from admission

Variable	Univariate analysis		Multivariate analysis[1]	
	OR (95%CI)	*P* value	OR (95%CI)	*P* value
Age < 2 yr	6 (1.1-37)	0.046		
Evolution > 7 d	10 (1.1-93)	0.041		
NT-proBNP > 5000 pg/mL	13 (1.4-122)	0.024		
LVEF < 30%	46 (4.4-392)	0.001	8 (0.56-135)	0.041

[1]Multivariate logistic regression was performed only on risk factors in univariate analyses for early and late poor outcome (age < 2 yr, evolution > 7 d, N-terminal pro-brain natriuretic peptide > 5000, left ventricular ejection fraction < 30%). ORs refer to the change in odds of poor early and late outcome when the predictor variables are presents. LVEF: Left ventricular ejection fraction; NT-proBNP: N-terminal pro-brain natriuretic peptide; OR: Odds ratio; CI: Confidence interval.

was 5%, and all cases of death occurred during the initial hospitalization. We observed LV dilation in 43% and LV dysfunction in 50% (14% severe) of cases on admission, reflecting the potential of myocarditis to produce important alterations in the early phases of the disease. Acute myocarditis in patients who present with LV systolic dysfunction can recover in weeks to months. Of note, we found a spontaneous complete recovery rate of initial LV dysfunction or dilation of 69% during the first year of follow-up. These outcomes are similar to those observed in two recent large prospective multicentric studies involving pediatric myocarditis[6,9] and highlight a contemporary good prognosis of acute myocarditis in children that could reflect the advances in the recognition and management of these patients. Also, this reinforces the need for aggressive initial management in the acute phase of the disease waiting for a possible recovery in most patients. Nevertheless, we found that myocarditis in children is still associated with a high rate of CHF, hospitalization, intensive care unit stay, use of cardiac medications, and inotropic support or mechanical circulatory support at the time of diagnosis. Also, 12% still suffered from LV dysfunction or dilation after 1 year. Hence, it would be useful to identify these high-risk patients in the early phase of the disease. The main finding of this study was that a severe depressed LV systolic function (LVEF < 30%) on admission was the only independent predictor for poor outcomes in pediatric myocarditis. However, in the univariate analysis we identified some features that could help clinicians detect these patients on admission. These factors were age < 2-years-old, > 7 d from the initial symptoms, and NT-proBNP > 5000 pg/mL. Of note, LVEF was associated with all these factors. As echocardiography is not widely available at emergency departments and requires some training and expertise, we think that the above mentioned clinical and biochemical factors could be useful to identify high-risk patients. Specifically, NT-proBNP levels seem to be very useful for the screening of LV dysfunction upon admission in children with myocarditis. We found that the diagnostic accuracy of NT-proBNP levels on admission for severe LV dysfunction on echocardiography was high and that those patients with concentrations less than 2000 pg/mL at admission probably will not have a severe LV dysfunction on echocardiography, and therefore they will have a good outcome.

Limitations

This study had several limitations. The retrospective nature without the establishment of inclusion criteria prior to the beginning of the study and the use of clinically diagnosed myocarditis could lead to the inclusion of patients who did not have myocarditis. The absence of cases of heart transplantation could be because our center does not have a heart transplant program. Therefore, it is possible that more severe cases of myocarditis were referred directly to hospitals with a heart transplant program. Although our mortality rate was low and consistent with the recent literature, it could also be influenced by this fact, and this could limit the risk factors provided. Also, the time of follow-up was short, and this could prevent the analysis of risk factors for long-term outcomes. Finally, none of our patients received immunomodulatory therapy, a promising therapeutic strategy as suggested by several randomized trials. This could impact the outcomes observed in our study, but this kind of therapy remains investigational mainly at this time and requires further elucidation. Of note, despite not using these treatments, our outcomes were similar to those studies that used them.

Conclusions

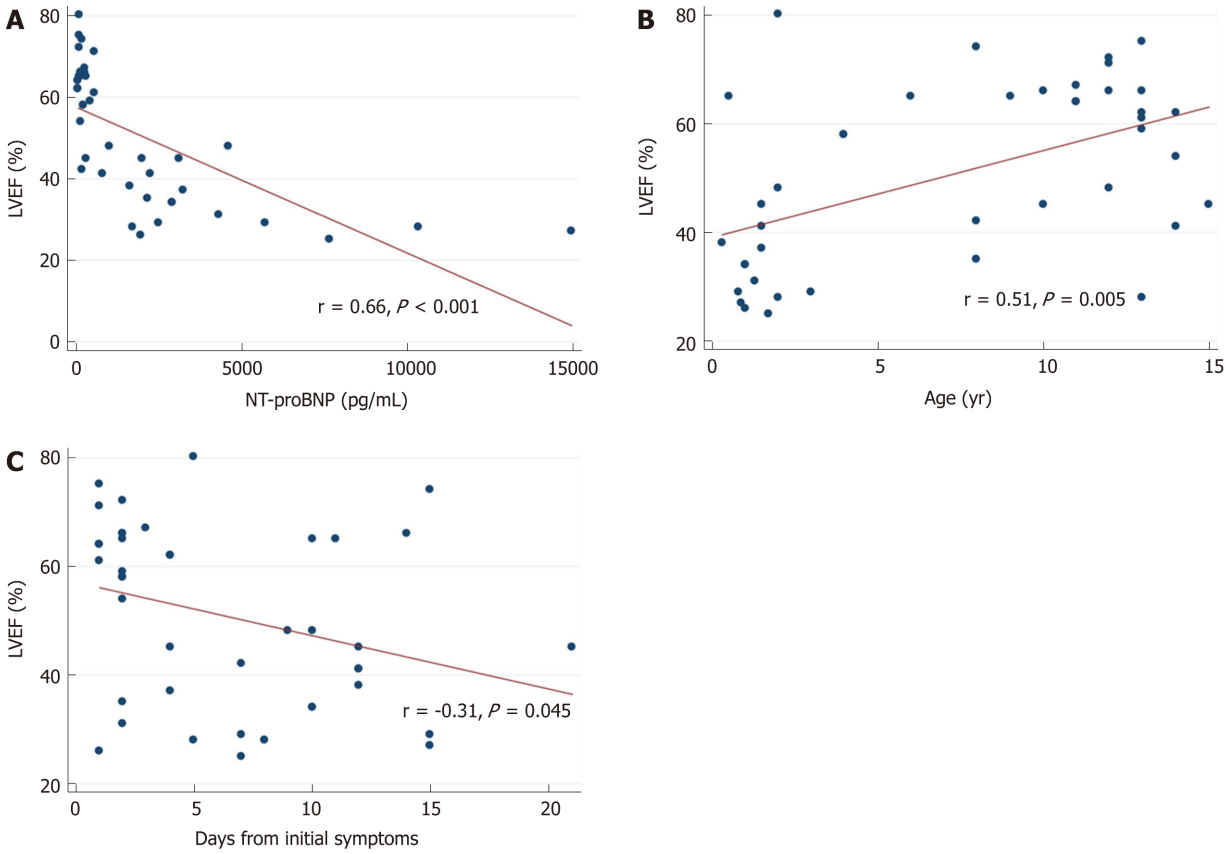

Figure 2 Correlations between left ventricular ejection fraction at admission and (A) N-terminal pro-brain natriuretic peptide levels, (B) age, and (C) days of evolution of the disease. NT-proBNP: N-terminal pro-brain natriuretic peptide.

The timely diagnosis of myocarditis in children is challenging due to the heterogeneous and unspecific clinical presentation and the low diagnostic accuracy of most non-invasive laboratory tests. Myocarditis should be considered among the differential diagnosis in infants with prolonged viral infections (overall with respiratory signs or symptoms) that does not improve and leads to multiple medical consultations. Echocardiography remains the most useful diagnostic tool for myocarditis, and the presence of severe LV dysfunction at admission was the primary predictor for poor outcomes. Younger ages, a prolonged course of the disease, and NT-proBNP levels are some factors that could help to identify these high-risk patients in ED.

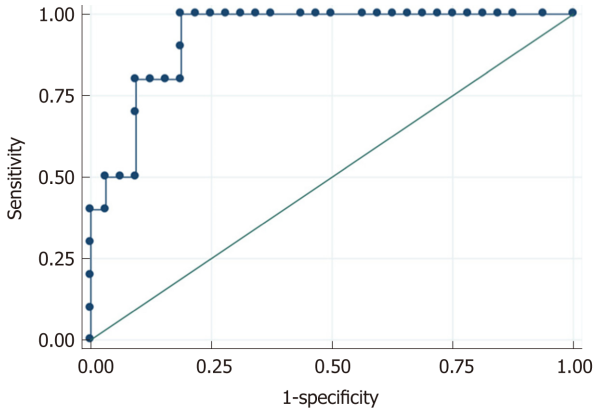

Figure 3 Area under receiver operating characteristic curve of N-terminal pro-brain natriuretic peptide for determining left ventricular ejection fraction < 30%. N-terminal pro-brain natriuretic peptide presented a high diagnostic accuracy for severe left ventricular systolic dysfunction on echocardiography with an area under curve of 0.931 (95%CI: 0.858-0.995, $P < 0.001$). The best cut-off point was 2000 pg/mL, with a sensitivity of 90%, specificity of 81%, positive predictive value of 60%, and negative predictive value of 96%.

ARTICLE HIGHLIGHTS

Research background

Pediatric myocarditis constitutes an important cause of morbidity and mortality in the form of death, heart transplant, and dilated cardiomyopathy. Pediatric myocarditis diagnosis is usually challenging. It is mainly due to its heterogeneous and unspecific clinical presentation, and the low accuracy of the currently available non-invasive diagnostic tests. Also, the gold standard for diagnosis, the endomyocardial biopsy has inherent risks and is not widely available. Of note, a diagnostic delay can lead to a subsequent elevated morbimortality.

Research motivation

We aimed to investigate the clinical presentation and the results of the non-invasive tests utilized in the diagnostic work-up of pediatric myocarditis at presentation.

Research objectives

Our main purpose was to provide clinical, biochemical, or echocardiographic clues in order to improve the early recognition of pediatric myocarditis at presentation in the emergency department. Also, we sought to identify predictors for poor outcome in pediatric myocarditis in order to identify high-risk patients that will need a more intensive therapy and close follow-up.

Research methods

We carried out a retrospective cross-sectional single-center study. A total of 42 patients between 2008 and 2017 were enrolled. Patients were divided into two groups: poor outcome and no poor outcome. We delineated the clinical presentation of our patients with myocarditis. Also, different clinical and diagnostic test variables were analyzed in order to find possible poor outcome predictors.

Research results

The clinical presentation of pediatric myocarditis was heterogeneous, ranging from asymptomatic to cardiogenic shock cases. Of note, pediatric myocarditis clinical presentation can mimic benign viral infections in children, usually in those younger patients that are not able to verbalize symptoms and debut as fulminant myocarditis. Conversely older patients presented with acute coronary syndrome-like myocarditis. There was no single non-invasive diagnostic test that led to rule out or rule in the diagnosis of pediatric myocarditis. Cardiac magnetic resonance imaging presented a high diagnostic accuracy, but was mostly useful only for older children with acute coronary syndrome-like presentation. Severe depressed left ventricle systolic function on echocardiography was the only independent predictor for poor outcome (death, transplant, or dilated cardiomyopathy). The presence of age < 2-years-old, a clinical course of more than 7 d from initial symptoms, or N-terminal pro-brain natriuretic peptide levels > 5000 pg/mL was associated with a severe depressed LV systolic function.

Research conclusions

A high grade of clinical suspicion is needed to make an early diagnosis of pediatric myocarditis, especially in infants who cannot verbalize their symptoms. This clinical suspicion must be used in combination with several findings of different non-invasive diagnostic tests in order to improve the prompt recognition of pediatric myocarditis. This study provided some clinical pictures that can help clinicians in this context. Echocardiography is a reliable diagnostic tool for pediatric myocarditis. Patients that present with a severe depressed LV systolic function have a poor outcome. Age younger than 2 years, prolonged course of disease, and higher N-terminal pro-brain natriuretic peptide levels are predictors of poor outcome that could be useful even in

centers where echocardiography is not available. The combined use of these predictors can lead to an early detection of high-risk patients in order to initiate adequate treatment and monitoring.

Research perspectives

This article reflects the challenge to diagnose pediatric myocarditis. Future studies should prospectively collect multicenter data on epidemiology, clinical presentation, and diagnostic value of currently available diagnostic tools in children with myocarditis to establish clinically meaningful criteria for the diagnosis of myocarditis. This will enhance the early recognition and subsequently the prognosis of these patients.

REFERENCES

1 **Kindermann I**, Barth C, Mahfoud F, Ukena C, Lenski M, Yilmaz A, Klingel K, Kandolf R, Sechtem U, Cooper LT, Böhm M. Update on myocarditis. *J Am Coll Cardiol* 2012; **59**: 779-792 [PMID: 22361396 DOI: 10.1016/j.jacc.2011.09.074]

2 **Shekerdemian L**, Bohn D. Acute viral myocarditis: Epidemiology and pathophysiology. *Pediatr Crit Care Me* 2006; **7**: S2 [DOI: 10.1097/01.PCC.0000244338.73173.70]

3 **Ghelani SJ**, Spaeder MC, Pastor W, Spurney CF, Klugman D. Demographics, trends, and outcomes in pediatric acute myocarditis in the United States, 2006 to 2011. *Circ Cardiovasc Qual Outcomes* 2012; **5**: 622-627 [PMID: 22828827 DOI: 10.1161/CIRCOUTCOMES.112.965749]

4 **Lipshultz SE**, Sleeper LA, Towbin JA, Lowe AM, Orav EJ, Cox GF, Lurie PR, McCoy KL, McDonald MA, Messere JE, Colan SD. The incidence of pediatric cardiomyopathy in two regions of the United States. *N Engl J Med* 2003; **348**: 1647-1655 [PMID: 12711739 DOI: 10.1056/NEJMoa021715]

5 **Klugman D**, Berger JT, Sable CA, He J, Khandelwal SG, Slonim AD. Pediatric patients hospitalized with myocarditis: a multi-institutional analysis. *Pediatr Cardiol* 2010; **31**: 222-228 [PMID: 19936586 DOI: 10.1007/s00246-009-9589-9]

6 **Butts RJ**, Boyle GJ, Deshpande SR, Gambetta K, Knecht KR, Prada-Ruiz CA, Richmond ME, West SC, Lal AK. Characteristics of Clinically Diagnosed Pediatric Myocarditis in a Contemporary Multi-Center Cohort. *Pediatr Cardiol* 2017; **38**: 1175-1182 [PMID: 28536746 DOI: 10.1007/s00246-017-1638-1]

7 **Sagar S**, Liu PP, Cooper LT. Myocarditis. *Lancet* 2012; **379**: 738-747 [PMID: 22185868 DOI: 10.1016/S0140-6736(11)60648-X]

8 **Levine MC**, Klugman D, Teach SJ. Update on myocarditis in children. *Curr Opin Pediatr* 2010; **22**: 278-283 [PMID: 20414115 DOI: 10.1097/MOP.0b013e32833924d2]

9 **Messroghli DR**, Pickardt T, Fischer M, Opgen-Rhein B, Papakostas K, Böcker D, Jakob A, Khalil M, Mueller GC, Schmidt F, Kaestner M, Udink Ten Cate FEA, Wagner R, Ruf B, Kiski D, Wiegand G, Degener F, Bauer UMM, Friede T, Schubert S; MYKKE Consortium. Toward evidence-based diagnosis of myocarditis in children and adolescents: Rationale, design, and first baseline data of MYKKE, a multicenter registry and study platform. *Am Heart J* 2017; **187**: 133-144 [PMID: 28454797 DOI: 10.1016/j.ahj.2017.02.027]

10 **Elamm C**, Fairweather D, Cooper LT. Pathogenesis and diagnosis of myocarditis. *Heart* 2012; **98**: 835-840 [PMID: 22442199 DOI: 10.1136/heartjnl-2012-301686]

11 **Baughman KL**. Diagnosis of myocarditis: death of Dallas criteria. *Circulation* 2006; **113**: 593-595 [PMID: 16449736 DOI: 10.1161/CIRCULATIONAHA.105.589663]

12 **Freedman SB**, Haladyn JK, Floh A, Kirsh JA, Taylor G, Thull-Freedman J. Pediatric myocarditis: emergency department clinical findings and diagnostic evaluation. *Pediatrics* 2007; **120**: 1278-1285 [PMID: 18055677 DOI: 10.1542/peds.2007-1073]

13 **Chang YJ**, Chao HC, Hsia SH, Yan DC. Myocarditis presenting as gastritis in children. *Pediatr Emerg Care* 2006; **22**: 439-440 [PMID: 16801847 DOI: 10.1097/01.pec.0000221346.64991.e7]

14 **Saji T**, Matsuura H, Hasegawa K, Nishikawa T, Yamamoto E, Ohki H, Yasukochi S, Arakaki Y, Joo K, Nakazawa M. Comparison of the clinical presentation, treatment, and outcome of fulminant and acute myocarditis in children. *Circ J* 2012; **76**: 1222-1228 [PMID: 22307381 DOI: 10.1253/circj.CJ-11-1032]

15 **Durani Y**, Egan M, Baffa J, Selbst SM, Nager AL. Pediatric myocarditis: presenting clinical characteristics. *Am J Emerg Med* 2009; **27**: 942-947 [PMID: 19857412 DOI: 10.1016/j.ajem.2008.07.032]

16 **Checchia PA**, Kulik TJ. Acute viral myocarditis: Diagnosis. *Pediatr Crit Care Me* 2006; **7**: S8 [DOI: 10.1097/01.PCC.0000244336.60719.8C]

17 **Kern J**, Modi R, Atalay MK, Kochilas LK. Clinical myocarditis masquerading as acute coronary syndrome. *J Pediatr* 2009; **154**: 612-615 [PMID: 19324224 DOI: 10.1016/j.jpeds.2008.10.018]

18 **Batra AS**, Epstein D, Silka MJ. The clinical course of acquired complete heart block in children with acute myocarditis. *Pediatr Cardiol* 2003; **24**: 495-497 [PMID: 14627323 DOI: 10.1007/s00246-002-0402-2]

19 **Ichikawa R**, Sumitomo N, Komori A, Abe Y, Nakamura T, Fukuhara J, Matsumura M, Miyashita M, Kanamaru H, Ayusawa M, Mugishima H. The follow-up evaluation of electrocardiogram and arrhythmias in children with fulminant myocarditis. *Circ J* 2011; **75**: 932-938 [PMID: 21343655 DOI: 10.1253/circj.CJ-10-0918]

20 **Balaji S**, Wiles HB, Sens MA, Gillette PC. Immunosuppressive treatment for myocarditis and borderline myocarditis in children with ventricular ectopic rhythm. *Br Heart J* 1994; **72**: 354-359 [PMID: 7833194 DOI: 10.1136/hrt.72.4.354]

21 **Dello Russo A**, Pieroni M, Santangeli P, Bartoletti S, Casella M, Pelargonio G, Smaldone C, Bianco M, Di Biase L, Bellocci F, Zeppilli P, Fiorentini C, Natale A, Tondo C. Concealed cardiomyopathies in competitive athletes with ventricular arrhythmias and an apparently normal heart: role of cardiac electroanatomical mapping and biopsy. *Heart Rhythm* 2011; **8**: 1915-1922 [PMID: 21782775 DOI: 10.1016/j.hrthm.2011.07.021]

22 **Pinamonti B**, Alberti E, Cigalotto A, Dreas L, Salvi A, Silvestri F, Camerini F. Echocardiographic findings in myocarditis. *Am J Cardiol* 1988; **62**: 285-291 [PMID: 3400607 DOI: 10.1016/0002-9149(88)90226-3]

23 **Angelini A**, Calzolari V, Calabrese F, Boffa GM, Maddalena F, Chioin R, Thiene G. Myocarditis mimicking acute myocardial infarction: role of endomyocardial biopsy in the differential diagnosis. *Heart* 2000; **84**: 245-250 [PMID: 10956283 DOI: 10.1136/heart.84.3.245]

24 **Friedrich MG**, Sechtem U, Schulz-Menger J, Holmvang G, Alakija P, Cooper LT, White JA, Abdel-Aty H, Gutberlet M, Prasad S, Aletras A, Laissy JP, Paterson I, Filipchuk NG, Kumar A, Pauschinger M, Liu P; International Consensus Group on Cardiovascular Magnetic Resonance in Myocarditis. Cardiovascular magnetic resonance in myocarditis: A JACC White Paper. *J Am Coll Cardiol* 2009; **53**: 1475-1487 [PMID: 19389557 DOI: 10.1016/j.jacc.2009.02.007]

25 **Lang RM**, Bierig M, Devereux RB, Flachskampf FA, Foster E, Pellikka PA, Picard MH, Roman MJ, Seward J, Shanewise JS, Solomon SD, Spencer KT, Sutton MS, Stewart WJ; Chamber Quantification Writing Group; American Society of Echocardiography's Guidelines and Standards Committee; European Association of Echocardiography. Recommendations for chamber quantification: a report from the American Society of Echocardiography's Guidelines and Standards Committee and the Chamber Quantification Writing Group, developed in conjunction with the European Association of Echocardiography, a branch of the European Society of Cardiology. *J Am Soc Echocardiogr* 2005; **18**: 1440-1463 [PMID: 16376782 DOI: 10.1016/j.echo.2005.10.005]

26 **Dec GW**, Waldman H, Southern J, Fallon JT, Hutter AM, Palacios I. Viral myocarditis mimicking acute myocardial infarction. *J Am Coll Cardiol* 1992; **20**: 85-89 [PMID: 1607543 DOI: 10.1016/0735-1097(92)90141-9]

27 **Hoyer MH**, Fischer DR. Acute myocarditis simulating myocardial infarction in a child. *Pediatrics* 1991; **87**: 250-253 [PMID: 1987539]

28 **Kühl U**, Pauschinger M, Bock T, Klingel K, Schwimmbeck CP, Seeberg B, Krautwurm L, Poller W, Schultheiss HP, Kandolf R. Parvovirus B19 infection mimicking acute myocardial infarction. *Circulation* 2003; **108**: 945-950 [PMID: 12925460 DOI: 10.1161/01.CIR.0000085168.02782.2C]

29 **Drossner DM**, Hirsh DA, Sturm JJ, Mahle WT, Goo DJ, Massey R, Simon HK. Cardiac disease in pediatric patients presenting to a pediatric ED with chest pain. *Am J Emerg Med* 2011; **29**: 632-638 [PMID: 20627219 DOI: 10.1016/j.ajem.2010.01.011]

30 **Lurz P**, Eitel I, Adam J, Steiner J, Grothoff M, Desch S, Fuernau G, de Waha S, Sareban M, Luecke C, Klingel K, Kandolf R, Schuler G, Gutberlet M, Thiele H. Diagnostic performance of CMR imaging compared with EMB in patients with suspected myocarditis. *JACC Cardiovasc Imaging* 2012; **5**: 513-524 [PMID: 22595159 DOI: 10.1016/j.jcmg.2011.11.022]

31 **Smith SC**, Ladenson JH, Mason JW, Jaffe AS. Elevations of cardiac troponin I associated with myocarditis. Experimental and clinical correlates. *Circulation* 1997; **95**: 163-168 [PMID: 8994432 DOI: 10.1016/S1062-1458(97)83068-1]

32 **Lippi G**, Salvagno GL, Guidi GC. Cardiac troponins in pediatric myocarditis. *Pediatrics* 2008; **121**: 864; author reply 864-864; author reply 865 [PMID: 18381554 DOI: 10.1542/peds.2008-0031]

33 **Koulouri S**, Acherman RJ, Wong PC, Chan LS, Lewis AB. Utility of B-type natriuretic peptide in differentiating congestive heart failure from lung disease in pediatric patients with respiratory distress. *Pediatr Cardiol* 2004; **25**: 341-346 [PMID: 15054559 DOI: 10.1007/s00246-003-0578-0]

34 **Welisch E**, Norozi K, Rauch R. N-terminal pro-brain natriuretic peptide level as a screening tool for cardiac involvement in paediatric diseases of extracardiac origin. *Clin Res Cardiol* 2011; **100**: 723-730 [PMID: 21487941 DOI: 10.1007/s00392-011-0317-0]

35 **Hammerer-Lercher A**, Geiger R, Mair J, Url C, Tulzer G, Lechner E, Puschendorf B, Sommer R. Utility of N-terminal pro-B-type natriuretic peptide to differentiate cardiac diseases from noncardiac diseases in young pediatric patients. *Clin Chem* 2006; **52**: 1415-1419 [PMID: 16690739 DOI: 10.1373/clinchem.2005.060608]

P- Reviewer: Karatza AA, Ciccone MM

S- Editor: Dou Y **L- Editor:** Filipodia **E- Editor:** Bian YN

World Journal of Clinical Cases

Submit a Manuscript: https://www.f6publishing.com

World J Clin Cases 2019 March 6; 7(5): 562-571

DOI: 10.12998/wjcc.v7.i5.562

ISSN 2307-8960 (online)

ORIGINAL ARTICLE

Observational Study

Safety of an improved patent ductus arteriosus occluder for transcatheter closure of perimembranous ventricular septal defects with abnormally attached tricuspid chordae tendineae

Lu He, Ya-Juan Du, Ge-Sheng Cheng, Yu-Shun Zhang

ORCID number: Lu He (0000-0003-0149-0606); Ya-Juan Du (0000-0003-3985-1649); Ge-Sheng Cheng (0000-0002-4605-2696); Yu-Shun Zhang (0000-0002-6395-2768).

Author contributions: He L and Zhang YS contributed to study concept and design; Du YJ and Cheng GS contributed to data analysis and interpretation and critical revision of the article; He L contributed to drafting of the article; all the authors read and approved the final manuscript.

Institutional review board statement: The study was approved by the ethics committee of Xi'an Jiaotong University Medical College First Affiliated Hospital (Xi'an, China).

Informed consent statement: All patients gave informed consent.

Conflict-of-interest statement: None.

STROBE statement: The authors have read the STROBE Statement-checklist of items, and the manuscript was prepared and revised according to the STROBE Statement-checklist of items.

Open-Access: This article is an open-access article which was selected by an in-house editor and fully peer-reviewed by external reviewers. It is distributed in accordance with the Creative Commons Attribution Non Commercial (CC BY-NC 4.0) license, which permits others to

Lu He, Ya-Juan Du, Ge-Sheng Cheng, Yu-Shun Zhang, Department of Structural Heart Disease, Xi'an Jiaotong University Medical College First Affiliated Hospital, Xi'an 710061, Shaanxi Province, China

Corresponding author: Yu-Shun Zhang, MD, PhD, Professor, Department of Structural Heart Disease, Xi'an Jiaotong University Medical College First Affiliated Hospital, 277 Yanta West Road, Xi'an 710061, Shaanxi Province, China. zys2889@sina.com
Telephone: +86-29-85324078
Fax: +86-29-85324078

Abstract

BACKGROUND

The off-label use of various devices has been reported for the transcatheter closure of perimembranous ventricular septal defects (PmVSD) because of serious complications, such as heart block and tricuspid regurgitation (TR), associated with conventional ventricular septal defect devices. However, whether certain defects such as PmVSD with abnormally attached tricuspid are fit for interventional treatment is still disputable.

AIM

To explore the feasibility and safety of transcatheter closure of PmVSD with abnormally attached tricuspid chordae tendineae using an improved patent ductus arteriosus (PDA) occluder.

METHODS

We retrospectively analyzed 20 patients diagnosed with PmVSD with abnormally attached tricuspid chordae tendineae who underwent interventional treatment using an improved PDA occluder at our center from January 2012 to January 2016. Baseline characteristics and procedural and follow-up data were analyzed.

RESULTS

All 20 patients achieved procedure success. No heart block occurred during the operation. One patient had a transient complete right bundle branch block within 48 h post-procedure and reverted to normal rhythm after intravenous injections of dexamethasone for 3 d. For all 20 patients, no residual shunt was observed by transthoracic echocardiography post-procedure. During the average follow-up period of 2.4 years, no severe TR was observed.

distribute, remix, adapt, build upon this work non-commercially, and license their derivative works on different terms, provided the original work is properly cited and the use is non-commercial. See: http://creativecommons.org/licenses/by-nc/4.0/

Manuscript source: Unsolicited manuscript

Received: December 22, 2018
Peer-review started: December 23, 2018
First decision: December 29, 2018
Revised: January 13, 2019
Accepted: January 29, 2019
Article in press: January 30, 2019
Published online: March 6, 2019

CONCLUSION
Using of the improved PDA occluder for the transcatheter closure of PmVSD with abnormally attached tricuspid chordae tendineae is a safe and promising treatment option. However, long-term follow-up in a large group of patients is still warranted.

Key words: Ventricular septal defect; Transcatheter; Patent ductus arteriosus occlude; Tricuspid regurgitation; Chordae tendineae

©The Author(s) 2019. Published by Baishideng Publishing Group Inc. All rights reserved.

Core tip: The aim of this study was to explore the feasibility and safety of transcatheter closure of perimembranous ventricular septal defects (PmVSD) with abnormally attached tricuspid chordae tendineae using an improved PDA occluder. A total of 20 patients diagnosed with PmVSD with abnormally attached tricuspid chordae tendineae who underwent interventional treatment using the improved patent ductus arteriosus (PDA) occluder were observed. All 20 patients achieved procedure success, and no residual shunt or severe tricuspid regurgitation was observed. Our study suggested that using of the improved PDA occluder for the transcatheter closure of PmVSD with abnormally attached tricuspid chordae tendineae is a safe and promising treatment option.

Citation: He L, Du YJ, Cheng GS, Zhang YS. Safety of an improved patent ductus arteriosus occluder for transcatheter closure of perimembranous ventricular septal defects with abnormally attached tricuspid chordae tendineae. *World J Clin Cases* 2019; 7(5): 562-571
URL: https://www.wjgnet.com/2307-8960/full/v7/i5/562.htm
DOI: https://dx.doi.org/10.12998/wjcc.v7.i5.562

INTRODUCTION

Transcatheter interventional therapy for certain types of perimembranous ventricular septal defects (PmVSD) is a substitute for surgical treatment. However, post-procedure complications of interventional therapy such as heart block[1-4] and tricuspid regurgitation (TR)[5,6] are often reported and appear serious, thus limiting the clinical application of this procedure. Furthermore, PmVSD are not infrequently complicated by the presence of aneurysmal fibrous tissue from the septal leaflet of the tricuspid valve, making the use of the device technically challenging and increasing the potential risk of inducing increased tricuspid insufficiency[7].

In some countries, such as China and India, tens of thousands of patients diagnosed with PmVSD are treated by transcatheter closure each year. However, with the increase in the number of interventional treatments, tricuspid insufficiency has been observed during follow-up. Although epidemiological data are lacking, these problems are not less serious than heart block. Some cases even require surgery to repair the tricuspid valve. Because the bilateral disc of the traditional symmetrical ventricular septal defect occluder is 2 mm longer than the waist, it is generally believed that interventional therapy is feasible when the attachment point of the tricuspid chordae tendineae to the defect on the right ventricular (RV) side is greater than 2 mm. However, during follow-up, after using of the traditional symmetrical occluder, tricuspid chordae tendineae rupture[6,8,9] or tricuspid valve stenosis[10,11] caused by the compression of the RV disc may occur even if the attachment point of the tricuspid chordae tendineae to the defect on the RV side is greater than 2 mm.

Using of the Amplatzer ductus occluder (ADO) in transcatheter closure of PmVSD has also been reported[12-14]. Because the ADO has no RV disc, theoretically, there is no special requirement for the distance between the attachment point of the tricuspid chordae tendineae and the RV side of the defect. Thus, the ADO can maximally avoid abrasion of the tricuspid chordae tendineae by the RV disc. However, the ADO has a longer waist (5-8 mm) than the traditional symmetrical VSD occluder. After occluder implantation, the waist will become longer because of the squeezing effect of the surrounding tissue. This longer waist may compress the tricuspid chordae tendineae, resulting in a moderate to large amount of TR. For patients diagnosed with PmVSD with abnormally attached tricuspid chordae tendineae, the indications for

interventional treatment and the most appropriate type of occluder remain controversial. Therefore, in the present study, we used an improved patent ductus arteriosus (PDA) occluder, which has no RV disc and a shorter waist, to explore the feasibility and safety of transcatheter closure of PmVSD with abnormally attached tricuspid chordae tendineae.

MATERIALS AND METHODS

Study population

Between January 2012 and January 2016, 360 cases of PmVSD received interventional therapy at the First Affiliated Hospital of Xi'an Jiaotong University. Among these cases, 20 with abnormally attached tricuspid chordae tendineae were selected for inclusion in a retrospective analysis based on transthoracic echocardiography (TTE). According to TTE findings, abnormally attached tricuspid chordae tendineae was defined by a distance of the attachment point of the tricuspid chordae tendineae to the defect on the RV side of 1-2 mm. This study was approved by the Regional Ethics Committee of our hospital, all patients or their parents signed informed consent, and patient anonymity was preserved.

Echocardiography

A GE-ViVid-E9 color Doppler ultrasound system (General Electric Corporation, Norfolk, Virginia) equipped with a 2-4 MHz transducer was used to perform TTE. All patients underwent TTE before the procedure. TTE was performed in the apical 5-chamber, long-axis, and short-axis parasternal view. The VSD sizes measured by TTE were 5.0-10.0 mm on the left ventricular (LV) side and 2.5-5.5 mm on the RV side. The ventricular septal rim below the aortic valve was 3.0-5.0 mm, and the distance of the attachment point of the tricuspid chordae tendineae to the defect on the RV side was 1.0-2.0 mm (Figures 1 and 2). Among the 20 patients, the attachment point of the tricuspid chordae tendineae was close to the inferior edge of the defect in 13 (65.0%) patients and close to the superior edge of the defect in 7 (35.0%).

The grading of TR has been well described previously[15]. The majority of parameters are qualitative or semiquantitative. Minor TR is defined as a small, central jet (usually < 4 cm^2 or < 20% of the right atrial area), moderate TR defined as a moderate central jet (usually 4-10 cm^2 or 20%-40% of the right atrial area), and severe TR as a large central jet (usually > 10 cm^2 or > 40% of the right atrial area).

Description of the improved PDA occluder

This study used an improved PDA occluder (Starway Medical Technology, Inc., Beijing, China), which is based on the ADO. The improved PDA occluder has no RV disc; the edge of the LV disc is 2 mm, and the waist is 5 mm. The shape of the occluder is similar to that of the ADO, but the waist is shorter, consistent with the designation of this device as the "improved PDA occlude". The size of the device is ranging from 6 to 12 mm. Figure 3 shows a schematic diagram of the improved PDA occluder and its advantages for the interventional therapy of PmVSD with abnormally attached tricuspid chordae tendineae.

Catheterization and device implantation technique

All patients received antibiotics 1 h before the procedure. The procedure was performed under 2% lidocaine local anesthesia for patients over 7 years of age, whereas general anesthesia with ketamine was used for patients under 7 years of age. Fluoroscopy was used to guide the device implantation only. The right femoral vein and artery were accessed, and heparin was administered according to the patient's body weight (80-100 IU/kg). Right and left cardiac catheterization was performed to evaluate the pulmonary vascular resistance. Hemodynamic parameters, including pulmonary arterial, aortic, atrial, and ventricular pressures, were recorded. Oximetric values were measured in the cardiac chambers and vessels and used to calculate Qp/Qs. Angiography in a single plane (45°-60° left anterior oblique/10°-25° cranial view) was performed to define the location and size of the VSD. Figure 4 shows left ventricle angiography performed before and after the procedure. Angiography of the ascending aorta was also performed in a 50° left atrial oblique view to check for aortic regurgitation (AR).

The technique of PmVSD closure was described in detail elsewhere[9]. An appropriately sized device (> 1-3 mm based on the defect size determined by TTE or angiography) was selected. The device was released when its proper position was obtained (left ventriculography was performed to confirm the proper position of the occluder) and interference with the aortic and tricuspid valve had been excluded (TTE confirmed the absence of AR and TR).

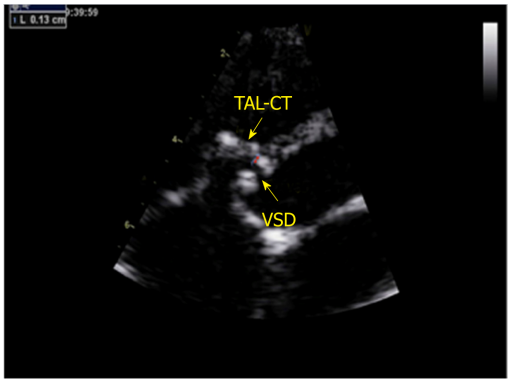

Figure 1 Non-standard aortic short-axis view. The red arrow shows the distance (1.3 mm) from the attachment point of the tricuspid anterior leaflet chordae tendineae to the inferior edge of the right ventricular side. TAL-CT: Tricuspid anterior leaflet chordae tendineae; VSD: Ventricular septal defects.

Follow-up protocol

After the procedure, one dose of antibiotic therapy was administered intravenously to prevent infective endocarditis. Holter monitoring was performed for one day, followed by electrocardiography performed daily before discharge. Patients were typically discharged 5 d after the procedure. Aspirin (3-5 mg/kg daily) was administered to all patients for 6 mo after the procedure. Clinical examination, TTE, and chest X-ray were performed before discharge, 1, 3, 6, and 12 mo post-procedure, and yearly thereafter.

Data analysis

The data analyses were performed using SPSS version 19.0. Summary statistics for normally distributed quantitative variables are expressed as the mean ± SD. For non-normally distributed variables, we use median and interquartile range (IQR). Categorical data are summarized as count and percentages. The objective of this article was to present the early experience with the improved PDA occluder for the interventional treatment of PmVSD with abnormally attached tricuspid chordae tendineae in a single-arm, single-center study; therefore, statistical comparisons between groups were not performed.

RESULTS

Patient characteristics

From January 2012 to January 2016, 360 patients diagnosed with PmVSD received interventional therapy at our center. We performed a retrospective analysis of 20 patients with abnormally attached tricuspid chordae tendineae selected by TTE.

The 20 patients included 12 males and 8 females with an age range of 4 to 52 (20.7 ± 12.3) years and a weight range of 15.5 to 83 (50.1 ± 17.5) kg. Among the 20 patients, 5 (25.0%) had a membranous VSD. The VSD size measured by TTE was 5.0-10.0 (7.3 ± 1.5) mm on the LV side and 2.5-5.5 (3.9 ± 0.8) mm on the RV side. The VSD size measured by angiography was 4.0-10.0 (6.7 ± 1.5) mm on the LV side and 2.5-4.5 (3.5 ± 0.6) mm on the RV side. The ventricular septal rim below the aortic valve was 3.0-5.0 (median 4.0) mm, and the attachment point of the tricuspid chordae tendineae to the defect on the RV side was 1.0-2.0 (median 1.8) mm. The attachment point of the tricuspid chordae tendineae was close to the inferior edge of the defect in 13 (65.0%) patients but was close to the superior edge of the defect in 7 (35.0%). One (5.0%) patient had minor AR, and one (5.0%) had minor TR. The average follow-up was 2.4 years. The baseline parameters and TTE data evaluated are listed in Table 1.

Procedural and follow-up data

Procedure success, defined as the ability to release the device without embolization or heart block during the procedure, was achieved in all 20 patients (100.0%). The 6 mm improved PDA occluder was implanted in 3 (15.0%) patients, 7 mm in 3 (15.0%), 8 mm in 5 (25.0%), 9 mm in 5 (25.0%), 10 mm in 3 (15.0%) and, 12 mm in 1 (5.0%). The average operation time was 49.3 ± 6.0 min, and the average fluoroscopy time was 24.3 ± 2.8 min.

No serious arrhythmia occurred during the procedure. One (5.0%) case of complete right bundle branch block occurred within 48 h after the procedure and reverted to

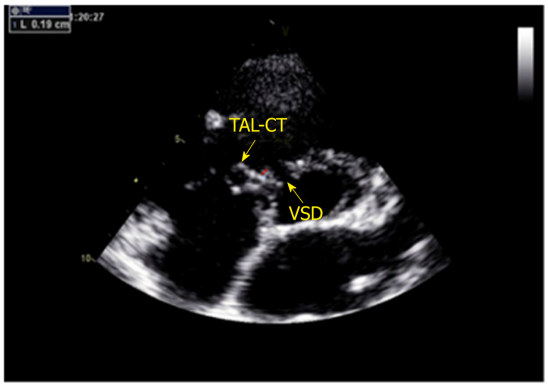

Figure 2 Non-standard aortic short-axis view. The red arrow shows the distance (1.9 mm) from the attachment point of the tricuspid septal leaflet chordae tendineae to the superior edge of the right ventricular side. TSL-CT: Tricuspid septal leaflet chordae tendineae; VSD: Ventricular septal defects.

normal rhythm after intravenous injections of dexamethasone for 3 d. At follow-ups 1, 3, 6, and 12 mo after the procedure and yearly thereafter, no serious new arrhythmia was found in any of the patients.

TTE was performed 48 h after occluder implantation. For all 20 patients, no residual shunt was observed by TTE post-procedure. Following the procedure, TR was increased in one (5.0%) patient (minor regurgitation). At follow-ups 1, 3, 6, and 12 mo after the procedure and yearly thereafter, one patient with aggravated TR exhibited no obvious change. No deaths occurred after the procedure. No AR was observed. The procedural and follow-up data are listed in Table 2.

DISCUSSION

Although the off-label use of a number of different devices, such as ADO, ADO II, and Amplatzer Vascular Plug I[10,14,16], has been described for interventional therapy of PmVSD, there is still controversy regarding whether PmVSD with abnormally attached tricuspid chordae tendineae is suitable for interventional therapy.

The most remarkable discovery from our study includes the high success rate of the procedure (100%), the ability to close moderately large defects up to 10 mm, and the absence of severe TR during or after the procedure. There was only one case of complete right bundle branch block within 48 h after the procedure, which reverted to normal rhythm after intravenous injections of dexamethasone for 3 d. Late-onset complete heart block was not observed for any of the 20 patients on routine follow-up through 2 years after the procedure.

Combined with initial 2 years of our experience with the closure of certain PmVSD, we tended to use ADO. Based on several heartening reports from other centers and our own experience, we put this change into practice[12,14,17,18]. However, during follow-up, moderate-to-severe TR occurred in some patients in the immediate or early postoperative period. We propose that when the attachment point of the tricuspid chordae tendineae is close to the defect on the RV side or when the occluder rim is adjacent to the chordae tendineae, the sharp rim of the RV disc can wear the chordae tendineae and increase the likelihood of iatrogenic TR. Additionally, the strain produced by the septum to the waist of the occluder may have an impact on the tricuspid valve and potentially cause TR or tricuspid valve rupture.

The bilateral disc rim of the symmetric PmVSD occluder is 2 mm longer than the waist; when an appropriately sized device (> 1-3 mm, based on the defect size measured by TTE or angiography) is selected, the actual condition of the occluder is in compression by the surrounding tissue of the defect. Therefore, the rims of the RV and LV discs are larger than 2 mm. Thus, the RV disc is longer, and the sharp rim of the RV disc can wear the chordae tendineae and increase the likelihood of iatrogenic TR. To prevent such damage, Lee *et al*[12] used ADO to treat 20 cases of PmVSD in South Korea. The ADO was successfully implanted in all patients without any significant complications[12]. Because the ADO has no RV disc, extrusion or abrasion of the tricuspid chordae tendineae is less likely to happen. However, the waist of the ADO is 6-8 mm, which will increase after occluder implantation due to extrusion of the surrounding tissue. The increased length of the waist may have an impact on the tricuspid valve and potentially cause severe TR or tricuspid valve rupture.

The risk of waist compression or erosion of the tricuspid valve is even greater for

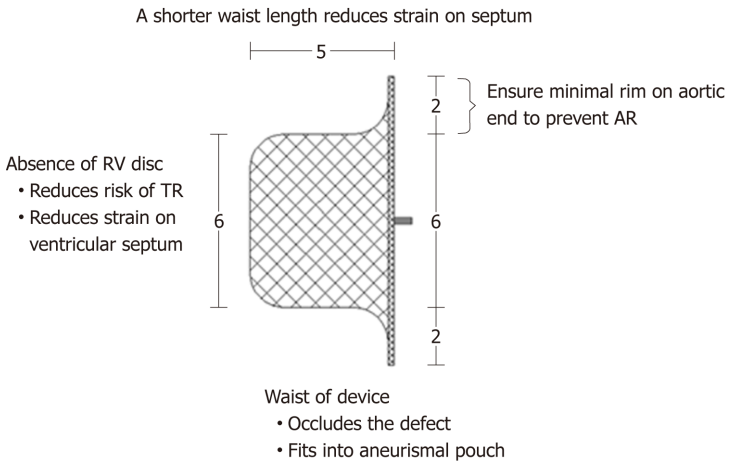

Figure 3 The improved patent ductus arteriosus occluder (6 mm) and its advantages for the closure of perimembranous ventricular septal defects with abnormally attached tricuspid chordae tendineae. RV: Right ventricular; TR: Tricuspid regurgitation; AR: Aortic regurgitation.

PmVSD with abnormally attached tricuspid chordae tendineae. Based on previous research results, the special improved PDA occluder, which has no RV disc and a shorter waist, was used in the present study (its advantages for the closure of PmVSD with abnormally attached tricuspid chordae tendineae are shown in Figure 1). After occluder implantation, the tissue surrounding the defect compresses the occluder. The RV disc of the occluder can then form a smooth edge, and the stretched length of the waist is far shorter than the waist of the ADO. Therefore, abrasion of the RV disc and an excessively long waist on the chordae tendineae are avoided.

In this study, procedure success was achieved in all 20 patients diagnosed with PmVSD with abnormally attached tricuspid chordae tendineae who underwent interventional treatment using the improved PDA occluder. No residual shunt was found by left ventriculography, and no AR was found by ascending aortic angiography immediately after the procedure. These outcomes may be attributable to the use of the improved PDA occluder, which has a short rim (2 mm) in the distal part. This rim is intended to be implanted in the space between the right coronary cusp and non-coronary cusp of the aortic valve and thus is unlikely to touch the aortic valve, protecting it from AR. No severe arrhythmia occurred in any patient during or after the procedure. Complete right bundle branch block occurred in one patient and reverted to normal rhythm. Complete right bundle branch block may have occurred because there was less contact with the left bundle branch than with the VSD occluder due to the shorter rim. The other crucial advantage of the improved PDA occluder is that it does not have a proximal disc and thus does not squeeze the His bundle.

Following the procedure, TR was increased in one patient (minor regurgitation) after the procedure. At the follow-up visits 1, 3, 6, and 12 mo after device implantation and yearly thereafter, one patient with aggravated TR exhibited no obvious change. This patient was 4 years old, and the defect was relatively large. Angiography showed a defect size of 9 mm on the LV side and 3.5 mm on the RV side, and an improved 10 mm PDA occluder was placed. The postoperative TTE examination revealed that the occluder had no cutting action on the tricuspid chordae tendineae because it had no RV disc. However, the occluder was relatively large and had a longer waist, so the RV disc compressed the chordae tendineae, thus causing TR. This result suggests that for large defects, especially for the relatively weak endocardial tissue and abnormally attached tricuspid chordae tendineae of pediatric patients, interventional treatment should be performed with caution. In these cases, the use of the improved PDA occluder with the shorter waist should be considered, which highlights the fact that the interventional therapy of PmVSD should follow the principle of individualization. The choice of occluder should depend on the defect size, morphology, and clinical features.

The results after an average follow-up of 2.4 years showed that the improved PDA device can be used in the interventional therapy of PmVSD with abnormally attached tricuspid chordae tendineae. The immediate and short-term curative effect was reliable, and no serious TR or other complications were observed.

In conclusion, although there is a concern that the improved PDA occluder is not designed for the interventional therapy of PmVSD, the improved PDA occluder might provide a valid and secure option in selected patients with abnormally attached

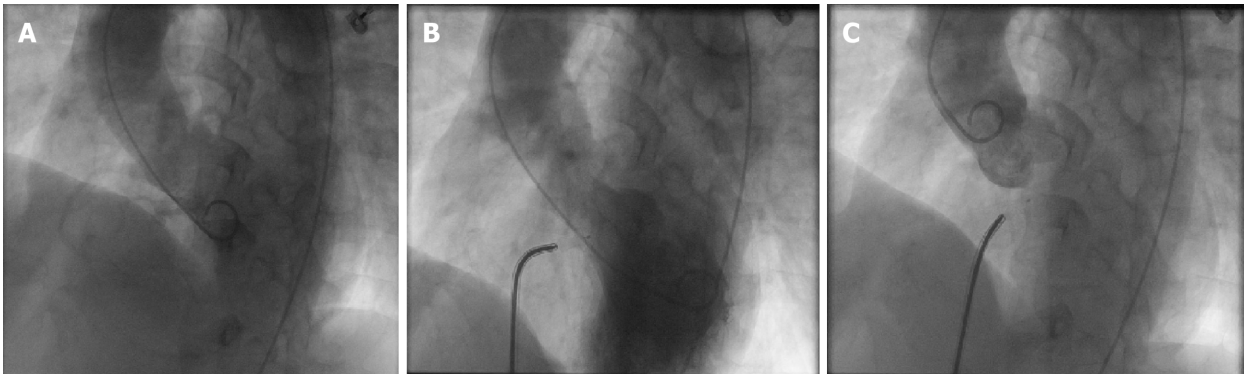

Figure 4 Left ventricle angiography performed before and after the procedure. A: Left ventricle angiography before the procedure showed perimembranous ventricular septal defects, the diameter of left ventricular side was about 8 mm, and right ventricular side was multiple-outlet with a diameter of about 1.5-2.5 mm; B: Left ventricle angiography after the procedure; C: Angiography of the ascending aorta after the procedure showed that there was no aortic insufficiency.

tricuspid chordae tendineae. The availability of the improved PDA occluder might allow a wider range of interventional therapy of PmVSD. However, longer follow-up in a large number of population is still warranted.

Table 1 Baseline characteristics and transthoracic echocardiography data of patients

Patients, *n*	20
Sex (M/F), *n* (%)	11 (55)/9 (45)
Age, yr, mean ± SD	20.7 ± 12.3
Weight, kg, mean ± SD	50.1 ± 17.5
Chest radiography	
Cardiomegaly, *n* (%)	8 (40.0)
Increased vascularity, *n* (%)	16 (80.0)
Echocardiography	
Defect size on LV side, mm, mean ± SD	7.3 ± 1.5
Defect size on RV side, mm, mean ± SD	3.9 ± 0.8
MVSA, *n* (%)	5 (25.0)
Ventricular septal rim below the aortic valve, mm, median (IQR)	4.0 (1.4)
Attachment point of the tricuspid chordae tendineae to the defect on RV side, mm, median (IQR)	1.8 (0.5)
Minor AR, *n* (%)	1 (5.0)
Minor TR, *n* (%)	1 (5.0)
Follow-up, yr, mean ± SD	2.4 ± 1.0

M: Male; F: Female; SD: Standard deviation; LV: Left ventricular; RV: Right ventricular; MVSA: Membranous ventricular septal aneurysm; IQR: Interquartile range; AR: Aortic regurgitation; TR: Tricuspid regurgitation.

Table 2 Procedural characteristics and post-procedural findings

Angiography	
Defect size on LV side, mm, mean ± SD	6.7 ± 1.5
Defect size on RV side, mm, mean ± SD	3.5 ± 0.6
Routine right and left heart catheterization	
sPAP, mmHg, mean ± SD	31.4 ± 4.4
mPAP, mmHg, mean ± SD	19.6 ± 3.6
Qp/Qs, mean ± SD	2.3 ± 0.4
Occluder size, *n* (%)	
6 mm	3 (15.0)
7 mm	3 (15.0)
8 mm	5 (25.0)
9 mm	5 (25.0)
10 mm	3 (15.0)
12 mm	1 (5.0)
Average operative time, min, mean ± SD	49.3 ± 6.0
Average fluoroscopy time, min, mean ± SD	24.3 ± 2.8
Post-procedural complications, *n* (%)	
CRBBB (transient)	1 (5.0)
Increased TR, *n* (%)	1 (5.0)
Sheath, Fr, median (IQR)	8.0 (2.0)

LV: Left ventricular; RV: Right ventricular; SD: Standard deviation; sPAP: Systolic pulmonary artery pressure; mPAP: Mean pulmonary artery pressure; Qp/Qs: Pulmonary-to-systemic flow ratio; CRBBB: Complete right bundle branch block; TR: Tricuspid regurgitation; IQR: Interquartile range.

ARTICLE HIGHLIGHTS

Research background

Whether certain defects such as perimembranous ventricular septal defects (PmVSD) with abnormally attached tricuspid chordae tendineae are fit for interventional treatment is still disputable. We explored the feasibility and safety of transcatheter closure of PmVSD with abnormally attached tricuspid chordae tendineae using an improved patent ductus arteriosus (PDA) occluder through an observational, single-center study.

Research motivation
The off-label use of various devices has been reported for the transcatheter closure of PmVSD because of serious complications, such as heart block and tricuspid regurgitation, associated with conventional ventricular septal defect devices. However, whether PmVSD with abnormally attached tricuspid chordae tendineae are suitable for interventional treatment has rarely been reported. Therefore, this study hopes to provide guidance for the choice of occluder which can be used in such defects. That might allow a wider range of interventional therapy of PmVSD.

Research objectives
The research objective of this study was to explore the feasibility and safety of transcatheter closure of PmVSD with abnormally attached tricuspid chordae tendineae using an improved PDA occluder.

Research methods
We retrospectively analyzed 20 patients diagnosed with PmVSD with abnormally attached tricuspid chordae tendineae who underwent interventional treatment using an improved PDA occluder at our center from January 2012 to January 2016. Baseline characteristics and procedural and follow-up data were analyzed. This study is a single-center, non-randomized, observational study.

Research results
Our research found that the improved PDA occluder might provide an valid and secure option in selected patients diagnosed with PmVSD with abnormally attached tricuspid chordae tendineae. Given its nature, the present study shares all of the limitations of observational studies. In our study, the mean follow-up time was only 2.4 years. Although the major complications of PmVSD closure usually appears within this time frame, the results may have been affected. The small sample size is another limitation of this study.

Research conclusions
In this single-center, non-randomized, observational study cohort, despite its small sample size, our study suggests that using of the improved PDA occluder for the transcatheter closure of PmVSD with abnormally attached tricuspid chordae tendineae is a safe and promising treatment option. The availability of the improved PDA occluder might allow a wider range of interventional therapy of PmVSD.

Research perspectives
We used the improved PDA occluder for transcatheter closure of PmVSD with abnormally attached tricuspid chordae tendineae as a breakthrough point, and concluded that using of the improved PDA occluder for the transcatheter closure of PmVSD with abnormally attached tricuspid chordae tendineae is a safe and promising treatment option. However, the number of patients is too small, and the single-center observational study still has its own shortcomings. So we still believe that the highest level of evidence in clinical studies is a multi-center, prospective, randomized controlled study.

REFERENCES

1 **Zhou T**, Shen XQ, Zhou SH, Fang ZF, Hu XQ, Zhao YS, Qi SS, Zhou Z, Li J, Lv XL. Atrioventricular block: a serious complication in and after transcatheter closure of perimembranous ventricular septal defects. *Clin Cardiol* 2008; **31**: 368-371 [PMID: 18727001 DOI: 10.1002/clc.20243]

2 **Wei Y**, Wang X, Zhang S, Hou L, Wang Y, Xu Y, Sun Q, Zhao H. Transcatheter closure of perimembranous ventricular septal defects (VSD) with VSD occluder: early and mid-term results. *Heart Vessels* 2012; **27**: 398-404 [PMID: 21618026 DOI: 10.1007/s00380-011-0153-1]

3 **Pedra CA**, Pedra SR, Esteves CA, Pontes SC, Braga SL, Arrieta SR, Santana MV, Fontes VF, Masura J. Percutaneous closure of perimembranous ventricular septal defects with the Amplatzer device: technical and morphological considerations. *Catheter Cardiovasc Interv* 2004; **61**: 403-410 [PMID: 14988905 DOI: 10.1002/ccd.10797]

4 **Butera G**, Carminati M, Chessa M, Piazza L, Micheletti A, Negura DG, Abella R, Giamberti A, Frigiola A. Transcatheter closure of perimembranous ventricular septal defects: early and long-term results. *J Am Coll Cardiol* 2007; **50**: 1189-1195 [PMID: 17868812 DOI: 10.1016/j.jacc.2007.03.068]

5 **Carminati M**, Butera G, Chessa M, De Giovanni J, Fisher G, Gewillig M, Peuster M, Piechaud JF, Santoro G, Sievert H, Spadoni I, Walsh K; Investigators of the European VSD Registry. Transcatheter closure of congenital ventricular septal defects: results of the European Registry. *Eur Heart J* 2007; **28**: 2361-2368 [PMID: 17684082 DOI: 10.1093/eurheartj/ehm314]

6 **Xu XD**, Liu SX, Bai Y, Zhang M, Zhao XX, Qin YW. Decreased tricuspid regurgitation following percutaneous closure of congenital perimembranous ventricular septal defect: immediate and 6-month echocardiographic assessment. *Heart Vessels* 2015; **30**: 611-617 [PMID: 24946869 DOI: 10.1007/s00380-014-0531-6]

7 **Anderson RH**, Wilcox BR. The surgical anatomy of ventricular septal defect. *J Card Surg* 1992; **7**: 17-35 [PMID: 1554976 DOI: 10.1111/j.1540-8191.1992.tb00773.x]

8 **Mertens L**, Meyns B, Gewillig M. Device fracture and severe tricuspid regurgitation after percutaneous closure of perimembranous ventricular septal defect: a case report. *Catheter Cardiovasc Interv* 2007; **70**: 749-753 [PMID: 17563097 DOI: 10.1002/ccd.21198]

9 **Fu YC**, Bass J, Amin Z, Radtke W, Cheatham JP, Hellenbrand WE, Balzer D, Cao QL, Hijazi ZM. Transcatheter closure of perimembranous ventricular septal defects using the new Amplatzer membranous VSD occluder: results of the U.S. phase I trial. *J Am Coll Cardiol* 2006; **47**: 319-325 [PMID: 16412854

DOI: 10.1016/j.jacc.2005.09.028]
10 **Arora R**, Trehan V, Kumar A, Kalra GS, Nigam M. Transcatheter closure of congenital ventricular septal defects: experience with various devices. *J Interv Cardiol* 2003; **16**: 83-91 [PMID: 12664821 DOI: 10.1046/j.1540-8183.2003.08006.x]
11 **Christiani LA**, Bergman F, Tress JC, Vanzillotta PP, Pedra CA. Severe tricuspid stenosis during percutaneous occlusion of perimembranous ventricular septal defect with the new Amplatzer device. *Congenit Heart Dis* 2006; **1**: 239-243 [PMID: 18377532 DOI: 10.1111/j.1747-0803.2006.00042.x]
12 **Lee SM**, Song JY, Choi JY, Lee SY, Paik JS, Chang SI, Shim WS, Kim SH. Transcatheter closure of perimembranous ventricular septal defect using Amplatzer ductal occluder. *Catheter Cardiovasc Interv* 2013; **82**: 1141-1146 [PMID: 23554093 DOI: 10.1002/ccd.24810]
13 **Mahimarangaiah J**, Subramanian A, Kikkeri Hemannasetty S, Chandra S, Karur S, Mandikal Kodandaramasastry U, Cholenahally Nanjappa M. Transcatheter closure of perimembranous ventricular septal defects with ductal occluders. *Cardiol Young* 2015; **25**: 918-926 [PMID: 25022868 DOI: 10.1017/S1047951114001255]
14 **El Said HG**, Bratincsak A, Gordon BM, Moore JW. Closure of perimembranous ventricular septal defects with aneurysmal tissue using the Amplazter Duct Occluder I: lessons learned and medium term follow up. *Catheter Cardiovasc Interv* 2012; **80**: 895-903 [PMID: 22907908 DOI: 10.1002/ccd.23074]
15 **Zoghbi WA**, Enriquez-Sarano M, Foster E, Grayburn PA, Kraft CD, Levine RA, Nihoyannopoulos P, Otto CM, Quinones MA, Rakowski H, Stewart WJ, Waggoner A, Weissman NJ; American Society of Echocardiography. Recommendations for evaluation of the severity of native valvular regurgitation with two-dimensional and Doppler echocardiography. *J Am Soc Echocardiogr* 2003; **16**: 777-802 [PMID: 12835667 DOI: 10.1016/S0894-7317(03)00335-3]
16 **Michel-Behnke I**, Le TP, Waldecker B, Akintuerk H, Valeske K, Schranz D. Percutaneous closure of congenital and acquired ventricular septal defects--considerations on selection of the occlusion device. *J Interv Cardiol* 2005; **18**: 89-99 [PMID: 15882154 DOI: 10.1111/j.1540-8183.2005.04051.x]
17 **Dilawar M**, Numan M, El-Sisi A, Gendi SM, Ahmad Z. Percutaneous closure of ventricular septal defect associated with tunnel-shaped aneurysm using the Amplatzer duct occluder. *Pediatr Cardiol* 2008; **29**: 366-370 [PMID: 17952490 DOI: 10.1007/s00246-007-9092-0]
18 **Tan CA**, Levi DS, Moore JW. Percutaneous closure of perimembranous ventricular septal defect associated with a ventricular septal aneurysm using the Amplatzer ductal occluder. *Catheter Cardiovasc Interv* 2005; **66**: 427-431 [PMID: 16208699 DOI: 10.1002/ccd.20499]

P- Reviewer: Arroyo-Martinez Q, Fekaj E
S- Editor: Ji FF **L- Editor:** Wang TQ **E- Editor:** Bian YN

World Journal of Clinical Cases

Submit a Manuscript: https://www.f6publishing.com

World J Clin Cases 2019 March 6; 7(5): 572-584

DOI: 10.12998/wjcc.v7.i5.572

ISSN 2307-8960 (online)

META-ANALYSIS

Adiponectin gene polymorphisms and risk of gestational diabetes mellitus: A meta-analysis

Lin-Ting Huang, Shi-Lan Wu, Xin Liao, Shu-Juan Ma, Hong-Zhuan Tan

ORCID number: Lin-Ting Huang (0000-0002-7352-9832); Shi-Lan Wu (0000-0003-0473-1313); Xin Liao (0000-0002-9640-8638); Shu-Juan Ma (0000-0002-7858-067X); Hong-Zhuan Tan (0000-0002-4292-5947).

Author contributions: Huang LT conceived the study, acquired, analyzed, and interpreted the data, and drafted the manuscript; Wu SL and Xin L acquired, analyzed, and interpreted the data and revised the manuscript; Ma SJ interpreted the data and revised the manuscript; Tan HZ conceived and designed the study and critically revised the manuscript. All author approved the final version of the manuscript.

Supported by the National Nature Science Foundation of China, No. 81773535.

Conflict-of-interest statement: The authors deny any conflict of interest.

Open-Access: This article is an open-access article which was selected by an in-house editor and fully peer-reviewed by external reviewers. It is distributed in accordance with the Creative Commons Attribution Non Commercial (CC BY-NC 4.0) license, which permits others to distribute, remix, adapt, build upon this work non-commercially, and license their derivative works on different terms, provided the original work is properly cited and the use is non-commercial. See: http://creativecommons.org/licenses/by-nc/4.0/

Manuscript source: Unsolicited

Lin-Ting Huang, Shi-Lan Wu, Xin Liao, Shu-Juan Wu, Hong-Zhuan Tan, Department of Epidemiology and Health Statistics, Xiangya School of Public Health, Central South University, Changsha 410083, Hunan Province, China

Corresponding author: Hong-Zhuan Tan, MD, PhD, Professor, Xiangya School of Public Health, Central South University, Changsha 410008, Hunan Province, China.
tanhz99@qq.com
Telephone: +86-731-88858435
Fax: +86-731-84805454

Abstract

BACKGROUND

Adiponectin (ADIPOQ) is an important factor involved in the regulation of both carbohydrate and lipid metabolism. Polymorphisms in the *ADIPOQ* gene are known to influence an individual's predisposition to metabolic syndrome and type 2 diabetes. Moreover, women with gestational diabetes mellitus (GDM) are at an increased risk of developing type 2 diabetes. Several studies have been conducted previously to assess the association between *ADIPOQ* polymorphisms and GDM; however, the results of the association are inconclusive.

AIM

To quantitatively evaluate the association between *ADIPOQ +45T/G*, *+276G/T*, and *-11377C/G* polymorphisms and the risk of GDM.

METHODS

A systematic search of EMBASE, PubMed, CNKI, Web of Science, and WANFANG DATA was conducted up to October 20, 2018. We calculated merged odds ratios (ORs) with 95% confidence intervals (CIs) using a fixed-effects or random-effects model depending on the between-study heterogeneity to evaluate the association between *AIDPOQ +45T/G*, *+276G/T*, and *-11377C/G* polymorphisms and the risk of GDM. Subgroup analysis was performed by ethnicity. Publication and sensitivity bias analyses were performed to test the robustness of the association. All statistical analyses were conducted using Stata12.0.

RESULTS

Nine studies of *+45T/G* included 1024 GDM cases and 1059 controls, five studies of *+276G/T* included 590 GDM cases and 595 controls, and five studies of *-11377C/G* included 722 GDM cases and 791 controls. Pooled ORs indicated that *+45T/G* increased GDM risk in Asians (allelic model: OR = 1.47, 95%CI: 1.27-1.70,

manuscript

Received: November 20, 2018
Peer-review started: November 21, 2018
First decision: December 15, 2018
Revised: December 24, 2018
Accepted: January 3, 2019
Article in press: January 3, 2019
Published online: March 6, 2019

P = 0.000; dominant model: OR = 1.54, 95%CI: 1.27-1.85, *P* = 0.000; recessive model: OR=2.00, 95%CI: 1.43-2.85, *P* = 0.000), not in South Americans (allelic model: OR = 1.21, 95%CI: 0.68-2.41, *P* = 0.510; dominant model: OR = 1.13, 95%CI: 0.59-2.15, *P* = 0.710; recessive model: OR = 2.18, 95%CI: 0.43-11.07, *P* = 0.350). There were no significant associations between *+276G/T* (allelic model: OR = 0.88, 95%CI: 0.74-1.05, *P* = 0.158; dominant model: OR = 0.91, 95%CI: 0.65-1.26, *P* = 0.561; recessive model: OR = 0.82, 95%CI: 0.64-1.05, *P* = 0.118) or *-11377C/G* (allelic model: OR = 0.96, 95%CI: 0.72-1.26, *P* = 0.750; dominant model: OR = 1.00, 95%CI: 0.73-1.37, *P* = 0.980; recessive model: OR = 0.90, 95%CI: 0.61-1.32, *P* = 0.570) and the risk of GDM.

CONCLUSION
Our meta-analysis shows the critical role of the *ADIPOQ +45T/G* polymorphism in GDM, especially in Asians. Studies focused on delineating ethnicity-specific factors with larger sample sizes are needed.

Key words: Gestational diabetes mellitus; Single nucleotide; Polymorphism; Adiponectin; Gene; Meta-analysis

©The Author(s) 2019. Published by Baishideng Publishing Group Inc. All rights reserved.

Core tip: No consensus is available in the literature about the association of adiponectin gene polymorphisms and the risk of gestational diabetes mellitus (GDM). As far as we know, only *+45T/G* was involved in a previous meta-analysis with a small sample size and obvious heterogeneity. We evaluated the association between *ADIPOQ +45T/G*, *+276G/T*, and *-11377C/G* polymorphisms and GDM with a bigger sample size, less heterogeneity. Moreover, subgroup analysis was performed by ethnicity.

Citation: Huang LT, Wu SL, Liao X, Ma SJ, Tan HZ. Adiponectin gene polymorphisms and risk of gestational diabetes mellitus: A meta-analysis. *World J Clin Cases* 2019; 7(5): 572-584
URL: https://www.wjgnet.com/2307-8960/full/v7/i5/572.htm
DOI: https://dx.doi.org/10.12998/wjcc.v7.i5.572

INTRUDUCTION

Gestational diabetes mellitus (GDM) is a condition of impaired glucose tolerance during pregnancy in women without a previous diagnosis of diabetes. It is associated with serious complications for both mother and child in the pre- and postnatal periods[1]. Many kinds of risk factors contribute to GDM, such as ethnicity, genetics, family history, dietary habits, and physical activity[1]. Obesity is a usual risk factor for GDM and can cause insulin resistance. Many biochemical mediators compounded in the adipose tissue and secreted in the circulatory system, such as resistin, adiponectin (ADIPOQ), and leptin, are suggested to correlate with obesity and insulin resistance[2].

ADIPOQ is produced in the adipose tissue and modulates various metabolic processes, including lipid metabolism, glucose and fatty acid oxidation. This hormone decreases insulin resistance, improves lipid metabolism, and exerts anti-inflammatory properties. Decreased plasma ADIPOQ levels were observed in patients with type 2 diabetes (T2D), metabolic syndrome, and obesity[3]. During normal pregnancy, ADIPOQ levels progressively decline, with its plasma concentration reaching even lower in GDM women[1]. Previous studies suggested that *ADIPOQ* gene single nucleotide polymorphisms (SNPs) could influence the concentration of plasma ADIPOQ and subsequently insulin sensitivity[4-6].

Studies have paid attention to the SNPs *+45T/G* in exon 2 and *+276G/C in* intron 2, *-11391G/A*, and *-11377C/G* in the promoter region. The two *ADIPOQ* linkage disequilibrium blocks are where these four variants located within. Block 1 comprises the promoter sequence spanning the region -14811 to -4120, and block 2 encompasses the exons in the region -450 to +4545[2]. The conclusions of these studies have been disputed regarding whether the metabolic phenotypes of GDM are influenced by the variability at this locus and which polymorphisms contribute to this effect. For example, Low *et al*[7] reported that a significant association was found between *SNP*

45T/G and GDM, and normal patients with the TT genotype had significantly higher plasma ADIPOQ levels compared to those with the TG or GG genotype. Beltcheva *et al*[1] reported that *-11377C/G* is associated with GDM. According to Daher *et al*[8], GDM is not associated with *+45T/G* and *-11377C/G* polymorphisms. Reasons for the conflicting results are small sample sizes in a single study and the hereditary difference of ethnicity.

As the results are discrepant and *+45T/G* was the only polymorphism which participated in the meta-analysis, our study was meant to evaluate whether and to what extent *ADIPOQ* gene polymorphisms contribute to GDM.

MATERIALS AND METHODS

Literature search strategy

Electronic databases PubMed, EMBASE, Web of Science, WANFANG DATA, and CNKI were used to search possibly association articles on human genetic studies of *ADIPOQ* and GDM that had been published up to 20 October 2018. The search terms used were: "Gestational diabetes mellitus" or "GDM" and "adiponectin" or "ADIPOQ" and "single nucleotide polymorphism" or "polymorphism".

Selection criteria and data extraction

We searched the database and identified 87 articles. The selection criteria of the publications were as follow: (1) well-designed case control studies on genetic association of ADIPOQ and the risk of GDM; (2) clear diagnostic criteria for GDM; (3) independent and sufficient genotype data must be contained in the original papers and the data can calculate odds ratios (ORs) and 95% confidence intervals (CIs); and (4) there should be at least two articles that have studied each polymorphism that we used in our meta-analysis. During the selection, we removed 25 articles for duplicate publication and excluded 49 articles for review, animal studies, case reports with unrelated outcomes or other diseases, and articles with no *ADIPOQ +45T/G*, *+276G/T*, or *-11377C/G* reported.

Finally, 13 articles were adopted in this meta-analysis. Among them, nine studies investigated *+45T/G*, five studies investigated *+276G/T*, and five studies investigated *-11377C/G*. A flow diagram of study selection is presented in Figure 1.

Data were extracted by two researchers independently. We have extracted the following information from every included study: first author, year of publication, country, ethnicity, matching criteria, genotyping method, numbers of cases and controls, minor allele frequency in controls, and Hardy-Weinberg equilibrium (HWE) status. We obtained the HWE status of controls by calculating from genotype distributions using STATA12.0. The Newcastle-Ottawa quality assessment scale (NOS) was used for quality assessment of primary studies. The study would be regarded as a high-quality study when it had an NOS scores ≥ 6 (Table 1)[9].

Statistical analysis

We used Stata12.0 software for statistical analyses. A fixed-effects or random-effects model was used to merge OR and 95%CI based on allelic models, recessive models, and dominant models to evaluate the association between each genetic variant and the risk of GDM. The *Z*-test was used for determining the significance of the merged OR. $P < 0.05$ was considered statistically significant.

We used the Cochran *Q* test to assess the heterogeneity among the studies and Higgins I^2 statistic for quantifying the heterogeneity. We used the random-effects model as the merging method when the variant association presented significant interstudy heterogeneity (*Q* test, *P*-value < 0.05, or $I^2 > 50\%$), otherwise, we used the fixed-effects model. Subgroup analysis was performed based on the ethnicity of the study population to evaluate ethnic-specific effects. Publication bias was tested by Begg's funnel plot.

The statistical methods of this study were reviewed by Shi-Min Hu from Department of Epidemiology and Health Statistics, Xiangya School of Public Health, Central South University.

RESULTS

Main characteristics of all the included studies

Thirteen studies were adopted in this meta-analysis; among them, nine studies were about the association of *+45T/G* and GDM[2,4,7,8,10-14], five studies were about the association of *+276G/T* and GDM[4,10,12-14], and five studies were about the association of

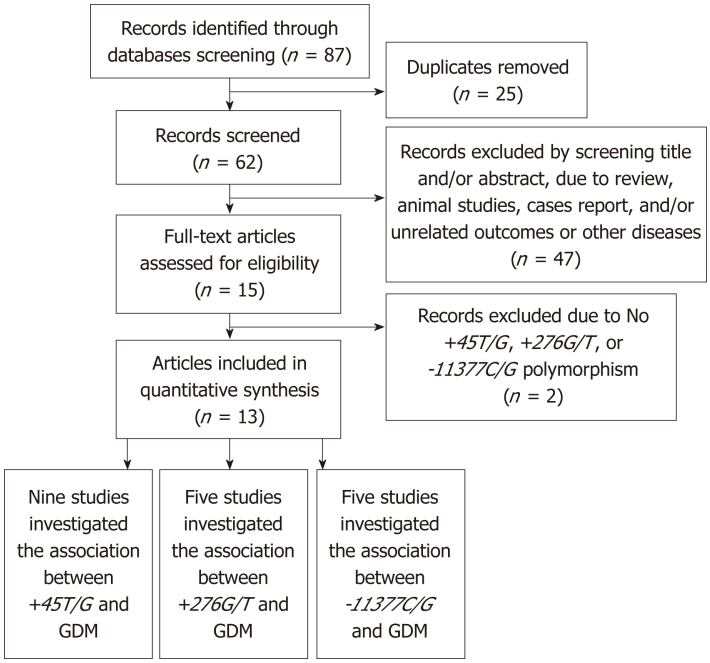

Figure 1 Flow diagram of study selection.

-11377C/G and GDM[1,3,8,15,16]. In total, 1667 GDM cases and 1682 controls were included; ten studies were from Asian descendants[2,4,7,10-15], two studies were from European descendants[1,3], and one study was from a South American descendant[8]. Detailed characteristics of all studies included are shown in Table 2.

Association between +45T/G and GDM

Nine articles evaluated the association of *+45T/G* and GDM; eight of them were conducted in Asia and 1 in South America, with a total of 1024 GDM cases and 1059 controls. Heterogeneity test revealed $P > 0.05$ and $I^2 < 50\%$; the fixed-effects model was used.

The pooled results suggested a significant association between *+45T/G* and GDM (allelic model: OR = 1.45, 95%CI: 1.26-1.67; dominant model: OR = 1.50, 95%CI: 1.25-1.79; recessive model: OR = 2.00, 95%CI: 1.42-2.84). Ethnicity-based subgroup analysis showed that *+45T/G* was associated with GDM in Asians (allelic model: OR = 1.47, 95%CI: 1.27-1.70; dominant model: OR = 1.54, 95%CI: 1.27-1.85; recessive model: OR = 2.00, 95%CI: 1.43-2.85). However, there was no association of *+45T/G* with the risk of GDM in South Americans (allelic model: OR = 1.21, 95%CI: 0.68-2.41; dominant model: OR = 1.13, 95%CI: 0.59-2.15; recessive model: OR=2.18, 95%CI: 0.43-11.07) (Figure 2 and Table 3).

Association between +276G/T and GDM

The association between *+276G/T* and the risk of GDM was investigated by five studies, including 590 GDM cases and 595 controls. Heterogeneity test revealed $P > 0.05$ and $I^2 < 50\%$, and the fixed-effects model was used.

The results showed that *+276G/T* was not associated with the risk of GDM (allelic model: OR = 0.88, 95%CI: 0.74-1.05; dominant model: OR = 0.91, 95%CI: 0.65-1.26; recessive model: OR = 0.82, 95%CI: 0.64-1.05) (Figure 3 and Table 3).

Association between -11377C/G and GDM

The association between *-11377C/G* and the risk of GDM was investigated by five studies, of which two were conducted in Asia, two conducted in Europe, and one in South America, with a total of 722 GDM cases and 791 controls. Heterogeneity test revealed $P < 0.05$ and $I^2 > 50\%$; the random-effects model was used.

The results showed that *-11377C/G* was not associated with the risk of GDM (allelic model: OR = 0.96, 95%CI: 0.72-1.26; dominant model: OR = 1.00, 95%CI: 0.73-1.37; recessive model: OR = 0.90, 95%CI: 0.61-1.32). Ethnicity-based subgroup analysis also showed that *-11377C/G* was not associated with GDM in Asian (allelic model: OR = 1.04, 95%CI: 0.77-1.41; dominant model: OR = 1.09, 95%CI: 0.79-1.50; recessive model: OR = 0.97, 95%CI: 0.51-1.86), European (allelic model: OR = 0.94, 95%CI: 0.45-1.96; dominant model: OR = 1.00, 95%CI: 0.42-2.33; recessive model: OR = 0.87, 95%CI: 0.51-1.49) and South American populations (allelic model: OR = 0.80, 95%CI: 0.50-1.29;

Table 1 Quality assessment of included case control studies using the Newcastle-Ottawa scale

Author	Yr	Selection				Comparability		Exposure			Score
		Case definition	Case representativeness	Control selection	Control definition	Important confounders	Every confounders	Ascertainment	Consistency	Non-response rate	
Low *et al*[7]	2011	1	1	0	1	1	0	1	1	1	7
Takhshid *et al*[2]	2015	1	1	1	1	0	0	1	1	1	7
Daher *et al*[8]	2011	1	1	1	1	1	0	1	1	1	8
Han *et al*[4]	2012	1	1	0	1	1	0	1	1	1	7
Gao *et al*[10]	2016	1	1	1	1	1	0	1	1	1	8
Luan *et al*[13]	2015	1	1	1	1	1	0	1	1	1	8
Li *et al*[12]	2017	1	1	1	1	1	0	1	1	1	8
Li *et al*[11]	2013	1	1	1	1	0	0	1	1	1	7
Zhang *et al*[14]	2014	1	1	1	1	1	0	1	1	1	8
Beltcheva *et al*[1]	2014	1	1	0	1	1	0	1	1	1	7
Pawlik *et al*[3]	2017	1	1	1	1	0	0	1	1	1	7
Chen *et al*[15]	2011	1	1	1	1	0	0	1	1	1	7
Wang *et al*[16]	2016	1	1	1	1	0	0	1	1	1	7

The quality evaluation content mainly includes three aspects: case selection, baseline comparability, and exposure factors with nine evaluation items. If the evaluation item is met, 1 point is obtained, otherwise 0, and the score ranges from 0 to 9.

dominant model: OR = 0.77, 95%CI: 0.44-1.36; recessive model: OR = 0.81, 95%CI: 0.51-1.86) (Figure 4 and Table 3).

Publication bias

We used the Egger regression asymmetry test and Begg's funnel plot to assess the public bias of the studies. The evidence of publication bias cannot be found in the meta-analysis of *+45T/G* (allelic model: continuity corrected *P*-value = 1.000, Egger regression asymmetry test *t* = -0.62, *P* = 0.554; recessive model: continuity corrected *P*-value = 0.466, Egger regression asymmetry test *t* = -0.15, *P* = 0.883), *+276G/T* (allelic model: continuity corrected *P*-value = 0.26, Egger regression asymmetry test *t* = -1.24, *P* = 0.282) and *-11377C/G* (allelic model: continuity corrected *P*-value = 0.221, Egger regression asymmetry test *t* = -2.48, *P* = 0.089)(Figure 5).

Sensitivity analysis

To assess the stability of the results, we performed the sensitivity analysis by sequentially excluding individual studies for each meta-analysis. For the association between *+45T/G*, *+276G/T*, or *-11377C/G* and GDM, there was no significant change of corresponding merged ORs when one study was sequentially excluded from every meta-analysis. Therefore, the results of our meta-analysis are stable and reliable (Figure 6).

DISCUSSION

ADIPOQ has been considered an important factor in regulating glucose and lipid metabolism. It is secreted by adipose tissue, which has a negative correlation with insulin resistance, T2D, and metabolic syndrome. ADIPOQ can increase insulin sensitivity, anti-inflammation, and anti-atherosclerosis, promote glucose uptake in muscle tissue, and inhibit intrahepatic synthetic glucose[17].

In the chromosomal region where the *ADIPOQ* gene is located, there are

Table 2 Detailed characteristics of all eligible studies for the association between *ADIPOQ* single nucleotide polymorphism and gestational diabetes mellitus

SNP	Author	Yr	Country	Ethnicity	Matching criteria	Method	Sample size		Genotype[1]		HWE
							Case	Control	Case	Control	
+45T/G	Low *et al*[7]	2011	Malaysia	Asian	NR	Taq PCR	26	53	11/13/2	35/17/1	0.51
	Takhshid *et al*[2]	2015	Iran	Asian	Age	PCR-RELF	65	70	37/28/0	54/16/0	0.28
	Daher *et al*[8]	2011	Brazil	SA	Race	PCR-RELF	79	169	61/15/3	134/32/3	0.51
	Han *et al*[4]	2012	China	Asian	NR	PCR-RELF	152	120	63/71/18	64/50/6	0.34
	Gao *et al*[10]	2016	China	Asian	Age, GW	PCR-RELF	150	150	59/66/25	81/57/12	0.66
	Luan *et al*[13]	2015	China	Asian	Age, GW	NR	60	60	33/21/6	29/26/5	0.81
	Li *et al*[12]	2017	China	Asian	Age, GW	PCR-RELF	130	130	53/63/14	63/60/7	0.13
	Li *et al*[11]	2013	China	Asian	NR	Sequencing	264	172	134/113/17	97/66/9	0.6
	Zhang *et al*[14]	2014	China	Asian	Age, BMI, GW	PCR-RELF	98	135	38/43/17	73/51/11	0.62
+276G/T	Han *et al*[4]	2012	China	Asian	NR	PCR-RELF	152	120	12/66/74	11/53/56	0.34
	Gao *et al*[10]	2016	China	Asian	Age, GW	PCR-RELF	150	150	15/69/66	15/60/75	0.66
	Luan *et al*[13]	2015	China	Asian	Age, GW	NR	60	60	7/26/27	3/25/32	0.81
	Li *et al*[12]	2017	China	Asian	Age, GW	PCR-RELF	130	130	64/58/8	60/56/14	0.13
	Zhang *et al*[14]	2014	China	Asian	Age, BMI, GW	PCR-RELF	98	135	10/45/43	13/54/68	0.62
-11377C/G	Beltcheva *et al*[1]	2014	Bulgaria	European	Age, BMI	TaqMan	130	130	80/44/6	66/50/14	0.34
	Pawlik *et al*[3]	2017	Poland	European	NR	TaqMan	204	207	92/91/21	115/75/17	0.34
	Daher *et al*[8]	2011	Brazil	SA	race	PCR-RELF	79	169	54/20/5	105/50/13	0.05
	Chen *et al*[15]	2011	China	Asian	NR	PCR-RELF	103	97	55/43/5	50/38/9	0.65
	Wang *et al*[16]	2016	China	Asian	NR	PCR-RELF	206	189	107/84/15	106/73/10	0.57

[1]Genotype is presented as wild type/heterozygous/homozygous. ADIPOQ: Adiponectin; GDM: Gestational diabetes mellitus; SNP: Single nucleotide polymorphism; SA: South American; GW: Gestational week; PCR-RELF: Polymerase chain reaction-restriction fragment length polymorphism; BMI: Body mass index; HWE: Hardy-Weinberg equilibrium; NR: Not reported.

susceptible sites of T2D and metabolic syndrome, and its SNPs can affect the level of ADIPOQ in blood, leading to obesity, insulin resistance, and the occurrence of T2D[15].

Plasma ADIPOQ levels gradually decreased with gestational week during pregnancy, consistent with the gradual decrease of insulin sensitivity[3], and plasma adiponectin levels decreased more significantly in GDM women. This phenomenon is closely related to the decreased transcriptional activity of *ADIPOQ* during pregnancy. Previous studies revealed the association of *ADIPOQ* SNPs, such as *+45T/G*[1,2,4,7,8,10-14], *+276G/T*[1,4,10,12,13,18], *-11377C/G*[1,3,8,15,16], *-3971A/G*[13,19], and *-11426A/G*[15,19], and the risk of GDM. A total of 66.7% (6 of 9) of the studies adopted in this meta-analysis reported that the *+45T/G* polymorphism increased the risk of GDM, and 40% (2 of 5) reported that the *-11377C/G* polymorphism was associated with GDM. A higher prevalence of the G allele was observed among women with GDM. All studies regarding *+276G/T* reported that this polymorphism had no association with the risk of GDM.

Thirteen studies were included in our study; nine studies were about *+45T/G*, with 1024 cases and 1059 controls, five studies were about *+276G/T*, with 590 cases and 595 controls, and five studies were about *-11377C/G*, with 722 cases and 791 controls. We not only had a larger sample size than previous studies but also performed subgroup analysis based on the ethnicity of the study population to evaluate ethnic-specific effects. *+45T/G* was proved by our meta-analysis to be a risk factor for GDM (allelic model: OR = 1.45, 95%CI: 1.26-1.67, P = 0.000), and 66.7% (6 of 9) of studies reported a positive result[2,4,7,10,12,14]. Subgroup analysis showed that *+45T/G* was associated with GDM in Asians (allelic model: OR = 1.47, 95%CI: 1.27-1.70, P = 0.000) but not in South Americans. In addition, no association of *+276G/T* or *-11377C/G* and the risk of GDM was observed.

Obvious heterogeneity was detected among the *-11377C/G* studies (allelic model: I^2 = 64.0%, P = 0.03, dominant model: I^2 = 55.0%, P = 0.06, recessive model: I^2 = 32.0%, P = 0.21). We used subgroup analysis based on ethnicity, and the heterogeneity could not be reduced, indicating that a small sample size and other reasons may have influenced the heterogeneity. The association of *-11377C/G* with the risk of GDM remains to be verified by further studies. No heterogeneity was found in the studies of *+45T/G* (allelic model: I^2 = 14.3%, P = 0.32, dominant model: I^2 = 18.1%, P = 0.28, recessive model: I^2 = 0.0%, P = 0.90) and *+276G/T* (allelic model: I^2 = 0.0%, P = 0.74,

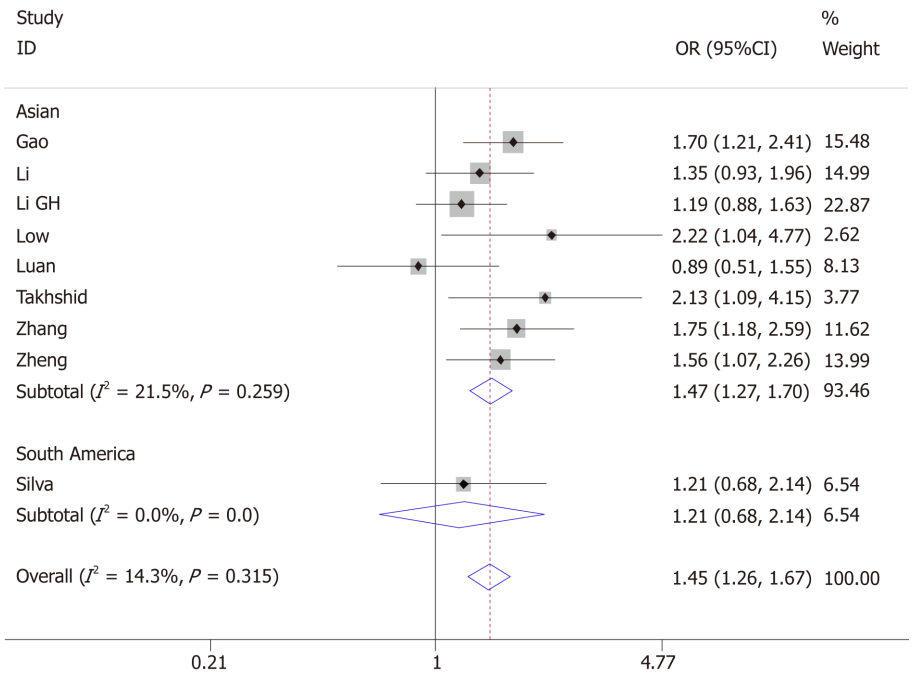

Figure 2 Forest plot for the association of *ADIPOQ +45T/G* polymorphism and gestational diabetes mellitus under the allelic model.

dominant model: I^2 = 0.0%, P = 0.78, recessive model: I^2 = 0.0%, P = 0.83), so the conclusion that *+45T/G* has, but *+276G/T* has no, association with the risk of GDM is relatively reliable. Begg's funnel plot was used to test publication bias. The test showed that there was no publication bias among the studies. Sensitivity analysis indicated that the results are stable and reliable.

The SNP *+45T/G* is a synonymous mutation (GGTGGG, Gly15Gly) at exon 2. The results of Yang *et al*[20] indicated that *+45T/G* polymorphism may influence the expression of *ADIPOQ* by influencing RNA splicing and stability. Some studies reported that the G allele of *+45T/G* polymorphism in the *ADIPOQ* gene is associated with obesity, insulin resistance, and T2D in several populations. Very few studies have investigated the association of *ADIPOQ +45T/G* polymorphism with GDM and the results of these studies were controversial.

As far as we know, only *+45T/G* was involved in a previous meta-analysis that reported no association of *ADIPOQ +45T/G* polymorphism with the risk of GDM (allelic model: OR = 1.17, 95%CI: 0.79-1.76; dominant model: OR = 0.86, 95%CI: 0.50-1.48; recessive model: OR = 1.21, 95%CI: 0.62-2.33)[21]. The reason for this controversy is most likely the following: (1) the small sample size (case number = 875, control number = 884); (2) obvious heterogeneity (all *P*-values for heterogeneity less than 0.01); and (3) false HWE status of 25% studies (2 of 8) involved in that meta-analysis will cause insufficient power which may lead to the false-negative results.

The role of *+276G/T* in the pathogenesis of metabolic syndrome and diabetes mellitus has also been reported to be contradictory. Commonly, the T allele has an association with a higher adiponectin level and protection against T2D[22,23], but some studies showed that T carriers have a higher risk of obesity and diabetes[24,25], or +276G/T polymorphism is not associated with T2D or GDM[26].

All the studies on *+276G/T* polymorphism included in our study came from the Chinese population. This result suggests that *+276G/T* in the Chinese population may associate with the risk of GDM. The studies about the association between *+276G/T* and GDM from other countries could not be found. Geographical, environmental, and genetic factors of different ethnic groups lead to different susceptibility to diabetes; therefore, we need more studies about the association between *+276G/T* and GDM of other ethnic groups to reach reliable conclusions.

Zhang *et al*[27] found that *ADIPOQ* gene promoter region has four transcription stimulatory protein (SP1) binding sites, while the G allele of *- 11377 C/G* in the promoter region can change the DNA sequence of one of the SP1 binding sites, leading to the loss of binding force to SP1. This may reduce the *ADIPOQ* gene transcription activity, inhibit the expression of genes, and lead to lower plasma ADIPOQ, which could associate with glucolipid metabolic abnormalities and insulin resistance. Consistent with the results of Vasseur *et al*[28], Petrone *et al*[29] reported that -

Table 3 Main results of the pooled odds ratios in meta-analysis for the association between *ADIPOQ* polymorphisms and gestational diabetes mellitus

SNP	N	Sample size		Allelic model		Dominant model		Recessive model	
		Case	Control	OR (95%CI)	P	OR (95%CI)	P	OR (95%CI)	P
+45T/G									
Total	10	1024	1059	1.45 (1.26-1.67)	0.000[a]	1.50 (1.25-1.79)	0.000[a]	2.00 (1.42-2.84)	0.000[a]
Subgroup									
Ethnicity									
Asian	8	945	890	1.47 (1.27-1.70)	0.000[a]	1.54 (1.27-1.85)	0.000[a]	2.00 (1.43-2.85)	0.000[a]
SA	1	79	169	1.21 (0.68-2.41)	0.510	1.13 (0.59-2.15)	0.710	2.18 (0.43-11.07)	0.350
+276G/T									
Total	5	590	595	0.88 (0.74-1.05)	0.158	0.91 (0.65-1.26)	0.561	0.82 (0.64-1.05)	0.118
-11377C/G									
Total	5	722	791	0.96 (0.72-1.26)	0.750	1.00 (0.73-1.37)	0.980	0.90 (0.61-1.32)	0.570
Subgroup									
Ethnicity									
Asian	2	309	286	1.04 (0.77-1.41)	0.800	1.09 (0.79-1.50)	0.600	0.97 (0.51-1.86)	0.930
SA	1	79	168	0.80 (0.50-1.29)	0.360	0.77 (0.44-1.36)	0.370	0.81 (0.28-2.34)	0.690
European	2	334	337	0.94 (0.45-1.96)	0.870	1.00 (0.42-2.33)	0.990	0.87 (0.51-1.49)	0.610

[a]$P < 0.01$. ADIPOQ: Adiponectin; SA: South American; GDM: Gestational diabetes mellitus; SNP: Single nucleotide polymorphism; N: Number of studies; OR: Odds ratio; CI: Confidence interval; NA: Not assessable.

11377G haplotype is associated with low plasma ADIPOQ levels and T2D. However, due to ethnic and geographical differences, the results of studies on the association between *ADIPOQ* gene *-11377C/G* polymorphism and diabetes mellitus are not completely consistent[30].

According to the literatures on *-11377C/G* polymorphism included in our studies, Asians accounted for 40%, Europeans for 40%, and South Americans for 20%. Due to the small sample size and large heterogeneity of each ethnic subgroup, our results, which are inconsistent with the previous studies, are unreliable.

The limitations of this study should be considered. First, the number of cases and controls involved in the meta-analysis for exploring the association of *ADIPOQ* and GDM in different ethnicities may have little power, and studies with larger sample sizes and multiple ethnicities are needed. Second, GDM has complicated cases, with genetic susceptibility, environmental triggers, and acquired dispositions, such as age, gestational weeks, condition of nutrition, and physique. In this meta-analysis, we failed to conduct a multivariate analysis of confounders. Therefore, further comprehensive studies with strict matching criteria for cases and controls are needed. Third, few studies have reported the association between polymorphisms and serum ADIPOQ levels, so genotype-phenotype analysis was prevented[21].

In conclusion, our meta-analysis reveals the association of the *ADIPOQ +45T/G* polymorphism and the risk of GDM; this polymorphism increases GDM risk in Asian populations. Another two polymorphisms, *+276G/T* and *-11377C/G*, seem to have no association with the risk of GDM. Prospective studies of high quality with larger sample sizes are required to reveal the association of *ADIPOQ* polymorphisms with GDM, the existence of ethnicity-specific factors, and the role that ADIPOQ polymorphisms play in pathology.

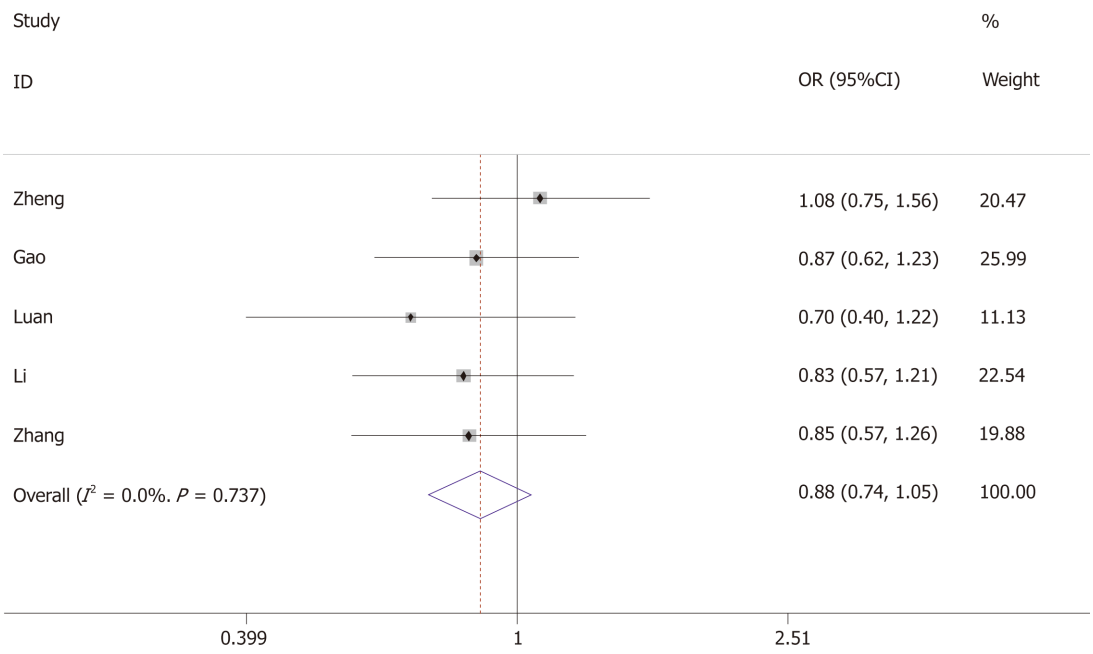

Figure 3 Forest plot for the association of *ADIPOQ +276G/T* polymorphism and gestational diabetes mellitus under the allelic model.

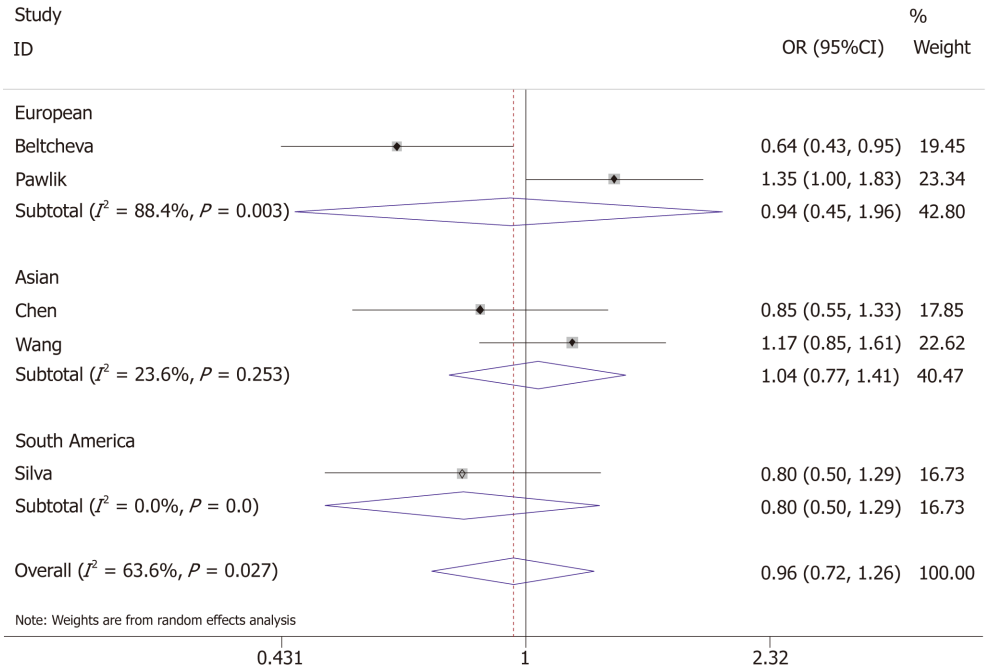

Figure 4 Forest plot for the association of *ADIPOQ -11377C/G* polymorphism and gestational diabetes mellitus under the allelic model.

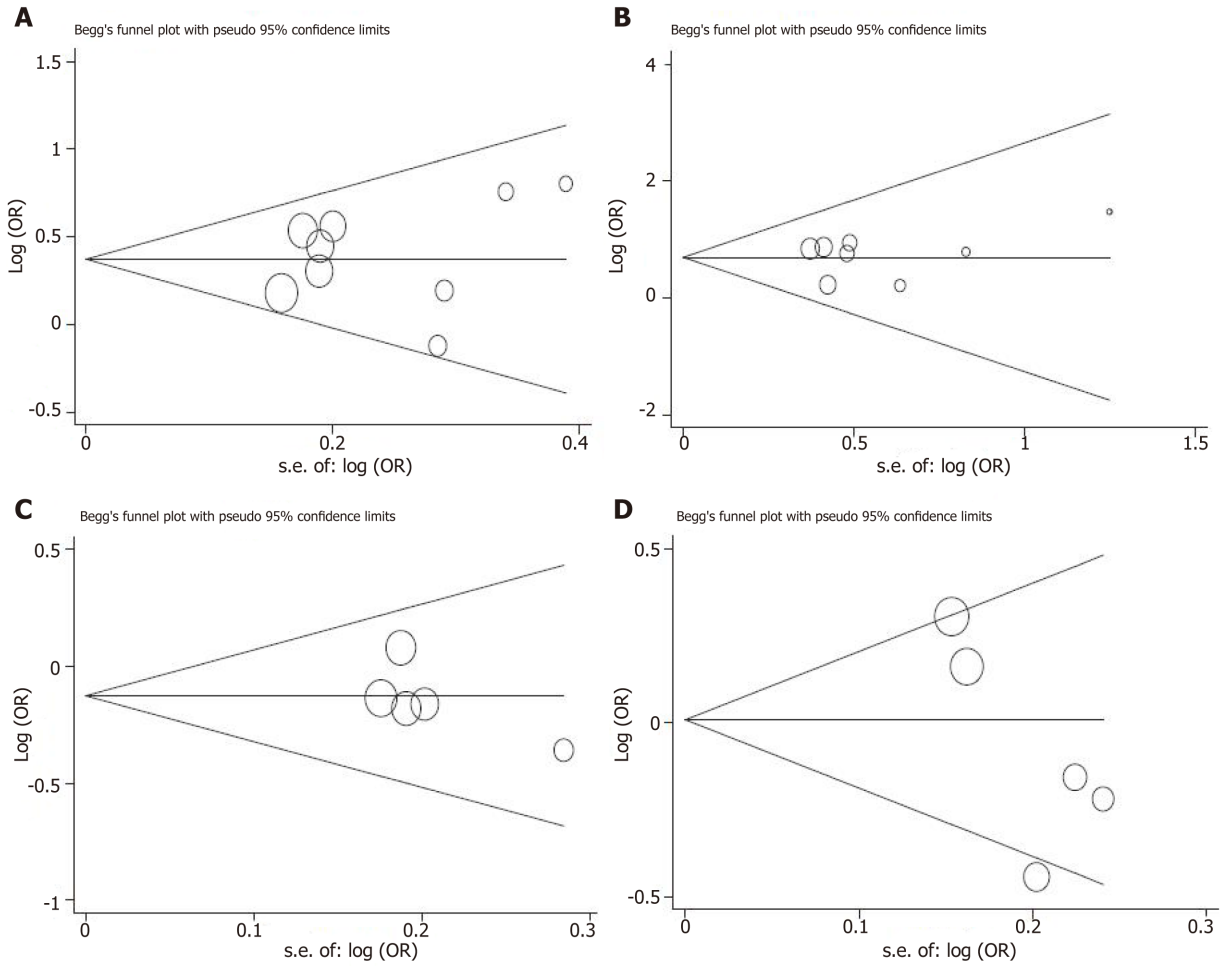

Figure 5 Begg's funnel plots for testing publication bias. A: *+45T/G* under allelic model; B: *+45T/G* under recessive model; C: *+276G/T* under allelic model; D: *-11377C/G* under allelic model. OR: Odds ratio.

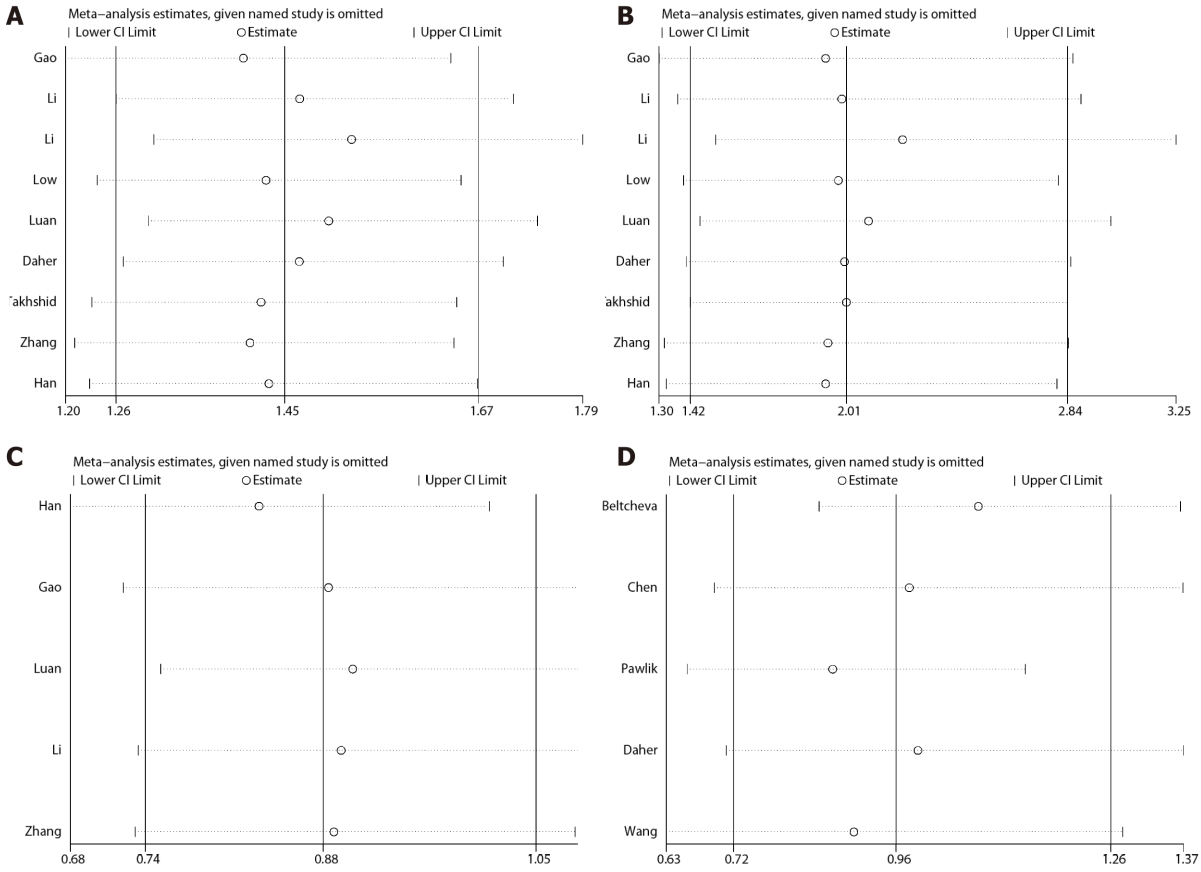

Figure 6 Sensitivity analysis between ADPIOQ polymorphisms and gestational diabetes mellitus in all studies. A: *+45T/G* under allelic model; B: *+45T/G* under recessive model; C: *+276G/T* under allelic model; D: *-11377C/G* under allelic model. CI: Confidence interval.

ARTICLE HIGHLIGHTS

Research background

Many biochemical mediators that are synthesized in the adipose tissue and secreted in the circulation, such as leptin, adiponectin (ADIPOQ), and resistin, are thought to be involved in obesity and insulin resistance. ADIPOQ is produced in the adipose tissue and regulates a variety of metabolic processes such as lipid metabolism, glucose and fatty acid oxidation. This hormone can reduce insulin resistance, improve lipid metabolism, and exert anti-inflammatory effects. Plasma ADIPOQ levels are decreased in patients with type 2 diabetes, metabolic syndrome, and obesity. Previous studies have shown that *ADIPOQ* single nucleotide polymorphisms can affect plasma ADIPOQ concentrations, which in turn affect insulin sensitivity.

Research motivation

Previous studies have evaluated the relationship between *ADIPOQ* polymorphisms and gestational diabetes mellitus (GDM), but the results of the association between *ADIPOQ* polymorphisms and GDM is uncertain.

Research objectives

We evaluated the association between *ADIPOQ* *+45T/G*, *+276G/T*, and *-11377C/G* polymorphisms and GDM with a bigger sample size and less heterogeneity. Moreover, subgroup analysis was performed by ethnicity.

Research methods

Potentially related articles on human fat metabolism and GDM gene research published before October 20, 2018 were retrieved through the electronic databases EMBASE, Web of Science, PubMed, WANFANG DATA, and China National Knowledge Infrastructure. A fixed-effects or random-effects model was used to calculate pooled odds ratios (ORs) with 95% confidence intervals (CIs), based on the between-study heterogeneity to evaluate the association between *AIDPOQ* *+45T/G*, *+276G/T*, and *-11377C/G* polymorphisms and the risk of GDM.

Research results

Nine *+45T/G* studies included 1024 GDM cases and 1059 controls, five *+276G/T* studies included 590 GDM cases and 595 controls, and five *-11377C/G* studies included 722 GDM cases

and 791 controls. Pooled ORs showed that *+45T/G* increased Asian GDM risk (allele model OR = 1.47, 95%CI: 1.27-1.70, P = 0.000; dominant model OR = 1.54, 95%CI: 1.27-1.85, P = 0.000; recessive mode: OR = 2.00, 95%CI: 1.43-2.85, P = 0.000), but not in South Americans (equal pattern: OR = 1.21, 95%CI: 0.68-2.41, P = 0.510; dominant model OR = 1.13, 95%CI: 0.59-2.15, P = 0.710; recessive mode OR = 2.18, 95%CI: 0.43-11.07, P = 0.350). There was no significant correlation between *+276G/T* (allele model OR = 0.88, 95%CI: 0.74-1.05, P = 0.158; dominant model OR = 0.91, 95%CI: 0.65-1.26, P = 0.561; recessive mode: OR = 0.82, 95%CI: 0.64-1.05, P = 0.118) or *-11377C/G* (equal pattern: OR = 0.96, 95%CI: 0.72-1.26, P = 0.750; dominant model OR = 1.00, 95%CI: 0.73-1.37, P = 0.980; recessive model: OR = 0.90, 95%CI: 0.61-1.32, P = 0.570) and GDM risk.

Research conclusions

Our meta-analysis reveals the association of the *ADIPOQ +45T/G* polymorphism and the risk of GDM; this polymorphism increases GDM risk in Asian populations.

Research perspectives

In order to reveal the association of *ADIPOQ* polymorphisms with GDM, the existence of ethnicity-specific factors, and the role that *ADIPOQ* polymorphisms play in pathology, studies focused on delineating ethnicity-specific factors with larger sample sizes are needed.

REFERENCES

1 **Beltcheva O**, Boyadzhieva M, Angelova O, Mitev V, Kaneva R, Atanasova I. The rs266729 single-nucleotide polymorphism in the adiponectin gene shows association with gestational diabetes. *Arch Gynecol Obstet* 2014; **289**: 743-748 [PMID: 24068295 DOI: 10.1007/s00404-013-3029-z]

2 **Takhshid MA**, Haem Z, Aboualizadeh F. The association of circulating adiponectin and + 45 T/G polymorphism of adiponectin gene with gestational diabetes mellitus in Iranian population. *J Diabetes Metab Disord* 2015; **14**: 30 [PMID: 25909078 DOI: 10.1186/s40200-015-0156-z]

3 **Pawlik A**, Teler J, Maciejewska A, Sawczuk M, Safranow K, Dziedziejko V. Adiponectin and leptin gene polymorphisms in women with gestational diabetes mellitus. *J Assist Reprod Genet* 2017; **34**: 511-516 [PMID: 28050671 DOI: 10.1007/s10815-016-0866-2]

4 **Han Y**, Zheng YL, Liu MH, Fan YP. Association of adiponectin gene single nucleotide polymorphism with gestational diabetes mellitus and pregnancy outcomes. *Shiyong Fuchanke Zazhi* 2012; **22**: 743-746

5 **Hara K**, Boutin P, Mori Y, Tobe K, Dina C, Yasuda K, Yamauchi T, Otabe S, Okada T, Eto K, Kadowaki H, Hagura R, Akanuma Y, Yazaki Y, Nagai R, Taniyama M, Matsubara K, Yoda M, Nakano Y, Tomita M, Kimura S, Ito C, Froguel P, Kadowaki T. Genetic variation in the gene encoding adiponectin is associated with an increased risk of type 2 diabetes in the Japanese population. *Diabetes* 2002; **51**: 536-540 [PMID: 11812766 DOI: 10.2337/diabetes.51.2.536]

6 **Menzaghi C**, Ercolino T, Di Paola R, Berg AH, Warram JH, Scherer PE, Trischitta V, Doria A. A haplotype at the adiponectin locus is associated with obesity and other features of the insulin resistance syndrome. *Diabetes* 2002; **51**: 2306-2312 [PMID: 12086965 DOI: 10.2337/diabetes.51.7.2306]

7 **Low CF**, Mohd Tohit ER, Chong PP, Idris F. Adiponectin SNP45TG is associated with gestational diabetes mellitus. *Arch Gynecol Obstet* 2011; **283**: 1255-1260 [PMID: 20552210 DOI: 10.1007/s00404-010-1548-4]

8 **Daher S**, Torloni MR, Gueuvoghlanian-Silva BY, Moron AF, Mattar R. Inflammatory mediator gene polymorphisms and gestational diabetes: A review of the literature. *J Reprod Immunol* 2011; **90**: 111-116 [PMID: 21684013 DOI: 10.1016/j.jri.2011.04.008]

9 **Stang A**. Critical evaluation of the Newcastle-Ottawa scale for the assessment of the quality of nonrandomized studies in meta-analyses. *Eur J Epidemiol* 2010; **25**: 603-605 [PMID: 20652370 DOI: 10.1007/s10654-010-9491-z]

10 **Gao Y**, Wang W, Wang SS. Association of Adiponectin Gene Single Nucleotide Polymorphism with Gestational Diabetes Mellitus. *Jilin Yixue* 2016; **6**: 1301-1302

11 **Li GH**, Kong LJ, Zhang L, Zhang WY. [Association of adiponectin gene polymorphisms +45T/G with gestational diabetes mellitus and neonate birth weight]. *Zhonghua Yixue Zazhi* 2013; **93**: 3770-3772 [PMID: 24548395]

12 **Li JY**, Ma S, Zhao J, Duan LJ, Sun HY. The correlation between single nucleotide polymorphism of adiponectin gene and gestational diabetes and its effect on pregnancy outcome. *Zhongguo Fuyoubaojian Zazhi* 2017; **22**: 5674-5677

13 **Luan YY**, Guo XH, Yang JH. Study on the correlation between the damage of adiponectin gene polymorphism with gestational impaired glucose. *Zhongguo Shiyanzhenduanxue Zazhi* 2015; **19**: 1093-1096

14 **Zhang C**, Liang XX. The relationship between adiponectin gene polymorphism of Guangxi Zhuang ethnic group and gestational diabetes. *Zhongguo Yishi Zazhi* 2014; **9**: 1221-1223 [DOI: 10.3760/cma.j.issn.1008-1372.2014.09.018]

15 **Chen ZY**, Du J. Relationship between diponectin gene polymorphism and gestational diabetes mellitus. *Xiandai Fuchanke Jinzhan* 2011; **20**: 718-721

16 **Wang XX**, Zhang L, Zhou GF, Pu XM. Study of the correlation between adiponectin gene polymorphism and gestational diabetes mellitus. *Zhongguo Fuyoubaojian Zazhi* 2016; **31**: 2546-2549

17 **Peng JJ**, Shi FX, Wang HY, Wang ZP, Yuan P. Correlation between adiponectin and gestaional diabetes mellitus. *Zhongguo Fuyoubaojian Zazhi* 2012; **27**: 1314-1316

18 **Zhang J**, Chi H, Xiao H, Tian X, Wang Y, Yun X, Xu Y. Interleukin 6 (IL-6) and Tumor Necrosis Factor α (TNF-α) Single Nucleotide Polymorphisms (SNPs), Inflammation and Metabolism in Gestational Diabetes Mellitus in Inner Mongolia. *Med Sci Monit* 2017; **23**: 4149-4157 [PMID: 28846666 DOI: 10.12659/MSM.903565]

19 **Chen XX**, Wei BR, Zhang LF, Yang YM. Association of -3771A/G Polymorphism in Promoter Region of Adiponectin Gene with Gestational Diabetes Mellitus. *Nanchangdaxue Xuebao Yixueban* 2013; **53**: 18-21

20 **Yang WS**, Tsou PL, Lee WJ, Tseng DL, Chen CL, Peng CC, Lee KC, Chen MJ, Huang CJ, Tai TY, Chuang LM. Allele-specific differential expression of a common adiponectin gene polymorphism related to obesity. *J Mol Med (Berl)* 2003; **81**: 428-434 [PMID: 12750819 DOI: 10.1007/s00109-002-0409-4]

21 **Xu F**, Zhang H, Qi H. No association of adiponectin +45 T/G polymorphism with the risk of gestational diabetes mellitus: Evidence from a meta-analysis. *J Renin Angiotensin Aldosterone Syst* 2016; **17**: 1470320316653283 [PMID: 27296394 DOI: 10.1177/1470320316653283]

22 **Liang Z**, Dong M, Cheng Q, Chen D. Gestational diabetes mellitus screening based on the gene chip technique. *Diabetes Res Clin Pract* 2010; **89**: 167-173 [PMID: 20554072 DOI: 10.1016/j.diabres.2010.04.001]

23 **Pollin TI**, Tanner K, O'connell JR, Ott SH, Damcott CM, Shuldiner AR, McLenithan JC, Mitchell BD. Linkage of plasma adiponectin levels to 3q27 explained by association with variation in the APM1 gene. *Diabetes* 2005; **54**: 268-274 [PMID: 15616038 DOI: 10.2337/diabetes.54.1.268]

24 **Beebe-Dimmer JL**, Zuhlke KA, Ray AM, Lange EM, Cooney KA. Genetic variation in adiponectin (ADIPOQ) and the type 1 receptor (ADIPOR1), obesity and prostate cancer in African Americans. *Prostate Cancer Prostatic Dis* 2010; **13**: 362-368 [PMID: 20697428 DOI: 10.1038/pcan.2010.27]

25 **Bouatia-Naji N**, Meyre D, Lobbens S, Séron K, Fumeron F, Balkau B, Heude B, Jouret B, Scherer PE, Dina C, Weill J, Froguel P. ACDC/adiponectin polymorphisms are associated with severe childhood and adult obesity. *Diabetes* 2006; **55**: 545-550 [PMID: 16443793 DOI: 10.2337/diabetes.55.02.06.db05-0971]

26 **Urbanek M**, Hayes MG, Lee H, Freathy RM, Lowe LP, Ackerman C, Jafari N, Dyer AR, Cox NJ, Dunger DB, Hattersley AT, Metzger BE, Lowe WL. The role of inflammatory pathway genetic variation on maternal metabolic phenotypes during pregnancy. *PLoS One* 2012; **7**: e32958 [PMID: 22479352 DOI: 10.1371/journal.pone.0032958]

27 **Zhang D**, Ma J, Brismar K, Efendic S, Gu HF. A single nucleotide polymorphism alters the sequence of SP1 binding site in the adiponectin promoter region and is associated with diabetic nephropathy among type 1 diabetic patients in the Genetics of Kidneys in Diabetes Study. *J Diabetes Complications* 2009; **23**: 265-272 [PMID: 18599322 DOI: 10.1016/j.jdiacomp.2008.05.004]

28 **Vasseur F**, Helbecque N, Dina C, Lobbens S, Delannoy V, Gaget S, Boutin P, Vaxillaire M, Leprêtre F, Dupont S, Hara K, Clément K, Bihain B, Kadowaki T, Froguel P. Single-nucleotide polymorphism haplotypes in the both proximal promoter and exon 3 of the APM1 gene modulate adipocyte-secreted adiponectin hormone levels and contribute to the genetic risk for type 2 diabetes in French Caucasians. *Hum Mol Genet* 2002; **11**: 2607-2614 [PMID: 12354786 DOI: 10.1093/hmg/11.21.2607]

29 **Petrone A**, Zavarella S, Caiazzo A, Leto G, Spoletini M, Potenziani S, Osborn J, Vania A, Buzzetti R. The promoter region of the adiponectin gene is a determinant in modulating insulin sensitivity in childhood obesity. *Obesity (Silver Spring)* 2006; **14**: 1498-1504 [PMID: 17030959 DOI: 10.1038/oby.2006.172]

30 **Enns JE**, Taylor CG, Zahradka P. Variations in Adipokine Genes AdipoQ, Lep, and LepR are Associated with Risk for Obesity-Related Metabolic Disease: The Modulatory Role of Gene-Nutrient Interactions. *J Obes* 2011; **2011**: 168659 [PMID: 21773001 DOI: 10.1155/2011/168659]

P- Reviewer: Pastromas S, Cengiz M

S- Editor: Dou Y **L- Editor:** Wang TQ **E- Editor:** Tan WW

World Journal of Clinical Cases

Submit a Manuscript: https://www.f6publishing.com

World J Clin Cases 2019 March 6; 7(5): 585-599

DOI: 10.12998/wjcc.v7.i5.585

ISSN 2307-8960 (online)

META-ANALYSIS

Maternal serum level of resistin is associated with risk for gestational diabetes mellitus: A meta-analysis

Shi-Min Hu, Meng-Shi Chen, Hong-Zhuan Tan

ORCID number: Shi-Min Hu (0000-0002-3284-2494); Meng-Shi Chen (0000-0002-9100-0967); Hong-Zhuan Tan (0000-0002-4292-5947).

Author contributions: Hu SM contributed to data acquisition, analysis, and interpretation and manuscript drafting; Chen MS contributed to data acquisition, analysis, and interpretation; Tan HZ contributed to data interpretation and manuscript revision; all authors approved the final version.

Supported by the National Natural Science Foundation of China, No. 81373088 and No. 81773535.

Conflict-of-interest statement: The authors deny any conflict of interest.

PRISMA 2009 Checklist statement: The authors have read the PRISMA 2009 Checklist, and the manuscript was prepared and revised according to the PRISMA 2009 Checklist.

Open-Access: This article is an open-access article which was selected by an in-house editor and fully peer-reviewed by external reviewers. It is distributed in accordance with the Creative Commons Attribution Non Commercial (CC BY-NC 4.0) license, which permits others to distribute, remix, adapt, build upon this work non-commercially, and license their derivative works on different terms, provided the original work is properly cited and the use is non-commercial. See: http://creativecommons.org/licenses/by-nc/4.0/

Shi-Min Hu, Meng-Shi Chen, Hong-Zhuan Tan, Department of Epidemiology and Health Statistics, Xiangya School of Public Health, Central South University, Changsha 410078, Hunan Province, China

Corresponding author: Hong-Zhuan Tan, PhD, Professor, Department of Epidemiology and Health Statistics, Xiangya School of Public Health, Central South University, 110 Xiangya Road, Changsha 410008, Hunan Province, China. tanhz99@qq.com
Telephone: +86-731-88858435
Fax: +86-731-84805454

Abstract

BACKGROUND

Resistin is most likely involved in the pathogenesis of gestational diabetes mellitus (GDM), but the existing findings are inconsistent.

AIM

To review the literature investigating the associations of the risk of GDM with serum level of resistin.

METHODS

A systematic literature search was performed using MEDLINE, EMBASE, and Web of Science (all databases). This meta-analysis included eligible studies that: (1) investigated the relationship between the risk of GDM and serum resistin; (2) included GDM cases and controls without GDM; (3) diagnosed GDM according to the oral glucose-tolerance test; (4) were performed in humans; (5) were published as full text articles in English; and (6) provided data with median and quartile range, median and minimum and maximum values, or mean and standard deviation. The pooled standardized mean difference (SMD) and 95% confidence interval (CI) were calculated to estimate the association between the risk of GDM and serum resistin. To analyze the potential influences of need for insulin in GDM patients and gestational age at blood sampling, we performed a subgroup analysis. Meta-regression with restricted maximum likelihood estimation was performed to assess the potentially important covariate exerting substantial impact on between-study heterogeneity.

RESULTS

The meta-analysis for the association between serum resistin level and GDM risk included 18 studies (22 comparisons) with 1041 cases and 1292 controls. The total results showed that the risk of GDM was associated with higher serum resistin level (SMD = 0.250, 95%CI: 0.116, 0.384). The "after 28 wk" subgroup, "no need

Manuscript source: Unsolicited manuscript

Received: December 18, 2018
Peer-review started: December 20, 2018
First decision: January 12, 2019
Revised: February 2, 2019
Accepted: February 18, 2019
Article in press: February 18, 2019
Published online: March 6, 2019

for insulin" subgroup, and "need for insulin" subgroup indicated that higher serum resistin level was related to GDM risk ("after 28 wk" subgroup: SMD = 0.394, 95%CI: 0.108, 0.680; "no need for insulin" subgroup: SMD = 0.177, 95%CI: 0.018, 0.336; "need for insulin" subgroup: SMD = 0.403, 95%CI: 0.119, 0.687). The "before 14 wk" subgroup, "14-28 wk" subgroup, and "no information of need for insulin" subgroup showed a nonsignificant association between serum resistin level and GDM risk ("before 14 wk" subgroup: SMD = 0.087, 95%CI: -0.055, 0.230; "14-28 wk" subgroup: SMD = 0.217, 95%CI: -0.003, 0.436; "no information of need for insulin" subgroup: SMD = 0.356, 95%CI: -0.143, 0.855). The postpartum subgroup included only one study and showed that higher serum resistin level was related to GDM risk (SMD = 0.571, 95%CI: 0.054, 1.087) The meta-regression revealed that no need for insulin in GDM patients, age distribution similar between cases and controls, and ELISA all had a significant impact on between-study heterogeneity.

CONCLUSION
This meta-analysis supports that the maternal serum resistin level is associated with GDM risk.

Key words: Resistin; Gestational diabetes mellitus; Meta-analysis; Gestational age

©The Author(s) 2019. Published by Baishideng Publishing Group Inc. All rights reserved.

Core tip: We conducted a meta-analysis of relevant high-quality studies, which revealed that the maternal serum resistin level is associated with gestational diabetes mellitus risk.

Citation: Hu SM, Chen MS, Tan HZ. Maternal serum level of resistin is associated with risk for gestational diabetes mellitus: A meta-analysis. *World J Clin Cases* 2019; 7(5): 585-599
URL: https://www.wjgnet.com/2307-8960/full/v7/i5/585.htm
DOI: https://dx.doi.org/10.12998/wjcc.v7.i5.585

INTRODUCTION

Gestational diabetes mellitus (GDM) is defined by varying degrees of glucose intolerance that is first detected during pregnancy[1]. In recent decades, the prevalence of GDM has been increasing and fluctuates from 1.7% to 11.6%[2]. Poorly controlled GDM is associated with an increase in the incidence of gestational hypertension, preeclampsia, polyhydramnios, fetal macrosomia, birth trauma, operative delivery, and neonatal hypoglycemia[3-5]. During pregnancy, insulin resistance is enhanced physiologically, which parallels the growth of the fetoplacental unit and facilitates the diversion of glucose to the fetus. When the compensatory increase in insulin is not sufficient to maintain glycemic homeostasis, pregnant women develop GDM.

Resistin, which was named after its insulin resistance ability by Steppan *et al*[6] in 2001, is a hormone with a molecular weight of 12.5 kDa that consists of 108 amino acids. Steppan *et al*[6] found anti-diabetic drugs called thiazolidinediones, which markedly lowered serum resistin levels in mice during treatment. The immunoneutralization of endogenous resistin improved blood glucose and insulin action in this model of type 2 diabetes. The treatment of normal mice with recombinant resistin impaired glucose tolerance and insulin action. Insulin-stimulated glucose uptake by adipocytes was enhanced by neutralization of resistin and reduced by resistin treatment[6]. The association between elevated circulating resistin and insulin resistance in patients with type 2 diabetes has also been revealed[7-11].

The results of studies on the association between resistin and GDM risk vary greatly. Some studies have suggested that elevated circulating resistin is a risk factor for GDM[12-26], while some have suggested that elevated circulating resistin is a protective factor[27-30], and others have suggested that resistin circulating level is not associated with GDM risk[31-52]. Variations in gestational age at sample collection, assay methods, fasting state, sample size, ethnicity, diagnosis criteria, severity of GDM, and definitions of controls could account for the considerable differences of the results of these studies. In a study performed by Steppan *et al*[6], they found that resistin expression was adipocyte-specific. However, recent reports suggest that resistin is

also expressed in multiple other tissues, such as pancreatic islets, skeletal muscles, mononuclear cells, placenta, and liver cells[51,53,54]. During pregnancy, the placenta synthesizes and secretes resistin into the maternal circulation[55,56]. One study found that resistin protein expression in placental tissue was much higher than that in subcutaneous adipose tissue in pregnant women's abdomens, suggesting that the placenta is a major contributor of resistin in pregnancy[57]. Several studies have shown that the maternal circulating level of resistin gradually increases with gestational age and decreases significantly after delivery[17-19,23,37,40,42,44]. This process of change is consistent with the growth and delivery of the placenta.

Notably, a previous meta-analysis published in 2013 that included 10 papers showed no association between circulating resistin levels and GDM[58]. However, the authors suggested that these results should be interpreted with caution owing to the large heterogeneity among the studies. Since 2013, there have been many high-quality articles on serum resistin levels and GDM. Therefore, we think it is necessary to conduct another meta-analysis, and since there is a sufficient number of articles, we can perform a meta-regression analysis and subgroup analysis to explore possible influencing factors. The purpose of this study was to review the literature on the association of resistin and GDM risk, and attempt to find potential influence factors to interpret the considerable differences of the results of these studies.

MATERIALS AND METHODS

Literature search

The databases MEDLINE, EMBASE, and Web of Science (all databases, including Web of Science Core Collection, BIOSIS Citation Index, *etc.*) were searched up to October 11, 2018 to find articles focused on the relationship between the risk of GDM and serum resistin level. The following keywords were used in PubMed and Web of Science: ("Diabetes, Gestational" [Mesh] OR "GDM" OR "gestational diabetes" OR "gestational diabetic" OR "diabetic pregnancy") AND ("resistin" [MeSH] OR resistin OR RETN OR ADSF OR RSTN OR XCP1 OR FIZZ3 OR RETN1). The following keywords were used in EMBASE: ("pregnancy diabetes mellitus"/exp OR "gestational diabetes" OR "gestational diabeti" OR "diabetic pregnancy" OR "gdm") AND ("resistin"/exp OR "resistin" OR "RETN" OR "ADSF" OR "RSTN" OR "XCP1" OR "FIZZ3" OR "RETN1"). We manually searched all the reference lists of the included studies and relevant reviews to find additional eligible studies.

Eligible studies, data extraction, and quality evaluation

This meta-analysis included eligible studies that: (1) investigated the relationship between the risk of GDM and serum resistin; (2) included GDM cases and controls without GDM; (3) diagnosed GDM according to the oral glucose-tolerance test; (4) were performed in humans; (5) were published as full text articles in English; and (6) provided data with median and quartile range, median and minimum and maximum values, or mean and standard deviation (SD). We excluded the studies with overlapping data. Information of the first author, study location (country), study design, year of publication, diagnostic criteria, number of patients and controls, gestational age at the time of blood sampling, assay methods, need for insulin in GDM patients, and the mean and SD of serum resistin levels was extracted. The quality of each included study was evaluated based on the Newcastle-Ottawa Scale (NOS) recommended by the Agency for Healthcare Research and Quality of the US[59]. Comparability of cases and controls on the basis of the design or analysis was evaluated based on whether the gestational age and body mass index (BMI) at blood sampling matched. The NOS total score of the literature included had to be greater than or equal to 5 points. Disputes were resolved by discussion with a third author during data extraction and quality evaluation. The equation "SD = SEM × $\sqrt{(n)}$" was used to calculate SD from the standard error of the mean (SEM). If we need to merge the data of subgroups, we used the following equations: $n = n_1 + n_2$, $\overline{x} = (n_1\overline{x}_1 + n_2\overline{x}_2)/(n_1 + n_2)$ and $SD = \sqrt{\{[(n_1\text{-}1)SD_1^2 + (n_2\text{-}1)SD_2^2 + n_1n_2/(n_1 + n_2)(\overline{x}_1^2 + \overline{x}_2^2 - 2\overline{x}_1\overline{x}_2)]/(n_1 + n_2 - 1)\}}$ [60]. The equation "SD = interquartile range/1.35" was used to calculate SD from interquartile ranges. And we treated the medians as means[61]. However, if we were provided with the minimum and maximum values, we calculated means and SDs according to the equations in the study of Hozo *et al*[62]. When serum resistin levels were measured in both nonfasting and fasting blood samples at the same gestational age, we chose the fasting result here.

Statistical analysis

The pooled standardized mean difference (SMD) and 95% confidence interval (CI)

were used to estimate the relationship between the risk of GDM and serum resistin. Subgroup analyses were performed to detect whether "need for insulin" or "gestational age at blood sampling" influenced the relationship between the risk of GDM and serum resistin. We divided the subjects into four subgroups according to the gestational age at blood sampling ("before 14 wk", "14-28 wk", "after 28 wk", and "postpartum"). If the gestational age of the included study did not completely overlap with the gestational age of the subgroup, we would assign the study into the subgroup with the most overlap with the gestational age of the study. The study of Kuzmicki *et al*[14] was assigned to the "14-28 wk" subgroup. The studies of Kralisch *et al*[39], Siddiqui *et al*[25], and Palik *et al*[17] were assigned to the subgroup of "after 28 wk". Additionally, based on the "need for insulin in GDM patients", the subjects were divided into three subgroups: (1) need for insulin; (2) no need for insulin; and (3) no information. The Z test was used to determine the significance of the pooled SMD, with α set at 0.05.

The Q test and the I^2 statistic were used to estimate the heterogeneity across studies[63,64]. If $P < 0.1$ in the Q test, and $I^2 > 50\%$, we used the random effects model to pool the data; and meta-regression with restricted maximum likelihood estimation (REML) was performed to assess the potentially important covariate exerting substantial impact on between-study heterogeneity. The following covariates were included in the meta-regression analysis: need for insulin (no need for insulin, need for insulin, OR no information; dummy variable), assay method (ELISA OR others), and maternal age distribution (similar between cases and controls OR different between cases and controls) in each study. Begg's funnel plot and Egger's test and sensitivity analysis were used to assess the publication bias and the stability of the results. STATA 12.0 software (Stata Corporation, College Station, TX) was the only analysis software in this meta-analysis. The statistical methods of this study were reviewed by Jun-Xia Yan from Department of Epidemiology and Health Statistics, Central South University, China.

RESULTS

Study selection

The process of study selection is shown in Figure 1. Three hundred and one records of potentially relevant studies were identified. Of these, 199 records were excluded based on their title and/or abstract ("repetitive publications": n = 132; "conference abstracts": n = 18; "reports of animal studies": n = 6; "reports of studies that investigated outcomes irrelevant to this meta-analysis": n = 31; "adipokines other than resistin": n = 1; "studies of which the biological material was not maternal blood": n = 11). A further 77 full-text articles were excluded because these were: (1) review, editorial, and opinion articles (n = 49); (2) studies in which interviewees were not grouped according to whether they had GDM (n = 11); (3) a study in which the controls were not pregnant women and had never been pregnant (n = 1); (4) papers with plasma resistin concentrations reported (n = 13); (5) non-full-text articles in English (n = 2); and (6) *RETN* gene study (n = 1). After in-depth analysis, seven more studies were excluded. The specific reasons for the exclusion and the detailed information of these seven papers are shown in Supplementary Table 1. The 18 studies (22 comparisons) that were ultimately selected for our meta-analysis included 1041 cases and 1292 controls (Tables 1 and 2).

Association between the risk of GDM and serum resistin level

The meta-analysis included 18 studies (22 comparisons) with 1041 cases and 1292 controls. The total results showed that higher serum resistin was associated with the risk of GDM (SMD = 0.250, 95%CI: 0.116, 0.384) (Table 3 and Figure 2). The "after 28 wk", "no need for insulin", and "need for insulin" subgroups indicated that higher serum resistin was related to the risk of GDM ("after 28 wk" subgroup: SMD = 0.394, 95%CI: 0.108, 0.680; "no need for insulin" subgroup: SMD = 0.177, 95%CI: 0.018, 0.336; "need for insulin" subgroup: SMD = 0.403, 95%CI: 0.119, 0.687). The "before 14 wk" subgroup, "14-28 wk" subgroup, and "no information of need for insulin" subgroup showed a nonsignificant association between serum resistin level and GDM risk ("before 14 wk" subgroup: SMD = 0.087, 95%CI: -0.055, 0.230; "14-28 wk" subgroup: SMD = 0.217, 95%CI: -0.003, 0.436; "no information of need for insulin" subgroup: SMD = 0.356, 95%CI: -0.143, 0.855). The postpartum subgroup included only one study and showed that higher serum resistin level was related to GDM risk (SMD = 0.571, 95%CI: 0.054, 1.087) (Table 3, Figures 3 and 4).

Table 4 summarizes results of meta-regression; "no need for insulin in GDM patients", "age distribution similar between cases and controls", and ELISA all had a

Table 1 Detailed characteristics of all eligible studies for the association between serum resistin levels and gestational diabetes mellitus

Ref.	Location	Study design	Number GDM/C	GDM diagnosis	Time for sampling	Assay method	Need for insulin *n* (%)	Resistin level, ng/mL mean ± SD		
								GDM	Control	*P*
Tsiotra *et al*[49], 2018	Greece	CC	15/23	75 g ADA	39 wk	LUMINEX xMAP	4 (26.7)	26.147 ± 7.337	23.440 ± 1.567	NS
Lobo *et al*[42], 2018	Brazil	CC	15/30	75 g IADPSG	< 14 wk	ELISA	0	14.047 ± 5.334	12.357 ± 4.747	NS
			18/28		14-20 wk		0	14.420 ± 6.157	14.219 ± 5.721	NS
Siddiqui *et al*[25], 2018	Saudi Arabia	CC	14/21	100 g ADA	24-32 wk	Randox evidence biochip analyzer	NI	9.1 ± 4.2	6.1 ± 1.6	0.02
Bagci *et al*[21], 2018	Turkey	CC	40/40	100 g NDDG	24-28 wk	ELISA	NI	16.78 ± 6.83	12.79 ± 5.02	0.004
Khanam *et al*[37], 2017	Australia	Cohort	52/71	75 g ADIPS	14 wk	Multiplex assay kits	0	0.667 ± 0.515	0.697 ± 0.249	NS
			52/71		18 wk		0	0.896 ± 0.547	0.806 ± 0.416	NS
Ravnsborg *et al*[45], 2016	Denmark	CC	199/208	75 g 2 h ≥ 9.0 mmol/L	8^{+1}-13^{+6} wk	ELISA	78 (39.2)	14.06 ± 6.43	13.22 ± 4.87	NS
Huang *et al*[13], 2016	China	CC	43/24	75 g IADPSG	37-40 wk	ELISA	17 (39.5)	19240 ± 5860	14570 ± 4890	< 0.05
Takhshid and Zare[48], 2015	Iran	CC	75/70	100 g Carpenter and Coustan	30 wk	ELISA	NI	13.0 ± 6.6	11.4 ± 6.9	NS
Boyadzhieva *et al*[32], 2013	Bulgaria	CC	127/109	75 g IADPSG	24-28 wk	BioVendor® kits	0	10.11 ± 2.2	9.09 ± 3.2	NS
Nanda *et al*[43], 2012	UK	CC	60/240	75 g fasting ≥ 6.0 mmol/L or 2 h ≥ 7.8 mmol/L	11-13 wk	ELISA	0	8.32 ± 4.58	8.28 ± 3.38	NS
Skvarca *et al*[47], 2012	Slovenia	CS	30/25	100 g Carpenter and Coustan	Approximately 27 wk	ELISA	0	2.00 ± 0.68	2.40 ± 1.26	NS
Akdeniz *et al*[31], 2011	Turkey	CC	20/22	ADA	Before delivery	ELISA	20 (100)	8.7 ± 2.1	8.1 ± 2.5	NS
Vitoratos *et al*[18], 2011	Greece	Cohort	30/30	100 g Carpenter and Coustan	26-28 wk	Sandwich immunoassay kit	0	0.21 ± 0.08	0.19 ± 0.12	NS
			30/30		38 wk		0	0.28 ± 0.2	0.21 ± 0.13	0.02
			30/30		The third postpartum day		0	0.25 ± 0.11	0.19 ± 0.10	0.03
Kleiblova *et al*[38], 2010	Czech Republic	CC	10/13	75 g Czech Diabetes Association	At delivery	ELISA	10 (100)	12.6 ± 4.2	10.9 ± 2.1	NS
Vitoratos *et al*[50], 2010	Greece	CC	30/30	100 g Carpenter and Coustan	24-26 wk	Sandwich immunoassay kit	0	0.1913 ± 0.1096	0.21 ± 0.0822	NS
Kralisch *et al*[39], 2009	Germany	CC	40/80	75 g ADA	G: 29 ± 3 wk; C: 28 ± 4 wk	ELISA	NI	6.5 ± 2.7	7.4 ± 3.3	NS
Kuzmicki *et al*[14], 2009	Poland	CC	81/82	75 g WHO	24-31 wk	Quantikine immunoassay kit	0	21.9 ± 5.9	19.0 ± 5.9	< 0.001
Palik *et al*[17], 2007	Hungary	CS	30/15	75 g WHO	26-30 wk	ELISA	30 (100)	15.76 ± 3.52	13.0 ± 3.60	< 0.001

CC: Case-control study; CS: Cross-sectional study; ADA: American Diabetes Association; IADPSG: International Association of Diabetic Pregnancy Study Group; WHO: World Health Organization; NDDG: National Diabetes Data Group; ADIPS: Australasian Diabetes in Pregnancy Society; RIA: Radio Immunoassay; NI: No information; NS: Non-significant.

Table 2 Quality assessment of the included studies based on scores of Newcastle-Ottawa Scale (case-control study version and cohort version)

Ref.	Case definition adequacy	Representativeness of cases	Selection of controls	Definition of controls	Comparability of cases and controls	Ascertainment of exposure	Same method of ascertainment for cases and controls	Non-response rate	Total quality score
Tsiotra *et al*[49], 2018	1	0	0	1	1	1	1	NI	5
Lobo *et al*[42], 2018	1	1	1	1	2	1	1	1	9
Siddiqui *et al*[25], 2018	1	0	0	1	1	1	1	NI	5
Bagci *et al*[21], 2018	1	0	0	1	1	1	1	NI	5
Ravnsborg *et al*[45], 2016	1	1	1	1	2	1	1	1	9
Huang *et al*[13], 2016	1	0	0	1	2	1	1	NI	6
Takhshid and Zare[48], 2015	1	0	0	1	2	1	1	NI	6
Boyadzhieva *et al*[32], 2013	1	1	1	1	1	1	1	NI	7
Nanda *et al*[43], 2012	1	1	0	1	1	1	1	NI	6
Skvarca *et al*[47], 2012	1	0	0	1	2	1	1	NI	6
Akdeniz *et al*[31], 2011	1	0	0	1	1	1	1	NI	5
Kleiblova *et al*[38], 2010	1	0	0	1	1	1	1	NI	5
Vitoratos *et al*[50], 2010	1	0	0	1	2	1	1	NI	6
Kralisch *et al*[39], 2009	1	0	0	1	2	1	1	NI	6
Kuzmicki *et al*[14], 2009	1	0	0	1	2	1	1	NI	6
Palik *et al*[17], 2007	1	0	0	1	1	1	1	NI	5

Ref.	Representativeness of the exposed cohort	Selection of the non-exposed cohort	Ascertainment of exposure	Demonstration that outcome of interest was not present at start of study	Comparability of cohorts	Assessment of outcome	Follow-up long enough for outcomes to occur	Adequacy of follow -up of cohorts	Total quality score
Khanam *et al*[37], 2017	0	1	1	1	2	1	1	0	7
Vitoratos *et al*[18], 2011	0	1	1	1	2	1	1	1	8

NI: No information.

significant impact on between-study heterogeneity. REML estimate of between-study variance tau2 decreased from 0.0482 to 0.02687, indicating that these variables can account for 44.3% of heterogeneity sources. No association was statistically significant when meta-regression was performed on the three strategies considered one by one. In the sensitivity analysis, no changes were observed in the significance of the results or in the corresponding pooled SMD (Figure 5). In the publication bias analysis, the results of Begg's funnel plot and the modified Egger linear regression test (Figure 6) showed no publication bias ($Z = 1.30$, $P = 0.195$; $t = 1.10$, $P = 0.284$).

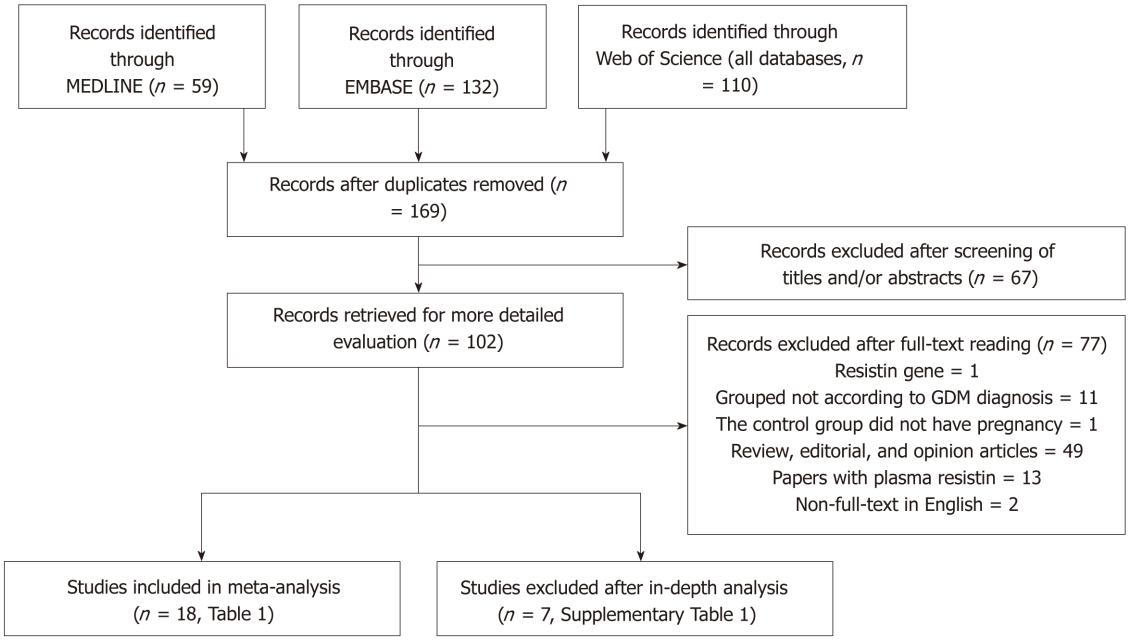

Figure 1 PRISMA flow diagram of the study selection process. GDM: Gestational diabetes mellitus.

DISCUSSION

The results of the studies focused on the association of maternal serum resistin level and GDM risk varied widely due to differences in study design type, ethnicity, diagnostic criteria for GDM, insulin use in GDM patients, inclusion criteria of the control group, the distribution equilibrium of maternal age, BMI, gestational age at sampling, sample size, serum/plasma selection, sample storage methods, and assay methods. To obtain a more reliable meta-analysis result, we set a threshold for the diagnostic criteria of GDM. To explore the possible influencing factors of the results, we performed subgroup analyses according to the gestational age at sampling and need for insulin in GDM patients. The total results showed that serum resistin level was associated with GDM. The results of the third trimester, "no need for insulin", and "need for insulin" subgroups were consistent with the total result.

The effect of resistin on blood glucose was confirmed in animal studies by highly evidence-based studies[6,65]. In a mouse model, Steppan *et al*[6] found that resistin levels were increased in diet-induced obesity, as well as in genetic models of obesity and insulin resistance. Neutralization of resistin reversibly reduced hyperglycemia in this model of diet-induced insulin resistance. The ability of recombinant resistin to produce glucose intolerance and insulin resistance is consistent with the opposite effects of immunoneutralization of endogenous resistin. Similar effects of resistin, *i.e.*, decreasing insulin-stimulated glucose uptake, were confirmed *in vitro* by using 3T3-L1 adipocytes[6]. Banerjee *et al*[65] studied the mechanism by which resistin regulates blood glucose, and they found that mice lacking resistin exhibited low blood glucose levels after fasting due to the impairment of hepatic glucose output. Resistin normally acts on the liver to inhibit the activation of adenosine monophosphate-activated protein kinase (AMPK). The key gluconeogenic enzymes glucose 6-phosphatase (*G6Pase*) and phosphoenolpyruvate carboxykinase (*PEPCK*) genes are both downregulated by activation of AMPK. Gene expression of *G6Pase* and *PEPCK* was markedly decreased in the liver of the resistin-null mice[65]. There have been no animal studies related to circulating resistin level and GDM risk.

The association between elevated serum resistin level and GDM was only found in the third-trimester subgroup when we divided the studies into four subgroups according to the gestational age. This may be because the serum level of resistin increases with gestational age[17-19,23,37,40,42,44], and the gap in resistin levels between GDM and the controls may also increase with increasing gestational age. Figure 3 shows this trend. Therefore, a study focusing on the association between the serum resistin level and GDM risk in the first and second trimesters would require a larger sample size than one focusing only on the third trimester. Choi *et al*[12] found higher circulating resistin levels in women with pGDM than in women with normal glucose tolerance during pregnancy and one year after delivery, suggesting that in addition to the placenta, other secretory organs such as adipose tissue may also contribute to the

Table 3 Summary of different comparative results of serum resistin level with gestational diabetes mellitus risk

Category		No. of comparisons	No. of cases	No. of controls	SMD (95%CI)	Z	*P*	I^2%	P_{het}
Overall		22	1041	1292	0.250 (0.116, 0.384)	3.65	0.000	53.1	0.002
Gestational age at blood sampling	Before 14 wk	4	326	549	0.087 (-0.055, 0.230)	1.20	0.229	0.0	0.550
	14-28 wk	8	408	415	0.217 (-0.003, 0.436)	1.93	0.053	55.5	0.028
	After 28 wk	9	277	298	0.394 (0.108, 0.680)	2.70	0.007	60.5	0.009
	Postpartum	1	30	30	0.571 (0.054, 1.087)	-	-	-	-
Need for insulin	No need for insulin	12	555	776	0.177 (0.018, 0.336)	2.18	0.029	43.7	0.052
	Need for insulin	6	317	305	0.403 (0.119, 0.687)	2.78	0.005	44.9	0.106
	No information	4	169	211	0.356 (-0.143, 0.855)	1.40	0.162	80.6	0.001

P_{het}: *P* value for heterogeneity; OR: Odds ratio; CI: Confidence interval; SMD: Standardized mean difference.

occurrence of GDM. A study on circulating resistin and fat mass compartments in pregnancy revealed that resistin levels are not related to BMI, total body fat mass, or abdominal subcutaneous fat mass but are related to abdominal visceral fat mass[66]. In this meta-analysis, the postpartum subgroup included only one study. Further research may be needed to focused on the postpartum. The results of the subgroup analysis, according to the need for insulin, showed that the pooled SMD of "need for insulin in GDM patients" was higher than the pooled SMD of "no need for insulin in GDM patients", suggesting that the serum level of resistin may be related to the severity of GDM. The research of Huang *et al*[13] showed that among pregnant women with GDM, the serum resistin levels of women with satisfactory glycemic control were lower than those in women with unsatisfactory glycemic control[13].

Studies on *RETN* (gene encoded resistin) mRNA and SNPs have also suggested that resistin is associated with GDM risk. The mRNA expression of *RETN* was increased in adipose tissue from GDM when compared to a non-GDM group, was related to insulin resistance level, and could be regulated by adrenomedullin and an adrenomedullin antagonist[13,67,68]. *RETN* rs1423096 and -420 C/G were found to be associated with GDM risk[48,69], and it has been reported that the G allele of -420 C/G in the *RETN* gene promoter was associated with an increase in circulating resistin[70,71].

In summary, our meta-analysis showed that higher maternal serum resistin level is related to GDM risk and suggested that the serum level of resistin may be related to the severity of GDM. Studies focusing on the association between the serum resistin level and GDM risk in the first and second trimesters would require a larger sample size than ones focusing only on the third trimester.

Table 4 Meta-regression analysis results

Covariate	Coefficient	Std. error	*t*	*P*	95%CI lower	95%CI upper
No need for insulin	-0.482	0.183	-2.64	0.017	-0.868	-0.097
Need for insulin	-0.169	0.190	-0.89	0.388	-0.570	0.233
Age distribution similar	0.298	0.126	2.37	0.030	0.033	0.563
ELISA	-0.399	0.160	-2.50	0.023	-0.737	-0.062

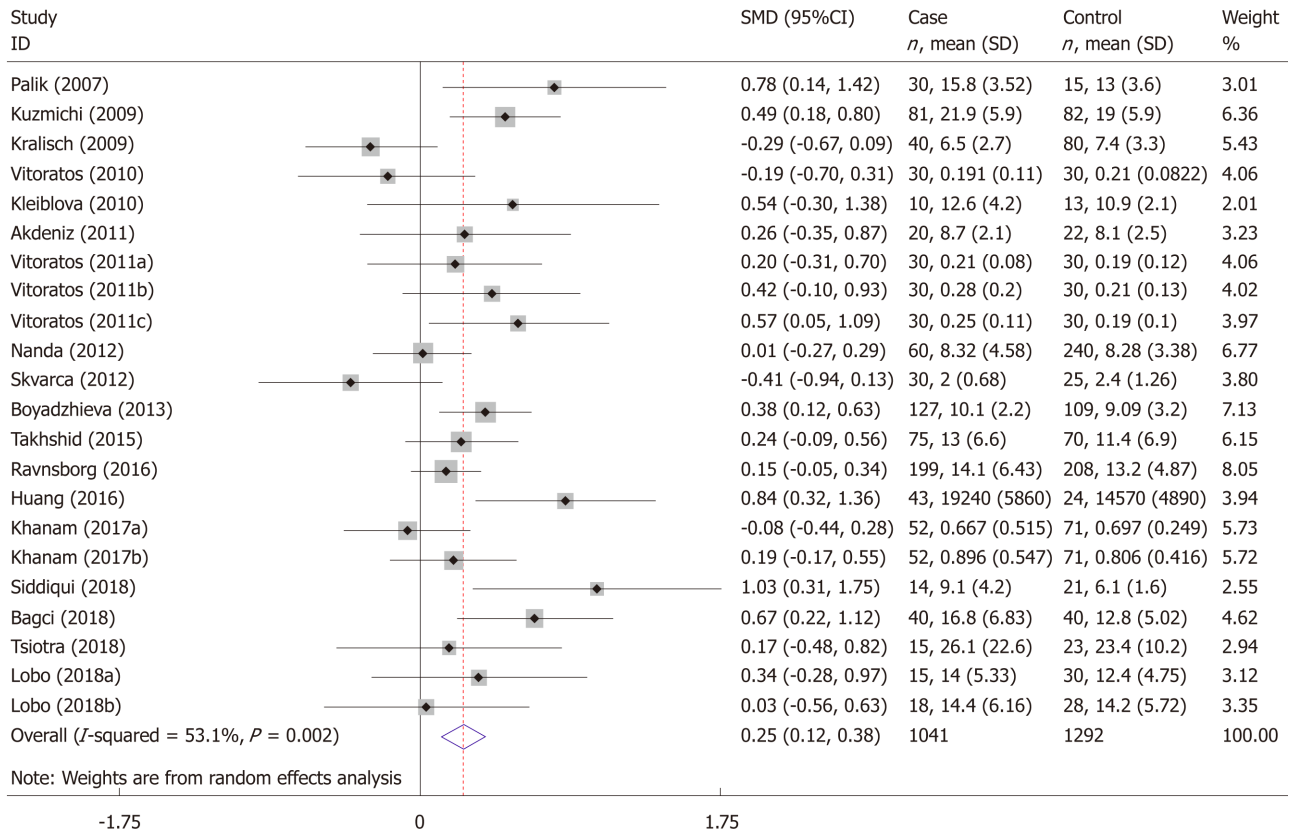

Figure 2 Meta-analysis for the association of serum resistin level with gestational diabetes mellitus risk using a random effects model.

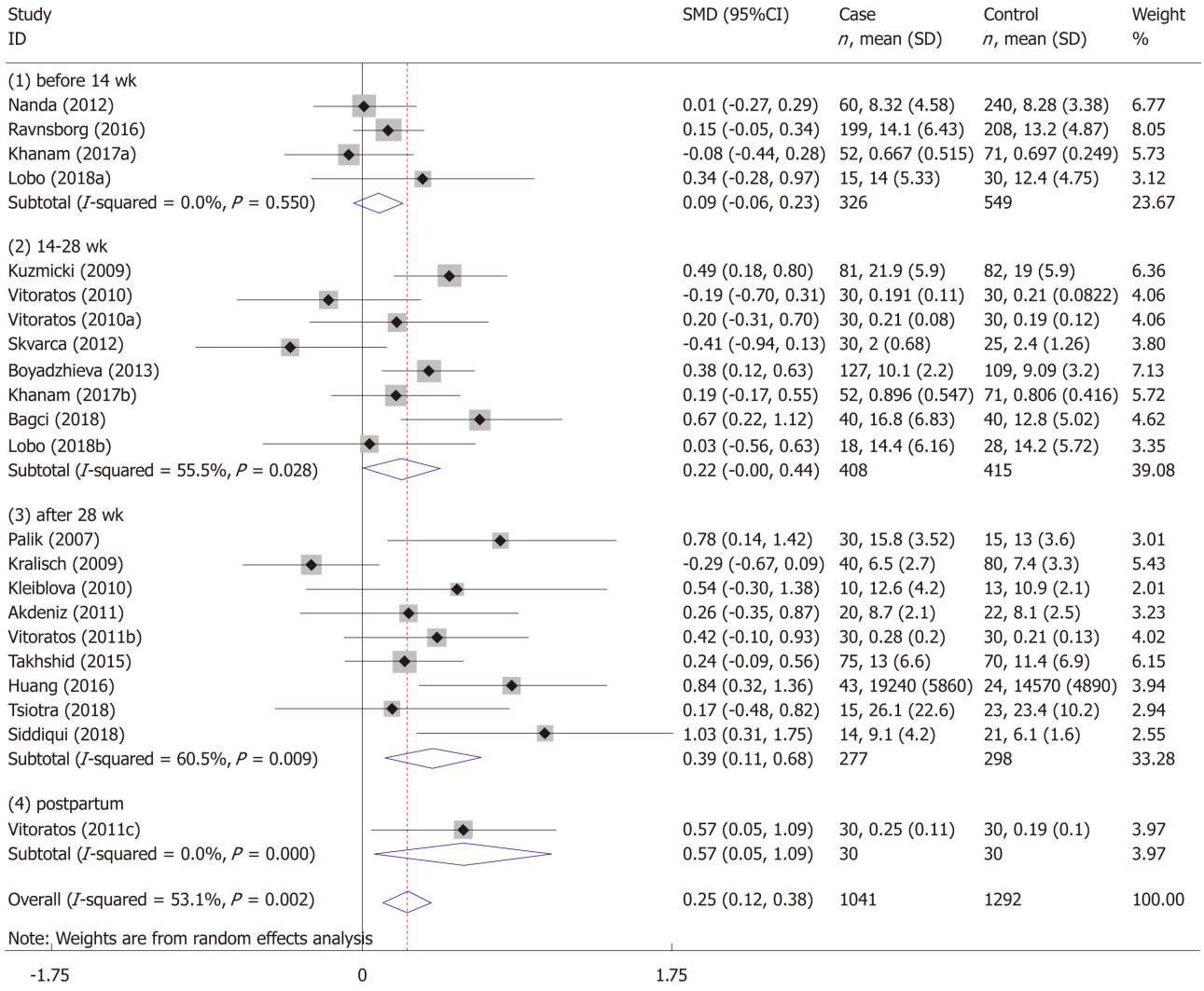

Figure 3 Gestational age at blood sampling subgroup analysis using a random effects model.

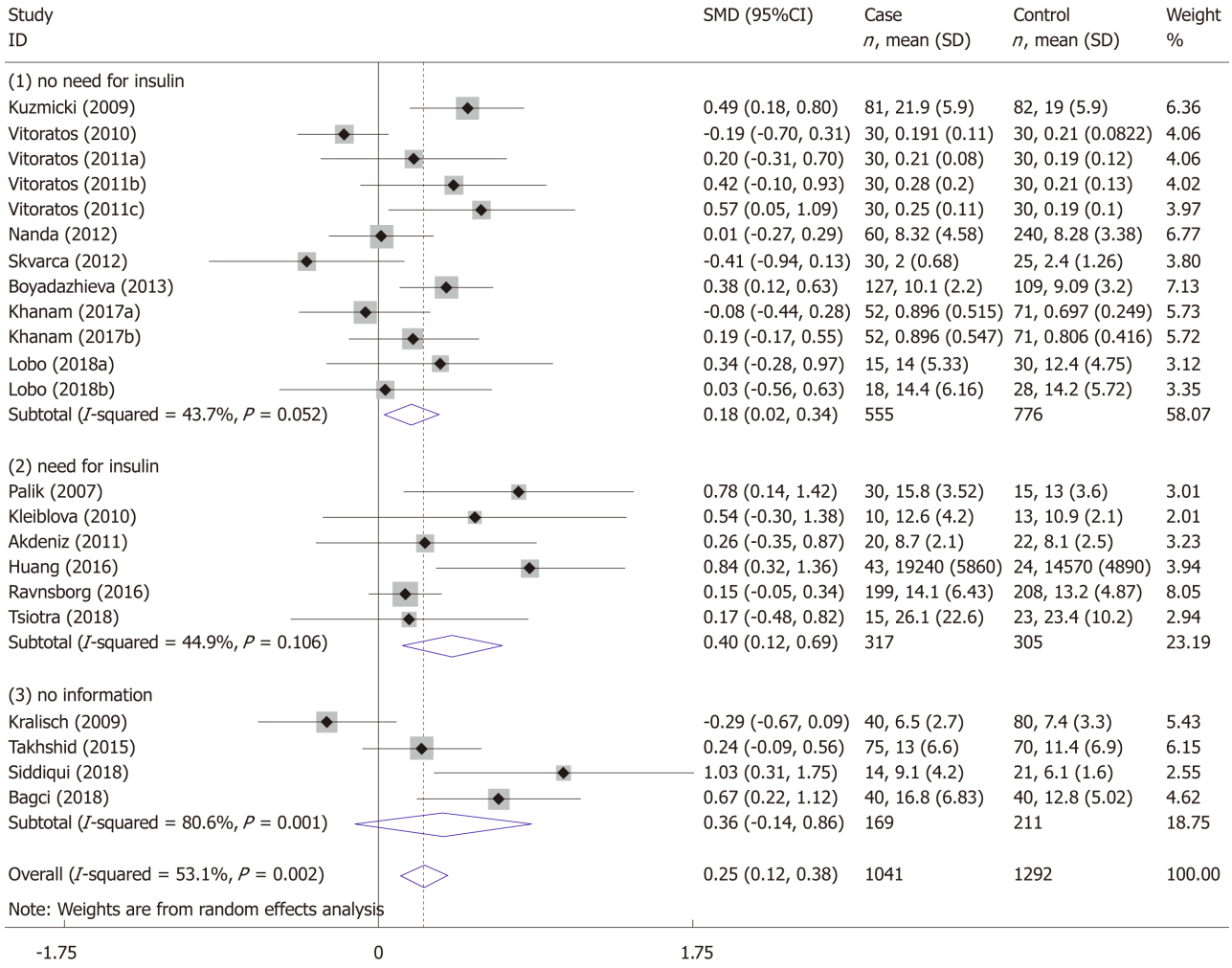

Figure 4 Need for insulin subgroup analysis using a random effects model.

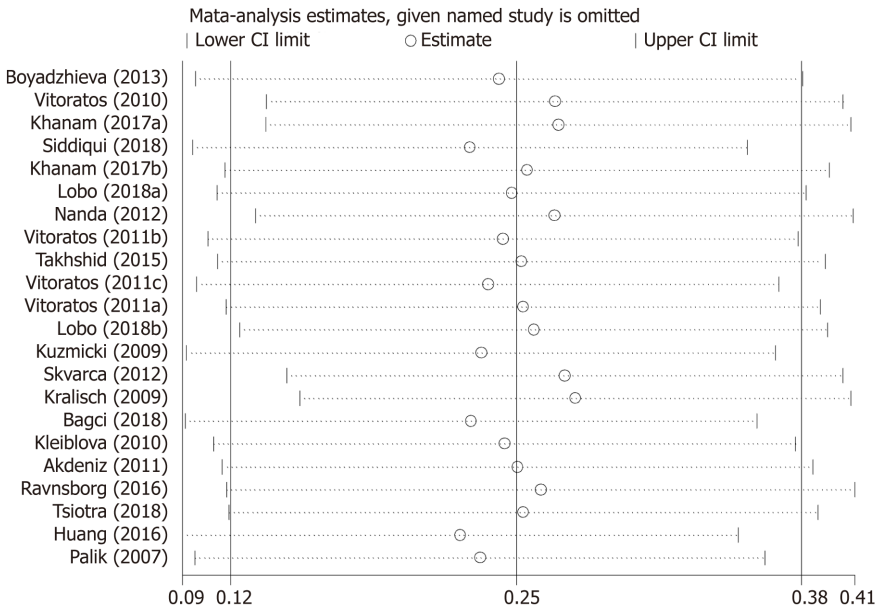

Figure 5 Results of sensitivity analysis of serum resistin level with gestational diabetes mellitus risk.

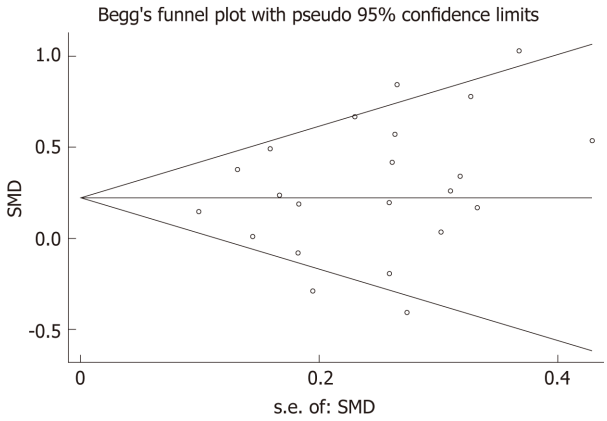

Figure 6 Begg's funnel plot for publication bias test of serum resistin level with gestational diabetes mellitus risk. SMD: Standardized mean difference.

ARTICLE HIGHLIGHTS

Research background

Resistin is most likely involved in the pathogenesis of gestational diabetes mellitus (GDM), but the existing findings are inconsistent.

Research motivation

To explore the sources of heterogeneity in the existing literature, we made the literature heterogeneity within an acceptable range by setting reasonable inclusion criteria. Based on this, we aimed to explore the relationship between serum level of resistin and GDM risk.

Research objectives

This article aims to review the studies investigating the association of GDM risk with serum resistin level.

Research methods

A systematic literature search was performed using MEDLINE, EMBASE, and Web of Science (all databases). We did subgroup analysis according to the need for insulin in GDM patients and gestational age at blood sampling. Meta-regression with restricted maximum likelihood estimation was performed to assess the potentially important covariate exerting substantial impact on between-study heterogeneity.

Research results

The meta-analysis included 18 studies (22 comparisons) with 1041 cases and 1292 controls. The total results showed that the risk of GDM was associated with serum resistin level. The results of subgroup are consistent with the total results. The meta-regression revealed that no need for insulin in GDM patients, age distribution similar between cases and controls, and ELISA all had a significant impact on between-study heterogeneity.

Research conclusions

This meta-analysis supports that the maternal serum resistin level is associated with GDM risk.

Research perspectives

In summary, our meta-analysis showed that higher maternal serum resistin level is related to GDM risk and suggested that the serum level of resistin may be related to the severity of GDM.

REFERENCES

1 **Buchanan TA**, Xiang AH. Gestational diabetes mellitus. *J Clin Invest* 2005; **115**: 485-491 [PMID: 15765129 DOI: 10.1172/Jci200524531]
2 **Schneider S**, Bock C, Wetzel M, Maul H, Loerbroks A. The prevalence of gestational diabetes in advanced economies. *J Perinat Med* 2012; **40**: 511-520 [PMID: 23120759 DOI: 10.1515/jpm-2012-0015]
3 **Li X**, Tan H, Huang X, Zhou S, Hu S, Wang X, Xu X, Liu Q, Wen SW. Similarities and differences between the risk factors for gestational hypertension and preeclampsia: A population based cohort study in south China. *Pregnancy Hypertens* 2016; **6**: 66-71 [PMID: 26955775 DOI: 10.1016/j.preghy.2015.11.004]
4 **He XJ**, Qin FY, Hu CL, Zhu M, Tian CQ, Li L. Is gestational diabetes mellitus an independent risk factor for macrosomia: a meta-analysis? *Arch Gynecol Obstet* 2015; **291**: 729-735 [PMID: 25388922 DOI: 10.1007/s00404-014-3545-5]
5 **Hartling L**, Dryden DM, Guthrie A, Muise M, Vandermeer B, Donovan L. Benefits and harms of treating gestational diabetes mellitus: a systematic review and meta-analysis for the U.S. Preventive Services Task Force and the National Institutes of Health Office of Medical Applications of Research. *Ann Intern Med*

2013; **159**: 123-129 [PMID: 23712381 DOI: 10.7326/0003-4819-159-2-201307160-00661]
6 **Steppan CM**, Bailey ST, Bhat S, Brown EJ, Banerjee RR, Wright CM, Patel HR, Ahima RS, Lazar MA. The hormone resistin links obesity to diabetes. *Nature* 2001; **409**: 307-312 [PMID: 11201732 DOI: 10.1038/35053000]
7 **Srinivasan M**, Meadows ML, Maxwell L. Assessment of Salivary Adipokines Resistin, Visfatin, and Ghrelin as Type 2 Diabetes Mellitus Biomarkers. *Biochem Res Int* 2018; **2018**: 7463796 [PMID: 29487749 DOI: 10.1155/2018/7463796]
8 **Tokuyama Y**, Osawa H, Ishizuka T, Onuma H, Matsui K, Egashira T, Makino H, Kanatsuka A. Serum resistin level is associated with insulin sensitivity in Japanese patients with type 2 diabetes mellitus. *Metabolism* 2007; **56**: 693-698 [PMID: 17445546 DOI: 10.1016/j.metabol.2006.12.019]
9 **Heidemann C**, Sun Q, van Dam RM, Meigs JB, Zhang C, Tworoger SS, Mantzoros CS, Hu FB. Total and high-molecular-weight adiponectin and resistin in relation to the risk for type 2 diabetes in women. *Ann Intern Med* 2008; **149**: 307-316 [PMID: 18765700 DOI: 10.7326/0003-4819-149-5-200809020-00005]
10 **Majdi MA**, Mohammadzadeh NA, Lotfi H, Mahmoudi R, Alipour FG, Shool F, Moghanloo MN, Porfaraj S, Zarghami N. Correlation of Resistin Serum Level with Fat Mass and Obesity-Associated Gene (FTO) rs9939609 Polymorphism in Obese Women with Type 2 Diabetes. *Diabetes Metab Syndr* 2017; **11** Suppl 2: S715-S720 [PMID: 28566238 DOI: 10.1016/j.dsx.2017.05.004]
11 **Santilli F**, Liani R, Di Fulvio P, Formoso G, Simeone P, Tripaldi R, Ueland T, Aukrust P, Davì G. Increased circulating resistin is associated with insulin resistance, oxidative stress and platelet activation in type 2 diabetes mellitus. *Thromb Haemost* 2016; **116**: 1089-1099 [PMID: 27709225 DOI: 10.1160/th16-06-0471]
12 **Choi SH**, Kwak SH, Youn BS, Lim S, Park YJ, Lee H, Lee N, Cho YM, Lee HK, Kim YB, Park KS, Jang HC. High plasma retinol binding protein-4 and low plasma adiponectin concentrations are associated with severity of glucose intolerance in women with previous gestational diabetes mellitus. *J Clin Endocrinol Metab* 2008; **93**: 3142-3148 [PMID: 18492757 DOI: 10.1210/jc.2007-1755]
13 **Huang H**, Xiao L, Wang A, Gu J, Ke H, Yan Y, Yang X. Correlation of resistin expression in maternal serum and subcutaneous adipose tissue with insulin resistance in gestational diabetes mellitus. *Int J Clin Exp Med* 2016; **9**: 18721-18727
14 **Kuzmicki M**, Telejko B, Szamatowicz J, Zonenberg A, Nikolajuk A, Kretowski A, Gorska M. High resistin and interleukin-6 levels are associated with gestational diabetes mellitus. *Gynecol Endocrinol* 2009; **25**: 258-263 [PMID: 19408175 DOI: 10.1080/09513590802653825]
15 **Liu DY**, Yu J, Zhou SX, Zhou Y, Li QM, Shi XY, Lin F, Shi QF. Study of levels of resistin in patients with gestational diabetes mellitus. *Dalian Yike Daxue Xuebao* 2008; **30**: 334-335, 343
16 **Oncul M**, Tuten A, Erman H, Gelisgen R, Benian A, Uzun H. Maternal and cord blood apelin, resistin and visfatin levels in gestational diabetes mellitus. *Minerva Med* 2013; **104**: 527-535 [PMID: 24101110 DOI: 10.1186/1471-2296-14-145]
17 **Palik E**, Baranyi E, Melczer Z, Audikovszky M, Szöcs A, Winkler G, Cseh K. Elevated serum acylated (biologically active) ghrelin and resistin levels associate with pregnancy-induced weight gain and insulin resistance. *Diabetes Res Clin Pract* 2007; **76**: 351-357 [PMID: 17010469 DOI: 10.1016/j.diabres.2006.09.005]
18 **Vitoratos N**, Deliveliotou A, Dimitrakaki A, Hassiakos D, Panoulis C, Deligeoroglou E, Creatsas GK. Maternal serum resistin concentrations in gestational diabetes mellitus and normal pregnancies. *J Obstet Gynaecol Res* 2011; **37**: 112-118 [PMID: 21159034 DOI: 10.1111/j.1447-0756.2010.01327.x]
19 **Chen D**, Fang Q, Chai Y, Wang H, Huang H, Dong M. Serum resistin in gestational diabetes mellitus and early postpartum. *Clin Endocrinol (Oxf)* 2007; **67**: 208-211 [PMID: 17547683 DOI: 10.1111/j.1365-2265.2007.02862.x]
20 **Akdeniz FT**, Akbulut Z, Sarı H, Aydın H, Dalan AB, Şit D, İspir T, Demirel GY. Effect of pro-inflammatory markers on gestational diabetes. *Turkish J Immunology* 2017; **5**: 45-50 [DOI: 10.25002/tji.2017.586]
21 **Bagci H**, Melekoglu R, Gursu MF, Akyol A, Bulmus FG. Associations between serum levels of adiponectin and resistin and metabolic parameters in pregnant women with gestational diabetes mellitus. *Clin Exp Obstet Gynecol* 2018; **45**: 539-543 [DOI: 10.12891/ceog4348.2018]
22 **Oh ES**, Han JH, Han SM, Im JA, Rhee EJ, Park CY, Oh KW, Lee WY. Adipokine Concentrations in Pregnant Korean Women with Normal Glucose Tolerance and Gestational Diabetes Mellitus. *Korean Diabetes J* 2009; **33**: 279-288 [DOI: 10.4093/kdj.2009.33.4.279]
23 **Noureldeen AF**, Qusti SY, Al-Seeni MN, Bagais MH. Maternal leptin, adiponectin, resistin, visfatin and tumor necrosis factor-alpha in normal and gestational diabetes. *Indian J Clin Biochem* 2014; **29**: 462-470 [PMID: 25298627 DOI: 10.1007/s12291-013-0394-0]
24 **Shang M**, Dong X, Hou L. Correlation of adipokines and markers of oxidative stress in women with gestational diabetes mellitus and their newborns. *J Obstet Gynaecol Res* 2018; **44**: 637-646 [PMID: 29399931 DOI: 10.1111/jog.13586]
25 **Siddiqui K**, George TP, Nawaz SS, Shehata N, El-Sayed AA, Khanam L. Serum adipokines (adiponectin and resistin) correlation in developing gestational diabetes mellitus: pilot study. *Gynecol Endocrinol* 2018; **34**: 502-506 [PMID: 29207892 DOI: 10.1080/09513590.2017.1411472]
26 **Zheng L**, Zhang H, Du J. Study on the Correlation of Serum Adiponectin and Resistin with Gestational Diabetes Mellitus Pregnant Women. *Zhongguo Yike Daxue Xuebao* 2011; **40**: 645-648 [DOI: 10.1007/s12264-011-1035-3]
27 **McManus R**, Summers K, de Vrijer B, Cohen N, Thompson A, Giroux I. Maternal, umbilical arterial and umbilical venous 25-hydroxyvitamin D and adipocytokine concentrations in pregnancies with and without gestational diabetes. *Clin Endocrinol (Oxf)* 2014; **80**: 635-641 [PMID: 24102192 DOI: 10.1111/cen.12325]
28 **Megia A**, Vendrell J, Gutierrez C, Sabaté M, Broch M, Fernández-Real JM, Simón I. Insulin sensitivity and resistin levels in gestational diabetes mellitus and after parturition. *Eur J Endocrinol* 2008; **158**: 173-178 [PMID: 18230823 DOI: 10.1530/EJE-07-0671]
29 **Park S**, Kim MY, Baik SH, Woo JT, Kwon YJ, Daily JW, Park YM, Yang JH, Kim SH. Gestational diabetes is associated with high energy and saturated fat intakes and with low plasma visfatin and adiponectin levels independent of prepregnancy BMI. *Eur J Clin Nutr* 2013; **67**: 196-201 [PMID: 23385969 DOI: 10.1038/ejcn.2012.207]
30 **Hossein-nezhad A**, Mirzaei K, Maghbooli Z, Rahmani M, Larijani B. Resistin, adiponectin and visfatin; can adipocytokines predict gestational diabetes mellitus and early post partum metabolic syndrome? *Iranian J Diabetes Lipid Disorders* 2010; **9**: 1-8

31 **Akdeniz N**, Kuyumcuoğlu U, Kale A, Arikan S, Kale E, Erdemoğlu M. Resistin may not associate with gestational diabetes mellitus although insulin resistance. *Clin Exp Obstet Gynecol* 2011; **38**: 236-238 [PMID: 21995154 DOI: 10.1111/j.1524-4741.2010.01035.x]

32 **Boyadzhieva M**, Atanasova I, Zacharieva S, Kedikova S. Adipocytokines during pregnancy and postpartum in women with gestational diabetes and healthy controls. *J Endocrinol Invest* 2013; **36**: 944-949 [PMID: 23685996 DOI: 10.3275/8968]

33 **Cortelazzi D**, Corbetta S, Ronzoni S, Pelle F, Marconi A, Cozzi V, Cetin I, Cortelazzi R, Beck-Peccoz P, Spada A. Maternal and foetal resistin and adiponectin concentrations in normal and complicated pregnancies. *Clin Endocrinol (Oxf)* 2007; **66**: 447-453 [PMID: 17302882 DOI: 10.1111/j.1365-2265.2007.02761.x]

34 **Fugmann M**, Uhl O, Hellmuth C, Hetterich H, Kammer NN, Ferrari U, Parhofer KG, Koletzko B, Seissler J, Lechner A. Differences in the serum nonesterified Fatty Acid profile of young women associated with a recent history of gestational diabetes and overweight/obesity. *PLoS One* 2015; **10**: e0128001 [PMID: 26011768 DOI: 10.1371/journal.pone.0128001]

35 **Georgiou HM**, Lappas M, Georgiou GM, Marita A, Bryant VJ, Hiscock R, Permezel M, Khalil Z, Rice GE. Screening for biomarkers predictive of gestational diabetes mellitus. *Acta Diabetol* 2008; **45**: 157-165 [PMID: 18496643 DOI: 10.1007/s00592-008-0037-8]

36 **Karatas A**, Tunçay Işikkent N, Ozlü T, Demirin H. Relationship of maternal serum resistin and visfatin levels with gestational diabetes mellitus. *Gynecol Endocrinol* 2014; **30**: 355-358 [PMID: 24512558 DOI: 10.3109/09513590.2014.887670]

37 **Guelfi KJ**, Ong MJ, Li S, Wallman KE, Doherty DA, Fournier PA, Newnham JP, Keelan JA. Maternal circulating adipokine profile and insulin resistance in women at high risk of developing gestational diabetes mellitus. *Metabolism Clinical And Experimental* 2017; **75**: 54-60 [PMID: 28935125 DOI: 10.1016/j.metabol.2017.08.003]

38 **Kleiblova P**, Dostalova I, Bartlova M, Lacinova Z, Ticha I, Krejci V, Springer D, Kleibl Z, Haluzik M. Expression of adipokines and estrogen receptors in adipose tissue and placenta of patients with gestational diabetes mellitus. *Mol Cell Endocrinol* 2010; **314**: 150-156 [PMID: 19682537 DOI: 10.1016/j.mce.2009.08.002]

39 **Kralisch S**, Stepan H, Kratzsch J, Verlohren M, Verlohren HJ, Drynda K, Lössner U, Blüher M, Stumvoll M, Fasshauer M. Serum levels of adipocyte fatty acid binding protein are increased in gestational diabetes mellitus. *Eur J Endocrinol* 2009; **160**: 33-38 [PMID: 18849305 DOI: 10.1530/EJE-08-0540]

40 **Kulik-Rechberger B**, Mora-Janiszewska O. [Serum resistin concentrations in cases of gestational diabetes mellitus with good glycemic control and in cord blood]. *Ginekol Pol* 2009; **80**: 432-436 [PMID: 19642599 DOI: 10.1055/s-0029-1185793]

41 **Lain KY**, Daftary AR, Ness RB, Roberts JM. First trimester adipocytokine concentrations and risk of developing gestational diabetes later in pregnancy. *Clin Endocrinol (Oxf)* 2008; **69**: 407-411 [PMID: 18284645 DOI: 10.1111/j.1365-2265.2008.03198.x]

42 **Lobo TF**, Torloni MR, Mattar R, Nakamura MU, Alexandre SM, Daher S. Adipokine levels in overweight women with early-onset gestational diabetes mellitus. *J Endocrinol Invest* 2018 [PMID: 29696612 DOI: 10.1007/s40618-018-0894-0]

43 **Nanda S**, Poon LC, Muhaisen M, Acosta IC, Nicolaides KH. Maternal serum resistin at 11 to 13 weeks' gestation in normal and pathological pregnancies. *Metabolism* 2012; **61**: 699-705 [PMID: 22146093 DOI: 10.1016/j.metabol.2011.10.006]

44 **Pagán A**, Sabater-Molina M, Olza J, Prieto-Sánchez MT, Blanco-Carnero JE, Parrilla JJ, Gil Á, Larqué E. A gene variant in the transcription factor 7-like 2 (TCF7L2) is associated with an increased risk of gestational diabetes mellitus. *Eur J Obstet Gynecol Reprod Biol* 2014; **180**: 77-82 [PMID: 25048152 DOI: 10.1016/j.ejogrb.2014.06.024]

45 **Ravnsborg T**, Andersen LL, Trabjerg ND, Rasmussen LM, Jensen DM, Overgaard M. First-trimester multimarker prediction of gestational diabetes mellitus using targeted mass spectrometry. *Diabetologia* 2016; **59**: 970-979 [PMID: 26818149 DOI: 10.1007/s00125-016-3869-8]

46 **Rottenkolber M**, Ferrari U, Holland L, Aertsen S, Kammer NN, Hetterich H, Fugmann M, Banning F, Weise M, Sacco V, Kohn D, Freibothe I, Hutter S, Hasbargen U, Lehmann R, Grallert H, Parhofer KG, Seissler J, Lechner A. The Diabetes Risk Phenotype of Young Women With Recent Gestational Diabetes. *J Clin Endocrinol Metab* 2015; **100**: E910-E918 [PMID: 25742512 DOI: 10.1210/jc.2014-3898]

47 **Skvarca A**, Tomazic M, Krhin B, Blagus R, Janez A. Adipocytokines and insulin resistance across various degrees of glucose tolerance in pregnancy. *J Int Med Res* 2012; **40**: 583-589 [PMID: 22613419 DOI: 10.1177/147323001204000220]

48 **Takhshid MA**, Zare Z. Resistin - 420 C/G polymorphism and serum resistin level in Iranian patients with gestational diabetes mellitus. *J Diabetes Metab Disord* 2015; **14**: 37 [PMID: 25945322 DOI: 10.1186/s40200-015-0165-y]

49 **Tsiotra PC**, Halvatsiotis P, Patsouras K, Maratou E, Salamalekis G, Raptis SA, Dimitriadis G, Boutati E. Circulating adipokines and mRNA expression in adipose tissue and the placenta in women with gestational diabetes mellitus. *Peptides* 2018; **101**: 157-166 [PMID: 29337272 DOI: 10.1016/j.peptides.2018.01.005]

50 **Vitoratos N**, Dimitrakaki A, Vlahos NF, Gregoriou O, Panoulis K, Christopoulos P, Creatsas G. Maternal and umbilical resistin levels do not correlate with infant birth weight either in normal pregnancies and or in pregnancies complicated with gestational diabetes. *J Matern Fetal Neonatal Med* 2010; **23**: 1019-1023 [PMID: 20082598 DOI: 10.3109/14767050903551459]

51 **Lappas M**, Yee K, Permezel M, Rice GE. Release and regulation of leptin, resistin and adiponectin from human placenta, fetal membranes, and maternal adipose tissue and skeletal muscle from normal and gestational diabetes mellitus-complicated pregnancies. *J Endocrinol* 2005; **186**: 457-465 [PMID: 16135665 DOI: 10.1677/joe.1.06227]

52 **Verhaeghe J**, van Bree R, Lambin S, Caluwaerts S. Adipokine profile and C-reactive protein in pregnancy: effects of glucose challenge response versus body mass index. *J Soc Gynecol Investig* 2005; **12**: 330-334 [PMID: 15979544 DOI: 10.1016/j.jsgi.2005.02.002]

53 **Minn AH**, Patterson NB, Pack S, Hoffmann SC, Gavrilova O, Vinson C, Harlan DM, Shalev A. Resistin is expressed in pancreatic islets. *Biochem Biophys Res Commun* 2003; **310**: 641-645 [PMID: 14521959 DOI: 10.1016/j.bbrc.2003.09.061]

54 **Sheng CH**, Di J, Jin Y, Zhang YC, Wu M, Sun Y, Zhang GZ. Resistin is expressed in human hepatocytes and induces insulin resistance. *Endocrine* 2008; **33**: 135-143 [PMID: 18446452 DOI: 10.1007/s12020-008-9065-y]

55 **Street ME**, Viani I, Ziveri MA, Volta C, Smerieri A, Bernasconi S. Impairment of insulin receptor signal

transduction in placentas of intra-uterine growth-restricted newborns and its relationship with fetal growth. *Eur J Endocrinol* 2011; **164**: 45-52 [PMID: 20930063 DOI: 10.1530/EJE-10-0752]
56 **Hauguel-de Mouzon S**, Guerre-Millo M. The placenta cytokine network and inflammatory signals. *Placenta* 2006; **27**: 794-798 [PMID: 16242770 DOI: 10.1016/j.placenta.2005.08.009]
57 **Zhou Y**, Zhang M, Guo W, Yu M, Xue K, Huang S, Chen Y, Zhu H, Xu L, Guo T. Expression of resistin protein in normal human subcutaneous adipose tissue and pregnant women subcutaneous adipose tissue and placenta. *J Huazhong Univ Sci Technolog Med Sci* 2006; **26**: 288-291 [PMID: 16961271 DOI: 10.1007/BF02829553]
58 **Lobo TF**, Torloni MR, Gueuvoghlanian-Silva BY, Mattar R, Daher S. Resistin concentration and gestational diabetes: a systematic review of the literature. *J Reprod Immunol* 2013; **97**: 120-127 [PMID: 23432878 DOI: 10.1016/j.jri.2012.10.004]
59 **Wells G**, Shea B, O'Connell J. The Newcastle-Ottawa Scale (NOS) for assessing the quality of nonrandomised studies in meta-analyses. 2018; Available from: URL: http://www.ohri.ca/programs/clinical_epidemiology/oxford.asp
60 **Zhang T**, Zhong W, editors. Applied methodology for evidence-based medicine. Changsha, China: Central South University Press. 2011
61 **Higgins JPT**, Green S, editors. Cochrane Handbook for Systematic Reviews of Interventions version 5.1.0. The Cochrane Collaboration. 2011
62 **Hozo SP**, Djulbegovic B, Hozo I. Estimating the mean and variance from the median, range, and the size of a sample. *BMC Med Res Methodol* 2005; **5**: 13 [PMID: 15840177 DOI: 10.1186/1471-2288-5-13]
63 **Whitehead A**, Whitehead J. A general parametric approach to the meta-analysis of randomized clinical trials. *Stat Med* 1991; **10**: 1665-1677 [PMID: 1792461 DOI: 10.1002/sim.4780101105]
64 **Higgins JP**, Thompson SG. Quantifying heterogeneity in a meta-analysis. *Stat Med* 2002; **21**: 1539-1558 [PMID: 12111919 DOI: 10.1002/sim.1186]
65 **Banerjee RR**, Rangwala SM, Shapiro JS, Rich AS, Rhoades B, Qi Y, Wang J, Rajala MW, Pocai A, Scherer PE, Steppan CM, Ahima RS, Obici S, Rossetti L, Lazar MA. Regulation of fasted blood glucose by resistin. *Science* 2004; **303**: 1195-1198 [PMID: 14976316 DOI: 10.1126/science.1092341]
66 **Ozias MK**, Li S, Hull HR, Brooks WM, Carlson SE. Relationship of circulating adipokines to body composition in pregnant women. *Adipocyte* 2014; **4**: 44-49 [PMID: 26167401 DOI: 10.4161/adip.29805]
67 **Dong Y**, Chauhan M, Betancourt A, Belfort M, Yallampalli C. Adipose Tissue Inflammation and Adrenomedullin Overexpression Contribute to Lipid Dysregulation in Diabetic Pregnancies. *J Clin Endocrinol Metab* 2018; **103**: 3810-3818 [PMID: 30020508 DOI: 10.1210/jc.2018-00905]
68 **Houshmand-Oeregaard A**, Hansen NS, Hjort L, Kelstrup L, Broholm C, Mathiesen ER, Clausen TD, Damm P, Vaag A. Differential adipokine DNA methylation and gene expression in subcutaneous adipose tissue from adult offspring of women with diabetes in pregnancy. *Clin Epigenetics* 2017; **9**: 37 [PMID: 28413567 DOI: 10.1186/s13148-017-0338-2]
69 **Urbanek M**, Hayes MG, Lee H, Freathy RM, Lowe LP, Ackerman C, Jafari N, Dyer AR, Cox NJ, Dunger DB, Hattersley AT, Metzger BE, Lowe WL. The role of inflammatory pathway genetic variation on maternal metabolic phenotypes during pregnancy. *PLoS One* 2012; **7**: e32958 [PMID: 22479352 DOI: 10.1371/journal.pone.0032958]
70 **Cho YM**, Youn BS, Chung SS, Kim KW, Lee HK, Yu KY, Park HJ, Shin HD, Park KS. Common genetic polymorphisms in the promoter of resistin gene are major determinants of plasma resistin concentrations in humans. *Diabetologia* 2004; **47**: 559-565 [PMID: 14740159 DOI: 10.1007/s00125-003-1319-x]
71 **Osawa H**, Yamada K, Onuma H, Murakami A, Ochi M, Kawata H, Nishimiya T, Niiya T, Shimizu I, Nishida W, Hashiramoto M, Kanatsuka A, Fujii Y, Ohashi J, Makino H. The G/G genotype of a resistin single-nucleotide polymorphism at -420 increases type 2 diabetes mellitus susceptibility by inducing promoter activity through specific binding of Sp1/3. *Am J Hum Genet* 2004; **75**: 678-686 [PMID: 15338456 DOI: 10.1086/424761]

P- Reviewer: Das U, Kai K
S- Editor: Ji FF **L- Editor:** Wang TQ **E- Editor:** Bian YN

World Journal of Clinical Cases

Submit a Manuscript: https://www.f6publishing.com

World J Clin Cases 2019 March 6; 7(5): 600-615

DOI: 10.12998/wjcc.v7.i5.600

ISSN 2307-8960 (online)

META-ANALYSIS

Docetaxel, cisplatin, and 5-fluorouracil compared with epirubicin, cisplatin, and 5-fluorouracil regimen for advanced gastric cancer: A systematic review and meta-analysis

Bo Li, Lian Chen, Hong-Liang Luo, Feng-Ming Yi, Yi-Ping Wei, Wen-Xiong Zhang

ORCID number: Bo Li (0000-0002-1438-4696); Lian Chen (0000-0001-5296-5806); Hong-Liang Luo (0000-0001-5221-7736); Feng-Ming Yi (0000-0001-9006-2042); Yi-Ping Wei (0000-0001-5364-8212); Wen-Xiong Zhang (0000-0003-2962-0847).

Author contributions: Li B conceptualized and designed the study, acquired, analyzed, and interpreted the data, and drafted the article; Chen L and Luo HL acquired, analyzed, and interpreted the data; Yi FM conceptualized and designed the study and analyzed and interpreted the data; Wei YP revised the article; Zhang WX conceptualized and designed the study, critically revised the manuscript, and approved the final version.

Supported by National Natural Science Foundation of China, No. 81560345.

Conflict-of-interest statement: The authors deny any conflict of interest.

PRISMA 2009 Checklist statement: The authors have read and revised according to the PRISMA 2009 Checklist.

Open-Access: This article is an open-access article which was selected by an in-house editor and fully peer-reviewed by external reviewers. It is distributed in accordance with the Creative Commons Attribution Non Commercial (CC BY-NC 4.0)

Bo Li, Yi-Ping Wei, Wen-Xiong Zhang, Department of Thoracic Surgery, The Second Affiliated Hospital of Nanchang University, Nanchang 330006, Jiangxi Province, China

Bo Li, Lian Chen, Jiangxi Medical College, Nanchang University, Nanchang 330006, Jiangxi Province, China

Hong-Liang Luo, Department of Gastrointestinal Surgery, The Second Affiliated Hospital of Nanchang University, Nanchang 330006, Jiangxi Province, China

Feng-Ming Yi, Department of Digestive Oncology, The Second Affiliated Hospital of Nanchang University, Nanchang 330006, Jiangxi Province, China

Corresponding author: Wen-Xiong Zhang, MD, Attending Doctor, Department of Thoracic Surgery, The Second Affiliated Hospital of Nanchang University, 1 Minde Road, Nanchang 330006, Jiangxi Province, China. zwx123dr@126.com
Telephone: +86-18720909414
Fax: +86-791-86311248

Abstract

BACKGROUND

As the first-line regimens for the treatment of advanced gastric cancer, both docetaxel, cisplatin, and 5-fluorouracil (DCF) and epirubicin, cisplatin, and 5-fluorouracil (ECF) regimens are commonly used in clinical practice, but there is still controversy about which is better.

AIM

To compare the efficacy and safety of DCF and ECF regimens by conducting this meta-analysis.

METHODS

Computer searches in PubMed, EMBASE, Ovid MEDLINE, Science Direct, Web of Science, The Cochrane Library and Scopus were performed to find the clinical studies of all comparisons between DCF and ECF regimens. We used progression-free survival (PFS), overall survival (OS), objective response rate (ORR), disease control rate (DCR), and adverse effects (AEs) as endpoints for analysis.

RESULTS

Our meta-analysis included seven qualified studies involving a total of 598

license, which permits others to distribute, remix, adapt, build upon this work non-commercially, and license their derivative works on different terms, provided the original work is properly cited and the use is non-commercial. See: http://creativecommons.org/licenses/by-nc/4.0/

Manuscript source: Unsolicited manuscript

Received: October 31, 2018
Peer-review started: October 31, 2018
First decision: December 12, 2018
Revised: December 20, 2018
Accepted: December 29, 2018
Article in press: December 30, 2018
Published online: March 6, 2019

patients. The pooled hazard ratios between the DCF and ECF groups were comparable in PFS (95%CI: 0.58-1.46, P = 0.73), OS (95%CI: 0.65-1.10, P = 0.21), and total AEs (95%CI: 0.93-1.29, P = 0.30). The DCF group was significantly better than the ECF group in terms of ORR (95%CI: 1.13-1.75, P = 0.002) and DCR (95%CI: 1.03-1.41, P = 0.02). However, the incidence rate of grade 3-4 AEs was also greater in the DCF group than in the ECF group (95%CI: 1.16-1.88, P = 0.002), especially for neutropenia and febrile neutropenia.

CONCLUSION
With better ORR and DCR values, the DCF regimen seems to be more suitable for advanced gastric cancer than the ECF regimen. However, the higher rate of AEs in the DCF group still needs to be noticed.

Key words: Gastric cancer; Chemotherapy; Docetaxel; Epirubicin; Cisplatin; 5-fluorouracil

©The Author(s) 2019. Published by Baishideng Publishing Group Inc. All rights reserved.

Core tip: This study is the first meta-analysis to compare docetaxel, cisplatin, and 5-fluorouracil (DCF) and epirubicin, cisplatin, and 5-fluorouracil (ECF) regimens for advanced gastric cancer. The results showed that progression-free survival (PFS), overall survival (OS), and total adverse effects (AEs) between the DCF and ECF groups were comparable. The DCF group was significantly better in terms of ORR and DCR than the ECF group. However, the incidence rate of grade 3-4 AEs was also greater in the DCF group than in the ECF group, especially for neutropenia and febrile neutropenia. Therefore, DCF regimen seems to be more suitable for advanced gastric cancer than the ECF regimen.

Citation: Li B, Chen L, Luo HL, Yi FM, Wei YP, Zhang WX. Docetaxel, cisplatin, and 5-fluorouracil compared with epirubicin, cisplatin, and 5-fluorouracil regimen for advanced gastric cancer: A systematic review and meta-analysis. *World J Clin Cases* 2019; 7(5): 600-615
URL: https://www.wjgnet.com/2307-8960/full/v7/i5/600.htm
DOI: https://dx.doi.org/10.12998/wjcc.v7.i5.600

INTRODUCTION

Gastric cancer has become the fifth most frequently diagnosed malignancy and the third leading cause of cancer-related deaths worldwide[1-3]. Most patients are unable to get timely diagnosis and effective treatment due to the lack of obvious symptoms in the early stage. Moreover, many patients are likely to relapse even after regular radiotherapy and chemotherapy[4]. Gastric cancer is sensitive to chemotherapy, and it is more clinically treated with combined chemotherapy for the purpose of palliative treatment[5,6].

Many regimens have been used for the treatment of patients with advanced gastric cancer, but none are considered standard. Recommended by clinical guidelines, docetaxel, cisplatin, and 5-fluorouracil (DCF) and epirubicin, cisplatin, and 5-fluorouracil (ECF) regimens are commonly used as first-line treatments for gastric cancer[7]. The results in some studies showed that the DCF group was better than the ECF group in terms of objective response rate (ORR), progression-free survival (PFS), and overall survival (OS)[8-9]. However, in other studies, opposite results were obtained, and the ECF regimen had better antitumor efficacy and better quality of life for advanced gastric cancer[10,11]. In a retrospective analysis from Turkey, Teker *et al* reported that DCF and ECF had similar efficacy and tolerability in treating advanced gastric cancer[12].

To solve the controversy, we conducted this meta-analysis of relevant studies to compare the survival outcomes [PFS, OS, ORR, and disease control rate (DCR)] and adverse effects (AEs) between DCF and ECF regimens.

MATERIALS AND METHODS

This meta-analysis was conducted according to the Preferred Reporting Items for Systematic Review and Meta-Analysis guidelines[13].

Search strategy

A systematic literature search of PubMed, EMBASE, Ovid Medline, ScienceDirect, Web of Science, The Cochrane Library and Scopus was performed up to August 31, 2018, combining the following mesh terms: "gastric cancer", "epirubicin", "docetaxel", and "chemotherapy". Our complete search for PubMed was: [docetaxel (Mesh Terms) OR docetaxel hydrate OR docetaxel trihydrate OR docetaxel anhydrous] AND [epirubicin (Mesh Terms) OR 4'-epidoxorubicin OR EPI-cell OR IMI28 OR NSC 256942 OR NSC256942 OR Ellence] AND [stomach neoplasm (Mesh Terms) OR gastric cancer OR stomach cancer OR stomach neoplasm OR gastric neoplasm OR cancers of stomach]. Search results were limited to original human studies, and search criteria were restricted to randomized controlled trials (RCTs) or cohort studies without language restriction. The search is supplemented by manually searching for references listed in all included studies.

Selection criteria and data extraction

We used the following criteria for selecting studies: (1) Population: Patients diagnosed with metastatic or advanced gastric cancer; (2) Intervention and comparison: DCF *vs* ECF; (3) Outcomes: PFS, OS, ORR, DCR, and AEs; and (4) Study design: High-quality RCTs and cohort studies. Studies without primary data, abstracts only, conference summary, meta-analysis, animal experiments, and duplicate data were excluded.

Data were independently extracted by two reviewers, including the following: (1) first author, year, dosage regimen, dosage and cycle, patient characteristics, and study design; (2) PFS, OS, ORR, and DCR; and (3) AEs (all-grade/grade 3-4). A third investigator resolved any disagreements about terms.

Quality assessment

The Jadad scale (5-point)[14] and the Newcastle-Ottawa Scale (NOS, 9-point)[15] were used to assess the methodological quality of RCTs and cohort studies, receptively. Three main items were included in the Jadad scale: Randomization, masking, and accountability of all patients. The NOS also included three main items: Patient selection, comparability, and exposure. The scores were allocated as stars to each study. RCTs achieving three or more stars were considered to be of high quality. Cohort studies achieving eight to nine stars were considered to be of high quality; six to seven stars were considered to be of medium quality.

Statistical analysis

Meta-analysis was performed with RevMan (Version 5.3) and STATA (Version 12.0). PFS and OS were analyzed by the pooled hazard ratio (HR); if the HR was less than 1, the result favored the DCF group; otherwise, it favored the ECF group. ORR, DCR, and AEs were analyzed by the pooled risk ratio. We extracted the HR of PFS and OS directly from studies or from Kaplan–Meier curves according to Tierney *et al*[16]. The heterogeneity test was evaluated by using the Q test and I^2 statistic. If $P > 0.1$ and $I^2 < 50\%$, the fixed effects model was used. Otherwise, the random effects model was used[17]. Begg's and Egger's tests were performed to assess possible publication bias. The result was considered statistically significant if the *P*-value was less than 0.05.

RESULTS

Study quality

We initially identified 965 potentially eligible studies. We further deleted the poor quality and repeated studies and ultimately included seven qualified studies (four RCTs and three cohort studies). A total of 598 cases of metastatic or advanced gastric cancer were included (257 patients in the DCF group and 341 patients in the ECF group). According to the Jadad scale and NOS, five studies were of high quality (four RCTs and one cohort study), and two cohort studies were of medium quality (Table 1). The selection procedure is shown in Figure 1, and the characteristics of the included studies are shown in Table 2.

Survival outcomes

Four studies including 288 patients reported PFS. No statistically significant difference was found between the two groups (95%CI: 0.58-1.46, $P = 0.73$), with significant heterogeneity ($P = 0.01$; $I^2 = 72\%$, Figure 2).

Table 1 Quality assessment of all included studies

Study	Selection	Comparability	Exposure	Randomization	Masking	Accountability of all patients	Quality (score)
Randomized controlled trial							
Sadighi *et al*[18], 2006				**	**	*	5
Roth *et al*[10], 2007				**	*	*	4
Gao *et al*[11], 2010				**	**	*	5
Babu *et al*[9], 2017				*	*	*	3
Retrospective study							
Abbasi *et al*[19], 2010	***	**	*				6
Kilickap *et al*[8], 2011	***	**	**				7
Teker *et al*[12], 2014	****	**	***				9

Five studies including 431 patients reported OS. No statistically significant difference was found between the two groups (95%CI: 0.65-1.10, P = 0.21), with acceptable heterogeneity (P = 0.33; I^2 = 13%, Figure 3).

Seven studies including 598 patients reported ORR. ORR was significantly greater in the DCF group than in the ECF group (95%CI: 1.13-1.75, P = 0.002), with no heterogeneity (P = 0.52; I^2 = 0%, Figure 4A).

Four studies including 351 patients reported DCR. DCR was significantly greater in the DCF group than in the ECF group (95%CI: 1.03-1.41, P = 0.02), with no heterogeneity (P = 0.97; I^2= 0%, Figure 4B).

Toxicities

We evaluated toxicities between the DCF and ECF groups based on total AEs (all-grade/grade 3-4). In subgroup analysis, we also evaluated the top ten reported AEs (all-grade/grade 3-4).

Four studies including 288 patients reported total all-grade AEs. No statistically significant difference was found between the two groups (95%CI: 0.93-1.29, P = 0.30), with significant heterogeneity (P = 0.03; I^2 = 66%, Figure 5). In the subgroup analysis, DCF induced a significantly greater rate of febrile neutropenia than ECF (95%CI: 1.05-4.00, P = 0.04). Similar incidence rates of leucopenia, neutropenia, thrombocytopenia, anemia, anorexia, nausea/vomiting, fatigue, diarrhea, and stomatitis were found between the two groups.

Four studies including 288 patients reported total grade 3-4 AEs. The incidence rate of grade 3-4 AEs was significantly greater in the DCF group than in the ECF group (95%CI: 1.16-1.88, P = 0.002), with significant heterogeneity (P = 0.07; I^2 = 57%, Figure 6). In the subgroup analysis, compared to ECF, DCF induced a significantly greater rate of neutropenia (95%CI: 1.25-2.16, P = 0.0003) and febrile neutropenia (95%CI: 1.17-4.12, P = 0.01). Similar incidence rates of leucopenia, anemia, anorexia, nausea/vomiting, fatigue, diarrhea, stomatitis, and paraesthesia were found between the two groups.

Sensitivity analysis and publication bias

In the analysis of PFS and total AEs (all-grade/grade 3-4), our results showed significant heterogeneity. We excluded a single study to evaluate the impact of the study on the pooled results. The results suggested that the outcomes of PFS, all-grade AEs, and grade 3-4 AEs were stable and reliable (Figure 7). The results of Begg's test and Egger's tests were as follows: ORR (P = 0.548; P = 0.491, Figure 8A), PFS (P = 0.089; P = 0.155, Figure 8B), and OS (P = 0.806; P = 0.481, Figure 8C). There was no evidence to identify significant publication bias.

DISCUSSION

Gastric cancer is still a worldwide malignant tumor with a high mortality rate[20]. At present, since screening gastric cancer is difficult to popularize, most patients are in an advanced stage and have lost the chance of radical operation when diagnosed[21]. Even if the tumors can be excised, there is a great chance of local recurrence after the operation[22]. Cisplatin-based combinations [particularly cisplatin and 5-fluorouracil (CF)] have been recognized as one of the preferred regimens for advanced gastric cancer. As improved regimens, both DCF and ECF regimens are superior to CF[23,24]. This study is the first meta-analysis to compare DCF and ECF regimens for advanced

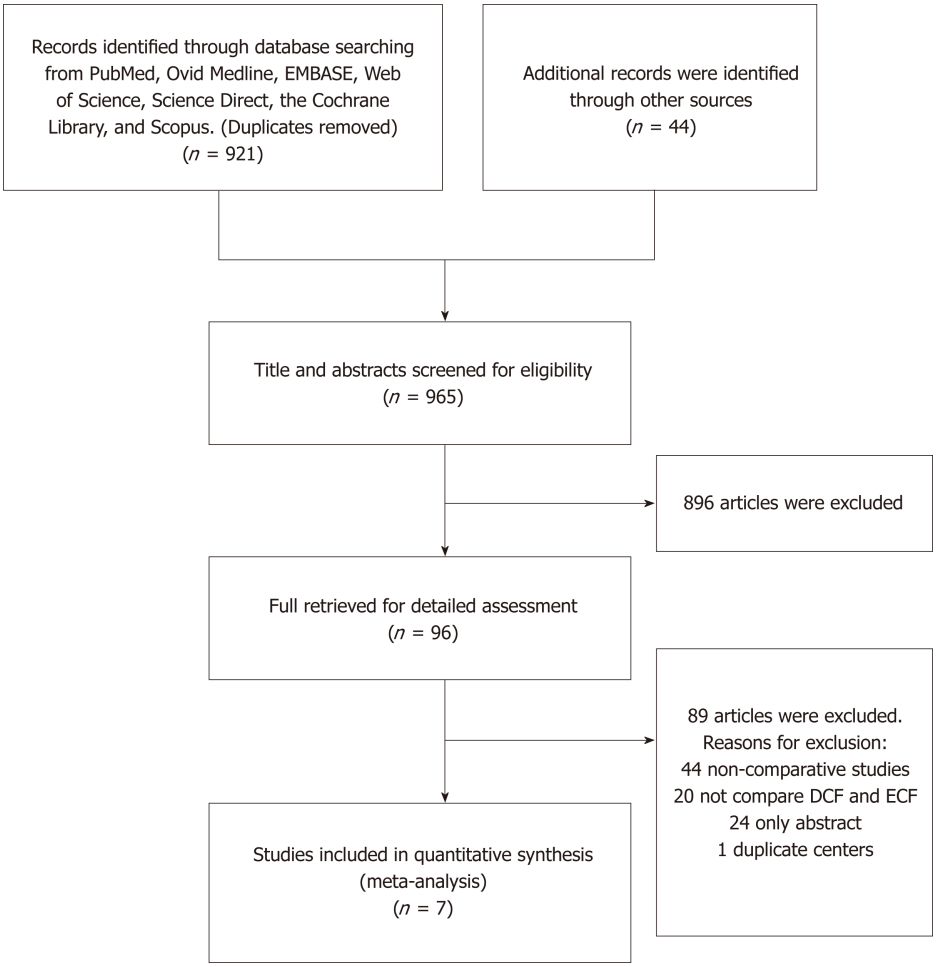

Figure 1 Flow chart of the study selection. ECF: Epirubicin, cisplatin, and 5-fluorouracil; DCF: Docetaxel, cisplatin, and 5-fluorouracil.

gastric cancer. The results showed that PFS, OS, and total AEs between the DCF and ECF groups were comparable. The DCF group was significantly better in terms of ORR and DCR than the ECF group. However, the incidence rate of grade 3-4 AEs was also greater in the DCF group than in the ECF group, especially for neutropenia and febrile neutropenia.

From our results, four studies[9,10,12,19] showed that DCF significantly prolonged the OS of patients compared with ECF, and three studies[8,9,19] showed that DCF significantly prolonged the PFS of patients compared with ECF. The results were beneficial to the translation of OS and PFS from the DCF regimen to the pooled median survival time of approximately 1 mo. However, no significant difference was found in OS or PFS between the two groups. Compared to non-docetaxel-containing regimens, Wagner *et al*[25] found that the results in OS and PFS might be extended slightly or without any difference[25]. Furthermore, the advantages of trivalent regimens containing docetaxel (DCF and FLO-T) might be offset by increased toxicity. Although our results did not show significant differences, it was possible that both regimens were effective in the treatment of advanced gastric cancer, probably because of the small number of cases. We looked forward to a larger scale of related research.

Our results showed an advantage in the improvement of ORR and DCR in the DCF group. Only one study[12] showed that the ORR of the DCF group was lower than that of the ECF group (26.2% *vs* 29.5%, respectively). These results might be because docetaxel had better efficacy, and the patient's response to this drug was relatively high. Its curative effect is largely related to its mechanism of action. Docetaxel is a taxane compound discovered in the 1990s. It mainly enhances tubulin aggregation and inhibits microtubule depolymerization, leading to the formation of stable non-functional microtubule bundles, thus destroying the mitosis of cancer cells to achieve anti-tumor effects. Compared with paclitaxel, it has stronger activity and broader anti-tumor spectrum. Epirubicin is an antibiotic anti-tumor drug, which belongs to a non-specific cell cycle anti-cancer drug. Its mechanism is to directly insert DNA nucleotide pairs to interfere with the transcription process and prevent the synthesis of RNA and DNA. Similar to our results, Petrioli *et al*[26] reported that docetaxel-based regimens

Table 2 Characteristics of the included studies

Ref.	Yr	Intervention and control	Samples	ORR (%)	OS	PFS	Design	Quality (score)
Sadighi *et al*[18]	2006	DCF: D 60 mg/m^2, d1, C 60 mg/m^2, d1, F 750 mg/m^2/d, d1-5 (21)	44	42.0	-	-	RCT	5/5
		ECF: E 60mg/m^2, d1, C 60 mg/m^2, d1, F 750 mg/m^2/d, d1-5 (21)	42	37.0	-	-		
Roth *et al*[10]	2007	DCF: D 85mg/m^2, d1, C 75 mg/m^2, d1, F 300 mg/m^2/d, d1-14 (21)	41	36.6	10.4	4.6	RCT	4/5
		ECF: E 50 mg/m^2, d1, C 60 mg/m^2, d1, F 200 mg/m^2/d, d1-21 (21)	40	25.0	8.3	4.9		
Abbasi *et al*[19]	2010	DCF: D 75mg/m^2, d1, C 75 mg/m^2, d1, F 750 mg/m^2/d, d1-5 (21)	30	56.3	10.81	6.81	RS	6/9
		ECF: E 50 mg/m^2, d1, C 60 mg/m^2, d1, F 200 mg/m^2/d, d1-21 (21)	113	31.3	8.06	5.13		
Gao *et al*[11]	2010	DCF: D 60 mg/m^2, d1, C 25 mg/m^2, d1-3, F 1000 mg/m^2, 46 h, pumping (21)	32	59.3	-	-	RCT	5/5
		ECF: E 50 mg/m^2, d1, C 25 mg/m^2, d1-3, F 1000 mg/m^2, 46 h, pumping (21)	32	32.6	-	-		
Kilickap *et al*[8]	2011	DCF: D 75 mg/m^2, d1, C 75 mg/m^2, d1, F 750 mg/m2/d, d1-5 (21)	40	40.0	9.6	5.8	RS	7/9
		ECF: E 50 mg/m^2, d1, C 60 mg/m^2, d1, F 250 mg/m^2/d, d1-21 (21)	40	30.0	10.1	4.4		
Teker *et al*[12]	2014	DCF: D 50-75 mg/m^2, d1, C 50-75 mg/m^2, d1, F 500-750 mg/m^2/d, d1-5 (21)	42	26.2	11	6.0	RS	9/9
		ECF: E 50 mg/m^2, d1, C 60 mg/m^2, d1, F 200 mg/m^2/d, d1-21 (21)	44	29.5	10	6.0		
Babu *et al*[9]	2017	DCF: D 75 mg/m^2, d1, C 60 mg/m^2, d1, F 750 mg/m^2/d, d1-5 (21)	28	46.4	12.5	7.5	RCT	3/5
		ECF: E 50 mg/m^2, d1, C 60 mg/m^2, d1, F 750 mg/m^2/d, d1-5 (21)	30	26.7	9.4	5.8		

ORR: Objective response rate; OS: Overall survival; PFS: Progression-free survival; ECF: Epirubicin, cisplatin, and 5-fluorouracil; DCF: Docetaxel, cisplatin, and 5-fluorouracil; RCT: Randomized controlled trial.

showed an increase in ORR compared with epirubicin-based regimens; however, no significant difference was found between the two groups[26]. A meta-analysis of DCF compared with non-docetaxel-containing regimens analyzed 12 RCTs for a total of 1089 cases with advanced gastric cancer. The results did not show any significant difference in CR or SD rates, but the DCF regimen can significantly increase the PR rate (38.8% *vs* 27.9%, respectively; 95%CI 1.16-1.65, P = 0.0003) compared with other regimens[27]. In four studies comparing docetaxel and non-docetaxel-containing regimens involving 1235 participants[24,28-30], the pooled ORRs were 43% and 30%, respectively (95%CI: 1.45-2.32, P = 0.002). In addition, due to higher response rates, individuals with good performance might have greater advantages from the three drug regimens, especially those containing docetaxel[25].

With respect to toxicity, hematological toxicity was confirmed to be the most common adverse event associated with the DCF regimen. In our analysis, we found high incidences of neutropenia and febrile neutropenia in the DCF group. Although it did not affect the efficacy of drugs, it might cause damage to other organs[31]. In recent years, many institutions have designed a number of improvements to regimens, such as DC or DF, capecitabine and oxaliplatin instead of 5-fluorouracil and cisplatin, or have changed the method of administration to weekly administration. Preliminary results showed that the AEs of the improved regimens were significantly lower than those of the DCF regimen, and the survival time seemed to be prolonged, but no significant difference was found in efficacy[32-33]. Based on the national comprehensive cancer network guidelines, DCF and ECF are considered high-risk and intermediate-risk regimens, respectively, for febrile neutropenia[7]. Phase I and phase II clinical studies have shown that docetaxel-induced toxicity is better tolerated when used weekly. The frequency of myelosuppression associated with neutropenia can also be reduced with weekly administration[34-37]. The AEs of DCF are acceptable only with appropriately selected patients and comprehensive toxicity management strategies. It is interesting to note that after appropriate dose reduction, the rates of neutropenia and febrile neutropenia were reduced with DCF. European and North American guidelines recommend the routine use of granulocyte colony-stimulating factor (G-CSF) prophylaxis when using chemotherapy regimens associated with a risk of neutropenia and febrile neutropenia[36,37]. Many studies have shown that G-CSF can control these two toxicities[38,39]. In this meta-analysis, we can see that the toxicity and side effects of the DCF regimen were relatively large, but with the improvement of medical level, the adverse reactions can be controlled and prevented. However, the combination of the three drugs should be carefully considered for the elderly and poor physique patients. Therefore, appropriate preventive measures should be taken in advance for patients who cannot tolerate the related toxicity.

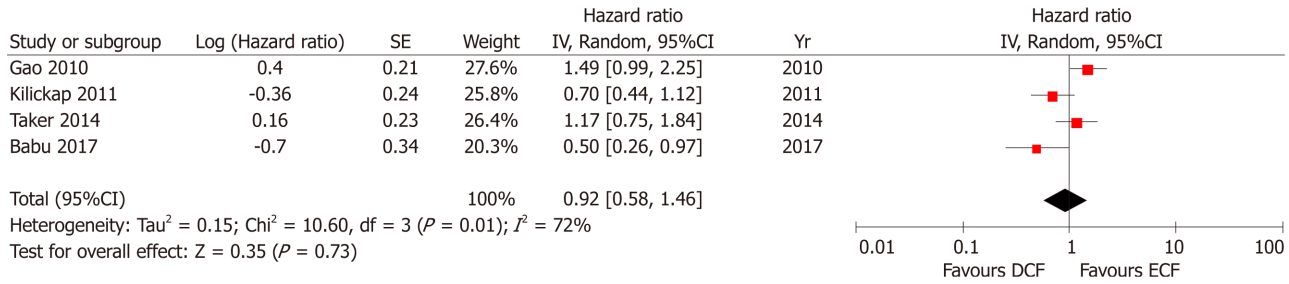

Figure 2 Forest plot of hazard ratio of progression-free survival associated with docetaxel, cisplatin, and 5-fluorouracil *vs* epirubicin, cisplatin, and 5-fluorouracil. ECF: Epirubicin, cisplatin, and 5-fluorouracil; DCF: Docetaxel, cisplatin, and 5-fluorouracil.

In addition, we should note that there are still some limitations in this meta-analysis: (1) not all of the studies are RCTs; (2) the total number of analyzed patients is small, which may not reflect the whole population; (3) significant heterogeneity existed in some comparisons; (4) some studies did not provide the data we have analyzed; (5) the number of AEs may not completely reflect the quality of life; and (6) the doses of anticancer agents were different in each study, which might increase heterogeneity between the included studies.

In conclusion, Both DCF and ECF are effective regimens for advanced gastric cancer, with comparable PFS, OS, and total AEs. The DCF regimen has greater advantages over the ECF regimen in terms of ORR and DCR. However, the incidence rate of grade 3-4 AEs is also higher in the DCF group. Due to the inherent limitations of the study, more large-scale and high-quality RCTs are needed to support this conclusion.

Study or subgroup	Log (Hazard ratio)	SE	Weight	Hazard ratio IV, Fixed, 95%CI	Yr
Abbasi 2010	0.27	0.29	21.2%	1.31 [0.74, 2.31]	2010
Gao 2010	-0.42	0.28	22.7%	0.66 [0.38, 1.14]	2010
Kilickap 2011	-0.07	0.31	18.5%	0.93 [0.51, 1.71]	2011
Taker 2014	-0.18	0.25	28.5%	0.84 [0.51, 1.36]	2014
Babu 2017	-0.69	0.44	9.2%	0.50 [0.21, 1.19]	2017
Total (95%CI)			100%	0.85 [0.65, 1.10]	

Heterogeneity: Chi^2 = 4.60, df = 4 (P = 0.33); I^2 = 13%
Test for overall effect: Z = 1.24 (P = 0.21)

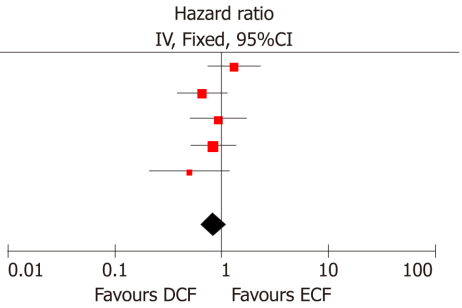

Figure 3 Forest plot of hazard ratio of overall survival associated with docetaxel, cisplatin, and 5-fluorouracil *vs* epirubicin, cisplatin, and 5-fluorouracil. ECF: Epirubicin, cisplatin, and 5-fluorouracil; DCF: Docetaxel, cisplatin, and 5-fluorouracil.

A

Study or subgroup	DCF Events	DCF Total	ECF Events	ECF Total	Weight	Risk ratio M-H, Fixed, 95%CI	Yr
Sadighi 2006	18	44	16	42	19.8%	1.07 [0.64, 1.81]	2006
Roth 2007	15	41	10	40	12.2%	1.46 [0.75, 2.86]	2007
Abbasi 2010	16	30	33	113	16.7%	1.83 [1.18, 2.84]	2010
Gao 2010	18	32	10	32	12.1%	1.80 [0.99, 3.27]	2010
Kilickap 2011	16	40	12	40	14.5%	1.33 [0.73, 2.45]	2011
Taker 2014	11	42	13	44	15.3%	0.89 [0.45, 1.75]	2014
Babu 2017	13	28	8	30	9.3%	1.74 [0.85, 3.56]	2017
Total (95%CI)		257		341	100%	1.41 [1.13, 1.75]	
Total everts	107		102				

Heterogeneity: Chi^2 = 5.16, df = 6 (P = 0.52); I^2 = 0%
Test for overall effect: Z = 3.03 (P = 0.002)

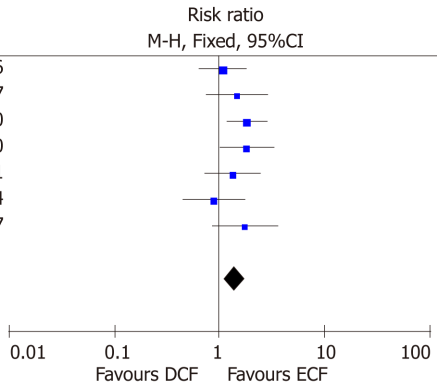

B

Study or subgroup	DCF Events	DCF Total	ECF Events	ECF Total	Weight	Risk ratio M-H, Fixed, 95%CI	Yr
Gao 2010	28	32	23	32	25.8%	1.22 [0.95, 1.57]	2010
Abbasi 2010	22	30	67	113	31.6%	1.24 [0.95, 1.61]	2010
Taker 2014	21	42	20	44	22.0%	1.10 [0.71, 1.71]	2014
Babu 2017	22	28	19	30	20.6%	1.24 [0.89, 1.73]	2017
Total (95%CI)		132		219	100%	1.20 [1.03, 1.41]	
Total everts	93		129				

Heterogeneity: Chi^2 = 0.24, df = 3 (P = 0.97); I^2 = 0%
Test for overall effect: Z = 2.28 (P = 0.02)

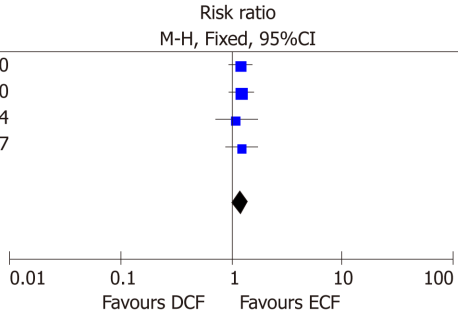

Figure 4 Forest plots of risk ratios of objective response rate (A) and disease control rate (B) associated with docetaxel, cisplatin, and 5-fluorouracil *vs* epirubicin, cisplatin, and 5-fluorouracil. ECF: Epirubicin, cisplatin, and 5-fluorouracil; DCF: Docetaxel, cisplatin, and 5-fluorouracil.

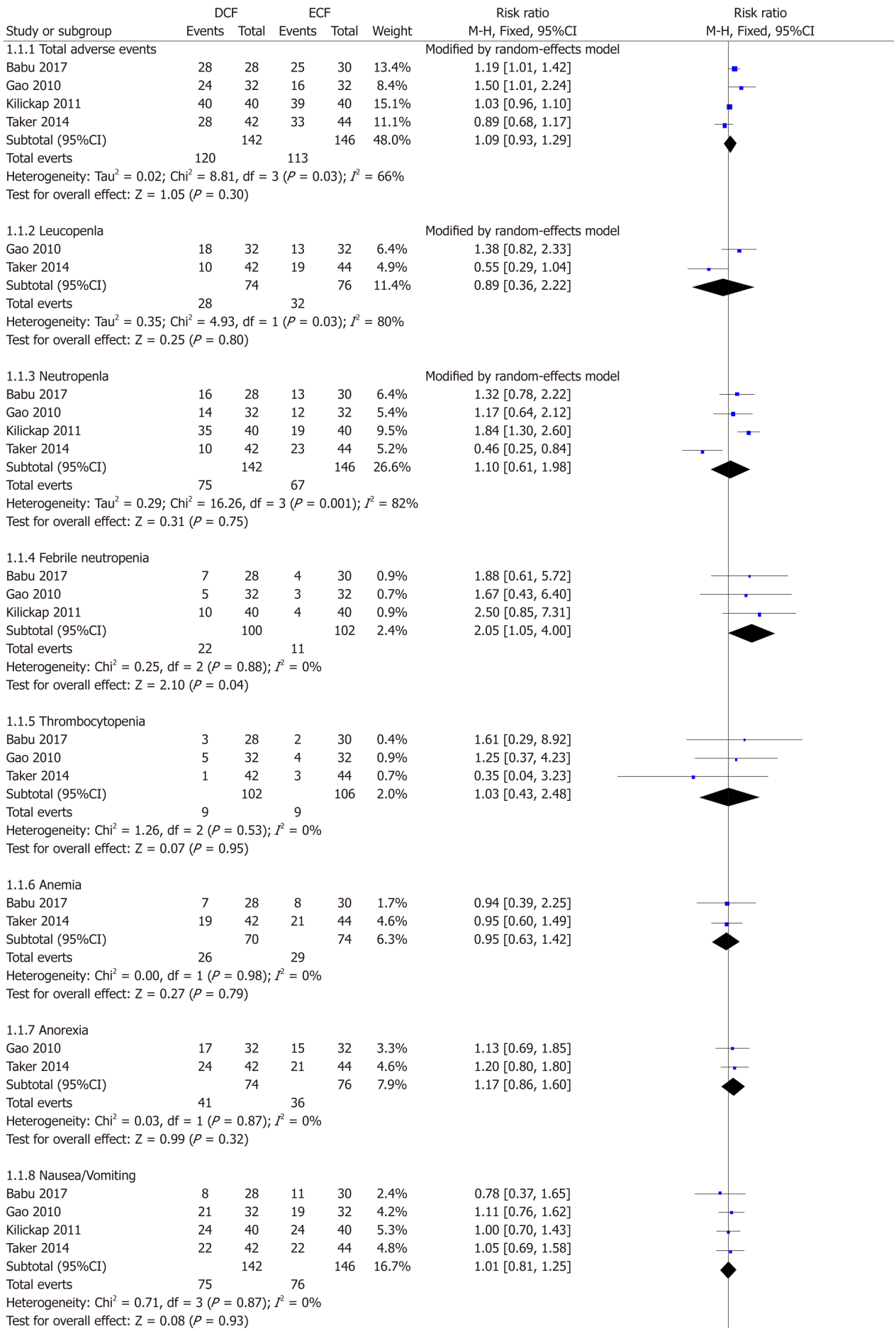
DCF
ECF
Risk ratio
Risk ratio
Study or subgroup
Events Total Events Total Weight
M-H, Fixed, 95%CI
M-H, Fixed, 95%CI
1.1.1 Total adverse events
Modified by random-effects model
Babu 2017 28 28 25 30 13.4% 1.19 [1.01, 1.42]
Gao 2010 24 32 16 32 8.4% 1.50 [1.01, 2.24]
Kilickap 2011 40 40 39 40 15.1% 1.03 [0.96, 1.10]
Taker 2014 28 42 33 44 11.1% 0.89 [0.68, 1.17]
Subtotal (95%CI) 142 146 48.0% 1.09 [0.93, 1.29]
Total everts 120 113
Heterogeneity: Tau² = 0.02; Chi² = 8.81, df = 3 (P = 0.03); I² = 66%
Test for overall effect: Z = 1.05 (P = 0.30)
1.1.2 Leucopenla
Modified by random-effects model
Gao 2010 18 32 13 32 6.4% 1.38 [0.82, 2.33]
Taker 2014 10 42 19 44 4.9% 0.55 [0.29, 1.04]
Subtotal (95%CI) 74 76 11.4% 0.89 [0.36, 2.22]
Total everts 28 32
Heterogeneity: Tau² = 0.35; Chi² = 4.93, df = 1 (P = 0.03); I² = 80%
Test for overall effect: Z = 0.25 (P = 0.80)
1.1.3 Neutropenla
Modified by random-effects model
Babu 2017 16 28 13 30 6.4% 1.32 [0.78, 2.22]
Gao 2010 14 32 12 32 5.4% 1.17 [0.64, 2.12]
Kilickap 2011 35 40 19 40 9.5% 1.84 [1.30, 2.60]
Taker 2014 10 42 23 44 5.2% 0.46 [0.25, 0.84]
Subtotal (95%CI) 142 146 26.6% 1.10 [0.61, 1.98]
Total everts 75 67
Heterogeneity: Tau² = 0.29; Chi² = 16.26, df = 3 (P = 0.001); I² = 82%
Test for overall effect: Z = 0.31 (P = 0.75)
1.1.4 Febrile neutropenia
Babu 2017 7 28 4 30 0.9% 1.88 [0.61, 5.72]
Gao 2010 5 32 3 32 0.7% 1.67 [0.43, 6.40]
Kilickap 2011 10 40 4 40 0.9% 2.50 [0.85, 7.31]
Subtotal (95%CI) 100 102 2.4% 2.05 [1.05, 4.00]
Total everts 22 11
Heterogeneity: Chi² = 0.25, df = 2 (P = 0.88); I² = 0%
Test for overall effect: Z = 2.10 (P = 0.04)
1.1.5 Thrombocytopenia
Babu 2017 3 28 2 30 0.4% 1.61 [0.29, 8.92]
Gao 2010 5 32 4 32 0.9% 1.25 [0.37, 4.23]
Taker 2014 1 42 3 44 0.7% 0.35 [0.04, 3.23]
Subtotal (95%CI) 102 106 2.0% 1.03 [0.43, 2.48]
Total everts 9 9
Heterogeneity: Chi² = 1.26, df = 2 (P = 0.53); I² = 0%
Test for overall effect: Z = 0.07 (P = 0.95)
1.1.6 Anemia
Babu 2017 7 28 8 30 1.7% 0.94 [0.39, 2.25]
Taker 2014 19 42 21 44 4.6% 0.95 [0.60, 1.49]
Subtotal (95%CI) 70 74 6.3% 0.95 [0.63, 1.42]
Total everts 26 29
Heterogeneity: Chi² = 0.00, df = 1 (P = 0.98); I² = 0%
Test for overall effect: Z = 0.27 (P = 0.79)
1.1.7 Anorexia
Gao 2010 17 32 15 32 3.3% 1.13 [0.69, 1.85]
Taker 2014 24 42 21 44 4.6% 1.20 [0.80, 1.80]
Subtotal (95%CI) 74 76 7.9% 1.17 [0.86, 1.60]
Total everts 41 36
Heterogeneity: Chi² = 0.03, df = 1 (P = 0.87); I² = 0%
Test for overall effect: Z = 0.99 (P = 0.32)
1.1.8 Nausea/Vomiting
Babu 2017 8 28 11 30 2.4% 0.78 [0.37, 1.65]
Gao 2010 21 32 19 32 4.2% 1.11 [0.76, 1.62]
Kilickap 2011 24 40 24 40 5.3% 1.00 [0.70, 1.43]
Taker 2014 22 42 22 44 4.8% 1.05 [0.69, 1.58]
Subtotal (95%CI) 142 146 16.7% 1.01 [0.81, 1.25]
Total everts 75 76
Heterogeneity: Chi² = 0.71, df = 3 (P = 0.87); I² = 0%
Test for overall effect: Z = 0.08 (P = 0.93)

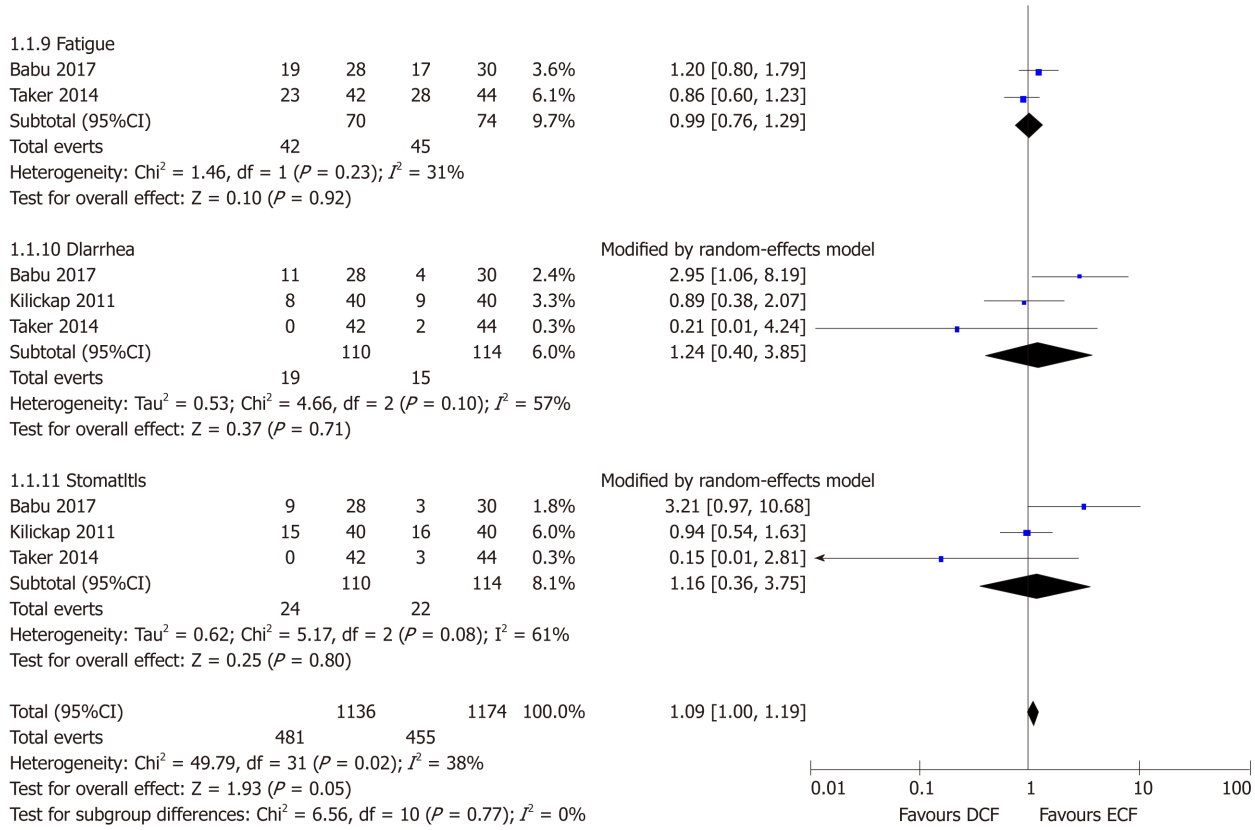

Figure 5 Forest plots of risk ratios of all-grade adverse effects associated with docetaxel, cisplatin, and 5-fluorouracil *vs* epirubicin, cisplatin, and 5-fluorouracil. ECF: Epirubicin, cisplatin, and 5-fluorouracil; DCF: Docetaxel, cisplatin, and 5-fluorouracil.

Study or subgroup	DCF Events	DCF Total	ECF Events	ECF Total	Weight	Risk ratio M-H, Fixed, 95%CI
2.1.1 Total grade 3-4 adverse events						Modified by random-effects model
Babu 2017	28	28	14	30	16.0%	2.10 [1.44, 3.07]
Gao 2010	24	32	16	32	14.6%	1.50 [1.01, 2.24]
Kilickap 2011	40	40	27	40	35.7%	1.47 [1.19, 1.83]
Taker 2014	28	42	27	44	21.2%	1.09 [0.79, 1.49]
Subtotal (95%CI)		142		146	87.6%	1.48 [1.16, 1.88]
Total everts	120		84			
Heterogeneity: Tau^2 = 0.03; Chi^2 = 6.91, df = 3 (P = 0.07); I^2 = 57%						
Test for overall effect: Z = 3.16 (P = 0.002)						
2.1.2 Leucopenla						
Gao 2010	4	32	3	32	1.4%	1.33 [0.32, 5.49]
Taker 2014	7	42	6	44	2.8%	1.22 [0.45, 3.34]
Subtotal (95%CI)		74		76	4.2%	1.26 [0.56, 2.86]
Total everts	11		9			
Heterogeneity: Chi^2 = 0.01, df = 1 (P = 0.92); I^2 = 0%						
Test for overall effect: Z = 0.55 (P = 0.58)						
2.1.3 Neutropenia						
Babu 2017	11	28	5	30	2.3%	2.36 [0.94, 5.93]
Gao 2010	2	32	2	32	1.0%	1.00 [0.15, 6.67]
Kilickap 2011	22	40	10	40	4.8%	2.20 [1.20, 4.03]
Roth 2007	32	41	24	40	11.6%	1.30 [0.96, 1.76]
Taker 2014	7	42	4	44	1.9%	1.83 [0.58, 5.81]
Subtotal (95%CI)		183		186	21.5%	1.65 [1.25, 2.16]
Total everts	74		45			
Heterogeneity: Chi^2 = 4.12, df = 4 (P = 0.39); I^2 = 3%						
Test for overall effect: Z = 3.58 (P = 0.0003)						
2.1.4 Febrile neutropenia						
Babu 2017	7	28	4	30	1.8%	1.88 [0.61, 5.72]
Roth 2007	17	41	7	40	3.4%	2.37 [1.10, 5.09]
Subtotal (95%CI)		69		70	5.2%	2.19 [1.17, 4.12]
Total everts	24		11			
Heterogeneity: Chi^2 = 0.12, df = 1 (P = 0.73); I^2 = 0%						
Test for overall effect: Z = 2.45 (P = 0.01)						
2.1.5 Anemia						
Babu 2017	1	28	1	30	0.5%	1.07 [0.07, 16.32]
Taker 2014	3	42	6	44	2.8%	0.52 [0.14, 1.96]
Subtotal (95%CI)		70		74	3.3%	0.60 [0.19, 1.95]
Total everts	4		7			
Heterogeneity: Chi^2 = 0.21, df = 1 (P = 0.64); I^2 = 0%						
Test for overall effect: Z = 0.85 (P = 0.40)						
2.1.6 Anorexia						Modified by random-effects model
Gao 2010	5	32	3	32	2.2%	1.67 [0.43, 6.40]
Taker 2014	1	42	4	44	0.9%	0.26 [0.03, 2.25]
Subtotal (95%CI)		74		76	3.1%	0.80 [0.13, 4.82]
Total everts	6		7			
Heterogeneity: Tau^2 = 0.92; Chi^2 = 2.09, df = 1 (P = 0.15); I^2 = 52%						
Test for overall effect: Z = 0.24 (P = 0.81)						
2.1.7 Nausea/Vomiting						
Babu 2017	0	28	1	30	0.7%	0.36 [0.02, 8.40]
Gao 2010	7	32	5	32	2.4%	1.40 [0.50, 3.95]
Kilickap 2011	8	40	6	40	2.9%	1.33 [0.51, 3.49]
Roth 2007	10	41	7	40	3.4%	1.39 [0.59, 3.30]
Taker 2014	2	42	3	44	1.4%	0.70 [0.12, 3.97]
Subtotal (95%CI)		183		186	10.7%	1.22 [0.73, 2.03]
Total everts	27		22			
Heterogeneity: Chi^2 = 1.17, df = 4 (P = 0.88); I^2 = 0%						
Test for overall effect: Z = 0.77 (P = 0.44)						
2.1.8 Fatigue						
Babu 2017	2	28	0	30	0.2%	5.34 [0.27, 106.70]
Taker 2014	3	42	2	44	0.9%	1.57 [0.28, 8.94]
Subtotal (95%CI)		70		74	1.2%	2.32 [0.54, 9.98]
Total everts	5		2			
Heterogeneity: Chi^2 = 0.49, df = 1 (P = 0.48); I^2 = 0%						
Test for overall effect: Z = 1.13 (P = 0.26)						

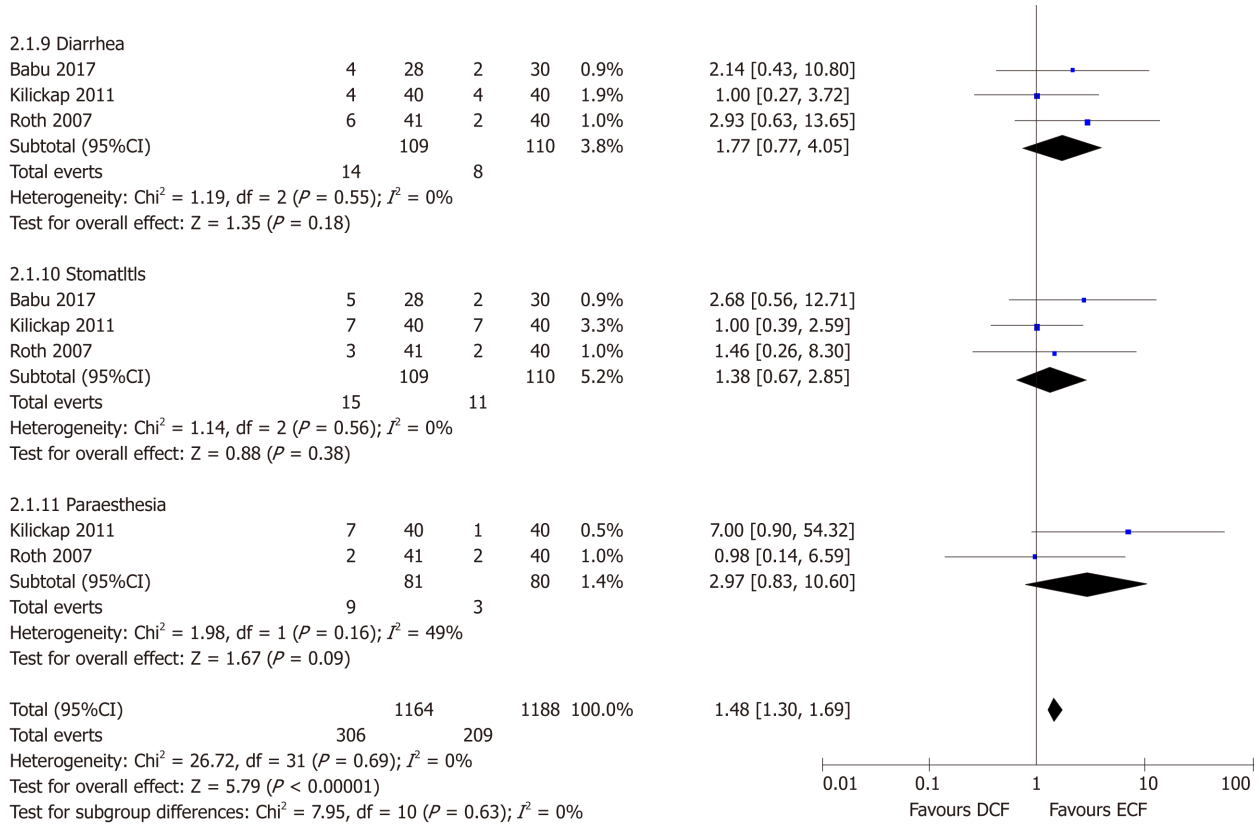

Figure 6 Forest plots of risk ratios of grade 3-4 adverse effects associated with docetaxel, cisplatin, and 5-fluorouracil *vs* epirubicin, cisplatin, and 5-fluorouracil. ECF: Epirubicin, cisplatin, and 5-fluorouracil; DCF: Docetaxel, cisplatin, and 5-fluorouracil.

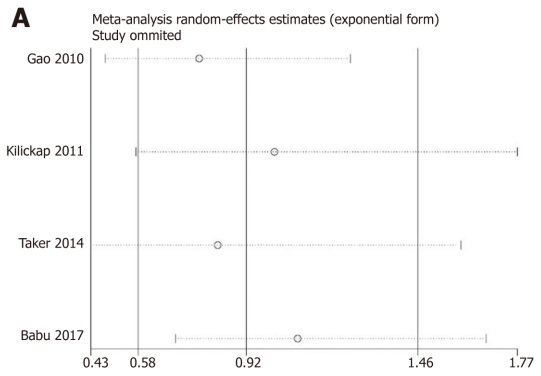

Study ommited	e^coef	(95%CI)	
Gao 2010	0.77302003	0.47942573	1.2464077
Kilickap 2011	1.0087584	0.57528448	1.7688526
Taker 2014	0.83125186	0.43408784	1.5917969
Babu 2017	1.0809172	0.69919729	1.6710334
Combined	0.92099216	0.58216494	1.457021

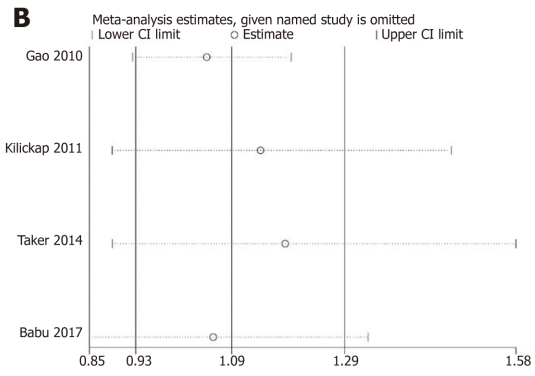

Study ommited	Estimate	(95%CI)	
Gao 2010	1.0485446	0.92074496	1.194083
Kilickap 2011	1.1411179	0.88590586	1.4698516
Taker 2014	1.1835881	0.88621151	1.5807523
Babu 2017	1.059528	0.84642333	1.3262863
Combined	1.0913749	0.9264195	1.2857017

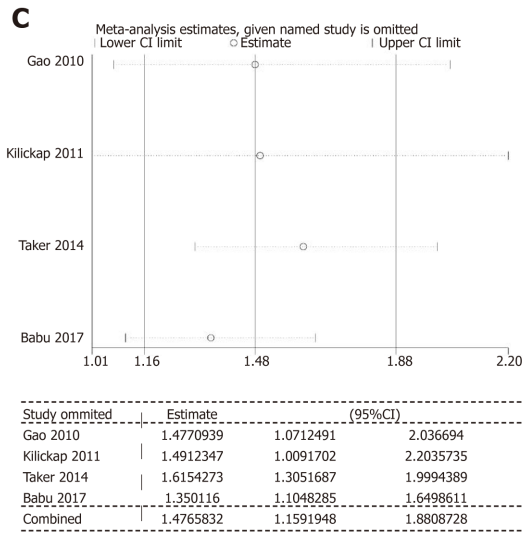

Study ommited	Estimate		(95%CI)
Gao 2010	1.4770939	1.0712491	2.036694
Kilickap 2011	1.4912347	1.0091702	2.2035735
Taker 2014	1.6154273	1.3051687	1.9994389
Babu 2017	1.350116	1.1048285	1.6498611
Combined	1.4765832	1.1591948	1.8808728

Figure 7 Meta-based influence analysis for comparisons of objective response rate (A), total adverse effects (B), and grade 3-4 adverse effects (C).

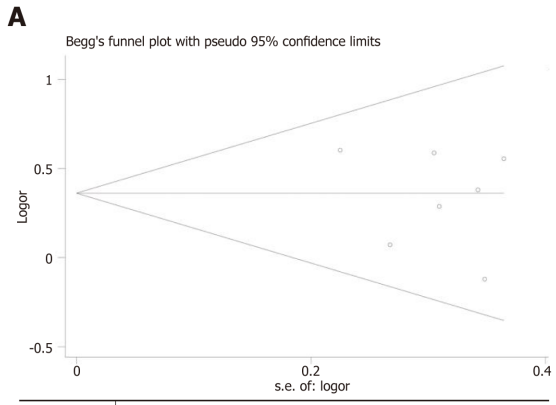

Std_Eff	Coef	Std. Err	*t*	*P* > |t|	(95%CI)	
Slope	0.8425367	0.6563998	1.28	0.256	-0.8447927	2.529866
Bias	-1.640456	2.208128	-0.74	0.491	-7.316631	4.035718

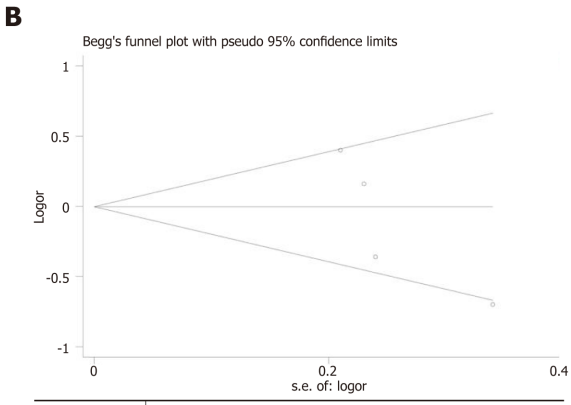

Std_Eff	Coef	Std. Err	*t*	*P* > |t|	(95%CI)	
Slope	1.999026	0.9068895	2.20	0.158	-1.903004	5.901057
Bias	-8.344442	3.727938	-2.24	0.155	-24.38446	7.69558

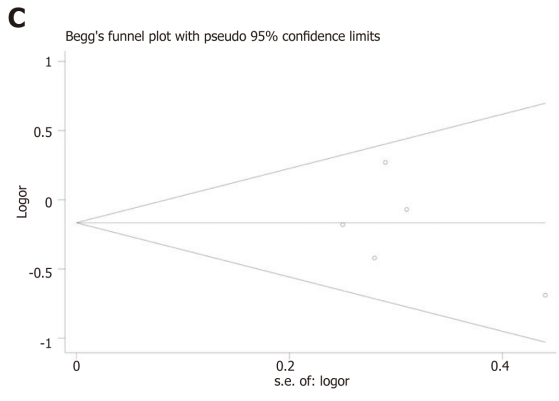

Std_Eff	Coef	Std. Err	*t*	*P* > |t|	(95%CI)	
Slope	0.5259134	0.8758762	0.60	0.591	-2.261516	3.313342
Bias	-2.354023	2.936912	-0.80	0.481	-11.70059	6.992541

Figure 8 Begg's and Egger's tests for comparisons of objective response rate (A), progression-free survival (B), and overall survival (C).

ARTICLE HIGHLIGHTS

Research background

Gastric cancer has always been a disease with high morbidity and mortality in the world. Because of the lack of obvious symptoms and signs in the early stage, many patients are found to

have been diagnosed in the advanced stage. At the same time, none of the first-line treatments for advanced gastric cancer is standard. At present, docetaxel, cisplatin, and 5-fluorouracil (DCF) and epirubicin, cisplatin, and 5-fluorouracil (ECF) are both effective first-line regimens for clinical use, but in many countries, different researchers have different opinions. There are still many disputes about the advantages and disadvantages of these two regimens. The results in some studies showed that the DCF group was better than the ECF group. However, in other studies, opposite results were obtained. To solve the controversy, we conducted this meta-analysis.

Research motivation

In many studies, both DCF and ECF regimens have shown good outcomes, but on the other hand, they also show many disadvantages, especially in the adverse effects (AEs). Since there is still much controversy in this field, and there is lack of evidence of evidence-based medicine in relevant fields to prove that which regimen is more suitable for clinical use, it is necessary to conduct relevant meta-analysis. This study therefore aimed to provide a more focused analysis through the evaluation of the survival outcomes and AEs between DCF and ECF regimens.

Research objectives

Our primary objective was to analyze the efficacy of the two first-line regimens in the treatment of advanced gastric cancer by obtaining the best and latest data from clinical trials. In the discussion section, we cited many frontier studies in related fields, and focused on the analysis of the reasons for the difference in therapeutic effect between DCF and ECF regimens. At the same time, we also hope that our research can play a guiding and helpful role in clinical medication.

Research methods

We conducted this meta-analysis according to the Preferred Reporting Items for Systematic Review and Meta-Analysis guidelines. Seven main databases were searched up to August 31, 2018. Search results were limited to original human studies, and search criteria were restricted to randomized controlled trials or cohort studies without language restriction. We selected studies according to the PICOS principle. The Jadad scale and the Newcastle-Ottawa Scale were used to assess quality of the studies, and RevMan and STATA were used to analyze the data. Progression-free survival (PFS) and overall survival (OS) were analyzed by the pooled hazard ratio. Objective response rate (ORR), disease control rate (DCR), and AEs were analyzed by the pooled risk ratio. The heterogeneity test was evaluated by using the Q test and I^2 statistic. If $P > 0.1$ and $I^2 < 50\%$, the fixed effects model was used. Otherwise, the random effects model was used.

Research results

Our meta-analysis included seven high quality articles and 598 patients with advanced gastric cancer for the final analysis to compare the efficacy and safety of the DCF regimen and ECF regimen. The results showed that DCF and ECF were both effective with comparable PFS (95%CI: 0.58-1.46, $P = 0.73$) and OS (95%CI: 0.65-1.10, $P = 0.21$). The DCF group showed significantly better ORR (95%CI: 1.13-1.75, $P = 0.002$) and DCR (95%CI: 1.03-1.41, $P = 0.02$) than the ECF group. We evaluated toxicities between the DCF and ECF groups based on total (all-grade/grade 3-4) AEs. The AEs between the two groups were only significantly different in the aspects of neutropenia (95%CI: 1.25-2.16, $P = 0.0003$) and febrile neutropenia (95%CI: 1.17-4.12, $P = 0.01$), while other toxicities showed no statistically significant differences between the two groups.

Research conclusions

This study is the latest meta-analysis to compare DCF and ECF regimens for advanced gastric cancer. From this result, we conclude that DCF regimen seems to be more suitable for advanced gastric cancer than the ECF regimen. This finding is extremely important for the research and guidance of clinical medication in related fields. DCF regimen, like most drugs, is not perfect and in some respects shows some unsatisfactory aspects. We cannot deny the effectiveness of DCF in the treatment of advanced gastric cancer, but we cannot ignore its side effects.

Research perspectives

Our evidence of evidence-based medicine is mainly based on the original clinical research, but at present it seems that the research in related fields is still very deficient, which directly leads to the great limitation of our access to clinical evidence. Although there is still much controversy about the first-line drug use in the treatment of advanced gastric cancer, because gastric cancer cells are relatively sensitive to chemotherapeutic drugs, it is expected that larger clinical trials in the future can be conducted for related research.

ACKNOWLEDGEMENTS

The authors thank Professor Ji-Chun Liu, MD, PhD (Department of Cardio-Thoracic Surgery, The Second Affiliated Hospital of Nanchang University) and Professor Xiao-Shu Cheng, MD, PhD (Department of Cardiology, The Second Affiliated Hospital of Nanchang University) for their advice.

REFERENCES

1 **Bray F**, Ferlay J, Soerjomataram I, Siegel RL, Torre LA, Jemal A. Global cancer statistics 2018: GLOBOCAN estimates of incidence and mortality worldwide for 36 cancers in 185 countries. *CA Cancer J Clin* 2018; **68**: 394-424 [PMID: 30207593 DOI: 10.3322/caac.21492]

2 **Wagner AD**, Wedding U. Advances in the pharmacological treatment of gastro-oesophageal cancer. *Drugs Aging* 2009; **26**: 627-646 [PMID: 19685930 DOI: 10.2165/11315740-000000000-00000]

3 **Ang TL**, Fock KM. Clinical epidemiology of gastric cancer. *Singapore Med J* 2014; **55**: 621-628 [PMID: 25630323 DOI: 10.11622/smedj.2014174]

4 **Das P**, Ajani JA. Gastric and gastro-oesophageal cancer therapy. *Expert Opin Pharmacother* 2005; **6**: 2805-2812 [PMID: 16318431 DOI: 10.1517/14656566.6.16.2805]

5 **Hu JK**, Chen ZX, Zhou ZG, Zhang B, Tian J, Chen JP, Wang L, Wang CH, Chen HY, Li YP. Intravenous chemotherapy for resected gastric cancer: meta-analysis of randomized controlled trials. *World J Gastroenterol* 2002; **8**: 1023-1028 [PMID: 12439918 DOI: 10.3748/wjg.v8.i6.1023]

6 **Hu JK**, Li CM, Chen XZ, Chen ZX, Zhou ZG, Zhang B, Chen JP. The effectiveness of intravenous 5-fluorouracil-containing chemotherapy after curative resection for gastric carcinoma: A systematic review of published randomized controlled trials. *J Chemother* 2007; **19**: 359-375 [PMID: 17855179 DOI: 10.1179/joc.2007.19.4.359]

7 **National Comprehensive Cancer Network**. National Comprehensive Cancer Network Practice guidelines in oncology-version V.1. 2018; (gastric cancer) Available from: https://www.nccn.org/professionals/physician_gls/pdf/gastric.pdf

8 **Kilickap S**, Yalcin S, Ates O, Tekuzman G. The first line systemic chemotherapy in metastatic gastric carcinoma: A comparison of docetaxel, cisplatin and fluorouracil (DCF) versus cisplatin and fluorouracil (CF); versus epirubicin, cisplatin and fluorouracil (ECF) regimens in clinical setting. *Hepatogastroenterology* 2011; **58**: 208-212 [PMID: 21510316]

9 **Babu KG**, Chaudhuri T, Lakshmaiah KC, Dasappa L, Jacob LA, Babu M, Rudresha AH, Lokesh KN, Rajeev LK. Efficacy and safety of first-line systemic chemotherapy with epirubicin, cisplatin plus 5-fluorouracil and docetaxel, cisplatin plus 5-fluorouracil regimens in locally advanced inoperable or metastatic gastric or gastroesophageal junction adenocarcinoma: A prospective phase II study from South India. *Indian J Cancer* 2017; **54**: 47-51 [PMID: 29199662 DOI: 10.4103/ijc.IJC_168_17]

10 **Roth AD**, Fazio N, Stupp R, Falk S, Bernhard J, Saletti P, Köberle D, Borner MM, Rufibach K, Maibach R, Wernli M, Leslie M, Glynne-Jones R, Widmer L, Seymour M, de Braud F; Swiss Group for Clinical Cancer Research. Docetaxel, cisplatin, and fluorouracil; docetaxel and cisplatin; and epirubicin, cisplatin, and fluorouracil as systemic treatment for advanced gastric carcinoma: a randomized phase II trial of the Swiss Group for Clinical Cancer Research. *J Clin Oncol* 2007; **25**: 3217-3223 [PMID: 17664469 DOI: 10.1200/JCO.2006.08.0135]

11 **Gao H**, Ding X, Wei D, Tao XU, Cheng P. Docetaxel versus epirubicin combined with cisplatin, leucovorin and fluorouracil for advanced gastric carcinoma as first line therapy: a randomized clinical trial. *Chin Clin Oncol* 2010; **15**: 529-533

12 **Teker F**, Yilmaz B, Kemal Y, Kut E, Yucel I. Efficacy and safety of docetaxel or epirubicin, combined with cisplatin and fluorouracil (DCF and ECF), regimens as first line chemotherapy for advanced gastric cancer: a retrospective analysis from Turkey. *Asian Pac J Cancer Prev* 2014; **15**: 6727-6732 [PMID: 25169516 DOI: 10.7314/APJCP.2014.15.16.6727]

13 **Moher D**, Liberati A, Tetzlaff J, Altman DG; PRISMA Group. Preferred reporting items for systematic reviews and meta-analyses: the PRISMA Statement. *Open Med* 2009; **3**: e123-e130 [PMID: 21603045]

14 **Jadad AR**, Moore RA, Carroll D, Jenkinson C, Reynolds DJ, Gavaghan DJ, McQuay HJ. Assessing the quality of reports of randomized clinical trials: is blinding necessary? *Control Clin Trials* 1996; **17**: 1-12 [PMID: 8721797 DOI: 10.1016/0197-2456(95)00134-4]

15 **Wells GA**, Shea BJ, O'Connell D, Peterson J, Welch V, Losos M. The newcastle-ottawa scale (nos) for assessing the quality of non-randomized studies in meta-analysis. *Appl Eng Agric* 2014; **18**: 727-734

16 **Tierney JF**, Stewart LA, Ghersi D, Burdett S, Sydes MR. Practical methods for incorporating summary time-to-event data into meta-analysis. *Trials* 2007; **8**: 16 [PMID: 17555582 DOI: 10.1186/1745-6215-8-16]

17 **Higgins JPT**, Green S, editors. *Cochrane handbook for systematic reviews of interventions (version 5.1.0)*. London: The Cochrane Collaboration 2011;

18 **Sadighi S**, Mohagheghi MA, Montazeri A, Sadighi Z. Quality of life in patients with advanced gastric cancer: a randomized trial comparing docetaxel, cisplatin, 5-FU (TCF) with epirubicin, cisplatin, 5-FU (ECF). *BMC Cancer* 2006; **6**: 274 [PMID: 17147808 DOI: 10.1186/1471-2407-6-274]

19 **Abbasi SY**, Taani HE, Saad A, Badheeb A, Addasi A. Advanced gastric cancer in jordan from 2004 to 2008: a study of epidemiology and outcomes. *Gastrointest Cancer Res* 2011; **4**: 122-127 [PMID: 22368735]

20 **Shah MA**, Janjigian YY, Stoller R, Shibata S, Kemeny M, Krishnamurthi S, Su YB, Ocean A, Capanu M, Mehrotra B, Ritch P, Henderson C, Kelsen DP. Randomized Multicenter Phase II Study of Modified Docetaxel, Cisplatin, and Fluorouracil (DCF) Versus DCF Plus Growth Factor Support in Patients With Metastatic Gastric Adenocarcinoma: A Study of the US Gastric Cancer Consortium. *J Clin Oncol* 2015; **33**: 3874-3879 [PMID: 26438119 DOI: 10.1200/JCO.2015.60.7465]

21 **Slagter AE**, Jansen EPM, van Laarhoven HWM, van Sandick JW, van Grieken NCT, Sikorska K, Cats A, Muller-Timmermans P, Hulshof MCCM, Boot H, Los M, Beerepoot LV, Peters FPJ, Hospers GAP, van Etten B, Hartgrink HH, van Berge Henegouwen MI, Nieuwenhuijzen GAP, van Hillegersberg R, van der Peet DL, Grabsch HI, Verheij M. CRITICS-II: a multicentre randomised phase II trial of neo-adjuvant chemotherapy followed by surgery versus neo-adjuvant chemotherapy and subsequent chemoradiotherapy followed by surgery versus neo-adjuvant chemoradiotherapy followed by surgery in resectable gastric cancer. *BMC Cancer* 2018; **18**: 877 [PMID: 30200910 DOI: 10.1186/s12885-018-4770-2]

22 **Fujitani K**, Yang HK, Mizusawa J, Kim YW, Terashima M, Han SU, Iwasaki Y, Hyung WJ, Takagane A, Park DJ, Yoshikawa T, Hahn S, Nakamura K, Park CH, Kurokawa Y, Bang YJ, Park BJ, Sasako M, Tsujinaka T; REGATTA study investigators. Gastrectomy plus chemotherapy versus chemotherapy alone for advanced gastric cancer with a single non-curable factor (REGATTA): a phase 3, randomised controlled trial. *Lancet Oncol* 2016; **17**: 309-318 [PMID: 26822397 DOI: 10.1016/S1470-2045(15)00553-7]

23 **Wagner AD**, Grothe W, Haerting J, Kleber G, Grothey A, Fleig WE. Chemotherapy in advanced gastric cancer: a systematic review and meta-analysis based on aggregate data. *J Clin Oncol* 2006; **24**: 2903-2909

[PMID: 16782930 DOI: 10.1200/JCO.2005.05.0245]
24 **Van Cutsem E**, Moiseyenko VM, Tjulandin S, Majlis A, Constenla M, Boni C, Rodrigues A, Fodor M, Chao Y, Voznyi E, Risse ML, Ajani JA; V325 Study Group. Phase III study of docetaxel and cisplatin plus fluorouracil compared with cisplatin and fluorouracil as first-line therapy for advanced gastric cancer: a report of the V325 Study Group. *J Clin Oncol* 2006; **24**: 4991-4997 [PMID: 17075117 DOI: 10.1200/JCO.2006.06.8429]
25 **Wagner AD**, Syn NL, Moehler M, Grothe W, Yong WP, Tai BC, Ho J, Unverzagt S. Chemotherapy for advanced gastric cancer. *Cochrane Database Syst Rev* 2017; **8**: CD004064 [PMID: 28850174 DOI: 10.1002/14651858.CD004064.pub4]
26 **Petrioli R**, Roviello G, Zanotti L, Roviello F, Polom K, Bottini A, Marano L, Francini E, Marrelli D, Generali D. Epirubicin-based compared with docetaxel-based chemotherapy for advanced gastric carcinoma: A systematic review and meta-analysis. *Crit Rev Oncol Hematol* 2016; **102**: 82-88 [PMID: 27083592 DOI: 10.1016/j.critrevonc.2016.04.001]
27 **Chen XL**, Chen XZ, Yang C, Liao YB, Li H, Wang L, Yang K, Li K, Hu JK, Zhang B, Chen ZX, Chen JP, Zhou ZG. Docetaxel, cisplatin and fluorouracil (DCF) regimen compared with non-taxane-containing palliative chemotherapy for gastric carcinoma: a systematic review and meta-analysis. *PLoS One* 2013; **8**: e60320 [PMID: 23593191 DOI: 10.1371/journal.pone.0060320]
28 **Al-Batran SE**, Pauligk C, Homann N, Hartmann JT, Moehler M, Probst S, Rethwisch V, Stoehlmacher-Williams J, Prasnikar N, Hollerbach S, Bokemeyer C, Mahlberg R, Hofheinz RD, Luley K, Kullmann F, Jäger E. The feasibility of triple-drug chemotherapy combination in older adult patients with oesophagogastric cancer: a randomised trial of the Arbeitsgemeinschaft Internistische Onkologie (FLOT65+). *Eur J Cancer* 2013; **49**: 835-842 [PMID: 23063354 DOI: 10.1016/j.ejca.2012.09.025]
29 **Fujii M**. Chemotherapy for advanced gastric cancer: ongoing phase III study of S-1 alone versus S-1 and docetaxel combination (JACCRO GC03 study). *Int J Clin Oncol* 2008; **13**: 201-205 [PMID: 18553228 DOI: 10.1007/s10147-008-0775-1]
30 **Wang J**, Xu R, Li J, Bai Y, Liu T, Jiao S, Dai G, Xu J, Liu Y, Fan N, Shu Y, Ba Y, Ma D, Qin S, Zheng L, Chen W, Shen L. Randomized multicenter phase III study of a modified docetaxel and cisplatin plus fluorouracil regimen compared with cisplatin and fluorouracil as first-line therapy for advanced or locally recurrent gastric cancer. *Gastric Cancer* 2016; **19**: 234-244 [PMID: 25604851 DOI: 10.1007/s10120-015-0457-4]
31 **Petrelli F**, Tomasello G, Ghidini M, Passalacqua R, Barni S. Modified schedules of DCF chemotherapy for advanced gastric cancer: a systematic review of efficacy and toxicity. *Anticancer Drugs* 2017; **28**: 133-141 [PMID: 27749286 DOI: 10.1097/CAD.0000000000000436]
32 **Van Cutsem E**, Boni C, Tabernero J, Massuti B, Middleton G, Dane F, Reichardt P, Pimentel FL, Cohn A, Follana P, Clemens M, Zaniboni A, Moiseyenko V, Harrison M, Richards DA, Prenen H, Pernot S, Ecstein-Fraisse E, Hitier S, Rougier P. Docetaxel plus oxaliplatin with or without fluorouracil or capecitabine in metastatic or locally recurrent gastric cancer: a randomized phase II study. *Ann Oncol* 2015; **26**: 149-156 [PMID: 25416687 DOI: 10.1093/annonc/mdu496]
33 **Tebbutt NC**, Cummins MM, Sourjina T, Strickland A, Van Hazel G, Ganju V, Gibbs D, Stockler M, Gebski V, Zalcberg J; Australasian Gastro-Intestinal Trials Group. Randomised, non-comparative phase II study of weekly docetaxel with cisplatin and 5-fluorouracil or with capecitabine in oesophagogastric cancer: the AGITG ATTAX trial. *Br J Cancer* 2010; **102**: 475-481 [PMID: 20068567 DOI: 10.1038/sj.bjc.6605522]
34 **Kimura Y**, Yano H, Taniguchi H, Iwazawa T, Danno K, Kagara N, Kanoh T, Ohnishi T, Tono T, Nakano Y, Monden T, Imaoka S. A phase I study of bi-weekly docetaxel for recurrent or advanced gastric cancer patients whose disease progressed by prior chemotherapy. *Jpn J Clin Oncol* 2011; **41**: 747-751 [PMID: 21498408 DOI: 10.1093/jjco/hyr050]
35 **Lee KW**, Kim BJ, Kim MJ, Han HS, Kim JW, Park YI, Park SR. A Multicenter Randomized Phase II Study of Docetaxel vs. Docetaxel Plus Cisplatin vs. Docetaxel Plus S-1 as Second-Line Chemotherapy in Metastatic Gastric Cancer Patients Who Had Progressed after Cisplatin Plus Either S-1 or Capecitabine. *Cancer Res Treat* 2017; **49**: 706-716 [PMID: 27764906 DOI: 10.4143/crt.2016.216]
36 **Smith TJ**, Bohlke K, Armitage JO. Recommendations for the Use of White Blood Cell Growth Factors: American Society of Clinical Oncology Clinical Practice Guideline Update. *J Oncol Pract* 2015; **11**: 511-513 [PMID: 29424584 DOI: 10.1200/JOP.2015.006742]
37 **Aapro MS**, Bohlius J, Cameron DA, Dal Lago L, Donnelly JP, Kearney N, Lyman GH, Pettengell R, Tjan-Heijnen VC, Walewski J, Weber DC, Zielinski C; European Organisation for Research and Treatment of Cancer. 2010 update of EORTC guidelines for the use of granulocyte-colony stimulating factor to reduce the incidence of chemotherapy-induced febrile neutropenia in adult patients with lymphoproliferative disorders and solid tumours. *Eur J Cancer* 2011; **47**: 8-32 [PMID: 21095116 DOI: 10.1016/j.ejca.2010.10.013]
38 **Li CP**, Chen JS, Chen LT, Yen CJ, Lee KD, Su WP, Lin PC, Lu CH, Tsai HJ, Chao Y. A phase II study of weekly docetaxel and cisplatin plus oral tegafur/uracil and leucovorin as first-line chemotherapy in patients with locally advanced or metastatic gastric cancer. *Br J Cancer* 2010; **103**: 1343-1348 [PMID: 20924378 DOI: 10.1038/sj.bjc.6605928]
39 **Liu Y**, Zhao G, Xu Y, He X, Li X, Chen H, Wu Q, Yao S, Yan G, Chen T. Multicenter Phase 2 Study of Peri-Irradiation Chemotherapy Plus Intensity Modulated Radiation Therapy With Concurrent Weekly Docetaxel for Inoperable or Medically Unresectable Nonmetastatic Gastric Cancer. *Int J Radiat Oncol Biol Phys* 2017; **98**: 1096-1105 [PMID: 28721893 DOI: 10.1016/j.ijrobp.2017.03.032]

P- Reviewer: Crumley ABC, Kimura A
S- Editor: Wang JL **L- Editor:** Wang TQ **E- Editor:** Tan WW

World Journal of Clinical Cases

Submit a Manuscript: https://www.f6publishing.com

World J Clin Cases 2019 March 6; 7(5): 616-622

DOI: 10.12998/wjcc.v7.i5.616

ISSN 2307-8960 (online)

CASE REPORT

Sustained complete response to erlotinib in squamous cell carcinoma of the head and neck: A case report

Mie Mie Thinn, Chung-Tzu Hsueh, Chung-Tsen Hsueh

ORCID number: Mie Mie Thinn (0000-0001-7605-2526); Chung-Tzu Hsueh (0000-0002-7574-9863); Chung-Tsen Hsueh (0000-0002-1409-0030).

Author contributions: Hsueh CT performed clinical examination and collected data; Thinn MM, Hsueh CT and Hsueh CT designed the report, analyzed the data and wrote the paper; all authors read and approved the final manuscript.

Informed consent statement: Informed written consent was obtained from the surviving spouse of deceased patient for publication of this report and any accompanying images.

Conflict-of-interest statement: The authors declare that they have no conflict of interest.

CARE Checklist (2016) statement: The authors have read the CARE Checklist (2016), and the manuscript was prepared and revised according to the CARE Checklist (2016).

Open-Access: This article is an open-access article which was selected by an in-house editor and fully peer-reviewed by external reviewers. It is distributed in accordance with the Creative Commons Attribution Non Commercial (CC BY-NC 4.0) license, which permits others to distribute, remix, adapt, build upon this work non-commercially, and license their derivative works on different terms, provided the original work is properly cited and the use is non-commercial. See: http://creativecommons.org/licen

Mie Mie Thinn, Division of Hematology and Medical Oncology, Loma Linda Veterans Administration Medical Center, Loma Linda, CA 92357, United States

Chung-Tzu Hsueh, Department of Dentistry, Cathay General Hospital, Taipei City 106, Taiwan

Chung-Tsen Hsueh, Division of Medical Oncology and Hematology, Department of Medicine, Loma Linda University, Loma Linda, CA 92357, United States

Corresponding author: Chung-Tsen Hsueh, MD, PhD, Professor, Division of Medical Oncology and Hematology, Department of Medicine, Loma Linda University, 11175 Campus Street, CSP 11015, Loma Linda, CA 92357, United States. chsueh@llu.edu
Telephone: +1-909-5588107
Fax: +1-909-5580219

Abstract

BACKGROUND

Squamous cell carcinoma of head and neck (SCCHN) is the fifth most common cancer worldwide. Inhibition of epidermal growth factor receptor signaling has been shown to be a critical component of therapeutic option. Herein, we report a case of durable complete response to erlotinib.

CASE SUMMARY

An 81-year-old Caucasian male who presented with metastatic poorly differentiated squamous cell carcinoma of right cervical lymph nodes (levels 2 and 3). Imaging studies including (18)F-fluorodeoxyglucose positron emission tomography/computed tomography (CT) and contrast-enhanced CT scan of neck and chest did not reveal any other disease elsewhere. Panendoscopic examination with random biopsy did not reveal malignant lesion in nasopharynx, oropharynx, and larynx. He underwent modified neck dissection and postoperative radiation. Within 2 mo after completion of radiation, he developed local recurrence at right neck, which was surgically removed. Two mo after the salvage surgery, he developed a second recurrence at right neck. Due to suboptimal performance status and his preference, he started erlotinib treatment. He achieved partial response after first 2 mo of erlotinib treatment, then complete response after total 6 mo of erlotinib treatment. He developed sever skin rash and diarrhea including *Clostridium difficile* infection during the course of erlotinib treatment requiring dose reduction and eventual discontinuation. He remained in complete remission for more than two years after discontinuation of erlotinib.

CONCLUSION

We report a case of metastatic SCCHN achieving durable complete response from

ses/by-nc/4.0/

Manuscript source: Invited manuscript

Received: December 19, 2018
Peer-review started: December 20, 2018
First decision: January 5, 2019
Revised: January 12, 2019
Accepted: January 29, 2019
Article in press: January 29, 2019
Published online: March 6, 2019

erlotinib. Patient experienced skin rash and diarrhea toxicities which were likely predictors of his treatment response.

Key words: Squamous cell carcinoma of head and neck; Epidermal growth factor receptor; Erlotinib; Complete response; Skin rash; Tyrosine kinase inhibitor; Case report

©The Author(s) 2019. Published by Baishideng Publishing Group Inc. All rights reserved.

Core tip: We present a patient with recurrent/metastatic squamous cell carcinoma of head and neck who had durable complete response after completion of 6-mo erlotinib treatment. Patient experienced severe skin rash and diarrhea toxicities from erlotinib. The severity of these adverse effects has been shown to be predictors of treatment response from inhibitors of epidermal growth factor receptor.

Citation: Thinn MM, Hsueh CT, Hsueh CT. Sustained complete response to erlotinib in squamous cell carcinoma of the head and neck: A case report. *World J Clin Cases* 2019; 7(5): 616-622
URL: https://www.wjgnet.com/2307-8960/full/v7/i5/616.htm
DOI: https://dx.doi.org/10.12998/wjcc.v7.i5.616

INTRODUCTION

Squamous cell carcinoma of head and neck (SCCHN) is the fifth most common cancer worldwide with a global yearly incidence of more than 600000 new cases and around 300000 annual deaths in 2012[1]. Early-stage disease is managed with either surgery or radiation. Two-third of patients present with locally advanced disease, and are generally treated with multimodality therapy, which commonly includes chemotherapy[2]. Tumor control and survival in SCCHN remain unsatisfactory. Even for those who have achieved complete response after initial treatment, the incidence of local recurrence is 50%-60% and the incidence of distant metastases is 20%-30%. Systemic therapy is the mainstay for metastatic disease and unsalvageable recurrence to improve survival and quality of life.

With recent advances in cancer biology, there appear to be common molecular events in SCCHN that are biologically significant in cell survival and invasion, and could be used for therapeutic development such as epidermal growth factor receptor (EGFR). Overexpression of EGFR and its ligand have been reported in 80% to 90% of SCCHN tumors compared with levels in normal mucosa of patients without cancer[3]. Increased EGFR expression has been reported to be a predictor of worse survival in SCCHN patients receiving surgery and chemotherapy[4,5]. The two targeting strategies for inhibition of EGFR are small-molecule tyrosine kinase inhibitors (TKIs) and monoclonal antibodies directed against the receptor. Cetuximab (a monoclonal antibody against EGFR) has been approved by United States Food and Drug Administration as initial treatment of locally advanced SCCHN in combination with radiation therapy, as first-line treatment of recurrent or metastatic SCCHN in combination with platinum-based therapy plus 5-fluorouracil, and as a single agent for recurrent or metastatic SCCHN progressing from prior platinum-based therapy[2]. Adding cetuximab to platinum-based chemotherapy with 5-fluorouracil as first-line treatment of recurrent or metastatic SCCHN significantly prolonged the median overall survival[6]. Herein, we report a case of sustained complete response to erlotinib, a TKI of EGFR, as first-line treatment for recurrent SCCHN.

CASE PRESENTATION

Chief complaints

An 81-year-old Caucasian male presented with right neck mass.

History of present illness

He had no history of cigarette smoking or alcohol use.

History of past illness

He had an extensive history of multiple skin lesions removed from his scalp, arms, chest and back over 10-15 years prior to presentation. Most of the skin lesions were squamous cell carcinoma except one lesion was in-situ melanoma. Other significant past medical history included diabetes mellitus type II, hypertension, hypothyroidism and remote cerebrovascular accident with mild residual dysarthria and right central vision loss.

Personal and family history

Family history was pertinent for mother died of liver cancer at age 86.

Physical examination upon admission

Physical examination was unremarkable except right neck lymphadenopathy.

Imaging examinations

Imaging studies including (18)F-fluorodeoxyglucose positron emission tomography/computed tomography (CT) and contrast-enhanced CT (CECT) scan of neck and chest revealed right cervical lymphadenopathy. The panendoscopic examination of ENT field did not reveal any abnormality, and the random biopsy of nasopharynx, oropharynx, and larynx showed no evidence of malignancy. Excisional biopsy of right neck mass turned out to be metastatic poorly differentiated squamous cell carcinoma. He underwent right modified neck dissection with seventeen lymph nodes removed from levels 2, 3, 4 and 5. Two of the two lymph nodes from level 2 had evidence of metastatic carcinoma with the largest focus being 2.5 cm and extracapsular extension being present. Three of the five lymph nodes from level 3 were positive for metastatic carcinoma with largest focus being 0.7 cm and extracapsular extension being present. None of the lymph nodes from level 4 or 5 were found to have any metastatic carcinoma. Shortly after postoperative intensity-modulated radiotherapy to right neck with total dose of 66 Gy, he developed local recurrence at right neck and underwent salvage surgery.

FINAL DIAGNOSIS

Two mo after salvage surgery, he was found to have palpable skin nodules over the right neck. CECT scan of the neck showed interval increase in the soft tissue thickening and diffuse subcutaneous thickening of the right neck. Focal skin irregularity and interval development of submental, right submandibular adenopathy as well as adenopathy at the right inferior parotid compatible with recurrent/metastatic SCCHN were noted (Figure 1).

TREATMENT

Treatment options were discussed including platinum based chemotherapeutic regimen and targeted therapy. Due to patient's preference and literature support (see discussion), erlotinib 150 mg orally per day was started. He tolerated the treatment well initially, and achieved partial response after 2 mo of treatment. Subsequently, he developed grade 3 toxicities including skin rash and diarrhea with *Clostridium difficile* infection requiring dose reduction of erlotinib from 150 mg to 100 mg daily.

OUTCOME AND FOLLOW-UP

He eventually had complete response after total 6 mo of treatment (Figure 2). Erlotinib was discontinued due to intolerance. He remained free of recurrent disease for more than two years. Subsequently he succumbed to death due to postoperative complication with respiratory failure after resection of an ulcerating skin lesion at right clavicular head.

DISCUSSION

Our patient presented with SCCHN of unknown primary with cervical lymph node metastasis. His primary site of origin has never been identified over the course of the subsequent workup and follow-up. Retrospective analyses indicate SCCHN of unknown primary represents about 3% of newly diagnosed SCCHN[7]. Most SCCHN of unknown primary may represent clinically occult oropharyngeal cancer. The

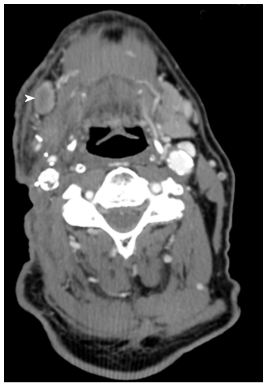

Figure 1 Contrast-enhanced computed tomography scan of neck prior to erlotinib treatment. Development of right neck focal skin irregularity and right submandibular lymphadenopathy (white arrowhead) consistent with metastases were noted.

management of SCCHN of unknown primary is aimed at curative for most patients; cervical lymphadenopathy indicates locally advanced disease and is amenable for multimodality treatment such as surgery and radiotherapy.

Our patient developed regional recurrence shortly after initial surgery with neck dissection and post-operative radiotherapy. Despite of salvage surgery, he developed recurrent disease at prior surgical site two mo later. Due to suboptimal performance status and patient's preference, he received systemic therapy with erlotinib, which is an EGFR TKI. EGFR TKIs inhibit EGFR and downstream signaling leading to apoptosis. Advantages of TKIs include the ease of oral administration. As shown in Table 1, erlotinib, lapatinib, gefitinib and afatinib have been studied in phase II/III trials[8-11]. Most of them showed promising activities in SCCHN, but failed to demonstrate improved survival compared to chemotherapy. A multicenter phase II study evaluated erlotinib in the treatment of recurrent or metastatic SCCHN showed the overall objective response rate of 4.3% in 115 patients. Forty-seven percent of patients received erlotinib at 150 mg daily throughout the entire study, 6% had dose escalations, and 46% required dose reductions and/or interruptions. Stable disease for a median duration of 16.1 wk was noted in 38% of patient. The median progression-free survival was 9.6 wk, and the median overall survival was 6 mo. Better overall survival was observed in patients who developed grade 2 or higher rash. Rash was the most common adverse event, observed in 79% of patients, followed by diarrhea, which was seen in 37% of patients. Most of the adverse events were mild to moderate[8].

Retrospective analyses of clinical trials investigating EGFR TKIs in SCCHN have shown skin rash and diarrhea are common toxicities and severity of these side effects correlates with therapeutic responses[12]. Skin rash has been shown to a predictor of response to EGFR TKI in patients with non-small cell lung cancer, likely due to skin injury caused by inhibition of EGFR signaling in epidermal cells[13]. Many factors may affect severity of skin rash including genetic variations in EGFR and metabolism of EGFR TKI[14]. Higher drug levels may result from polymorphisms in metabolizing enzymes such as cytochrome P450 family. The severe skin rash and diarrhea toxicities seen in our case are likely predictors of good treatment response from erlotinib.

In non-small cell lung carcinoma, patients with activating mutations in the EGFR tyrosine kinase domain are sensitive to EGFR TKIs. However, the incidence of this type of EGFR mutations is low and fails to predict sensitivity to EGFR TKIs in SCCHN[15]. Van Allen *et al*[16] reported a patient with locally advanced SCCHN achieving a near-complete pathological response after 13 d of neoadjuvant erlotinib treatment. After surgical resection, histologic evaluation revealed 2 residual foci (approximately 2 mm each) of invasive, moderately differentiated squamous cell carcinoma within the primary site but there was no evidence of lymph node metastasis. The patient did not receive adjuvant therapy and had no evidence of disease recurrence 24 mo postoperatively. Whole exome sequencing of the pretreatment tumor revealed a MAPK1 E322K somatic mutation, which was further implicated in mediating erlotinib sensitivity. This response to erlotinib occurred in the context of an activating somatic MAPK1 E322K mutation, which led to increased EGFR ligand production and EGFR activation in preclinical studies[17].

Recent adoption of next-generation sequencing in genomic testing of tumor has provided opportunity to advance precision medicine. Dumbrava *et al*[18] reported a case of metastatic SCCHN who progressed on a phase II clinical trial with erlotinib,

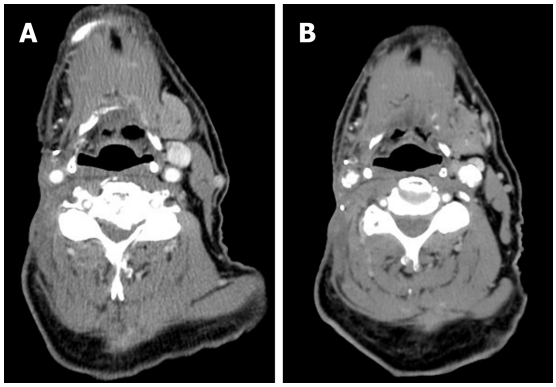

Figure 2 Contrast-enhanced computed tomography scan of neck. A: After completion of 6-mo erlotinib treatment; B: Seven mo after discontinuation of erlotinib treatment. Both showed resolution of right neck focal skin irregularity and right submandibular lymphadenopathy as shown in **Figure 1**.

docetaxel and cisplatin. Patient's tumor was subsequently biopsied and found to have amplification of fibroblast growth factor genes by next-generation sequencing. Patient was treated with fibroblast growth factor receptor inhibitor on clinical trial and achieved complete response for about 9 mo[18].

CONCLUSION

We report a case of durable complete response to erlotinib in SCCHN. Patient experienced skin rash and diarrhea toxicities which were likely predictors of his treatment response. The use of next-generation sequencing in genomic profiling of tumor samples may select patients who will likely respond to targeted therapy.

Table 1 Outcome of single-agent epidermal growth factor receptor tyrosine kinase inhibitor studies in recurrent/metastatic squamous cell carcinoma of head and neck

Agent	Phase/publication	Control arm	RR (%)	OS (mo)
Erlotinib	II/Soulieres[8]	None	4.3	6
Lapatinib	II/de Souza[11]	None	0	9.6-5.2 (lower on prior EGFR inhibitor exposure)
Gefitinib	III/Stewart[9]	Methotrexate	2.7 (250 mg/d); 7.6 (500 mg/d)	5.6 (250 mg/d); 6 (500 mg/d)
Afatinib	III/Machiels[10]	Methotrexate	10	6.8

RR: Response rate; OS: Overall survival; EGFR: Epidermal growth factor receptor.

REFERENCES

1 **Ferlay J**, Soerjomataram I, Dikshit R, Eser S, Mathers C, Rebelo M, Parkin DM, Forman D, Bray F. Cancer incidence and mortality worldwide: sources, methods and major patterns in GLOBOCAN 2012. *Int J Cancer* 2015; **136**: E359-E386 [PMID: 25220842 DOI: 10.1002/ijc.29210]

2 **Marur S**, Forastiere AA. Head and Neck Squamous Cell Carcinoma: Update on Epidemiology, Diagnosis, and Treatment. *Mayo Clin Proc* 2016; **91**: 386-396 [PMID: 26944243 DOI: 10.1016/j.mayocp.2015.12.017]

3 **Grandis JR**, Tweardy DJ. Elevated levels of transforming growth factor alpha and epidermal growth factor receptor messenger RNA are early markers of carcinogenesis in head and neck cancer. *Cancer Res* 1993; **53**: 3579-3584 [PMID: 8339264]

4 **Rubin Grandis J**, Melhem MF, Gooding WE, Day R, Holst VA, Wagener MM, Drenning SD, Tweardy DJ. Levels of TGF-alpha and EGFR protein in head and neck squamous cell carcinoma and patient survival. *J Natl Cancer Inst* 1998; **90**: 824-832 [PMID: 9625170 DOI: 10.1093/jnci/90.11.824]

5 **Etienne MC**, Pivot X, Formento JL, Bensadoun RJ, Formento P, Dassonville O, Francoual M, Poissonnet G, Fontana X, Schneider M, Demard F, Milano G. A multifactorial approach including tumoural epidermal growth factor receptor, p53, thymidylate synthase and dihydropyrimidine dehydrogenase to predict treatment outcome in head and neck cancer patients receiving 5-fluorouracil. *Br J Cancer* 1999; **79**: 1864-1869 [PMID: 10206306 DOI: 10.1038/sj.bjc.6690297]

6 **Vermorken JB**, Mesia R, Rivera F, Remenar E, Kawecki A, Rottey S, Erfan J, Zabolotnyy D, Kienzer HR, Cupissol D, Peyrade F, Benasso M, Vynnychenko I, De Raucourt D, Bokemeyer C, Schueler A, Amellal N, Hitt R. Platinum-based chemotherapy plus cetuximab in head and neck cancer. *N Engl J Med* 2008; **359**: 1116-1127 [PMID: 18784101 DOI: 10.1056/NEJMoa0802656]

7 **Strojan P**, Ferlito A, Medina JE, Woolgar JA, Rinaldo A, Robbins KT, Fagan JJ, Mendenhall WM, Paleri V, Silver CE, Olsen KD, Corry J, Suárez C, Rodrigo JP, Langendijk JA, Devaney KO, Kowalski LP, Hartl DM, Haigentz M, Werner JA, Pellitteri PK, de Bree R, Wolf GT, Takes RP, Genden EM, Hinni ML, Mondin V, Shaha AR, Barnes L. Contemporary management of lymph node metastases from an unknown primary to the neck: I. A review of diagnostic approaches. *Head Neck* 2013; **35**: 123-132 [PMID: 22034046 DOI: 10.1002/hed.21898]

8 **Soulieres D**, Senzer NN, Vokes EE, Hidalgo M, Agarwala SS, Siu LL. Multicenter phase II study of erlotinib, an oral epidermal growth factor receptor tyrosine kinase inhibitor, in patients with recurrent or metastatic squamous cell cancer of the head and neck. *J Clin Oncol* 2004; **22**: 77-85 [PMID: 14701768 DOI: 10.1200/JCO.2004.06.075]

9 **Stewart JS**, Cohen EE, Licitra L, Van Herpen CM, Khorprasert C, Soulieres D, Vodvarka P, Rischin D, Garin AM, Hirsch FR, Varella-Garcia M, Ghiorghiu S, Hargreaves L, Armour A, Speake G, Swaisland A, Vokes EE. Phase III study of gefitinib compared with intravenous methotrexate for recurrent squamous cell carcinoma of the head and neck [corrected]. *J Clin Oncol* 2009; **27**: 1864-1871 [PMID: 19289630 DOI: 10.1200/JCO.2008.17.0530]

10 **Machiels JP**, Haddad RI, Fayette J, Licitra LF, Tahara M, Vermorken JB, Clement PM, Gauler T, Cupissol D, Grau JJ, Guigay J, Caponigro F, de Castro G, de Souza Viana L, Keilholz U, Del Campo JM, Cong XJ, Ehrnrooth E, Cohen EE; LUX-H&N 1 investigators. Afatinib versus methotrexate as second-line treatment in patients with recurrent or metastatic squamous-cell carcinoma of the head and neck progressing on or after platinum-based therapy (LUX-Head & Neck 1): an open-label, randomised phase 3 trial. *Lancet Oncol* 2015; **16**: 583-594 [PMID: 25892145 DOI: 10.1016/S1470-2045(15)70124-5]

11 **de Souza JA**, Davis DW, Zhang Y, Khattri A, Seiwert TY, Aktolga S, Wong SJ, Kozloff MF, Nattam S, Lingen MW, Kunnavakkam R, Stenson KM, Blair EA, Bozeman J, Dancey JE, Vokes EE, Cohen EE. A phase II study of lapatinib in recurrent/metastatic squamous cell carcinoma of the head and neck. *Clin Cancer Res* 2012; **18**: 2336-2343 [PMID: 22371453 DOI: 10.1158/1078-0432.CCR-11-2825]

12 **Cohen EE**, Halpern AB, Kasza K, Kocherginsky M, Williams R, Vokes EE. Factors associated with clinical benefit from epidermal growth factor receptor inhibitors in recurrent and metastatic squamous cell carcinoma of the head and neck. *Oral Oncol* 2009; **45**: e155-e160 [PMID: 19586795 DOI: 10.1016/j.oraloncology.2009.05.637]

13 **Ruan Y**, Jiang J, Guo L, Li Y, Huang H, Shen L, Luan M, Li M, Du H, Ma C, He L, Zhang X, Qin S. Genetic Association of Curative and Adverse Reactions to Tyrosine Kinase Inhibitors in Chinese advanced Non-Small Cell Lung Cancer patients. *Sci Rep* 2016; **6**: 23368 [PMID: 26988277 DOI: 10.1038/srep23368]

14 **Liu S**, Kurzrock R. Toxicity of targeted therapy: Implications for response and impact of genetic polymorphisms. *Cancer Treat Rev* 2014; **40**: 883-891 [PMID: 24867380 DOI: 10.1016/j.ctrv.2014.05.003]

15 **Perisanidis C**. Prevalence of EGFR Tyrosine Kinase Domain Mutations in Head and Neck Squamous Cell Carcinoma: Cohort Study and Systematic Review. *In Vivo* 2017; **31**: 23-34 [PMID: 28064216 DOI: 10.21873/invivo.11020]

16 **Van Allen EM**, Lui VW, Egloff AM, Goetz EM, Li H, Johnson JT, Duvvuri U, Bauman JE, Stransky N, Zeng Y, Gilbert BR, Pendleton KP, Wang L, Chiosea S, Sougnez C, Wagle N, Zhang F, Du Y, Close D,

Johnston PA, McKenna A, Carter SL, Golub TR, Getz G, Mills GB, Garraway LA, Grandis JR. Genomic Correlate of Exceptional Erlotinib Response in Head and Neck Squamous Cell Carcinoma. *JAMA Oncol* 2015; **1**: 238-244 [PMID: 26181029 DOI: 10.1001/jamaoncol.2015.34]

17 **Wen Y**, Li H, Zeng Y, Wen W, Pendleton KP, Lui VW, Egloff AM, Grandis JR. MAPK1E322K mutation increases head and neck squamous cell carcinoma sensitivity to erlotinib through enhanced secretion of amphiregulin. *Oncotarget* 2016; **7**: 23300-23311 [PMID: 27004400 DOI: 10.18632/oncotarget.8188]

18 **Dumbrava EI**, Alfattal R, Miller VA, Tsimberidou AM. Complete Response to a Fibroblast Growth Factor Receptor Inhibitor in a Patient With Head and Neck Squamous Cell Carcinoma Harboring FGF Amplifications. *JCO Precision Oncology* 2018; 1-7 [DOI: 10.1200/PO.18.00100]

P- Reviewer: Bhalla AS, Dasgupta S
S- Editor: Ji FF **L- Editor:** A **E- Editor:** Bian YN

World Journal of Clinical Cases

Submit a Manuscript: https://www.f6publishing.com

World J Clin Cases 2019 March 6; 7(5): 623-627

DOI: 10.12998/wjcc.v7.i5.623

ISSN 2307-8960 (online)

CASE REPORT

Exercise-induced anaphylaxis with an Ayurvedic drug as cofactor: A case report

Francesca Losa, Margherita Deidda, Davide Firinu, Maria Luisa Di Martino, Maria Pina Barca, Stefano Del Giacco

ORCID number: Francesca Losa (0000-0003-2315-4558); Margherita Deidda (0000000222112594); Davide Firinu (0000-0002-5768-391X); Maria Luisa Di Martino (0000-0001-5878-2090); Maria Pina Barca (0000-0002-0335-6438); Stefano Del Giacco (0000-0002-4517-1749).

Author contributions: Losa F, Deidda M and Firinu D were responsible for the data analysis and interpretation and contributed to writing the manuscript; Losa F, Firinu D and Di Martino ML were responsible for the data selection and clinical interpretation of the data; all authors read and approved the final manuscript.

Informed consent statement: The patient gave written consent, however, the authors made efforts to remove identifying information to protect the privacy of the patient.

Conflict-of-interest statement: There are no conflicts of interest relevant to this article to disclose from any of the authors.

CARE Checklist (2016) statement: The authors have read the CARE Checklist (2016), and the manuscript was prepared and revised according to the CARE Checklist (2016).

Open-Access: This article is an open-access article which was selected by an in-house editor and fully peer-reviewed by external reviewers. It is distributed in accordance with the Creative Commons Attribution Non

Francesca Losa, Margherita Deidda, Davide Firinu, Maria Luisa Di Martino, Maria Pina Barca, Stefano Del Giacco, Department of Medical Sciences and Public Health and Unit of Allergy and Clinical Immunology, University Hospital "Duilio Casula", University of Cagliari, Monserrato 09042, Italy

Corresponding author: Davide Firinu, MD, PhD, Assistant Professor, Doctor, Research Fellow, Department of Medical Sciences and Public Health and Unit of Allergy and Clinical Immunology, University Hospital "Duilio Casula", University of Cagliari, Asse Didattico "E1" Medicina, Cittadella Universitaria, Cagliari 09142, Italy. davide.firinu@unica.it
Telephone: +39-70-51096128
Fax: +39-70-51096227

Abstract

BACKGROUND

The practice of Indian Ayurvedic medicine is spreading in Western countries and Shilajit is one of the most used drugs, for its antioxidant activities and immunomodulatory effects. Albeit Shilajit has showed a high degree of safety, it can act as cofactor of anaphylaxis, especially in condition at high risk, such as mast cell activation syndrome (MCAS). We reported this case to sensitize practitioners to investigate to the use of complementary and alternative medicine, in case of exercise-induced anaphylaxis (EIAn).

CASE SUMMARY

A 43-year-old woman, working as a dance teacher, developed urticaria after ingestion of rice, tuna and Shilajit, which did not respond to intramuscular corticosteroids. Subsequently, she developed dyspnoea and hypotension with loss of consciousness that arose 1 h after sexual activity. The patient did not refer personal history of atopy. Specific IgE for main food allergens resulted negative, with total IgE levels of 14 IU/L. Oral provocation test with Shilajit was not perfomed because the patient refused, but we performed prick-by-prick and patch test that resulted negative. Serum tryptase at the time of anaphylaxis was 20.6 μg/L that fell down to of 10.6 μg/L after therapy, but has remained at the high value after two days and during the follow-up. We performed an analysis of the *c-KIT* gene in peripheral blood, which was negative. We felt the diagnosis consistent with EIAn in a patient with a possible MCAS.

CONCLUSION

In Western countries the use of drugs from Ayurvedic medicine is more common than in the past. These substances can be cofactors of anaphylaxis in patients with

Commercial (CC BY-NC 4.0) license, which permits others to distribute, remix, adapt, build upon this work non-commercially, and license their derivative works on different terms, provided the original work is properly cited and the use is non-commercial. See: http://creativecommons.org/licenses/by-nc/4.0/

Manuscript source: Invited manuscript

Received: December 19, 2018
Peer-review started: December 20, 2018
First decision: January 19, 2019
Revised: February 3, 2019
Accepted: February 18, 2019
Article in press: February 18, 2019
Published online: March 6, 2019

risk factors.

Key words: Indian Ayurvedic medicine; Anaphylaxis; Exercise-induced anaphylaxis; Mast cell activation syndrome; Case report

©The Author(s) 2019. Published by Baishideng Publishing Group Inc. All rights reserved.

Core tip: This case report describes, for the first time, the role of drugs belonging to complementary and alternative medicine (CAM) in triggering anaphylaxis. Owing to the increase in their consumption in Western countries, these drugs should be considered as potential cofactor in conditions with a high risk of anaphylaxis, such as exercise-induced anaphylaxis and mast cell activation syndrome. This experience may be useful to give insight to practitioners about CAM and potential adverse drug reactions.

Citation: Losa F, Deidda M, Firinu D, Martino MLD, Barca MP, Giacco SD. Exercise-induced anaphylaxis with an Ayurvedic drug as cofactor: A case report. *World J Clin Cases* 2019; 7(5): 623-627
URL: https://www.wjgnet.com/2307-8960/full/v7/i5/623.htm
DOI: https://dx.doi.org/10.12998/wjcc.v7.i5.623

INTRODUCTION

Anaphylaxis is defined as a "severe, life-threatening systemic hypersensitivity reaction"[1]. The most common triggers are medications, insect stings, and foods. Exercise-induced anaphylaxis (EIAn) is a rare, unpredictable, and potentially fatal syndrome in which the occurrence of anaphylaxis coincides with exercise or physical activity. EIAn may occur after the ingestion of food, either pre- or post-exercise (Food-Dependent Exercise-Induced Anaphylaxis - FDEIAn), or independently of food ingestion (Non-Food Dependent Exercise-Induced Anaphylaxis[2]. When a Non-Food-Dependent form is identified, patients should be evaluated for mast cell activation syndrome (MCAS), which encompasses a group of diseases characterized by symptoms due to release of mast-cell mediators[3]. Shilajit is a herbo-mineral compound, derived from mountain regions of Asia, and consists of organic substances, divided into variable humic and non-humic proportions. The active components of Shilajit are dibenzo-alpha-pyrones and related metabolites; organic acids, such as fulvic acid; and inorganic constituents. It is one of most commonly used drugs in Indian Ayurvedic medicine, a complementary and alternative medicine (CAM). No data are available regarding anaphylaxis or allergic reactions elicited by Shilajit[4]. Here, we report a case of a woman who developed anaphylaxis after intense physical activity and ingestion of Shilajit.

CASE PRESENTATION

Chief complaints and history of present illness

A 43-year-old woman, a dance teacher, started taking a drug containing Shilajit in April 2017, at a dose of 400 mg/d. In July, she decided to increase the dose to 800 mg/d. The first day of the Shilajit dose increase, taken with a meal of rice and tuna, she developed urticaria, after one hour from the meal, immediately subsequent to intense physical activity. The hives appeared on thorax, neck, and arms and decreased after intramuscular corticosteroids, but did not disappear completely. The patient decided to stop taking Shilajit. Despite the symptoms, the patient also went to the beach that day and sunbathed for hours. The next day, one hour after sexual activity and a meal based again on rice, she developed angioedema, dyspnea, and hypotension with syncope that resolved after the administration of adrenaline, intravenous corticosteroids, and H1 and H2 antihistamines in the Emergency Department. She denied the assumption of alcohol, menses and she did not present sign or symptoms of infection.

Personal and family history

The patient's personal history and laboratory results were not suggestive of allergy, as

summarized in Table 1.

Laboratory examinations

Serum tryptase (ST) level at the time of anaphylaxis was 20.6 μg/L (normal level: 1–15 μg/L), and its progression is shown in Figure 1. Prick-by-prick and patch-testing with Shilajit were negative in the patient and in the controls, which were tested to exclude a false-positive result. Exercise test after a meal without Shilajit was negative, and an oral provocation test was not performed, due to patient refusal. To evaluate the hypothesis of an underlying MCAS, despite being the first anaphylaxis episode, we performed an analysis of the c-KIT gene in peripheral blood, which was negative (allele-specific real time quantitative PCR assay, ABI PRISM 7500 FAST, ThermoScientific, Uppsala, Sweden). We did not perform bone marrow biopsy, due to a low probability of clonal mast-cell syndrome, according to the Spanish Network on Mastocytosis (REMA) protocol[5]. During hospitalization, oral prednisone and antihistamines were administered and rapidly tapered until discontinuation.

FINAL DIAGNOSIS

Urticarial.

TREATMENT

At discharge, we prescribed epinephrine auto-injector and she was advised to avoid potential triggers, such as intense physical activity, for at least four hours after meals.

OUTCOME AND FOLLOW-UP

In the following months, the patient did not experience further episodes of urticaria or other symptoms. She did not change her eating habits, including the intake of rice and tuna, or physical activity. ST remained elevated during the follow-up.

DISCUSSION

The use of CAM drugs from Asia is rapidly increasing in Western countries. Shilajit is one of the substances most used in Ayurvedic medicine for its therapeutic antioxidant and anti-inflammatory properties, as well as its alleged antioxidant and immunomodulatory effects[4]. There has been only one *in vitro* study where fulvic acid has shown an inhibitory effect on human leukemia basophil (KU812) cells[6]. The active constituent of Shilajit are dibenzo-α-pyrones and related metabolites and fulvic acid. The pure extract of Shilajit is often made impure by contaminations of mycotoxins, heavy metal ions or reactive free radicals, so it is mandatory purify the substance before the use[7]. No studies on the pharmacokinetics and pharmaco-dynamics are available and there are no reports of adverse or hypersensitivity reactions to Shilajit, its components, or other drugs belonging to CAM[8].

MCAS is characterized by recurrent symptoms due to the release of mast-cell mediators, which correspond to an increase of ST level. Moreover, a prompt response to anti-mediator therapy and the exclusion of primary and secondary causes of mast cell activation are required for diagnosis[9]. MCAS is one of the differential diagnoses in cases of anaphylaxis. Although hymenoptera stings are the triggers responsible for most of the life-threatening reactions, drugs and foods can also cause anaphylaxis, in association with physical activity or exposure to heat. The case we here report was challenging for the time interval between the ingestion of Shilajit at an increased dose and the physical activity, in conjunction with a negative diagnostic work-up, which made a diagnosis of FEIAn not likely. On the contrary, the time course of the reaction and the presence of several triggers made more likely a diagnosis of EIAn. Moreover, the lack of other episodes of anaphylaxis in the past twelve months and during the follow-up is not consistent with a diagnosis of idiopathic anaphylaxis[10]. The persistent increase of ST level over time raises the suspicion of MCAS.

Both elevated basal ST level (> 20 μg/L) and an increase of 20% plus 2 μg/L over the basal level are suggestive of mast cell activation and satisfy MCAS criteria. We performed a c-KIT mutational analysis by rtPCR using peripheral blood, and the results were negative. The sensitivity of this technique on peripheral blood is quite low. Indeed, some MCAS patients may carry the D816V KIT mutation but there are

Table 1 Patient characteristics and laboratory data

Patient characteristics	Laboratory data
Age, yr	43
BMI, kg/m^2	23
Family history of atopy	Negative
ADR (antibiotics, NSAID, anesthetics, contrast agents)	No
Bone mineral density	T score - 0.7
FEV1	Normal
Chest radiograph	Normal
Abdomen ultrasonography	Normal
Skin Prick Test (foods and aeroallergens)	Negative
Blood test results	
Total IgE	14.8 KU/L
Specific IgE[1]	
Wheat	0.00 KU/L
rTri a 19	0.00 KU/L
rTri a 14 LPT	0.00 KU/L
Alpha-amilase	0.00 KU/L
Rice	0.00 KU/L
Oats	0.00 KU/L
Barley	0.00 KU/L
Tuna	0.00 KU/L
Soy	0.00 KU/L
rPru p 3	0.00 KU/L
Nut	0.00 KU/L
Walnut	0.00 KU/L
Latex	0.04 KU/L

[1]ImmunoCAP, Phadia 250, ThermoScientific. Normal range 0-100 kUA Cut-off 0.10 kUA/L. BMI: Body mass index; NSAID: Nonsteroidal antiinflammatory drug; FEV1: Forced expiratory volume in one second.

also cases of mastocytosis that do not[11]. In the presence of a single episode of anaphylaxis and with no c-KIT mutation detectable, we chose not to perform a bone marrow biopsy and to monitor our patient over time according to the REMA indications. The REMA group has proposed a scoring model to predict the presence of clonal mast cells in patients with history of anaphylaxis without skin mastocytosis, before performing a bone marrow study. Our patient had a score of 1, which indicated a low probability of clonal mast-cell activation disorder[5].

Considering the whole clinical picture and the laboratory outcomes, the persistence of elevated ST and the lack of anaphylaxis recurrences after suspending the culprit drug we felt the diagnosis consistent with EIAn in a patient with a possible MCAS.

The main limitations in the diagnostic work-up were the lack of information about the pharmacokinetics of Shilajit and the refuse of the patient to undergo to an oral challenge with the drug. Nevertheless, the occurrence of urticaria immediately after the increase in Shilajit dose and anaphylaxis in association with well-known triggers brought us to consider Shilajit as a key cofactor for anaphylaxis. Data from the literature suggest that augmenting factors take place in more than 30% of occurrence of anaphylaxis, so physicians have to investigate during anamnesis about cofactors[12].

This case is the first example reported of a CAM drug potentially eliciting anaphylaxis. Thus, because the consumption of these drugs is increasing in Western countries, Shilajit might be regarded as a potential cofactor, especially in people with features of mast-cells related disorders.

CONCLUSION

CAM drugs can potentially elicit anaphylaxis. In case of EIAn it is mandatory to investigate the presence of mast cell disorders. More studies are necessary about pharmacokinetics and pharmacodynamics of CAM drugs

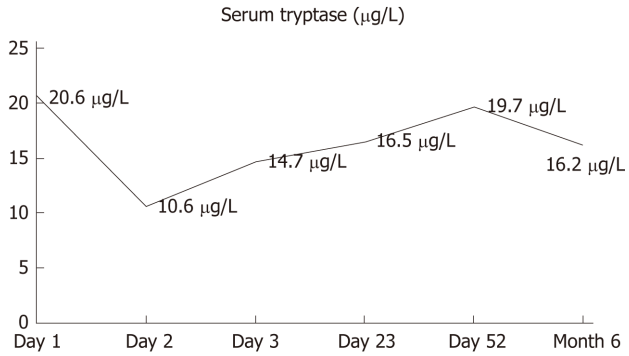

Figure 1 Evolution of serum tryptase.

REFERENCES

1 **Muraro A**, Roberts G, Worm M, Bilò MB, Brockow K, Fernández Rivas M, Santos AF, Zolkipli ZQ, Bellou A, Beyer K, Bindslev-Jensen C, Cardona V, Clark AT, Demoly P, Dubois AE, DunnGalvin A, Eigenmann P, Halken S, Harada L, Lack G, Jutel M, Niggemann B, Ruëff F, Timmermans F, Vlieg-Boerstra BJ, Werfel T, Dhami S, Panesar S, Akdis CA, Sheikh A; EAACI Food Allergy and Anaphylaxis Guidelines Group. Anaphylaxis: guidelines from the European Academy of Allergy and Clinical Immunology. *Allergy* 2014; **69**: 1026-1045 [PMID: 24909803 DOI: 10.1111/all.12437]

2 **Ansley L**, Bonini M, Delgado L, Del Giacco S, Du Toit G, Khaitov M, Kurowski M, Hull JH, Moreira A, Robson-Ansley PJ. Pathophysiological mechanisms of exercise-induced anaphylaxis: an EAACI position statement. *Allergy* 2015; **70**: 1212-1221 [PMID: 26100553 DOI: 10.1111/all.12677]

3 **Onnes MC**, Tanno LK, Elberink JN. Mast Cell Clonal Disorders: Classification, Diagnosis and Management. *Curr Treat Options Allergy* 2016; **3**: 453-464 [PMID: 27942432 DOI: 10.1007/s40521-016-0103-3]

4 **Wilson E**, Rajamanickam GV, Dubey GP, Klose P, Musial F, Saha FJ, Rampp T, Michalsen A, Dobos GJ. Review on shilajit used in traditional Indian medicine. *J Ethnopharmacol* 2011; **136**: 1-9 [PMID: 21530631 DOI: 10.1016/j.jep.2011.04.033]

5 **Alvarez-Twose I**, González-de-Olano D, Sánchez-Muñoz L, Matito A, Jara-Acevedo M, Teodosio C, García-Montero A, Morgado JM, Orfao A, Escribano L. Validation of the REMA score for predicting mast cell clonality and systemic mastocytosis in patients with systemic mast cell activation symptoms. *Int Arch Allergy Immunol* 2012; **157**: 275-280 [PMID: 22042301 DOI: 10.1159/000329856]

6 **Motojima H**, O Villareal M, Han J, Isoda H. Microarray analysis of immediate-type allergy in KU812 cells in response to fulvic acid. *Cytotechnology* 2011; **63**: 181-190 [PMID: 21331654 DOI: 10.1007/s10616-010-9333-6]

7 **Agarwal SP**, Khanna R, Karmarkar R, Anwer MK, Khar RK. Shilajit: a review. *Phytother Res* 2007; **21**: 401-405 [PMID: 17295385 DOI: 10.1002/ptr.2100]

8 **Bielory L**. Complementary and Alternative Medicine in Allergy-Immunology: More Information is Needed. *J Allergy Clin Immunol Pract* 2018; **6**: 99-100 [PMID: 29310770 DOI: 10.1016/j.jaip.2017.09.024]

9 **Akin C**. Mast cell activation syndromes presenting as anaphylaxis. *Immunol Allergy Clin North Am* 2015; **35**: 277-285 [PMID: 25841551 DOI: 10.1016/j.iac.2015.01.010]

10 **Nwaru BI**, Dhami S, Sheikh A. Idiopathic Anaphylaxis. *Curr Treat Options Allergy* 2017; **4**: 312-319 [PMID: 28890861 DOI: 10.1007/s40521-017-0136-2]

11 **Kristensen T**, Vestergaard H, Møller MB. Improved detection of the KIT D816V mutation in patients with systemic mastocytosis using a quantitative and highly sensitive real-time qPCR assay. *J Mol Diagn* 2011; **13**: 180-188 [PMID: 21354053 DOI: 10.1016/j.jmoldx.2010.10.004]

12 **Muñoz-Cano R**, Pascal M, Araujo G, Goikoetxea MJ, Valero AL, Picado C, Bartra J. Mechanisms, Cofactors, and Augmenting Factors Involved in Anaphylaxis. *Front Immunol* 2017; **8**: 1193 [PMID: 29018449 DOI: 10.3389/fimmu.2017.01193]

P- Reviewer: Exbrayat JM, Moneim AA, Rangel-Corona R
S- Editor: Ji FF **L- Editor:** A **E- Editor:** Bian YN

World Journal of Clinical Cases

Submit a Manuscript: https://www.f6publishing.com

World J Clin Cases 2019 March 6; 7(5): 628-635

DOI: 10.12998/wjcc.v7.i5.628

ISSN 2307-8960 (online)

CASE REPORT

Diagnostic detection with cardiac tomography and resonance of extremely rare coronary anomaly: A case report and review of literature

Nicolò Schicchi, Marco Fogante, Gian Marco Giuseppetti, Andrea Giovagnoni

ORCID number: Nicolò Schicchi (0000-0002-9851-9526); Marco Fogante (0000-0003-2993-5718); Gian Marco Giuseppetti (0000-0001-9373-5134); Andrea Giovagnoni (0000-0002-5264-652X).

Author contributions: Schicchi N interpreted the imaging and contributed to manuscript drafting; Fogante M reviewed the literature and contributed to manuscript drafting; Giuseppetti GM and Giovagnoni A were responsible for the revision of the manuscript for important intellectual content; all authors issued final approval for the version to be submitted.

Informed consent statement: Informed written consent was obtained from the patient's parents for publication of this report and any accompanying images.

Conflict-of-interest statement: The authors declare that they have no conflict of interest.

CARE Checklist (2016) statement: The authors have read the CARE Checklist (2016), and the manuscript was prepared and revised according to the CARE Checklist (2016).

Open-Access: This article is an open-access article which was selected by an in-house editor and fully peer-reviewed by external reviewers. It is distributed in accordance with the Creative Commons Attribution Non Commercial (CC BY-NC 4.0) license, which permits others to distribute, remix, adapt, build

Nicolò Schicchi, Gian Marco Giuseppetti, Andrea Giovagnoni, Department of Radiology, Azienda Ospedaliero-Universitaria Ospedali Riuniti, Ancona 60126, Italy

Marco Fogante, Department of Radiology, Università Politecnica delle Marche, Ancona 60126, Italy

Corresponding author: Marco Fogante, MD, Research Scientist, Radiologist, Department of Radiology, Università Politecnica delle Marche, Via Tronto 10, Ancona 60126, Italy.
m.fogante@pm.univpm.it
Telephone: +39-33-38949603

Abstract

BACKGROUND

The association of two congenital coronary artery anomalies (CAAs) is extremely rare but represents one of the main cause of sudden cardiac death in young athletes. Although coronary angiography (CX-A) is still widely used in childhood, cardiac magnetic resonance (C-MRI) and cardiac computed tomography (C-CT) have recently taken on an increasing diagnostic role in early detection of CAAs and concomitant congenital cardiac malformations.

CASE SUMMARY

A healthy 10-year-old male patient was referred to the Radiological Department of our Institution due to no evidence of left coronary artery in echocardiographic examination. With C-MRI was detected marked myocardial trabeculation and was suspected anomalous origin and course of left circumflex (LCx) artery and of left anterior descending (LAD) artery. With third generation Dual Source C-CT 192x2-sections (SOMATOM Force, Siemens, Germany) was confirmed anomalous origin of LCx artery from right pulmonary artery associated with anomalous origin of LAD artery from right coronary artery with course in front of right ventricular outflow tract. The patient underwent surgical treatment with reimplantation of the anomalous LCX and LAD arteries into the wall of ascending aorta, with no postoperative complications. The patient remained asymptomatic and follow-up C-MRI scan four months after operation showed complete success of surgery treatment.

CONCLUSION

This case highlights the diagnostic potential of C-CT and C-MRI in evaluation of CAAs and of cardiac morphology and functionality, with very low radiation dose

upon this work non-commercially, and license their derivative works on different terms, provided the original work is properly cited and the use is non-commercial. See: http://creativecommons.org/licenses/by-nc/4.0/

Manuscript source: Unsolicited manuscript

Received: December 24, 2018
Peer-review started: December 25, 2018
First decision: December 29, 2018
Revised: January 9, 2019
Accepted: January 26, 2019
Article in press: January 26, 2019
Published online: March 6, 2019

and without the risks related to invasive procedure.

Key words: Coronary anomalies; Cardiac computed tomography; Cardiac magnetic resonance; Case report; Coronary artery anomalies

©The Author(s) 2019. Published by Baishideng Publishing Group Inc. All rights reserved.

Core tip: Congenital coronary artery anomalies (CAAs) represent one of the main causes of sudden cardiac death in young athletes. For this reason, early detection of CAAs is essential. We present an extremely rare case of association of two congenital coronary anomalies, characterized by anomalous origin of left circumflex artery from right pulmonary artery and anomalous origin of left anterior descending artery from right coronary artery with course in front of right ventricular outflow tract. This case highlights the diagnostic potential of cardiac computed tomography and cardiac magnetic resonance in evaluation of CAAs and of cardiac morphology and functionality, with very low radiation dose and without the risks related to invasive procedure.

Citation: Schicchi N, Fogante M, Giuseppetti GM, Giovagnoni A. Diagnostic detection with cardiac tomography and resonance of extremely rare coronary anomaly: A case report and review of literature. *World J Clin Cases* 2019; 7(5): 628-635
URL: https://www.wjgnet.com/2307-8960/full/v7/i5/628.htm
DOI: https://dx.doi.org/10.12998/wjcc.v7.i5.628

INTRODUCTION

Congenital coronary artery anomalies (CAAs) are uncommon and frequently associated with other cardiac malformations. Extremely rare is the contemporary association of two CAAs[1,2]. With adequate coronary collateralisation, the clinical course may be silent but, sometimes, patients may had severe clinical outcomes, including sudden cardiac death (SDC), and need surgical treatment in infancy. For these reasons, early detection and exact delineation of coronary origin and course are essential[3,4]. Most of CAAs are diagnosed by invasive procedure, like coronary angiography (CX-A), or during surgical treatment.

Here we describe the first case of a pediatric male patient with origin of left circumflex (LCx) artery from right pulmonary artery (RPA) associated with origin of left anterior descending (LAD) artery from right coronary artery (RCA). These anomalies were suspected with cardiac magnetic resonance (C-MRI) and confirmed with cardiac computed tomography (C-CT) with very low radiation dose and without the risks related to invasive procedure, like CX-A.

CASE PRESENTATION

Chief complaints

A healthy 10-year-old male patient (weight 53.3 kg and height 158.4 cm) was referred to the Radiological Department of our Institution.

History of present illness

He had not familiarity and risk factors for cardio-vascular diseases, congenital heart disease, arrhythmias and SCD. Karate practitioner (3 times/wk) without problems. Asymptomatic for chest pain, dyspnea, palpitation and syncope episodes.

History of past illness

The patient had a free previous medical history. In particular, born at term (38 wk), childbirth without any complications and birth weight was 2.4 kg. Regular growth.

Physical examination

Physical examination revealed no sign of cardiopathy and without any cardiac added noises at chest auscultation. The patient's temperature was 36 °C, heart rate was 72 bpm, respiratory rate was 13 breaths per minute, blood pressure was 110/70 mmHg and oxygen saturation in room air was 98%.

Laboratory examinations

Blood analysis revealed normal haematocrit and platelet count. The blood biochemistries, as well as urine analysis were normal. Creatinine value was 0.9 mg/dL and creatinine clearance was 106 mL/min (estimated with Cockcroft-Gault formula).

Imaging examinations

Electrocardiography showed sinus rhythm, correct atrial-ventricular conduction (QRS 0.09 ms) and non-specific alterations of ventricular recovery (QTc 0.39 ms). Echocardiographic findings included normal volumes of left ventricle and atrium. Normal function of atrioventricular, aortic e pulmonary valves. No septal defects. Normal diameter of ascending aorta. No pericardial effusion. RCA origin high and ectatic. Left coronary artery origin and course not detect. For these reasons, patient was undergoing to C-MRI.

Further diagnostic work-up

C-MRI (Achieva, Philips Medical Systems, The Netherlands) using a 1.5-T scanner was performed. Was used a 32-channel MR cardiac array coil with patient in prone position. C-MRI protocol consisted of balanced steady-state free precession (BSSFP) cine-imaging, T2-weighted and T1-weighted inversion recovery images, and sequences for late enhancement evaluation. Contrast agent dose was 0.2 mL/kg (gadobutrol, 1.0 mmol/mL) with flow injection rate of 2.0 mL/s. BSSFP sequences were acquired in the three cardiac axis, T2-weighted and T1-weighted in transversal cardiac axis, and sequences after contrast agent in short cardiac axis covering the entire left ventricle. The exam showed concordance in atrial-ventricular and ventricular-artery communication, regular return of superior vena cava and pulmonary veins. Left ventricle normal for volume, thickening of posterior wall with multiple mitral accessory ropes. Regular contractile functionality (ejection fraction of 71%). Accentuated endocardial trabeculation. Regular volume of left atrium. Regular right cardiac sections. Probable anomalies of origin and course of LCx and LAD arteries. For this reason, the patient was scanned with third generation Dual Source C-CT 192 × 2-sections (SOMATOM Force, Siemens, Germany). Patient remained in sinus rhythm before examination without receiving βblocker. Patient received a non-ionic low-osmolality contrast agent Visipaque 320 mgI/mL (iodixanol; GE Healthcare Life Sciences, Chalfont, United Kingdom), with a volume of 30 mL and flow injection rate of 5 mL/sec followed by saline injection at same volume and velocity. The scanning area began from the upper limit of the sternum to 1 cm below the diaphragm with superior to inferior direction. The parameters used for the exam were: 70 kV of tube voltage; automatic tube current modulation technique (CAREdose); rotation time, 0.28 sec; detector array, 192 × 0.6 mm; slice thickness, 0.75 mm and convolution kernel of B26. Was applied prospective ECG-triggered axial coronary protocol in a step-and-shoot scan mode and the exposure time was adjusted between 40%-70% of the cardiac cycle. After the examination, radiation CT dose index, dose length product and effective dose were recorded. Then the raw data was post-processed and was included the capture of the optimal images, multi-plane and maximum intensity projection reconstructions and volume rendering representations. C-CT confirmed anomalous origin of LCx artery from RPA associated with anomalous origin of LAD artery from RCA with proximal-medium course in front of RVOT and presences of coronary interconnections. Moreover, the examination showed the origin of a small diagonal branch from the left coronary sinus for the vascularization of the left ventricle wall (Figures 1-5).

FINAL DIAGNOSIS

The final diagnosis of the presented case is anomalous origin of LCx artery from RPA associated with anomalous origin of LAD artery from RCA with proximal-medium course in front of RVOT and presences of coronary interconnections.

TREATMENT

The young patient underwent surgical treatment. The procedure began with standard median sternotomy, chest opening, thymus removal and pericardium opening. Then were cannulated the innominate artery and right atrium for cardiopulmonary bypass. After pulmonary arteries were clamped, the child was cooled down to 16 °C core temperature and circulatory arrest was commenced. Primarily, LCX was dissected

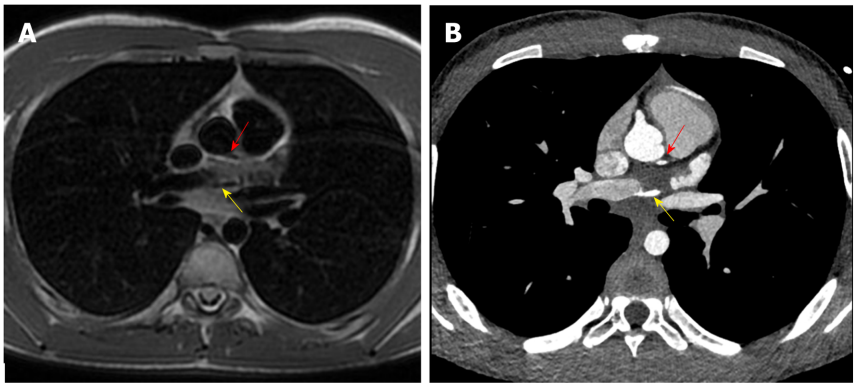

Figure 1 Origin of left circumflex artery and small diagonal branch. A: Origin of left circumflex artery from right pulmonary artery (yellow arrow) and origin of a small diagonal branch from the left coronary sinus for the left ventricle (red arrow) evaluated with 1.5 T cardiac magnetic resonance; B: Origin of left circumflex artery from right pulmonary artery (yellow arrow) and origin of a small diagonal branch from the left coronary sinus for the left ventricle (red arrow) evaluated with third generation dual source cardiac computed tomography.

from the RPA with a generous cuff, and was re-implanted into the wall of the aorta. Secondly, LAD was dissected from RCA and re-implated into the wall of aorta. Finally, after full rewarming, the operation was concluded and the sternum was closed.

OUTCOME AND FOLLOW-UP

The patient had an uneventful postoperative clinical course. At follow-up visit, two months after surgical treatment (one month after hospital discharge), the patient was asymptomatic. Follow-up C-MRI, four months after operation, showed complete success of surgery treatment.

DISCUSSION

Based on scientific works present in literature, the prevalence of CAAs in general population is around 1%; with a range from 0.3% to 5.6% in studies on patients undergoing CX-A, and in approximately 1% of routine autopsy. About 26% of CAAs are associated with other congenital cardiac malformations[5-7]. Separate origin of the LAD and LCX represents the commonest CAA with an incidence of 0.41%, followed by LCX arising from the RCA, with an incidence of 0.37%[8-10]. These anomalies, could be asymptomatic, but in some cases may lead to myocardial infarction, arrhythmia, ventricular aneurysm, mitral regurgitation, cardiomyopathy and SCD and they represent the second most common cause of SDC in young athletes. Therefore, the symptoms depend to the expansion of collateral vessels from coronary arteries. For this reason, patients need surgical treatment in early infancy[3,4]. Some potential pathogenetic mechanisms have been proposed to explain ischaemia and SCD, such as endothelial injury of the anomalous coronary artery with consequent sudden coronary spasm or modification of physiologic blood circulation. Another possible cause of ischemia is the acute angle of take-off of the anomalous vessel and the related slit-like orifice, which may become kinked and occluded during exercise[11-14]. Otherwise, it is interesting to note that in nearly 15% of patients with CAAs, myocardial ischemia can develop in the absence of atherosclerosis. For this reasons, early detection of CAAs and concomitant congenital cardiac malformations are crucial[15-17].

Although CX-A is still widely used in childhood, C-MRI and C-CT have recently taken on an increasing role in the diagnosis of CAAs. Indeed the association, of these two non- invasive examinations, allows the evaluation of cardiac morphology and functionality, with high spatial and temporal resolution, and permits to assess, exactly, coronary anatomy, without the risks related to invasive procedure and patient sedation and with a very low radiation dose[18-25].

Here we reported the case of a 10-year-old male patient with anomalous origin of LCx artery from RPA associated with anomalous origin and course of LAD artery from RCA in front of RVOT. This association was suspected with C-MRI and confirmed with C-CT without the necessity of CX-A, or other invasive procedures. To

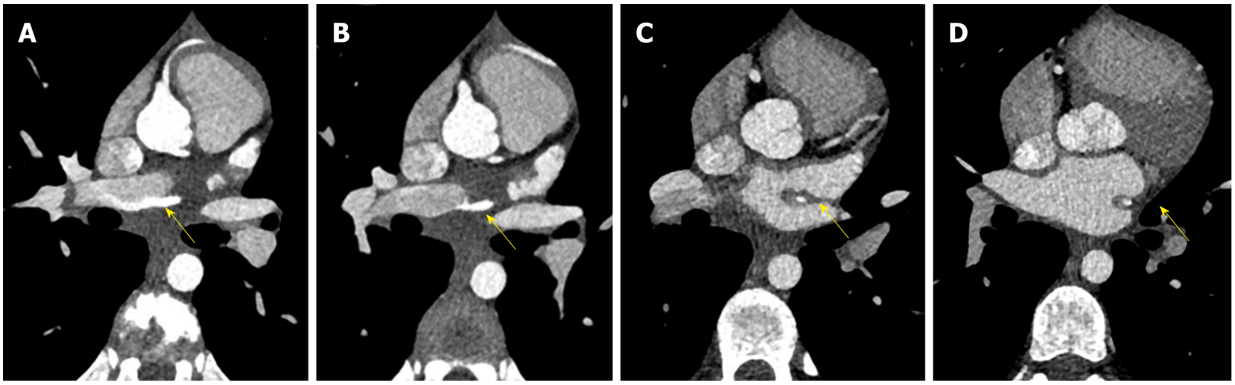

Figure 2 Course of circumflex artery. A-D: Course of circumflex artery between two left pulmonary veins shown with third generation dual source cardiac computed tomography (yellow arrow).

the best of our knowledge, the presented case is the first one in scientific literature that describes this anomaly association. Moreover, of 12 similar cases of CAAs reported in literature, only 2 were detected and confirmed with C-MRI or C-CT, the others were diagnosed with CX-A or during surgical treatment[26-37]. Our patient was a healthy child with no previous serious or recurrent or unusual cardiac symptoms. Electrocardiography examination was regular but with echocardiography, left coronary artery origin and course was not detect. For these reasons patient was undergoing to C-MRI. This exam provided informations on cardiac morphology and functionality and allowed to suspect anomalous origin and course of coronary arteries. Subsequently, third generation dual source C-CT electrocardiogram-gated, with high spatial resolution, guaranteed the detection of exact origin and course of coronary arteries, estimation of their diameter, and visualization of collateral vessels from coronary arteries. The radiation dose was very low, as summarized in Table 1, with effective dose of 3.87 mSv and without risks related to an invasive procedure and patient sedation. The patient had an uneventful postoperative clinical course and follow-up C-MRI showed complete success of surgery treatment.

CONCLUSION

Although CX-A is still widely used in childhood for the diagnosis of CAAs, C-MRI allows the evaluation of cardiac morphology and functionality and C-CT, with high spatial resolution, allows to evaluate, with high diagnostic accuracy, CAAs in children, without the risks related to invasive procedure and patient sedation and with a very low radiation dose.

Table 1 Dose report

	kV	mAs / ref.	CTDIvol (mGy)	DLP (mGycm)
Scout_AP	120	19	0.07	2.5
Test Bolus	70	70	5.62	5.6
DS_CorAdSeq	70	428/588	6.54	102.0
Total				110.0

Dose report for coronary examination with third generation dual source cardiac computed tomography. CTDIvol: CT dose index; DLP: Dose length product.

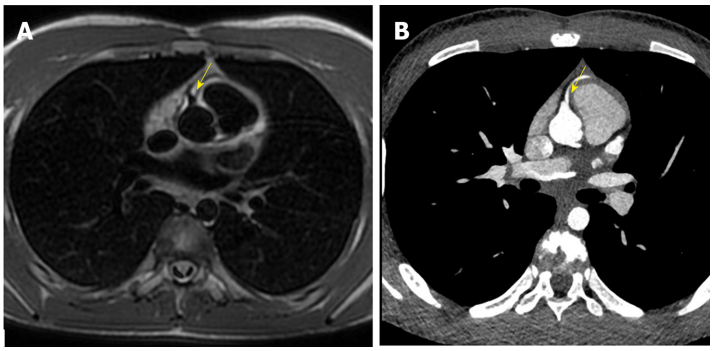

Figure 3 Origin of left anterior descending artery. A: Origin of left anterior descending artery from right coronary artery evaluated with 1.5 T cardiac magnetic resonance (yellow arrow); B: Origin of left anterior descending artery from right coronary artery evaluated with third generation dual source cardiac computed tomography (yellow arrow).

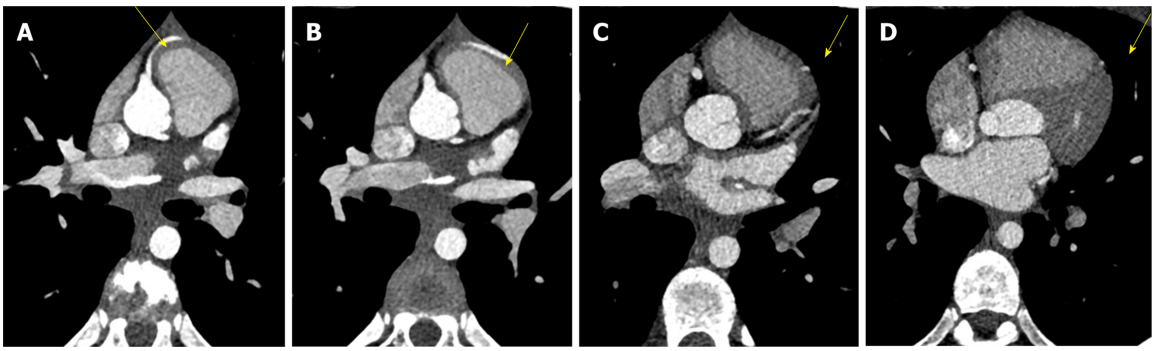

Figure 4 Course of left anterior descending artery. A-D: Course of left anterior descending artery in front of right ventricular outflow tract shown with third generation dual source cardiac computed tomography.

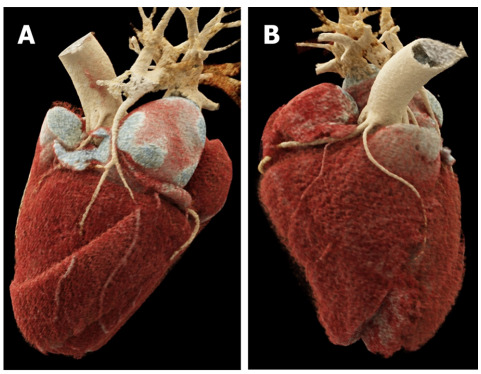

Figure 5 Coronary artery anomalies in volume rendering reconstruction. A: Left circumflex artery from right pulmonary artery; B: Left anterior descending artery from right coronary artery.

REFERENCES

1 **Angelini P**. Coronary artery anomalies: an entity in search of an identity. *Circulation* 2007; **115**: 1296-1305 [PMID: 17353457 DOI: 10.1161/CIRCULATIONAHA.106.618082]
2 **Goo HW**. Coronary artery imaging in children. *Korean J Radiol* 2015; **16**: 239-250 [PMID: 25741188 DOI: 10.3348/kjr.2015.16.2.239]
3 **Spicer DE**, Henderson DJ, Chaudhry B, Mohun TJ, Anderson RH. The anatomy and development of normal and abnormal coronary arteries. *Cardiol Young* 2015; **25**: 1493-1503 [PMID: 26675596 DOI: 10.1017/S1047951115001390]
4 **Gavrielatos G**, Letsas KP, Pappas LK, Antonellis I, Kardaras F. Anomalous origin of the entire coronary system with separate ostia within the right sinus of valsalva: a rare congenital anomaly and a review of the literature. *Cardiology* 2007; **107**: 209-212 [PMID: 16946599 DOI: 10.1159/000095419]
5 **Young PM**, Gerber TC, Williamson EE, Julsrud PR, Herfkens RJ. Cardiac imaging: Part 2, normal, variant, and anomalous configurations of the coronary vasculature. *AJR Am J Roentgenol* 2011; **197**: 816-826 [PMID: 21940568 DOI: 10.2214/AJR.10.7249]
6 **Angelini P**. Coronary artery anomalies--current clinical issues: definitions, classification, incidence, clinical relevance, and treatment guidelines. *Tex Heart Inst J* 2002; **29**: 271-278 [PMID: 12484611 DOI: 10.1109/43.88921]
7 **Angelini P**, Velasco JA, Flamm S. Coronary anomalies: incidence, pathophysiology, and clinical relevance. *Circulation* 2002; **105**: 2449-2454 [PMID: 12021235 DOI: 10.1161/01.CIR.0000016175.49835.57]
8 **Yamanaka O**, Hobbs RE. Coronary artery anomalies in 126,595 patients undergoing coronary arteriography. *Cathet Cardiovasc Diagn* 1990; **21**: 28-40 [PMID: 2208265 DOI: 10.1002/ccd.1810210110]
9 **Yurtdaş M**, Gülen O. Anomalous origin of the right coronary artery from the left anterior descending artery: review of the literature. *Cardiol J* 2012; **19**: 122-129 [PMID: 22461044 DOI: 10.5603/CJ.2012.0023]
10 **Alexander RW**, Griffith GC. Anomalies of the coronary arteries and their clinical significance. *Circulation* 1956; **14**: 800-805 [PMID: 13374855 DOI: 10.1161/01.CIR.14.5.800]
11 **Frescura C**, Basso C, Thiene G, Corrado D, Pennelli T, Angelini A, Daliento L. Anomalous origin of coronary arteries and risk of sudden death: a study based on an autopsy population of congenital heart disease. *Hum Pathol* 1998; **29**: 689-695 [PMID: 9670825 DOI: 10.1016/S0046-8177(98)90277-5]
12 **Camarda J**, Berger S. Coronary artery abnormalities and sudden cardiac death. *Pediatr Cardiol* 2012; **33**: 434-438 [PMID: 22322562 DOI: 10.1007/s00246-012-0168-0]
13 **Burke AP**, Farb A, Virmani R, Goodin J, Smialek JE. Sports-related and non-sports-related sudden cardiac death in young adults. *Am Heart J* 1991; **121**: 568-575 [PMID: 1825009 DOI: 10.1016/0002-8703(91)90727-Y]
14 **Drory Y**, Turetz Y, Hiss Y, Lev B, Fisman EZ, Pines A, Kramer MR. Sudden unexpected death in persons less than 40 years of age. *Am J Cardiol* 1991; **68**: 1388-1392 [PMID: 1951130 DOI: 10.1016/0002-9149(91)90251-F]
15 **Basso C**, Maron BJ, Corrado D, Thiene G. Clinical profile of congenital coronary artery anomalies with origin from the wrong aortic sinus leading to sudden death in young competitive athletes. *J Am Coll Cardiol* 2000; **35**: 1493-1501 [PMID: 10807452 DOI: 10.1016/S0735-1097(00)00566-0]
16 **Maron BJ**, Thompson PD, Puffer JC, McGrew CA, Strong WB, Douglas PS, Clark LT, Mitten MJ, Crawford MD, Atkins DL, Driscoll DJ, Epstein AE. Cardiovascular preparticipation screening of competitive athletes: addendum: an addendum to a statement for health professionals from the Sudden Death Committee (Council on Clinical Cardiology) and the Congenital Cardiac Defects Committee (Council on Cardiovascular Disease in the Young), American Heart Association. *Circulation* 1998; **97**: 2294 [PMID: 9631885 DOI: 10.1161/01.CIR.97.22.2294]
17 **Taylor AJ**, Rogan KM, Virmani R. Sudden cardiac death associated with isolated congenital coronary artery anomalies. *J Am Coll Cardiol* 1992; **20**: 640-647 [PMID: 1512344 DOI: 10.1016/0735-1097(92)90019-J]
18 **Sun Z**, Lin C, Davidson R, Dong C, Liao Y. Diagnostic value of 64-slice CT angiography in coronary artery disease: a systematic review. *Eur J Radiol* 2008; **67**: 78-84 [PMID: 17766073 DOI: 10.1016/j.ejrad.2007.07.014]
19 **Abdulla J**, Abildstrom SZ, Gotzsche O, Christensen E, Kober L, Torp-Pedersen C. 64-multislice detector computed tomography coronary angiography as potential alternative to conventional coronary angiography: a systematic review and meta-analysis. *Eur Heart J* 2007; **28**: 3042-3050 [PMID: 17981829 DOI: 10.1093/eurheartj/ehm466]
20 **Mowatt G**, Cook JA, Hillis GS, Walker S, Fraser C, Jia X, Waugh N. 64-Slice computed tomography angiography in the diagnosis and assessment of coronary artery disease: systematic review and meta-analysis. *Heart* 2008; **94**: 1386-1393 [PMID: 18669550 DOI: 10.1136/hrt.2008.145292]
21 **Miller JM**, Rochitte CE, Dewey M, Arbab-Zadeh A, Niinuma H, Gottlieb I, Paul N, Clouse ME, Shapiro EP, Hoe J, Lardo AC, Bush DE, de Roos A, Cox C, Brinker J, Lima JA. Diagnostic performance of coronary angiography by 64-row CT. *N Engl J Med* 2008; **359**: 2324-2336 [PMID: 19038879 DOI: 10.1056/NEJMoa0806576]
22 **Min JK**, Shaw LJ, Berman DS. The present state of coronary computed tomography angiography a process in evolution. *J Am Coll Cardiol* 2010; **55**: 957-965 [PMID: 20202511 DOI: 10.1016/j.jacc.2009.08.087]
23 **Bonello B**, Kilner PJ. Review of the role of cardiovascular magnetic resonance in congenital heart disease, with a focus on right ventricle assessment. *Arch Cardiovasc Dis* 2012; **105**: 605-613 [PMID: 23177489 DOI: 10.1016/j.acvd.2012.04.005]
24 **Fratz S**, Chung T, Greil GF, Samyn MM, Taylor AM, Valsangiacomo Buechel ER, Yoo SJ, Powell AJ. Guidelines and protocols for cardiovascular magnetic resonance in children and adults with congenital heart disease: SCMR expert consensus group on congenital heart disease. *J Cardiovasc Magn Reson* 2013; **15**: 51 [PMID: 23763839 DOI: 10.1186/1532-429X-15-51]
25 **Kilner PJ**. The role of cardiovascular magnetic resonance in adults with congenital heart disease. *Prog Cardiovasc Dis* 2011; **54**: 295-304 [PMID: 22014496 DOI: 10.1016/j.pcad.2011.07.006]
26 **Honey M**, Lincoln JC, Osborne MP, de Bono DP. Coarctation of aorta with right aortic arch. Report of surgical correction in 2 cases: one with associated anomalous origin of left circumflex coronary artery from the right pulmonary artery. *Br Heart J* 1975; **37**: 937-945 [PMID: 127600 DOI:

10.1136/hrt.37.9.937]
27 **Garcia CM**, Chandler J, Russell R. Anomalous left circumflex coronary artery from the right pulmonary artery: first adult case report. *Am Heart J* 1992; **123**: 526-528 [PMID: 1736592 DOI: 10.1016/0002-8703(92)90673-J]
28 **Sarioglu T**, Kinoglu B, Saltik L, Eroglu A. Anomalous origin of circumflex coronary artery from the right pulmonary artery associated with subaortic stenosis and coarctation of the aorta. *Eur J Cardiothorac Surg* 1997; **12**: 663-665 [PMID: 9370415 DOI: 10.1016/S1010-7940(97)00166-8]
29 **Korosoglou G**, Ringwald G, Giannitsis E, Katus HA. Anomalous origin of the left circumflex coronary artery from the pulmonary artery. A very rare congenital anomaly in an adult patient diagnosed by cardiovascular magnetic resonance. *J Cardiovasc Magn Reson* 2008; **10**: 4 [PMID: 18272006 DOI: 10.1186/1532-429X-10-4]
30 **Danov V**, Kornovski V, Hazarbasanov D, Panayotov P. Anomalous origin of left circumflex coronary artery from the right pulmonary artery in adult. *Thorac Cardiovasc Surg* 2009; **57**: 114-115 [PMID: 19241316 DOI: 10.1055/s-2008-1038513]
31 **Jayagopal PB**, Pai BV, Jayasree HN, Thomas A. Anomalous origin of left circumflex artery from pulmonary artery. *Indian Heart J* 2014; **66**: 214-215 [PMID: 24814119 DOI: 10.1016/j.ihj.2013.12.027]
32 **Jaworski R**, Kansy A, Łaniewski-Wołłk P. Anomalous origin of circumflex coronary artery from right pulmonary artery in a hypoplastic left heart syndrome child. *Kardiochir Torakochirurgia Pol* 2014; **11**: 210-212 [PMID: 26336423 DOI: 10.5114/kitp.2014.43853]
33 **Sekelyk R**, Mykychak Y, Fedevych O, Yemets I. Anomalous origin of circumflex coronary artery from right pulmonary artery associated with coarctation of the aorta: a case report of surgical treatment. *World J Pediatr Congenit Heart Surg* 2014; **5**: 97-99 [PMID: 24403364 DOI: 10.1177/2150135113505294]
34 **Liu B**, Fursevich D, O'Dell MC, Flores M, Feranec N. Anomalous Left Circumflex Coronary Artery Arising from the Right Pulmonary Artery: A Rare Cause of Aborted Sudden Cardiac Death. *Cureus* 2016; **8**: e499 [PMID: 27014533 DOI: 10.7759/cureus.499]
35 **Al-Muhaya MA**, Syed A, Najjar AHA, Mofeed M, Al-Mutairi M. Anomalous origin of circumflex coronary artery from right pulmonary artery associated with atrial septal defect. *J Saudi Heart Assoc* 2017; **29**: 219-222 [PMID: 28652677 DOI: 10.1016/j.jsha.2017.02.001]
36 **Daylan A**, Ertugay S, Apaydın AZ, Oğuz E. Circumflex coronary artery originating from the right pulmonary artery in adult. *Asian Cardiovasc Thorac Ann* 2017; **25**: 528-530 [PMID: 28610440 DOI: 10.1177/0218492317717419]
37 **Bo I**, Semple T, Cheasty E, Rubens MB, Ho SY, Rigby ML, Nicol ED. Left circumflex coronary artery from the pulmonary artery in scimitar syndrome. *Pediatr Radiol* 2018; **48**: 632-637 [PMID: 29541807 DOI: 10.1007/s00247-017-4067-7]

P- Reviewer: Altarabsheh SE, Falconi M, Kharlamov AN, Najafi M
S- Editor: Ji FF **L- Editor:** A **E- Editor:** Bian YN

World Journal of Clinical Cases

Submit a Manuscript: https://www.f6publishing.com

World J Clin Cases 2019 March 6; 7(5): 636-641

DOI: 10.12998/wjcc.v7.i5.636

ISSN 2307-8960 (online)

CASE REPORT

Fatal meningococcal meningitis in a 2-year-old child: A case report

Aleksander Mularski, Czesław Żaba

ORCID number: Aleksander Mularski (0000-0002-3392-1813); Czesław Żaba (0000-0001-7522-4568).

Author contributions: Mularski A and Żaba C performed the postmortem examination, reviewed the literature and contributed to manuscript drafting.

Informed consent statement: No informed written consent was needed as the medicolegal autopsy was carried out at a prosecutor's request.

Conflict-of-interest statement: The authors declare that they have no conflict of interest.

CARE Checklist (2016) statement: The authors have read the CARE Checklist (2016), and the manuscript was prepared and revised according to the CARE Checklist (2016).

Open-Access: This article is an open-access article which was selected by an in-house editor and fully peer-reviewed by external reviewers. It is distributed in accordance with the Creative Commons Attribution Non Commercial (CC BY-NC 4.0) license, which permits others to distribute, remix, adapt, build upon this work non-commercially, and license their derivative works on different terms, provided the original work is properly cited and the use is non-commercial. See: http://creativecommons.org/licenses/by-nc/4.0/

Manuscript source: Unsolicited manuscript

Received: December 20, 2018
Peer-review started: December 20, 2018

Aleksander Mularski, Department of Legal and Forensic Medicine, Poznan University of Medical Sciences, Poznan 60-781, Poland

Czesław Żaba, Institute of Forensic Research, Cracow 31-033, Poland

Corresponding author: Aleksander Mularski, MD, Academic Fellow, Medical Assistant, Department of Legal and Forensic Medicine, Poznan University of Medical Sciences, Święcickiego 6, Poznan 60-781, Poland. aleksander.mularski@gmail.com
Telephone: +48-61-8546410
Fax: +48-61-8546410

Abstract

BACKGROUND

In fatal cases of meningococcal septicemia, bacteriological diagnosis may not be straightforward due to postmortem replication and relocation of endogenic microflora. In medicolegal practice, aside from routine autopsy and histopathology, also other diagnostic methods, such as microbiological tests, immunohistochemistry and polymerase chain reaction (PCR), are used to examine body fluids and tissues.

CASE SUMMARY

We present the case of sudden death in a 2-year-old child. The patient died approximately 30 min after hospital admission before any routine diagnostic procedures were undertaken. Presence of whole-body rash and fulminant course of the disease raised suspicion of meningococcal septicemia. An autopsy was performed seven days after death when the body showed the signs of late postmortem decomposition. No etiological factor of septicemia could be identified based on macro- and microscopic findings. However, PCR demonstrated the presence of genetic material of group W *Neisseria meningitidis* in patient's cerebrospinal fluid and blood.

CONCLUSION

Microbiological PCR should be conducted postmortem whenever a specific etiological factor could not be identified with conventional methods.

Key words: Meningococcal infection; Molecular microbiology; Waterhouse-Friderichsen syndrome; *Neisseria meningitidis*; Autopsy; Cerebrospinal fluid; Case report

©The Author(s) 2019. Published by Baishideng Publishing Group Inc. All rights reserved.

Core tip: We present the case of a 2-year-old patient who died suddenly with the signs of meningococcal septicemia. No etiological factor of the septicemia could be identified

First decision: January 5, 2019
Revised: January 14, 2019
Accepted: January 29, 2019
Article in press: January 30, 2019
Published online: March 6, 2019

based on macro- and microscopic findings during an autopsy carried out seven days postmortem. However, the genetic material of group W *Neisseria meningitidis* was detected in cerebrospinal fluid samples based on polymerase chain reaciton (PCR). Our observations imply that microbiological PCR can be helpful in medicolegal practice, especially when an autopsy is delayed and the results of conventional bacteriological examination are unavailable or seem controversial.

Citation: Mularski A, Żaba C. Fatal meningococcal meningitis in a 2-year-old child: A case report. *World J Clin Cases* 2019; 7(5): 636-641
URL: https://www.wjgnet.com/2307-8960/full/v7/i5/636.htm
DOI: https://dx.doi.org/10.12998/wjcc.v7.i5.636

INTRODUCTION

Acute infections of the central nervous system still constitute a diagnostic and therapeutic challenge. Their course is severe, they usually co-exist with systemic infections, and are associated with high mortality. *Neisseria meningitidis* (*N. meningitidis*) infections are a particular threat since they may occur epidemically or pandemically, rather than sporadically or endemically. Although up to 12 serological groups have been identified among *N. meningitidis* strains, more than 90% of infections are caused by A, B, C, Y and W group isolates. Identification of *N. meningitidis* serogroups that predominate in a given country is vital for the development of local vaccination strategies.

Clinical presentation of *N. meningitidis* infections is similar like in the case of other bacterial neuroinfections. A common, albeit not pathognomonic symptom of meningococcal septicemia is purpuric rash, present in 10%-50% of cases. Aside from the rash, adrenal hemorrhages (Waterhouse-Friderichsen syndrome, WFS) can be observed in fulminant infections, especially in children. In fatal cases, bacteriological diagnosis may not be straightforward due to postmortem replication and relocation of endogenic microflora. In medicolegal practice, aside from routine autopsy and histopathology, also other diagnostic methods, such as microbiological tests, immunohistochemistry and polymerase chain reaction (PCR), are used to examine body fluids and tissues[1-5].

CASE PRESENTATION

Clinical summary

A 2-year-old boy was admitted to the Pediatric Emergency Room in an extremely poor general condition, with apnea, asystole, immeasurable oxygen saturation and the signs of severe brain injury (Glasgow Coma Scale 3). Based on the information from his father, the boy had a fever and adipsia for several hours and vomited twice. The symptoms appeared in the afternoon a day before the hospital admission; based on this presentation, a non-specific upper respiratory infection had been diagnosed by a family physician in an outpatient setting.

The patient passed away 30 min post-admission despite a resuscitation attempt undertaken at the Emergency Room. Examination of blood samples obtained at admission revealed normal leukocyte count with a decrease in neutrophil fraction and an increase in lymphocyte, monocyte and basophile percentages, elevated concentrations of urea, creatinine and C-reactive protein, considerable hypoglycemia, increased activity of aspartate aminotransferase with normal activity of alanine aminotransferase, a significant rise in lactate dehydrogenase, and procalcitonin above the upper detection limit.

Based on medical history, clinical and laboratory findings, patient's death was attributed to septic shock. However, a medicolegal autopsy was requested by the prosecutor to establish the cause of death ultimately and to evaluate the correctness of outpatient medical treatment.

Pathological findings

The autopsy was performed seven days after the patient's death. External examination of the body revealed purpuric rash, more pronounced on the face, arms and chest, along with the signs of early decomposition (Figure 1). Cerebrospinal fluid

(CSF) and blood samples were obtained aseptically before opening the body cavities. CSF was collected by means of suboccipital puncture, and blood by transthoracic puncture of the heart. Moreover, brain, lung, liver, spleen, heart and kidney samples were obtained, as aseptically as possible. Internal examination revealed massive hemorrhages in both adrenal glands (Figure 2), and petechiae in esophageal mucosa, thymus, subepicardial and subpleural tissue (Figure 3). No evidence of meningitis was found on macroscopic examination.

Histological findings

The macroscopic findings were confirmed on microscopic examination. The evidence of unspecific passive congestion was found in the brain, thymus, lungs, liver and spleen, along with fiber waviness in the heart. Moreover, massive hemorrhages at the corticomedullary junction were identified in both adrenal glands (Figure 4).

Microbiological studies and PCR

Since the autopsy was carried out seven days after the patient's death, no microbiological studies were performed. However, the genetic material of group W *N. meningitidis* was detected in CSF samples using PCR. Due to the positive result of the test, other samples (skin, brain, lungs, liver, spleen, heart and kidneys) were not subjected to PCR examination.

FINAL DIAGNOSIS

Based on the results of autopsy, microscopic and genetic examination it was concluded that the boy died due to septic shock associated with a severe meningococcal disease with concomitant WFS, caused by group W *N. meningitidis*.

TREATMENT

Not applicable.

OUTCOME AND FOLLOW-UP

Not applicable.

DISCUSSION

N. meningitidis is a fastidious, encapsulated, aerobic Gram-negative diplococcus being a leading cause of fatal sepsis and meningitis worldwide. Each case of suspected bacterial meningitis should be considered a medical emergency, since in untreated cases, mortality due to this condition may approximate 100%. The epidemiological profile of *N. meningitidis* varies from population to population and may change over time. This pathogen may be an etiological factor of meningococcal sepsis and WFS, a rare, life-threatening condition. In meningococcal WFS, initially macular rash progresses to large purpuric lesions penetrating deep into the skin and eventually causing subcutaneous necrosis. While WFS is usually associated with meningococcal infection, it may sporadically have different etiology, which puts particular emphasis on the correctness of causal factor identification[3-7].

Mortality due to meningococcal infections, especially WFS, can be decreased if these conditions are diagnosed early. Still some patients die despite medical treatment, especially if meningococcal disease is initially misdiagnosed as a common viral infection (cold, influenza, gastritis); in virtually all such cases, the correctness of medical intervention needs to be verified postmortem. Without adequate knowledge of basic clinical aspects of sepsis, patient's history, symptoms and course of the disease, and circumstances of death, postmortem diagnostic findings can be easily misinterpreted. This, in turn, may result in erroneous medicolegal opinion about the cause of death and/or correctness of medical treatment[8]. Postmortem diagnosis of fulminant meningococcal sepsis is particularly challenging if no CSF samples were obtained from a living patient. The evaluation can be further compromised due to the incompleteness of medical documentation or complete lack thereof, sudden death, and a serious delay in the autopsy.

During the medicolegal autopsy, the pathologist should carefully examine the cadaver for all potential abnormalities and signs of inflammation present on external

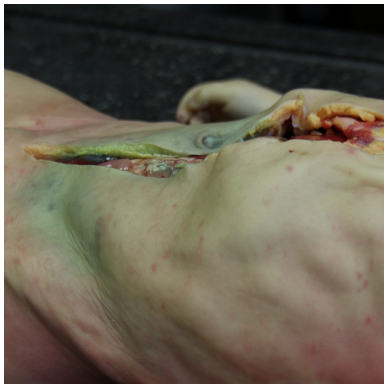

Figure 1 Purpuric rash on the chest and arms. Early decomposition.

and internal examination. Although sepsis does not produce any pathognomonic lesions that can be identified by microscopic examination, the latter should be a vital component of each postmortem evaluation[9].

Examination of the CSF is of paramount importance for the diagnosis of all forms of meningitis. Other materials that can be examined microbiologically postmortem include blood (especially from the heart), urine, nasal discharge, throat and skin swabs. However, several *Neisseria* species, among them *N. meningitidis*, can colonize nasopharynx and skin in healthy humans, and thus, their isolation from these locations should be interpreted with care[10].

Early administration of antibiotics may hinder microbiological confirmation of meningococcal disease. Further, isolation of the bacteria from the blood or CSF obtained postmortem may not necessarily correspond to a true positive result but may be associated with the agonal spread, translocation after death or contamination. Most of the above seem to be unrelated to the cause of death[11-13].

Postmortem detection of meningococcemia based on the presence of specific meningococcal capsular polysaccharides in the blood is a well-established diagnostic option. The results of the test are rarely false positive, even when conducted long after death, on blood samples with heavy bacterial load and/or deep hemolysis, stored for a long time at 40°C, and containing anticoagulant[14].

Both laboratory and clinical studies demonstrated that PCR, especially real-time PCR, are sensitive and specific enough to detect meningococcal disease. Also other new diagnostic tests, *e.g.*, fluorescence in situ hybridization and mass spectrometry, are suitable for this purpose. Nevertheless, none of these methods has been validated as a postmortem test. Only a few previously published reports documented the accuracy of late postmortem molecular identification of *N. meningitidis* in the CSF and other body fluids, such as blood from the heart and vitreous humor[2,11,15,16]. Our hereby presented experiences add to this sparse evidence, demonstrating that detection of *N. meningitidis* in the CSF obtained up to 7 days after death is still possible.

CONCLUSION

Postmortem isolation of *N. meningitidis* from the CSF of the patient who died seven days earlier is an important finding from both medical and medicolegal perspective. Our observations imply that PCR can be helpful in medicolegal practice, especially when an autopsy is delayed and the results of conventional bacteriological examination seem controversial. Postmortem PCR is a valuable instrument to determine the etiology of WFS diagnosed with conventional tests. Plausibly, suboccipital puncture, although more technically demanding, is a more appropriate route of CSF collection than traditional sampling from the cavities, due to a lower risk of secondary bacterial contamination. However, this hypothesis needs to be verified in future prospective studies. To summarize, our hereby presented findings imply that molecular microbiology should be accepted wider as a technique for postmortem evaluation.

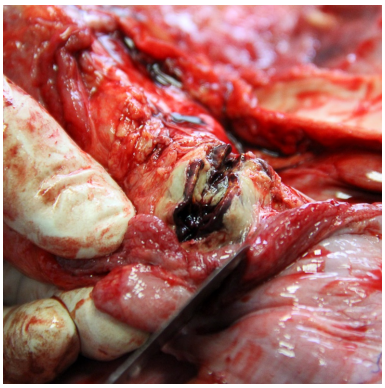

Figure 2 Hemorrhages in the adrenal gland.

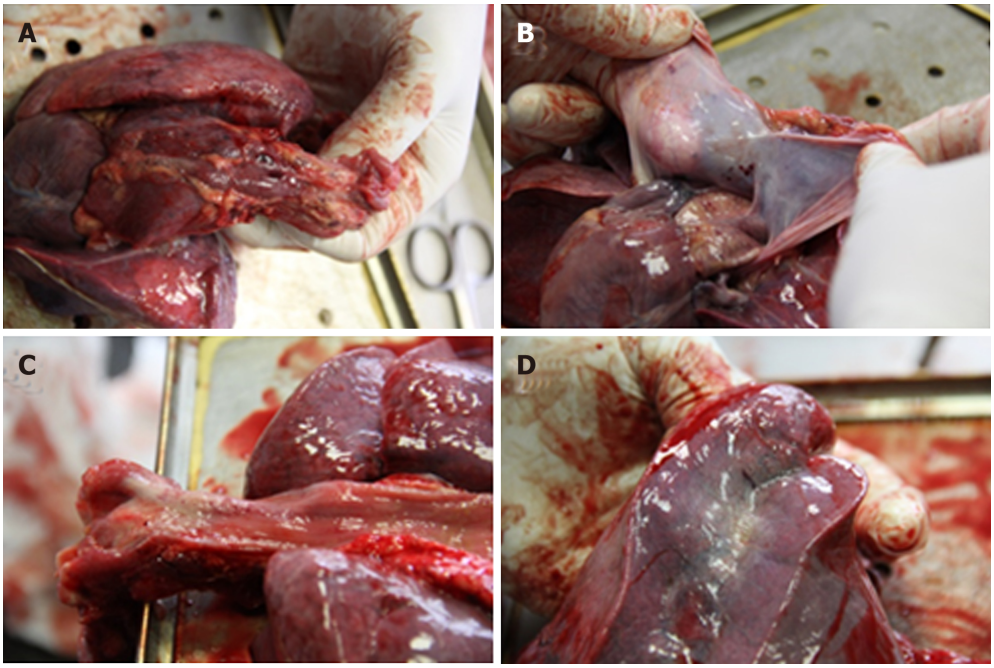

Figure 3 Petechiae. A: Thymus; B: Pericardial sack; C: Esophageal mucosa; D: Subpleural.

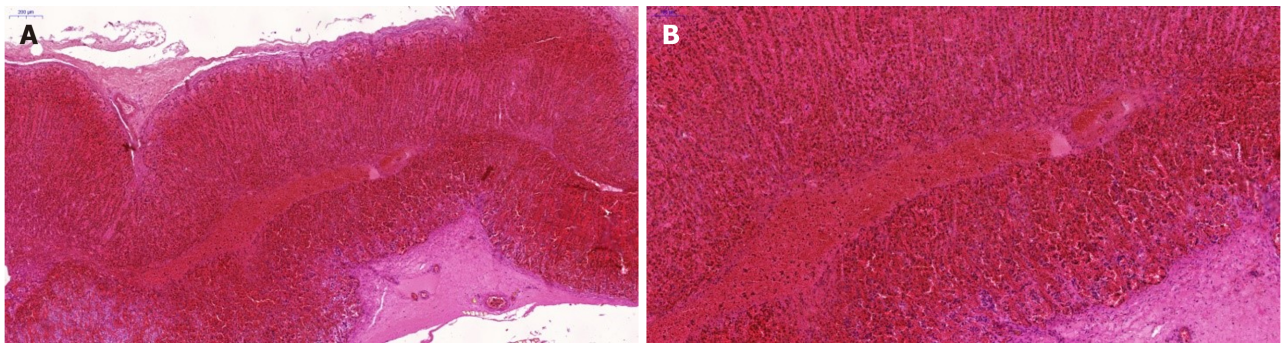

Figure 4 Adrenal gland, hematoxylin and eosin. A: 50 ×; B: 100 ×.

REFERENCES

1 **Albrecht A**, Hryniewicz W, Kuch A, Przyjalkowski W, Skoczyńska A, Szenborn L. Rekomendacje postepowania w zakażeniach bateryjnych ośrodkowego układu nerwowego [Recommendations for the management of bacterial infections within the central nervous system]. Warsaw: National Medicines Institute 2012; Available from: URL: http://antybiotyki.edu.pl/wp-content/uploads/Rekomendacje/reko-

mendacje-ukl-nerwowy_2011.pdf
2 **Ridpath AD**, Halse TA, Musser KA, Wroblewski D, Paddock CD, Shieh WJ, Pasquale-Styles M, Scordi-Bello I, Del Rosso PE, Weiss D. Postmortem diagnosis of invasive meningococcal disease. *Emerg Infect Dis* 2014; **20**: 453-455 [PMID: 24565379 DOI: 10.3201/eid2003.131245]
3 **Hamilton D**, Harris MD, Foweraker J, Gresham GA. Waterhouse-Friderichsen syndrome as a result of non-meningococcal infection. *J Clin Pathol* 2004; **57**: 208-209 [PMID: 14747454 DOI: 10.1036/JCP.2003.9936]
4 **Kim KS**. Acute bacterial meningitis in infants and children. *Lancet Infect Dis* 2010; **10**: 32-42 [PMID: 20129147 DOI: 10.1016/S1473-3099(09)70306-8]
5 **Tattoli L**, Marzullo A, Di Vella G, Solarino B. Postmortem detection of Neisseria meningitidis in case of Waterhouse-Friderichsen syndrome from fulminant meningococcal disease in an adult patient. *Rom J Leg Med* 2015; **23**: 29-32 [DOI: 10.4323/rjlm.2015.29]
6 **Bollero D**, Stella M, Gangemi EN, Spaziante L, Nuzzo J, Sigaudo G, Enrichens F. Purpura fulminans in meningococcal septicaemia in an adult: a case report. *Ann Burns Fire Disasters* 2010; **23**: 43-47 [PMID: 21991197]
7 **Rouphael NG**, Stephens DS. Neisseria meningitidis: biology, microbiology, and epidemiology. *Methods Mol Biol* 2012; **799**: 1-20 [PMID: 21993636 DOI: 10.1007/978-1-61779-346-2_1]
8 **Rorat M**, Jurek T, Simon K. Post-mortem diagnostics in cases of sepsis. Part 1. Aetiology, epidemiology and microbiological tests. *Arch Med Sadowej Kryminol* 2014; **64**: 280-294 [PMID: 25909922 DOI: 10.5114/amsik.2014.50532]
9 **Rorat M**, Jurek T, Simon K. Post-mortem diagnostics in cases of sepsis. Part 2. Biochemical and morphological examinations. *Arch Med Sadowej Kryminol* 2015; **65**: 55-66 [PMID: 26007162]
10 **Ploy MC**, Garnier F, Languepin J, Fermeaux V, Martin C, Denis F. Interest of postmortem-collected specimens in the diagnosis of fulminant meningococcal sepsis. *Diagn Microbiol Infect Dis* 2005; **52**: 65-66 [PMID: 15878445 DOI: 10.1016/j.diagmicrobio.2004.12.012]
11 **Bryant PA**, Li HY, Zaia A, Griffith J, Hogg G, Curtis N, Carapetis JR. Prospective study of a real-time PCR that is highly sensitive, specific, and clinically useful for diagnosis of meningococcal disease in children. *J Clin Microbiol* 2004; **42**: 2919-2925 [PMID: 15243039 DOI: 10.1128/JCM.42.7.2919-2925.2004]
12 **Weber MA**, Klein NJ, Hartley JC, Lock PE, Malone M, Sebire NJ. Infection and sudden unexpected death in infancy: a systematic retrospective case review. *Lancet* 2008; **371**: 1848-1853 [PMID: 18514728 DOI: 10.1016/S0140-6736(08)60798-9]
13 **Morris J**, Harrison L, Partridge S. Practical and theoretical aspects of postmortem bacteriology. *Curr Diagn Pathol* 2007; **13**: 65-74 [DOI: 10.1016/j.cdip.2006.07.005]
14 **Challener RC**, Morrissey AM, Jacobs MR. Postmortem diagnosis of meningococcemia by detection of capsular polysaccharides. *J Forensic Sci* 1988; **33**: 336-346 [PMID: 3131479 DOI: 10.1016/0379-0738(88)90108-9]
15 **Palmiere C**, Vanhaebost J, Ventura F, Bonsignore A, Bonetti LR. Cerebrospinal fluid PCR analysis and biochemistry in bodies with severe decomposition. *J Forensic Leg Med* 2015; **30**: 21-24 [PMID: 25623190 DOI: 10.1016/j.jflm.2014.12.012]
16 **Maujean G**, Guinet T, Fanton L, Malicier D. The interest of postmortem bacteriology in putrefied bodies. *J Forensic Sci* 2013; **58**: 1069-1070 [PMID: 23551205 DOI: 10.1111/1556-4029.12155]

P- Reviewer: Fiore M, Krishnan T, Pourshafie MR
S- Editor: Ji FF **L- Editor:** A **E- Editor:** Bian YN

World Journal of Clinical Cases

Submit a Manuscript: https://www.f6publishing.com

World J Clin Cases 2019 March 6; 7(5): 642-649

DOI: 10.12998/wjcc.v7.i5.642

ISSN 2307-8960 (online)

CASE REPORT

Perioperative topical ascorbic acid for the prevention of phacoemulsification-related corneal endothelial damage: Two case reports and review of literature

Chia-Yi Lee, Hung-Ta Chen, Yi-Jen Hsueh, Hung-Chi Chen, Chieh-Cheng Huang, Yaa-Jyuhn James Meir, Chao-Min Cheng, Wei-Chi Wu

ORCID number: Chia-Yi Lee (0000-0002-5719-0488); Hung-Ta Chen (0000-0003-3229-5408); Yi-Jen Hsueh (0000-0003-3380-7188); Hung-Chi Chen (0000-0002-1117-7878); Chieh-Cheng Huang (0000-0003-1773-8450); Yaa-Jyuhn James Meir (0000-0002-8562-5995); Chao-Min Cheng (0000-0002-8644-1960); Wei-Chi Wu (0000-0003-3760-7255).

Author contributions: Lee CY and Chen HT contributed equally to this work. All authors gave approval of the final version.

Supported by the Chang Gung Memorial Hospital, No. CMRPG3F1471~2 and No. CMRPG3G0031~3; the Ministry of Science and Technology No. MOST 106-2314-B-182A-042-34 and No. MOST 107-2314-B-182A-088-MY3.

Informed consent statement: Informed written consent was obtained from the patient for publication of this report and any accompanying images.

Conflict-of-interest statement: The authors declare that they have no conflicts of interest.

CARE Checklist (2016) statement: The authors have read the CARE Checklist (2013), and the manuscript was prepared and revised according to the CARE Checklist (2016).

Open-Access: This article is an open-access article which was

Chia-Yi Lee, Department of Ophthalmology, Show Chwan Memorial Hospital, Changhua 50093, Taiwan

Chia-Yi Lee, Department of Optometry, College of Medicine and Life Science, Chung Hwa University of Medical Technology, Tainan 71241, Taiwan

Hung-Ta Chen, Department of Internal Medicine, Taipei City Hospital- Heping Branch, Taipei 10341, Taiwan

Yi-Jen Hsueh, Hung-Chi Chen, Wei-Chi Wu, Department of Ophthalmology, Chang Gung Memorial Hospital, Linkou 20012, Taiwan

Yi-Jen Hsueh, Hung-Chi Chen, Chieh-Cheng Huang, Chao-Min Cheng, Center for Tissue Engineering, Chang Gung Memorial Hospital, Linkou 20012, Taiwan

Hung-Chi Chen, Wei-Chi Wu, Department of Medicine, College of Medicine Chang Gung University, Taoyuan 33305, Taiwan

Chieh-Cheng Huang, Chao-Min Cheng, Institute of Biomedical Engineering, National Tsing Hua University, Hsinchu 30010, Taiwan

Yaa-Jyuhn James Meir, Department of Biomedical Sciences, College of Medicine Chang Gung University, Taoyuan 33305, Taiwan

Corresponding author: Hung-Chi Chen, MD, PhD, Attending Ophthalmologist, Department of Ophthalmology, Chang Gung Memorial Hospital, No. 5, Fuxing Street, Guishan District, Taoyuan 33305, Taiwan. mr3756@cgmh.org.tw
Telephone: +886-3-3281200
Fax: +886-3-3287798

Abstract

BACKGROUND

The current case report describes successful phacoemulsification with the aid of perioperative topical ascorbic acid (AA) in two patients with corneal endothelial disorders to prevent postoperative corneal endothelial decompensation.

CASE SUMMARY

Two eyes of two patients underwent phacoemulsification with pre-existing corneal endothelial disorders including Fuchs corneal endothelial dystrophy

selected by an in-house editor and fully peer-reviewed by external reviewers. It is distributed in accordance with the Creative Commons Attribution Non Commercial (CC BY-NC 4.0) license, which permits others to distribute, remix, adapt, build upon this work non-commercially, and license their derivative works on different terms, provided the original work is properly cited and the use is non-commercial. See: http://creativecommons.org/licenses/by-nc/4.0/

Manuscript source: Unsolicited manuscript

Received: November 17, 2018
Peer-review started: November 19, 2018
First decision: December 29, 2018
Revised: January 16, 2019
Accepted: January 26, 2019
Article in press: January 26, 2019
Published online: March 6, 2019

(Patient 1) and endotheliitis (Patient 2). Topical AA was applied to both patients at least one month before and after with a frequency of four times per day. After the surgery, both eyes improved best-corrected visual acuity (BCVA) and there was limited human corneal endothelial cell loss without signs of corneal endothelial decompensation, such as deteriorated BCVA or persistent corneal edema during the follow-up of at least two years.

CONCLUSION
Perioperative administration of topical AA may be an alternative therapy to the triple procedure in patients expecting to undergo cataract surgery.

Key words: Ascorbic acid; Fuchs corneal endothelial dystrophy; Endotheliitis; Human corneal endothelial cell; Phacoemulsification; Case report

©The Author(s) 2019. Published by Baishideng Publishing Group Inc. All rights reserved.

Core tip: Perioperative topical ascorbic acid (AA) was instilled in two patients with low corneal endothelial cell density who were scheduled for cataract surgery. After the surgery, both patients showed improved visual acuity without corneal decompensation. Perioperative topical AA is promising for prevention of corneal endothelial dysfunction in high-risk patients undergoing phacoemulsification; it may be considered as an alternative therapy.

Citation: Lee CY, Chen HT, Hsueh YJ, Chen HC, Huang CC, Meir YJJ, Cheng CM, Wu WC. Perioperative topical ascorbic acid for the prevention of phacoemulsification-related corneal endothelial damage: Two case reports and review of literature. *World J Clin Cases* 2019; 7(5): 642-649
URL: https://www.wjgnet.com/2307-8960/full/v7/i5/642.htm
DOI: https://dx.doi.org/10.12998/wjcc.v7.i5.642

INTRODUCTION

Phacoemulsification has been used to treat cataract for decades, while human corneal endothelial cells (HCECs) loss remains a major complication[1]. Fuchs endothelial corneal dystrophy (FECD) is a dystrophic disorder of HCECs that are vulnerable to external damage[2]. Recently, corneal endotheliitis has been demonstrated to be an inflammatory process with viral origin, *e.g.*, cytomegalovirus (CMV), that destroys HCECs and leads to severe visual impairment[3]. Because corneal decompensation with severe HCECs loss is common in patients with impaired HCECs, including corneal endothelial dystrophy, post-traumatic status and corneal endotheliitis[4,5], adequate management is advocated to prevent corneal decompensation after phacoemulsification.

Triple procedures, combining endothelial keratoplasty, phacoemulsification and intraocular lens implantation, have been successfully performed in patients with concomitant cataract and corneal decompensation[6], while limited sources of corneal donor tissues result in long waiting lists[7]. Also, several complications following triple procedure have been reported, such as secondary glaucoma, graft dislocation requiring re-surgery and graft rejection leading to graft failure[8,9]. We therefore wonder if there are potential strategies to prevent corneal endothelial loss other than surgical triple procedures.

Theoretically, ascorbic acid (AA) can be an ideal ocular nutritional supplement[10]. Two in vitro studies have shown that AA and L-AA 2-phosphate prolonged the lifespan and inhibited apoptosis of murine corneal endothelial cells[11] and HCECs[12], probably through anti-oxidant effects. On the other hand, topical AA can be used alone to manage alkali burns which decrease the incidence of corneal ulcerations and perforation in rabbits[13], or combined with topical steroids to treat alkali burns without significant side effects[14,15]. Furthermore, animal studies showed that AA applied to the irrigating solution can serve as free-radical scavengers to prevent endothelial cell damage from phacoemulsification[16,17]. Still, it remains unclear whether topical AA can prevent HCECs loss after phacoemulsification. In addition, although AA has been used for protective agent of HCECs by intraoperative or

postoperative administration[17-19], the perioperative instillation of AA has not been used before.

Herein, we report the use of topical AA before and after cataract surgery to reduce HCECs loss in patients with pre-existing corneal endothelial disorders. The novel effect of perioperative topical AA, which obviated the need for corneal transplantation, is demonstrated in two patients with FECD and CMV corneal endotheliitis respectively.

CASE PRESENTATION

Chief complaint

Patient 1: A 41-year-old man presented with blurry vision in the right eye.

Patient 2: A 51-year-old man was referred to our clinic due to whitish left cornea.

History of present illness

Patient 1: The symptom persisted for months without exacerbating or relieving factors.

Patient 2: The symptom persisted for 3 wk and had gradually progressed.

History of past illness

Patient 1: The patient reported no known systemic illness or previous surgery.

Patient 2: The patient revealed no known systemic illness or previous surgery.

Personal and family history

Patient 1: The patient revealed no known personal and family history.

Patient 2: The patient revealed no known personal and family history.

Physical examination

Patient 1: The best-corrected visual acuity (BCVA) in the right eye was 20/60. Slit lamp examination revealed cataract with right predominance.

Patient 2: On examination, BCVA was 20/50 in the left eye and the silt-lamp microscope revealed bilateral cataract with mild corneal edema in the left eye (Figure 1A).

Laboratory examinations

Patient 1: No laboratory examination was performed due to the absence of indication.

Patient 2: Intracameral tapping of left eye was arranged, and real-time quantitative polymerase chain reaction exam reported a positive result for CMV.

Imaging examinations

Patient 1: Specular microscopy showed bilateral guttate formations (Figure 2).

Patient 2: The specular microscope revealed ECD of 1273/mm^2 with disciform lesions in the left eye.

FINAL DIAGNOSIS

Patient 1: The final diagnosis of the case was bilateral cataract with right predominant and bilateral FECD.

Patient 2: The final diagnosis of the case was bilateral cataracts and CMV endotheliitis in the left eye.

TREATMENT

Patient 1: Phacoemulsification was performed, and postoperative BCVA in the right eye was 20/200; nevertheless, our patient continued to complain of blurry vision and tingling of the right eye. Specular microscopy revealed pseudophakic bullous keratopathy and Descemet's stripping. Automated endothelial keratoplasty was performed as salvage surgery. After keratoplasty, a clear cornea graft with enhanced

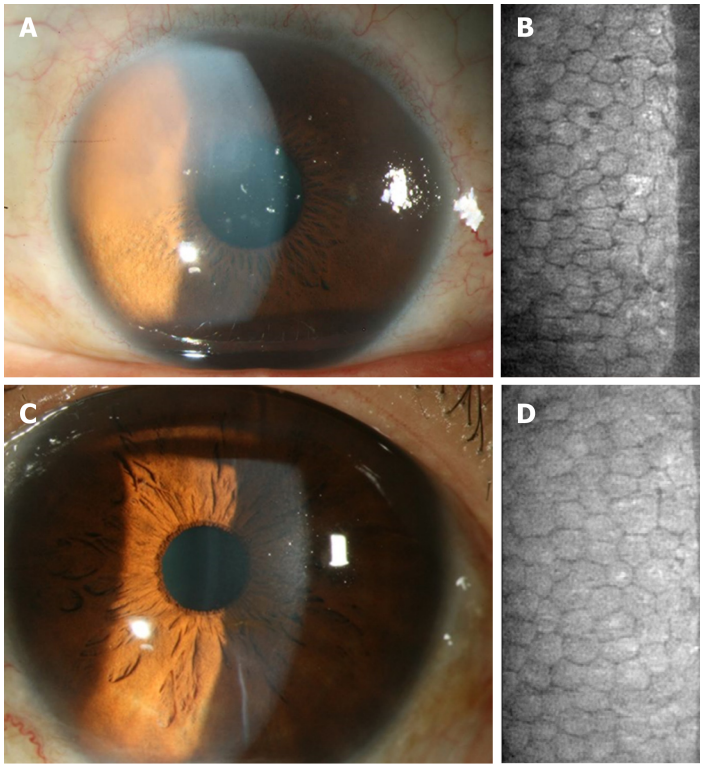

Figure 1 The corneal endothelium condition before and after cataract surgery in the left eye of Patient 2. A: Preoperative corneal appearance *via* silt-lamp biomicroscope; B: Preoperative corneal endothelial cell density *via* specular microscope; C: Postoperative corneal appearance *via* silt-lamp biomicroscope; D: Postoperative corneal endothelial cell density *via* specular microscope.

endothelial cell density (ECD) of 2075/mm^2 and improved BCVA of 20/25 in the right eye were observed. Two years later, a left eye cataract was found with BCVA of 20/200 (Figure 3A) and another phacoemulsification was planned. The preoperative ECD was 1365/mm^2 in the left eye (Figure 3B). To prevent a similar scenario of corneal decompensation, we prescribed AA (50 mg/mL, Vitacicol, Taiwan Biotech CO., LTD., Taoyuan, Taiwan) eye drops four times daily one month before and after surgery. In addition, excessive intracameral medications, including lidocaine and carbachol, were avoided intraoperatively.

Patient 2: Acyclovir and famciclovir were sequentially prescribed for the suspicion of herpetic simplex virus endotheliitis; however, upper corneal edema and a few keratic precipitates emerged. Topical valganciclovir and systemic ganciclovir were prescribed for the CMV endotheliitis, and the CMV endotheliitis subsided. Meanwhile, AA (50 mg/mL) was used for the scheduled cataract surgery with a frequency of four times daily one month perioperatively. The ECD was 1048/mm^2 before surgery (Figure 1B).

OUTCOME AND FOLLOW-UP

Patient 1: Only mild stromal edema was observed postoperatively without bullae, while improved visual acuity was reported by the patient. The BCVA in the left eye was 20/30 with clear cornea and ECD of 1239/mm^2 two years postoperatively (Figure 3C and D).

Patient 2: After the surgery, the visual acuity had improved without signs of corneal decompensation. The postoperative ECD was 1017/mm^2 in the left eye with BCVA of 20/20 at the latest visit (Figure 1C and D).

DISCUSSION

In the corneal endothelium, oxidative stress may increase lipid peroxidation, leading to cellular impairment and apoptosis of HCECs[20]. FECD is featured by elevated cell apoptosis resulting from higher oxidative stress and oxygen-induced damage on

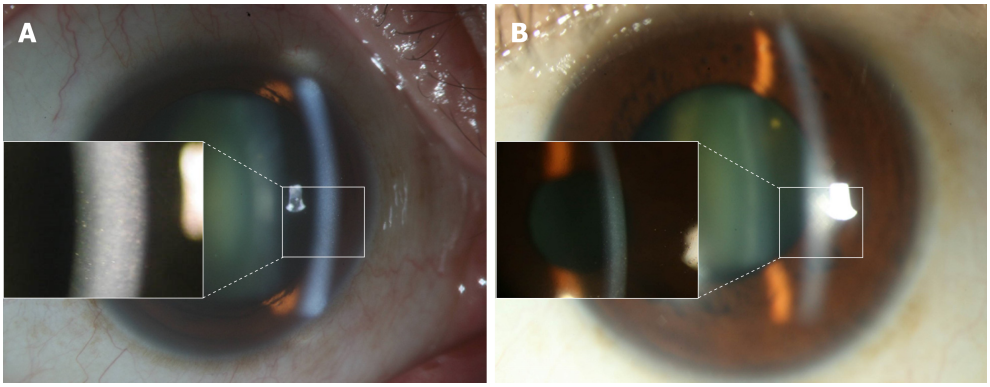

Figure 2 The appearance of Fuchs endothelial corneal dystrophy in Patient 1. A: External eye appearance and guttate formation (left bracket) in the right eye; B: External eye appearance and guttate formation (left bracket) in the left eye.

DNA[20,21]. Although oxidative stress has not been demonstrated in CMV corneal endotheliitis, apoptosis has been detected in CMV retinitis in cell line models[22]. In addition, oxygen free radicals generated by high-intensity ultrasound oscillations in water during phacoemulsification have been shown to damage the corneal endothelium[23]. Since HCECs of the two patients enrolled were impaired with ECD below 1500 cell/mm^2, the double damage of phacoemulsification and concurrent FECD or CMV endotheliitis increased the risks of developing corneal decompensation or even pseudophakic bullous keratopathy. To prevent the oxidative damage, we arranged anti-oxidant therapy with topical AA and reached acceptable visual outcome with fair corneal condition. To our knowledge, this is the first experience to show the effectiveness of topical AA in the prevention of phacoemulsification-related corneal endothelial damage.

The AA has been widely applied in immune and inflammatory disorders due to its antioxidant properties recently[24]. In the field of ophthalmology, previous studies illustrated that AA may be associated with the development of cataract, age-related macular degeneration and diabetic macular edema and owns the potential as a therapeutic agent[10,25-27]. About the cornea, postoperatively topical instillation and oral administration of AA preserve the integrity of corneal stroma in refractive procedures[18,19], while intracameral irrigation of AA during phacoemulsification may decrease corneal endothelial injury in animal studies[17,28]. Still, the effectiveness of perioperative AA instillation on the protection of HCECs demonstrated in the current study has rarely been reported elsewhere. The AA we administrated in the current study was 50 mg/mL, which was much higher than the concentration of AA in the general culture medium. However, the corneal endothelium is immersed in an environment where aqueous humor is recycled every one to two hours and the bioavailability of topical medications is only approximately one to five percent[29]. As a result, we adopted a much higher concentration of AA than that of the ordinary culture medium and followed a humanly possible administration protocol of four times a day in the hope to reach similar concentration of AA in the culture medium. The favorable preservation of HCECs and absence of complications in our two patients verifies the current concentration of AA as acceptable whether in terms of efficacy or safety.

The first patient was diagnosed with FECD. In a previous study, 35 of 89 eyes needed to undergo endothelial keratoplasty, but no improvement in BCVA was found in those eyes that underwent endothelial keratoplasty[6]. By comparison, BCVA in the left eye of the first patient recovered prominently. Our findings suggest that perioperative anti-oxidant supplements can improve and preserve HCECs and visual outcomes compatible with the degree of the traditional approach. Furthermore, graft dislocation and pupillary block glaucoma occasionally occur in patients undergoing triple surgery despite excellent visual outcome[30], while current management avoids these complications.

For patients with corneal endotheliitis who require cataract surgery, previous studies focused only on postoperative infection[31], or did not provide adequate details regarding postoperative status[5]. In the current study, the second patient was diagnosed with CMV endotheliitis and low ECD, while the final BCVA was 20/20, showing much improvement with similar ECD values observed postoperatively. A possible explanation is that phacoemulsification-related oxidative stress can be alleviated by AA and that the anti-inflammatory effect of AA may also reduce the inflammation from both phacoemulsification and CMV endotheliitis[32].

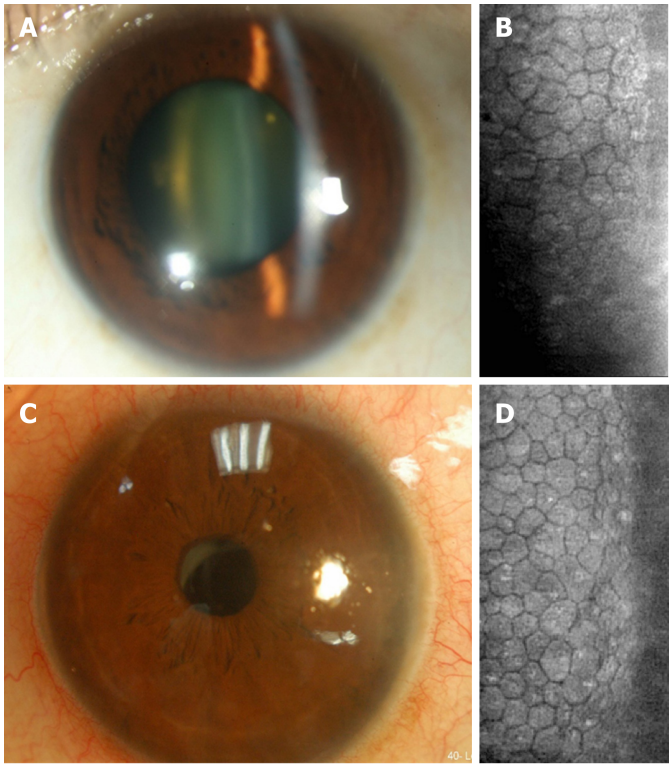

Figure 3 The corneal endothelium condition before and after cataract surgery in the left eye of Patient 1. A: Preoperative corneal appearance *via* silt-lamp biomicroscope; B: Preoperative corneal endothelial cell density *via* specular microscope; C: Postoperative corneal appearance *via* silt-lamp biomicroscope; D: Postoperative corneal endothelial cell density *via* specular microscope.

Comparison of the current study to two previous studies concerning the application of phacoemulsification in low ECD patients is illustrated in Table 1. The two previous studies applied a soft-shell technique to reduce possible mechanical impact[4,5]. We did not perform the soft-shell technique but rather used an ophthalmic Viscoat viscoelastic device and irrigation with balanced salt solution. Furthermore, we did not alter the perioperative medications except AA among all eyes undergoing cataract surgery mentioned in this report. Collectively, the use of perioperative topical AA alone ended up with similar HCECs loss compared to previous experiences[4,5]. Moreover, the major etiology of low ECD in a previous study was primary angle closure glaucoma with acute attack or laser iridotomy[4], possibly inducing less damage to HCECs than HCECs-origin lesions such as FECD.

CONCLUSION

Perioperative topical AA showed both safety and promise for prevention of HCECs dysfunction in high-risk patients undergoing phacoemulsification and may be considered an alternative therapy. Further large prospective studies are required to determine the optimal dose.

Table 1 Comparison of different modifications of cataract surgery in patients with low endothelial count

	Hayashi 2011	Yamazoe 2011	Lee 2019
Technique to preserve EC	Soft shell technique	Soft shell technique	Perioperative AA
Case number	50	61	2
Mean age (yr)	68.9	72.3	45.5
Gender (M to F, %)	24 to 76	23 to 77	100 to 0
Leading etiology (%)	PACG (38)	FCED (33)	FCED and CMV endotheliitis (50)
Mean preOP ECD	805.0	692.9	1206.5
Energy (mJ)	27.3 ± 10.1	NA	30.4
Time (Sec)	57.5 ± 28.3	NA	72.8
Mean EC loss (%)	5.1	11.5	6.1

EC: Endothelial cells; AA: Ascorbic acid; M: Male; F: Female; PACG: Primary angle closure glaucoma; FCED: Fuchs corneal endothelial dystrophy; CMV: Cytomegalovirus; preOP: Preoperative; ECD: Endothelial cell density.

REFERENCES

1 **Rosado-Adames N**, Afshari NA. The changing fate of the corneal endothelium in cataract surgery. *Curr Opin Ophthalmol* 2012; **23**: 3-6 [PMID: 22134364 DOI: 10.1097/ICU.0b013e32834e4b5f]
2 **Adamis AP**, Filatov V, Tripathi BJ, Tripathi RC. Fuchs' endothelial dystrophy of the cornea. *Surv Ophthalmol* 1993; **38**: 149-168 [PMID: 8235998 DOI: 10.1016/0039-6257(93)90099-S]
3 **Chee SP**, Bacsal K, Jap A, Se-Thoe SY, Cheng CL, Tan BH. Corneal endotheliitis associated with evidence of cytomegalovirus infection. *Ophthalmology* 2007; **114**: 798-803 [PMID: 17207531 DOI: 10.1016/j.ophtha.2006.07.057]
4 **Hayashi K**, Yoshida M, Manabe S, Hirata A. Cataract surgery in eyes with low corneal endothelial cell density. *J Cataract Refract Surg* 2011; **37**: 1419-1425 [PMID: 21684110 DOI: 10.1016/j.jcrs.2011.02.025]
5 **Yamazoe K**, Yamaguchi T, Hotta K, Satake Y, Konomi K, Den S, Shimazaki J. Outcomes of cataract surgery in eyes with a low corneal endothelial cell density. *J Cataract Refract Surg* 2011; **37**: 2130-2136 [PMID: 21908173 DOI: 10.1016/j.jcrs.2011.05.039]
6 **van Cleynenbreugel H**, Remeijer L, Hillenaar T. Cataract surgery in patients with Fuchs' endothelial corneal dystrophy: when to consider a triple procedure. *Ophthalmology* 2014; **121**: 445-453 [PMID: 24289914 DOI: 10.1016/j.ophtha.2013.09.047]
7 **Rosenfeld E**, Varssano D. The corneal transplant score: a simple corneal graft candidate calculator. *Graefes Arch Clin Exp Ophthalmol* 2013; **251**: 1771-1775 [PMID: 23649668 DOI: 10.1007/s00417-013-2358-8]
8 **Sridhar MS**, Murthy S, Bansal AK, Rao GN. Corneal triple procedure: indications, complications, and outcomes: a developing country scenario. *Cornea* 2000; **19**: 333-335 [PMID: 10832694 DOI: 10.1097/00003226-200005000-00015]
9 **Covert DJ**, Koenig SB. New triple procedure: Descemet's stripping and automated endothelial keratoplasty combined with phacoemulsification and intraocular lens implantation. *Ophthalmology* 2007; **114**: 1272-1277 [PMID: 17433835 DOI: 10.1016/j.ophtha.2006.12.030]
10 **Bartlett H**, Eperjesi F. An ideal ocular nutritional supplement? *Ophthalmic Physiol Opt* 2004; **24**: 339-349 [PMID: 15228513 DOI: 10.1111/j.1475-1313.2004.00218.x]
11 **Serbecic N**, Beutelspacher SC. Vitamins inhibit oxidant-induced apoptosis of corneal endothelial cells. *Jpn J Ophthalmol* 2005; **49**: 355-362 [PMID: 16187034 DOI: 10.1007/s10384-005-0209-9]
12 **Shima N**, Kimoto M, Yamaguchi M, Yamagami S. Increased proliferation and replicative lifespan of isolated human corneal endothelial cells with L-ascorbic acid 2-phosphate. *Invest Ophthalmol Vis Sci* 2011; **52**: 8711-8717 [PMID: 21980003 DOI: 10.1167/iovs.11-7592]
13 **Pfister RR**, Paterson CA. Ascorbic acid in the treatment of alkali burns of the eye. *Ophthalmology* 1980; **87**: 1050-1057 [PMID: 7243199 DOI: 10.1016/S0161-6420(80)35126-9]
14 **Brodovsky SC**, McCarty CA, Snibson G, Loughnan M, Sullivan L, Daniell M, Taylor HR. Management of alkali burns : an 11-year retrospective review. *Ophthalmology* 2000; **107**: 1829-1835 [PMID: 11013181 DOI: 10.1016/S0161-6420(00)00289-X]
15 **Davis AR**, Ali QK, Aclimandos WA, Hunter PA. Topical steroid use in the treatment of ocular alkali burns. *Br J Ophthalmol* 1997; **81**: 732-734 [PMID: 9422923 DOI: 10.1136/bjo.81.9.732]
16 **Nemet AY**, Assia EI, Meyerstein D, Meyerstein N, Gedanken A, Topaz M. Protective effect of free-radical scavengers on corneal endothelial damage in phacoemulsification. *J Cataract Refract Surg* 2007; **33**: 310-315 [PMID: 17276276 DOI: 10.1016/j.jcrs.2006.10.031]
17 **Rubowitz A**, Assia EI, Rosner M, Topaz M. Antioxidant protection against corneal damage by free radicals during phacoemulsification. *Invest Ophthalmol Vis Sci* 2003; **44**: 1866-1870 [PMID: 12714617 DOI: 10.1167/iovs.02-0892]
18 **Stojanovic A**, Ringvold A, Nitter T. Ascorbate prophylaxis for corneal haze after photorefractive keratectomy. *J Refract Surg* 2003; **19**: 338-343 [PMID: 12777030]
19 **Kasetsuwan N**, Wu FM, Hsieh F, Sanchez D, McDonnell PJ. Effect of topical ascorbic acid on free radical tissue damage and inflammatory cell influx in the cornea after excimer laser corneal surgery. *Arch Ophthalmol* 1999; **117**: 649-652 [PMID: 10326963 DOI: 10.1001/archopht.117.5.649]
20 **Jurkunas UV**, Bitar MS, Funaki T, Azizi B. Evidence of oxidative stress in the pathogenesis of fuchs endothelial corneal dystrophy. *Am J Pathol* 2010; **177**: 2278-2289 [PMID: 20847286 DOI: 10.2353/ajpath.2010.100279]
21 **Czarny P**, Kasprzak E, Wielgorski M, Udziela M, Markiewicz B, Blasiak J, Szaflik J, Szaflik JP. DNA damage and repair in Fuchs endothelial corneal dystrophy. *Mol Biol Rep* 2013; **40**: 2977-2983 [PMID:

23275192 DOI: 10.1007/s11033-012-2369-2]
22 **Cinatl J**, Blaheta R, Bittoova M, Scholz M, Margraf S, Vogel JU, Cinatl J, Doerr HW. Decreased neutrophil adhesion to human cytomegalovirus-infected retinal pigment epithelial cells is mediated by virus-induced up-regulation of Fas ligand independent of neutrophil apoptosis. *J Immunol* 2000; **165**: 4405-4413 [PMID: 11035078 DOI: 10.4049/jimmunol.165.8.4405]
23 **Augustin AJ**, Dick HB. Oxidative tissue damage after phacoemulsification: influence of ophthalmic viscosurgical devices. *J Cataract Refract Surg* 2004; **30**: 424-427 [PMID: 15030835 DOI: 10.1016/S0886-3350(03)00577-7]
24 **Sorice A**, Guerriero E, Capone F, Colonna G, Castello G, Costantini S. Ascorbic acid: its role in immune system and chronic inflammation diseases. *Mini Rev Med Chem* 2014; **14**: 444-452 [PMID: 24766384 DOI: 10.2174/1389557514666140428112602]
25 **Schmidl D**, Garhöfer G, Schmetterer L. Nutritional supplements in age-related macular degeneration. *Acta Ophthalmol* 2015; **93**: 105-121 [PMID: 25586104 DOI: 10.1111/aos.12650]
26 **May JM**. Ascorbic acid repletion: A possible therapy for diabetic macular edema? *Free Radic Biol Med* 2016; **94**: 47-54 [PMID: 26898503 DOI: 10.1016/j.freeradbiomed.2016.02.019]
27 **Jalal D**, Koorosh F, Fereidoun H. Comparative study of plasma ascorbic acid levels in senile cataract patients and in normal individuals. *Curr Eye Res* 2009; **34**: 118-122 [PMID: 19219683 DOI: 10.1080/02713680802632599]
28 **M Padua IR**, P Valdetaro G, B Lima T, K Kobashigawa K, E S Silva P, Aldrovani M, M Padua PP, Laus JL. Effects of intracameral ascorbic acid on the corneal endothelium of dogs undergoing phacoemulsification. *Vet Ophthalmol* 2018; **21**: 151-159 [PMID: 28714237 DOI: 10.1111/vop.12490]
29 **Hughes PM**, Olejnik O, Chang-Lin JE, Wilson CG. Topical and systemic drug delivery to the posterior segments. *Adv Drug Deliv Rev* 2005; **57**: 2010-2032 [PMID: 16289435 DOI: 10.1016/j.addr.2005.09.004]
30 **Terry MA**, Shamie N, Chen ES, Phillips PM, Shah AK, Hoar KL, Friend DJ. Endothelial keratoplasty for Fuchs' dystrophy with cataract: complications and clinical results with the new triple procedure. *Ophthalmology* 2009; **116**: 631-639 [PMID: 19201480 DOI: 10.1016/j.ophtha.2008.11.004]
31 **Zarei-Ghanavati S**, Alizadeh R, Yoo SH. Herpes Simplex Virus Endotheliitis following Descemet's Membrane Endothelial Keratoplasty. *J Ophthalmic Vis Res* 2015; **10**: 184-186 [PMID: 26425323 DOI: 10.4103/2008-322X.163764]
32 **Ellulu MS**, Rahmat A, Patimah I, Khaza'ai H, Abed Y. Effect of vitamin C on inflammation and metabolic markers in hypertensive and/or diabetic obese adults: a randomized controlled trial. *Drug Des Devel Ther* 2015; **9**: 3405-3412 [PMID: 26170625 DOI: 10.2147/DDDT.S83144]

P- Reviewer: Teragawa H; Kim CH
S- Editor: Dou Y **L- Editor:** A **E- Editor:** Bian YN

World Journal of Clinical Cases

Submit a Manuscript: https://www.f6publishing.com

World J Clin Cases 2019 March 6; 7(5): 650-655

DOI: 10.12998/wjcc.v7.i5.650

ISSN 2307-8960 (online)

CASE REPORT

Application of computer-assisted navigation in treating congenital maxillomandibular syngnathia: A case report

Li-Qin Lin, Shan-Shan Bai, Min Wei

ORCID number: Li-Qin Lin (0000-0003-0003-8722); Shan-Shan Bai (0000-0002-1065-7730); Min Wei (0000-0002-6974-6287).

Author contributions: Lin LQ and Bai SS are co-first authors and contributed equally to this work; all authors contributed to this work.

Supported by Ninth People's Hospital affiliated to Shanghai Jiao Tong University, School of Medicine "Multi-Disciplinary Team" Clinical Research Project, No. 201701011.

Informed consent statement: The relatives of the individual in this manuscript have provided informed written consent to publish this case.

Conflict-of-interest statement: The authors have no conflicts of interest to declare. None of the authors have received funding from any organization with a real or potential interest in the subject matter, materials, equipment, software, or devices discussed.

CARE Checklist (2016) statement: The authors have read the CARE Checklist (2016), and the manuscript was prepared and revised according to the CARE Checklist (2016).

Open-Access: This article is an open-access article which was selected by an in-house editor and fully peer-reviewed by external reviewers. It is distributed in accordance with the Creative Commons Attribution Non Commercial (CC BY-NC 4.0)

Li-Qin Lin, Shan-Shan Bai, Min Wei, Department of Plastic and Reconstructive Surgery, Shanghai Ninth People's Hospital, Shanghai Jiao Tong University School of Medicine, Shanghai 200011, China

Corresponding author: Min Wei, MD, PhD, Doctor, Full Professor, Surgeon, Department of Plastic and Reconstructive Surgery, Shanghai Ninth People's Hospital, Shanghai Jiao Tong University School of Medicine, 639 Zhizaoju Road, Shanghai 200011, China.
drwm1010@sina.com
Telephone: +86-137-01671615

Abstract

BACKGROUND

Congenital maxillomandibular syngnathia is an extremely rare disorder characterized by craniofacial malformations and inability to open the mouth adequately, which leads to problems with feeding, swallowing, and breathing as well as temporomandibular joint ankylosis. The main goal of the surgery is to release the ankylosis, establish functioning mandible, and prevent re-fusion. However, surgical procedures for this disease are rarely reported.

CASE SUMMARY

Here, we report a 7-mo-old girl with bilateral maxillomandibular syngnathia. The patient presented with difficulty in feeding, breathing, sounding, and swallowing and had developmental dysplasia. For treatment, we performed bone isolation by computer-assisted navigation and used silicone to fix the wound surface to prevent refusion of bone. To our knowledge, this is the only syngnathia case in the literature treated using computer-assisted navigation. With the guidance of precise navigation, we were able to minimize operation time by at least one hour, the patient's blood vessels, nerves, and tooth germs were well protected, and excessive bleeding was avoided. After six weeks, the patient showed improvement in mouth opening and no major issues of feeding.

CONCLUSION

Application of computer-assisted navigation can significantly improve accuracy, effectiveness, and surgical safety in correcting congenital maxillomandibular syngnathia.

Key words: Craniofacial abnormalities; Mandibular diseases; Maxilla; Computer-assisted navigation; Case report

©The Author(s) 2019. Published by Baishideng Publishing Group Inc. All rights reserved.

license, which permits others to distribute, remix, adapt, build upon this work non-commercially, and license their derivative works on different terms, provided the original work is properly cited and the use is non-commercial. See: http://creativecommons.org/licenses/by-nc/4.0/

Manuscript source: Unsolicited manuscript

Received: November 9, 2018
Peer-review started: November 13, 2018
First decision: December 29, 2018
Revised: January 28, 2019
Accepted: January 29, 2019
Article in press: January 30, 2019
Published online: March 6, 2019

Core tip: Congenital maxillomandibular fusion is a rare anomaly of the craniofacial region. We report a 7-mo-old girl with bilateral maxillomandibular syngnathia. We performed bony isolation by computer-assisted navigation, a first-of-its-kind treatment approach for syngnathia. The operation time was minimized by at least one hour, and the patient's blood vessels, nerves, and tooth germs were well protected, and bleeding was minimized. There were major improvements in the patient's status. We concluded that application of computer-assisted navigation can significantly improve accuracy, effectiveness, and surgical safety in difficult-to-treat deformity.

Citation: Lin LQ, Bai SS, Wei M. Application of computer-assisted navigation in treating congenital maxillomandibular syngnathia: A case report. *World J Clin Cases* 2019; 7(5): 650-655
URL: https://www.wjgnet.com/2307-8960/full/v7/i5/650.htm
DOI: https://dx.doi.org/10.12998/wjcc.v7.i5.650

INTRODUCTION

Congenital craniofacial disorders represent approximately 20% of all birth defects. Syngnathia, a rare craniofacial disorder, is characterized by fusion of the hard and soft tissues of the jaw. The first case of syngnathia was reported by Burket in 1936 in a patient who had multiple diagnoses, including temporomandibular joint (TMJ) ankyloses, fusion of gums, associated facial hemiatrophy, and Horner syndrome[1]. A significant complication in syngnathia patients is restricted mouth opening, which results in feeding, swallowing, and respiration problems. Early recognition and treatment are critical for normal growth and development. The aim of the case report is to introduce the application of computer-assisted navigation during syngnathia corrective surgery.

CASE PRESENTATION

Chief complaints

A 7-month-old girl with a clinical diagnosis of congenital maxillomandibular fusion was referred to the Department of Plastic and Reconstructive Surgery, Shanghai Ninth People's Hospital, Shanghai Jiao Tong University School of Medicine for surgery. She was suffering from bilateral maxillomandibular syngnathia and inability to open mouth.

History of present illness

The patient was fed through a straw by his grandmother.

History of past illness

She had no past history of surgery and was not taking any medication.

Personal and family history

She was the first child of the parents (mother 28 years old, father 30 years old) and was born *via* an uncomplicated vaginal delivery. The parents did not have a history of consanguineous marriage. A similar symptom was not observed in other patient's family members.

Physical examination upon admission

Physical examination revealed sever retardation - she was 73 cm tall and weight 5.5 kg - but did not reveal any congenital or systemic problems. She also presented with difficulty in feeding, breathing, sounding, and swallowing. The patient had difficulty in opening her mouth more than 1 mm in diameter. In her oral cavity, the upper and lower gums were completely fused and two deciduous teeth in the mandible were visible (Figure 1). Otherwise no abnormalities were noted.

Laboratory examinations

No abnormality was seen in routine blood tests, biochemical tests, or ECG.

Imaging examinations

Figure 1 Facial features and preoperative intraoral view of the patient. A: Frontal view of the patient; B: Profile view of the patient; C: Intraoral view. Maxillary and mandibular arches were fused.

A three-dimensional CT scan showed bilateral maxillomandibular fusion and very little oral cavity (Figure 2). These observations are consistent with TMJ ankyloses, a typical clinical feature in syngnathia patients.

FINAL DIAGNOSIS

Congenital maxillomandibular syngnathia.

TREATMENT

The purpose of the surgery was to separate the fused mandible and maxilla to open the mouth, which would solve the patient's feeding issues. The patient underwent a prophylactic tracheostomy to prevent obstruction of airway during surgery 7 d in advance. Then, we prepared for computer-assisted navigation. Three-dimensional CT data were saved in the Dicom (digital imaging and communications in medicine) format and were imported into Mimics 10.0 software (Materialise, Leuven, Belgium) and the iPlan software of the VectorVision2 navigation system (BrainLAB, Feldkirchen, Germany). The anatomical landmarks were measured and analyzed on the basis of three-dimensional images. We chose the line from preauricular to marginal mandibular as the incision site. Operation simulations were performed to affirm the position of osteotomy line and the level of mandibular opening and its fixed position. The patient underwent general anaesthesia and the skin was sterilized. A navigation bracket was installed to the patient's head first, and then face scanning by a laser scanner was performed for surface registration. The surgical instrument was registered at last. Registration accuracy (0.8 mm) was verified using the navigation pointer. The tip position and orientation of the probe were viewed continuously on screen (Figure 3). The oral space was exposed by retractors, the skin and subcutaneous tissue of incision were cut open, and the bilateral jaw lateral surface was exposed by blunt separation. It was easy to detect and isolate the mandible using the navigation system. Real-time position was verified by the navigation probe to avoid damaging important nerves, vessels, and dental germs. After the mandible was sawed off, silicone was fixed on the wound surface to prevent refusion of bone. Negative pressure drainage was put in the bilateral mandibles prior to suturing the incision. Perioperative bleeding was 100 mL. The patient was admitted to SICU after surgery.

OUTCOME AND FOLLOW-UP

Immediately following surgery, the patient had difficulty swallowing, so we used a nasogastric tube for feeding. The patient was discharged from the hospital one week later and was instructed to perform mouth opening and swallowing exercises. Follow-up three-dimensional CT scans of the face confirmed separation and bony healing. After six months, there was no recurrence. After eight months, the patient was 91 cm in height, weighed 11 kg, and could pronounce several single words; thus, we concluded that the surgery was successful.

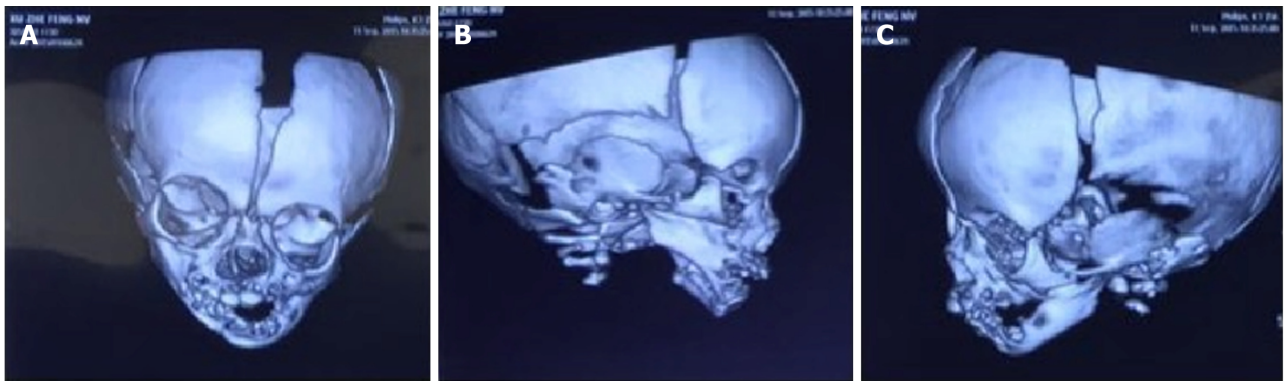

Figure 2 Three-dimensional computed tomography images demonstrating bony fusion of bilateral maxillaries to the mandibles. A: Frontal view; B: Right lateral view; C: Left lateral view.

DISCUSSION

Syngnathia is a rare human congenital condition. It involves connection between soft tissues or fusion between bony tissues and varies in severity from single mucosal bands (synechiae) to complete bone fusion (synotosis)[2]. Syngnathia is often accompanied by additional congenital defects, such as microglossia, micrognathia, and TMJ abnormalities. There are approximately 60 cases of congenital bony syngnathia reported in the literature[3], which reveal a high degree of variability in the location and extent of jaw fusion, and indicate that bony syngnathia may be isolated or syndromic. It is estimated that only 18% of cases are associated with known syndromes, such as aglossia-adactylia syndrome or hemifacial microsomia[4]. In the reported cases, women commonly display an isolated form of syngnathia, whereas men display a more complex pattern of disease. Syngnathia is usually detected immediately after birth because the baby is not able to open the mouth to feed normally. Notably, patients presenting with complete bilateral synostosis of the upper and lower jaw represent the least common and most severe form of syngnathia.

The etiology and pathogenesis of syngnathis remain unknown, and it is an extremely rare condition involving abnormal development of the splanchnocranium, which is the part of the skull that is derived from the branchial arches[2]. Various etiologies have been proposed, including environmental insults, medications such as meclizine, persistence of the buccopharyngeal membrane, and amniotic constriction bands[5,6]. Villanueva-García and colleagues have suggested the possibility of an autosomal recessive occurrence[7]. Moreover, a recent molecular genetics study showed that the *Foxc1* and *Fgf8* genes play a role in regulating mammalian jaw patterning and mutations in these genes may underlie the pathogenesis of syngnathia[4]. However, given that our patient had no other congenital abnormalities and there was no significant family history, a genetic or syndromic cause is unlikely.

Surgical division of the fusion must be carried out as soon as possible, which is necessary for normal feeding, removing airway obstruction, and allowing normal mandibular growth. Delay in surgical treatment increases the possibility of TMJ ankylosis, which leads to a lack of mandibular growth and facial deformities. The main goal of the surgery described in this care report was to release syngnathia and prevent recurrence. New management techniques, such as distraction, have been reported in congenital maxillomandicular[8]. Since most syngnathia patients are infants, major surgical challenges are intraoperative blood loss and damage to nerves and dental germs. Another challenge stems from the lack of comprehensive guidelines to ensure patient safety during this type of surgery.

In the present case, we applied computer-assisted navigation to instruct our surgical approach. Computer navigation has emerged as an essential technology for guiding and verifying operations, such as reconstruction of mandible or orbital bone, orthognathia, and many other of craniofacial surgeries[9,10]. We can understand the correlations among surgical devices, incisions, and peripheral anatomic sites in real-time easily *via* computer navigation, and also can check the distance between the operation positions to the position designed preoperatively. With the precise guidance of computer navigation, our operative time was minimized by at least one hour. Moreover, the patients' blood vessels, nerves, and tooth germs were all well protected and perioperative bleeding was minimized.

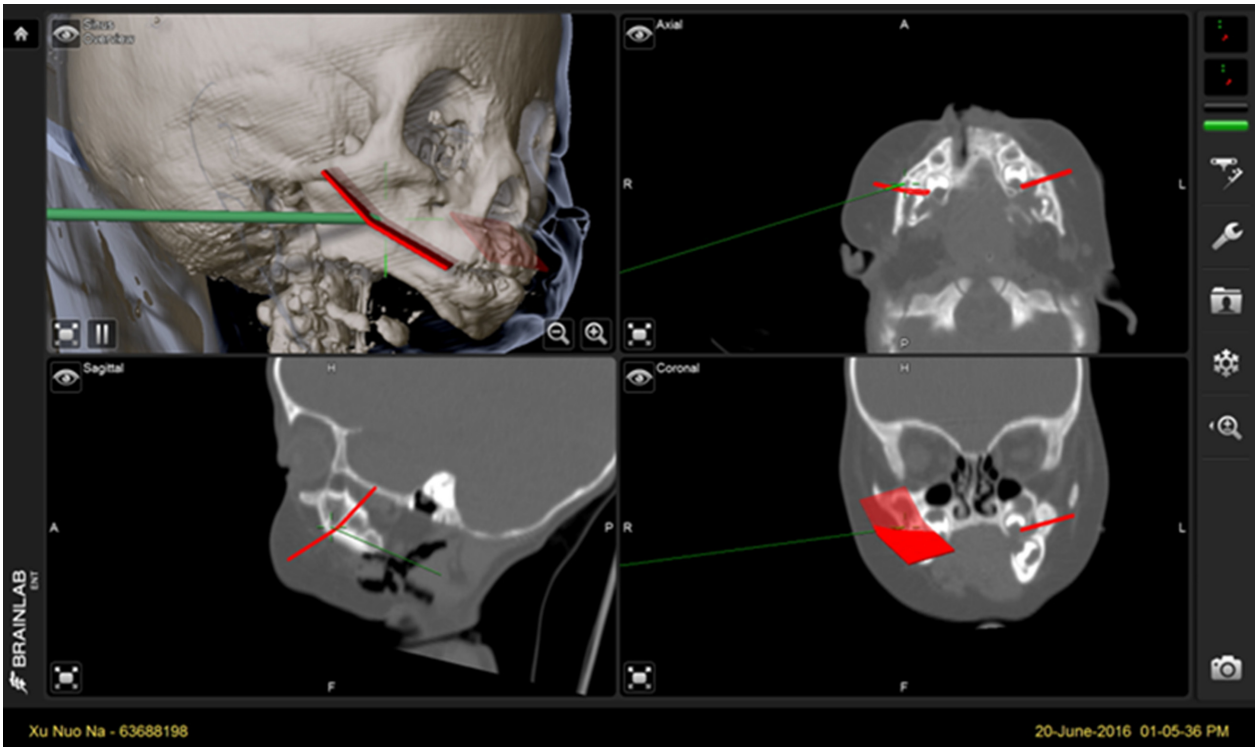

Figure 3 Screenshot of the navigation system. The pointer indicates arrival at the target site.

CONCLUSION

We have demonstrated a novel approach to treating complex zygomaticomandibular syngnathia. Distraction techniques, like the one used here, should prove useful in addressing other craniofacial malformations. To our knowledge, this is the only syngnathia case in the literature treated using distraction techniques. In the future, our approach could be optimized to manage and prevention recurrence in other syngnathia patients.

ACKNOWLEDGEMENTS

The authors would like to thank the research staff and clinical personnel of the Shanghai 9th People's Hospital for their outstanding performance and patient care.

REFERENCES

1 **Martín LP**, Pérez MM, García EG, Martín-Moro JG, González JI, García MB. Atypical case of congenital maxillomandibular fusion with duplication of the craniofacial midline. *Craniomaxillofac Trauma Reconstr* 2011; **4**: 113-120 [PMID: 22655122 DOI: 10.1055/s-0031-1279674]
2 **Broome M**, Vial Y, Jacquemont S, Sergi C, Kamnasaran D, Giannoni E. Complete Maxillo-Mandibular Syngnathia in a Newborn with Multiple Congenital Malformations. *Pediatr Neonatol* 2016; **57**: 65-68 [PMID: 23778189 DOI: 10.1016/j.pedneo.2013.04.009]
3 **Al-Mahdi AH**, Koppel DA, Al-Jumaily HA, Mohammed AA, Boyd D. Congenital Bilateral Zygomatico-Maxillo-Mandibular Fusion Associated With Gum Fusion. *J Craniofac Surg* 2016; **27**: e20-e23 [PMID: 26703053 DOI: 10.1097/SCS.0000000000002293]
4 **Inman KE**, Purcell P, Kume T, Trainor PA. Interaction between Foxc1 and Fgf8 during mammalian jaw patterning and in the pathogenesis of syngnathia. *PLoS Genet* 2013; **9**: e1003949 [PMID: 24385915 DOI: 10.1371/journal.pgen.1003949]
5 **Fallahi HR**, Naeini M, Mahmoudi M, Javaherforoosh F. Congenital zygomatico-maxillo-mandibular fusion: a brief case report and review of literature. *Int J Oral Maxillofac Surg* 2010; **39**: 930-933 [PMID: 20466517 DOI: 10.1016/j.ijom.2010.04.003]
6 **Turksen Z**, Ozakpinar HR, Tellioglu AT. A case of syngnathia, cleft palate and hypospadias: an isolated case or syndromic syngnathism? *J Craniomaxillofac Surg* 2012; **40**: 8-10 [PMID: 21501960 DOI: 10.1016/j.jcms.2011.02.004]
7 **Villanueva-García D**, Contreras-Masse G, Villa-Guillén M, Ramón-García G, Murguía-De Sierra T. Syngnathism in an infant born to consanguineous parents. *Am J Med Genet A* 2009; **149A**: 2303-2305 [PMID: 19725127 DOI: 10.1002/ajmg.a.32734]
8 **Konaş E**, Aliyev A, Tunçbilek G. Congenital maxillomandibular syngnathia: a new management

technique using distraction techniques. *J Craniofac Surg* 2015; **26**: e68-e70 [PMID: 25569423 DOI: 10.1097/SCS.0000000000001239]

9 **Rahimov CR**, Farzaliyev IM, Fathi HR, Davudov MM, Aliyev A, Hasanov E. The Application of Virtual Planning and Navigation Devices for Mandible Reconstruction and Immediate Dental Implantation. *Craniomaxillofac Trauma Reconstr* 2016; **9**: 125-133 [PMID: 27162568 DOI: 10.1055/s-0035-1566159]

10 **Varley I**, White L, Salvi SM, Lee N. Digital import of orbital implants to enhance navigation in reconstruction of the deep orbit. *Orbit* 2016; **35**: 20-23 [PMID: 26679992 DOI: 10.3109/01676830.2015.1099691]

P- Reviewer: Karatza AA; Rolle U

S- Editor: Dou Y **L- Editor:** Wang TQ **E- Editor:** Bian YN

World Journal of Clinical Cases

Submit a Manuscript: https://www.f6publishing.com

World J Clin Cases 2019 March 6; 7(5): 656-662

DOI: 10.12998/wjcc.v7.i5.656

ISSN 2307-8960 (online)

CASE REPORT

Concomitant paraganglioma and thyroid carcinoma: A case report

Bo Lin, Hong-Yu Yang, Hui-Jun Yang, Shi-Yue Shen

ORCID number: Bo Lin (0000-0001-8867-5755); Hong-Yu Yang (0000-0003-4547-9775); Hui-Jun Yang (0000-0001-7096-5535); Shi-Yue Shen (0000-0003-2367-0675).

Author contributions: Yang HY designed the study; Yang HY and Yang HJ contributed surgical treatment and follow-up data collection; Lin B and Shen SY analyzed the data; Lin B wrote the paper; Yang HY revised the manuscript; all authors read and approved the final manuscript.

Informed consent statement: The patient provided written informed consent.

Conflict-of-interest statement: The authors state that they have no conflicts of interest.

CARE Checklist (2016) statement: The manuscript was prepared and revised according to the CARE Checklist (2016).

Open-Access: This article is an open-access article which was selected by an in-house editor and fully peer-reviewed by external reviewers. It is distributed in accordance with the Creative Commons Attribution Non Commercial (CC BY-NC 4.0) license, which permits others to distribute, remix, adapt, build upon this work non-commercially, and license their derivative works on different terms, provided the original work is properly cited and the use is non-commercial. See: http://creativecommons.org/licenses/by-nc/4.0/

Manuscript source: Unsolicited manuscript

Bo Lin, Hong-Yu Yang, Hui-Jun Yang, Shi-Yue Shen, Department of Oral and Maxillofacial Surgery, Peking University Shenzhen Hospital, Shenzhen 518036, Guangdong Province, China

Corresponding author: Hong-Yu Yang, PhD, Professor, Surgeon, Department of Oral and Maxillofacial Surgery, Peking University Shenzhen Hospital, 1120 Lianhua Road, Futian District, Shenzhen 518036, Guangdong Province, China. yanghongyu0520@163.com
Telephone: +86-755-83923333
Fax: +86-755-83923333

Abstract

BACKGROUND

Paraganglioma/pheochromocytoma and medullary thyroid carcinoma can coexist and are often found in multiple endocrine neoplasia (MEN). However, very few cases highlight papillary thyroid carcinoma. We present herein a rare case of head and neck paraganglioma associated with papillary thyroid carcinoma.

CASE SUMMARY

A 51-year-old man presented to our department with right-sided neck swelling and hypertension. Physical examination showed neck masses with obvious pulsation. Concentrations of serum calcium, phosphorus, parathormone, thyroid stimulating hormone, free thyroxine, and calcitonin were within normal limits. Enhanced computed tomography revealed an irregular solid nodule, located in the carotid artery bifurcation. A low-density nodule of the thyroid isthmus with a spot-like dense shadow was also detected. The diagnosis of carotid body tumor was raised and an ultrasound-guided fine needle aspiration biopsy of the thyroid nodule revealed papillary thyroid carcinoma. The patient underwent surgery for lesion excision, total thyroidectomy, and neck dissection, and the pathology was reported as paraganglioma and papillary carcinoma. Genetic studies showed negative results for germline mutation of succinate dehydrogenase subunit D on 11q23. He was treated with ^{131}I after surgery and remained disease-free so far.

CONCLUSION

The presence of concomitant paraganglioma and thyroid papillary carcinoma could be either coincidental or a result of an unknown mutation.

Key words: Paraganglioma; Thyroid carcinoma; Multiple endocrine tumors; Case report

©The Author(s) 2019. Published by Baishideng Publishing Group Inc. All rights reserved.

Core tip: The presence of concomitant paraganglioma and thyroid papillary carcinoma is

Received: January 19, 2019
Peer-review started: January 22, 2019
First decision: January 26, 2019
Revised: February 1, 2019
Accepted: February 18, 2019
Article in press: February 18, 2019
Published online: March 6, 2019

extremely rare. We present a case of a head and neck paraganglioma associated with papillary thyroid carcinoma in a 51-year-old man. The major characteristics and imaging features of the lesion are discussed.

Citation: Lin B, Yang HY, Yang HJ, Shen SY. Concomitant paraganglioma and thyroid carcinoma: A case report. *World J Clin Cases* 2019; 7(5): 656-662
URL: https://www.wjgnet.com/2307-8960/full/v7/i5/656.htm
DOI: https://dx.doi.org/10.12998/wjcc.v7.i5.656

INTRODUCTION

Carotid body tumors represent approximately 65% of head and neck paragangliomas, followed by glomus jugulare and glomus tympanicum tumors[1].

A paraganglioma can partly or wholly be associated with other tumors such as kidney cancer, parathyroid adenoma, thyroid carcinoma, gastrointestinal stromal tumors, and astrocytoma[2].

Coexistence of paraganglioma/pheochromocytoma (PHEO) and medullary thyroid carcinoma (MTC) is strongly suggestive of multiple endocrine neoplasia (MEN), in such cases, succinate dehydrogenase subunit B (SDHB) and subunit D (SDHD) mutation was frequently reported as positive[3,4].

Herein, we report a patient with a combination of paraganglioma and papillary thyroid carcinoma. The tumors were surgically removed with minimal blood loss and temporary neurological loss. An analysis of RET porto-oncogene mutation yielded negative results. To our best knowledge, this unusual association of the two tumors represents a novel entity.

In addition, we summarize the clinical manifestations and the imaging and pathological features of the tumors.

CASE PRESENTATION

Chief complaints

A 51-year-old man was admitted to our department with a year-long history of swelling on the right-sided neck.

History of present illness

He also had a history of hypertension for three years, but without any medical treatment, and his blood pressure and heart rate at presentation were 150/94 mmHg and 83 beats/min, respectively.

History of past illness

He was diagnosed with diabetes three years ago and took metformin to control the blood sugar levels. He did not describe other constitutional symptoms such as episodes of diaphoresis, weight loss, or palpitations.

Personal and family history

The family history was unremarkable.

Physical examination upon admission

Obvious pulsation could be found on the right-sided neck masses. The masses were firm in texture and are not accompanied by pain. Cranial nerve examinations were intact, and the otolaryngology examination was negative.

Laboratory examinations

Concentrations of serum calcium, phosphorus, and parathormone were normal. Besides, radiotracer-labeled metaiodobenzyl-guanidine scintigraphy and serum and urine catecholamine and metanephrine levels were negative. Laboratory tests combined with abdominal computed tomography (CT) excluded the diagnosis of a PHEO. Serum thyroid stimulating hormone and free thyroxine, calcitonin, and carcinoembryonic antigen were within normal limits.

Imaging examinations

Enhanced CT revealed two irregular solid nodules, consisting of 3.5 × 3.6 × 4.0 cm soft tissue density located in the right carotid artery bifurcation with heterogeneous reinforcement. The mass surrounded both the internal and external carotid arteries; however, a clear boundary between the tumor and the artery could be found. At the same time, a low-density nodule of the thyroid isthmus measuring about 11 mm in diameter with a spot-like dense shadow could be seen. Carotid angiography demonstrated a blood-rich tumor at the carotid bifurcation that surrounded the internal and external carotid arteries. Figure 1 shows the paraganglioma and thyroid cancer, respectively (Figure 1 A and B), which were displayed simultaneously in the same section (Figure 1C).

Ultrasound showed a hypoechoic mass near the isthmus measuring about 18 × 15 × 12 mm in size. The boundary of the mass was unclear and calcification could be seen in the internal echo. An ultrasound-guided fine needle aspiration biopsy (FNAB) of the thyroid nodule revealed papillary thyroid carcinoma.

FINAL DIAGNOSIS

Based on the clinical characteristics and radiographic results, a combination of carotid body tumor and thyroid papillary carcinoma was raised.

TREATMENT

The patient underwent thyroidectomy, neck dissection, and surgery for removal of the right-sided lesion.

During surgery, the dissection of the encapsulated mass from the carotid bifurcation was performed. The internal carotid artery and external carotid artery remained intact. Total thyroidectomy removed a nodular left lobe and normal-appearing right lobe, isthmus, and pyramidal lobe, with right-side selective neck dissection (levels II-V).

Total thyroidectomy removed a nodular left lobe and normal-appearing right lobe, isthmus, and pyramidal lobe, with right-side selective neck dissection (levels II-V).

Upon microscopic analysis, the tumor at the carotid artery bifurcation appeared to have rich blood supply, formed by epithelial cells lying in a trabecular pattern and arranged in a "Zellballen" structure (Figure 2). In the thyroid tumor, the cells lining the papillary structures showed nuclear grooves and nuclear clearing, which are characteristic nuclear features of papillary thyroid carcinoma (Figure 3). The final histopathologic diagnosis was paraganglioma and thyroid papillary carcinoma. Immunohistochemical staining revealed positive staining for chromogranin and synaptophysin; the sustentacular cells stained positively for S100 protein.

Analysis of the *RET* proto-oncogene mutation, von Hippel Lindau (*VHL*) mutation, *SDHB* mutation, and *SDHD* mutation showed negative results.

OUTCOME AND FOLLOW-UP

Nifedipine was administered after the operation as the patient continued to be hypertensive. The patient experienced two weeks of hoarseness after operation without other neurological symptoms. He was treated with ^{131}I after surgery and so far disease-free. The patient is still being followed.

DISCUSSION

Paragangliomas are rare neuroendocrine neoplasms that originate from chromaffin cells of the adrenal medulla. CBT is a form of head and neck paraganglioma arising at the carotid bifurcation.

MEN is characterized by thyroid, adrenal medulla, and parathyroid neuroendocrine cell proliferation or tumor, and the clinical manifestations are MTC, PHEO, and primary parathyroid primary hyperparathyroidism[5,6]. A few cases were reported to exhibit combinations of PHEO, abdominal paraganglioma, and papillary thyroid carcinoma[7,8]. However, the coexistence of head and neck paraganglioma and papillary thyroid carcinoma was extremely rare and only reported in three cases (Table 1).

Clinically, thyroid masses, as well as symptoms of increased secretion of catecholamines such as paroxysmal hypertension, headache, palpitations, and

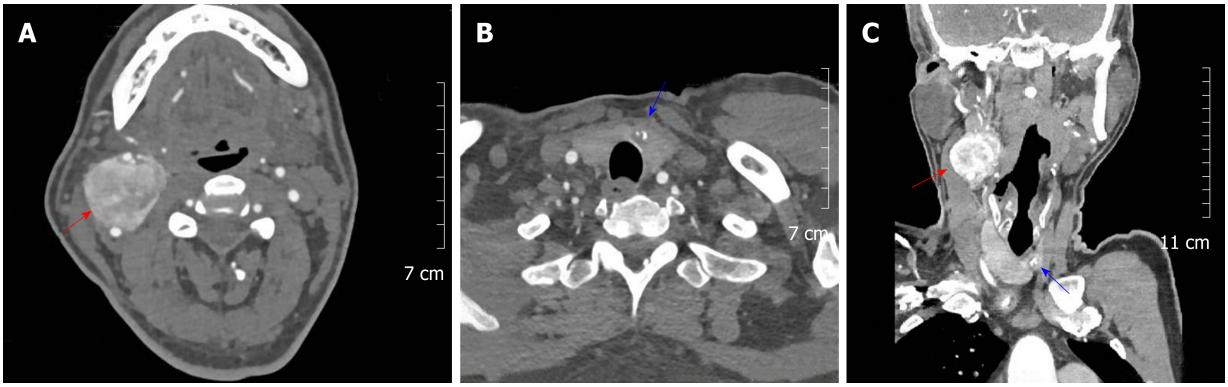

Figure 1 Preoperative images of the tumor. A: The paraganglioma located in the carotid artery bifurcation (red arrow); B: A low-density nodule of the thyroid isthmus with a high-density calcification can be seen (blue arrow); C: Enhanced computed tomography showing coexistence of paraganglioma (red arrow) and thyroid carcinoma (blue arrow).

sweating are most common. The high blood pressure in our patient raised the suspicion of MEN, but the normal serum and urine catecholamine and metanephrine levels and abdominal ultrasound eliminate PHEO.

When an endocrine gland tumor is discovered, the possibility of MEN should be considered and screened for. Serum calcitonin is a special indicator for the diagnosis of MTC, which can be more than 1000 pg/mL. CT, digital subtraction angiography (DSA), and MRI are helpful to locate the paraganglioma, while ultrasonography and FNAB are more reliable for detection of thyroid tumors.

CT angiography (CTA) is required for preoperative diagnosis and treatment strategies. It can significantly improve the recognition of tumors and identify the anatomical relationship between the tumor and important blood vessels. Correct diagnosis of CBT by careful clinical physical examination is not difficult, but the advantage of CTA is that it can help identify the "feeding artery" of the tumor and provide critical information for surgery.

Moreover, it was through CT that an asymptomatic thyroid tumor was found, which could further confirm the diagnosis.

RET was identified as a *MEN-2* susceptibility gene in 1993, and the gene carrier's penetrance rate is almost 100%[9]. In head and neck paraganglioma, a mutation of the D subunit of the *SDH* gene is identified in 50%-94% of cases, while a mutation of the B subunit is identified in 10%-20% of cases[10]. Neumann *et al*[18] suggested that whether thyroid malignancies are also components of SDHB or SDHD related disease awaits further confirmation. The genetic testing in the reported cases is reviewed in Table 1. The results of these studies indicate that the PTC-PGL/PHEO seems to have a heterogeneous genetic background. However, the genetic testing of our cases is not the same as previous studies. Whether this association is coincidental or has a genetic underlying relationship remains identification.

Onset involves multiple organs, and the treatment emphasizes multidisciplinary cooperation. Different lesions are mainly treated by related specialists, but it is necessary to avoid isolated treatment of a single subject. Removal of the paraganglioma and papillary cancer was the optimal treatment in this case, but it was necessary to exclude PHEO, as otherwise, other procedures could have induced hypertensive crisis. However, paraganglioma resection at the carotid bifurcation remains a challenge for surgeons because of its rich blood supply.

To our best understanding and knowledge, no known syndrome or conceivable interrelationships among the tumors explained this combination presentation. This case highlights that the presence of concomitant paraganglioma and thyroid papillary carcinoma could be either coincidental or a result of an underlying unknown mutation.

ACKNOWLEDGEMENT

The authors thank Ms. YJ Huang for her support of the study.

Table 1 Literature review

Author (yr)	Topography	Diagnosis	Genetic testing
Rasquin *et al*[11], 2018	Adrenal	PTC and PHEO	*EGLN1, FH, KIF1B, MEN1, NF1, RET, SDHAF2, SDHC, SDHD, TMEM127, VHL*, and *SDHA*: (-)
Bugalho, *et al*[7], 2015	Carotid body	PTC and PGL/PHEO	*VHL, SDHB, SDHC, SDHD, SDHAF2, TMEM127, MAX, PTEN*: (-)
	Adrenal	PTC and PGL/PHEO	*SDHB* (+)
	Adrenal	PTC and PGL/PHEO	*VHL, SDHB, SDHC, SDHD, SDHAF2, TMEM127, MAX, PTEN*: (-)
	Adrenal	PTC and PGL/PHEO	*SDHB* (+)
Huguet *et al*[12], 2013	Adrenal	PTC and PGLs	*SDHD* (+)
Papathomas *et al*[13], 2013	Carotid body	PTC and PGL and PHEO	*SDHD* (+)
Sisson *et al*[8], 2012	Adrenal	PTC and PHEO and PA	Not performed
Nasser *et al*[14], 2009	Adrenal	PTC and PHEO	*RET*: (-)
Zbuk *et al*[15], 2007	Carotid body	PTC and PGLs	*PTEN* (+), *SDHC* (+)
Yang *et al*[16], 2007	Adrenal	PTC and PHEO and PGL	*RET, VHL, SDHB, SDHD*: (-)
Hashiba *et al*[17], 2006	Adrenal	PTC and PHEO	Not performed
Neumann *et al*[18], 2004	Adrenal	PTC and PGL	*SDHB* (+)
	Adrenal	PTC and PGL	*SDHD* (+)

PTC: Papillary thyroid carcinoma; PHEO: Pheochromocytoma; PGL: Paraganglioma; PA: Pituitary adenoma; SDHD: Succinate dehydrogenase subunit D; SDHB: Succinate dehydrogenase subunit B; VHL: Von Hippel-Lindau mutation.

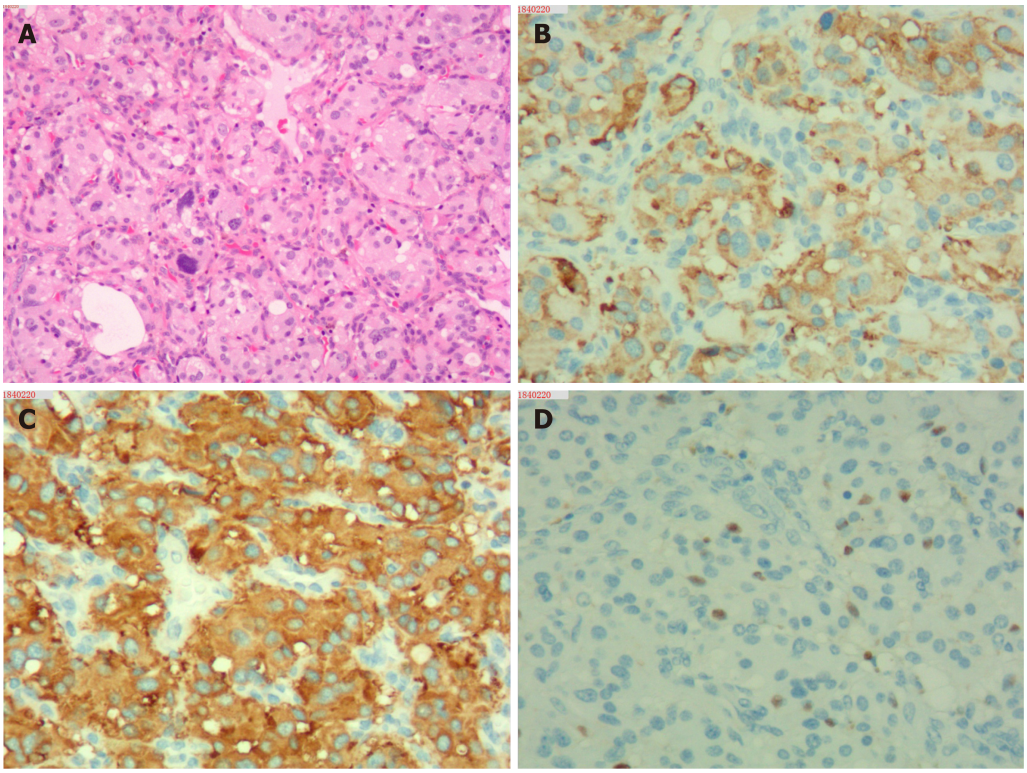

Figure 2 Microscopic features of the paraganglioma. A: Hematoxylin-Eosin (HE) staining (100 ×) showing well-defined solid nests of tumor cells, rounded by a fibrovascular tissue; B-C: Immunohistochemical staining of the tumor showing that the chief cells are intensively positive for chromogranin (B) and synaptophysin (C); D: Sustentacular cells are positive for S-100 protein.

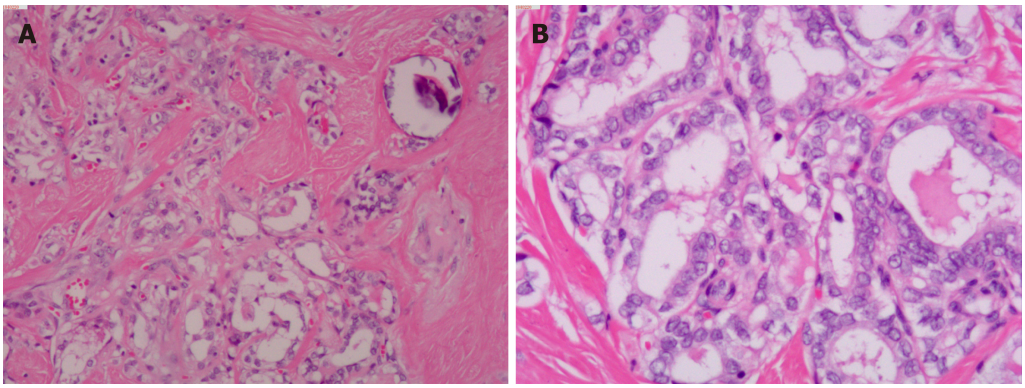

Figure 3 Microscopic features of the papillary thyroid carcinoma. A: Hematoxylin-Eosin (HE) staining (40 ×) showing that the papillae in papillary thyroid carcinoma are composed of cuboidal cells; B: HE staining (100 ×) showing nuclear changes including nuclear clearing and overlapping nuclei.

REFERENCES

1 **Lee JH**, Barich F, Karnell LH, Robinson RA, Zhen WK, Gantz BJ, Hoffman HT; American College of Surgeons Commission on Cancer; American Cancer Society. National Cancer Data Base report on malignant paragangliomas of the head and neck. *Cancer* 2002; **94**: 730-737 [PMID: 11857306 DOI: 10.1002/cncr.10252]

2 **Brandi ML**, Gagel RF, Angeli A, Bilezikian JP, Beck-Peccoz P, Bordi C, Conte-Devolx B, Falchetti A, Gheri RG, Libroia A, Lips CJ, Lombardi G, Mannelli M, Pacini F, Ponder BA, Raue F, Skogseid B, Tamburrano G, Thakker RV, Thompson NW, Tomassetti P, Tonelli F, Wells SA, Marx SJ. Guidelines for diagnosis and therapy of MEN type 1 and type 2. *J Clin Endocrinol Metab* 2001; **86**: 5658-5671 [PMID: 11739416 DOI: 10.1210/jcem.86.12.8070]

3 **Chandrasekharappa SC**, Guru SC, Manickam P, Olufemi SE, Collins FS, Emmert-Buck MR, Debelenko LV, Zhuang Z, Lubensky IA, Liotta LA, Crabtree JS, Wang Y, Roe BA, Weisemann J, Boguski MS, Agarwal SK, Kester MB, Kim YS, Heppner C, Dong Q, Spiegel AM, Burns AL, Marx SJ. Positional cloning of the gene for multiple endocrine neoplasia-type 1. *Science* 1997; **276**: 404-407 [PMID: 9103196 DOI: 10.1126/science.276.5311.404]

4 **Decker RA**, Peacock ML, Watson P. Hirschsprung disease in MEN 2A: increased spectrum of RET exon 10 genotypes and strong genotype-phenotype correlation. *Hum Mol Genet* 1998; **7**: 129-134 [PMID: 9384613 DOI: 10.1093/hmg/7.1.129]

5 **Skogseid B**, Rastad J, Gobl A, Larsson C, Backlin K, Juhlin C, Akerström G, Oberg K. Adrenal lesion in multiple endocrine neoplasia type 1. *Surgery* 1995; **118**: 1077-1082 [PMID: 7491526 DOI: 10.1016/S0039-6060(05)80117-5]

6 **Shepherd JJ**. The natural history of multiple endocrine neoplasia type 1. Highly uncommon or highly unrecognized? *Arch Surg* 1991; **126**: 935-952 [PMID: 1677802 DOI: 10.1001/archsurg.1991.01410320017001]

7 **Bugalho MJ**, Silva AL, Domingues R. Coexistence of paraganglioma/pheochromocytoma and papillary thyroid carcinoma: a four-case series analysis. *Fam Cancer* 2015; **14**: 603-607 [PMID: 26071763 DOI: 10.1007/s10689-015-9818-8]

8 **Sisson JC**, Giordano TJ, Avram AM. Three endocrine neoplasms: an unusual combination of pheochromocytoma, pituitary adenoma, and papillary thyroid carcinoma. *Thyroid* 2012; **22**: 430-436 [PMID: 22385288 DOI: 10.1089/thy.2011.0345]

9 **Machens A**. Early malignant progression of hereditary medullary thyroid cancer. *N Engl J Med* 2004; **350**: 943 [PMID: 14985494 DOI: 10.1056/NEJM200402263500917]

10 **Astuti D**, Hart-Holden N, Latif F, Lalloo F, Black GC, Lim C, Moran A, Grossman AB, Hodgson SV, Freemont A, Ramsden R, Eng C, Evans DG, Maher ER. Genetic analysis of mitochondrial complex II subunits SDHD, SDHB and SDHC in paraganglioma and phaeochromocytoma susceptibility. *Clin Endocrinol (Oxf)* 2003; **59**: 728-733 [PMID: 14974914 DOI: 10.1046/j.1365-2265.2003.01914.x]

11 **Rasquin L**, Prater J, Mayrin J, Minimo C. Simultaneous Pheochromocytoma, Paraganglioma, and Papillary Thyroid Carcinoma without Known Mutation. *Case Rep Endocrinol* 2018; **2018**: 6358485 [PMID: 30405919 DOI: 10.1155/2018/6358485]

12 **Huguet I**, Walker L, Karavitaki N, Byrne J, Grossman AB. Dandy-Walker malformation, papillary thyroid carcinoma, and SDHD-associated paraganglioma syndrome. *J Clin Endocrinol Metab* 2013; **98**: 4595-4596 [PMID: 24152682 DOI: 10.1210/jc.2013-3015]

13 **Papathomas TG**, Gaal J, Corssmit EP, Oudijk L, Korpershoek E, Heimdal K, Bayley JP, Morreau H, van Dooren M, Papaspyrou K, Schreiner T, Hansen T, Andresen PA, Restuccia DF, van Kessel I, van Leenders GJ, Kros JM, Looijenga LH, Hofland LJ, Mann W, van Nederveen FH, Mete O, Asa SL, de Krijger RR, Dinjens WN. Non-pheochromocytoma (PCC)/paraganglioma (PGL) tumors in patients with succinate dehydrogenase-related PCC-PGL syndromes: a clinicopathological and molecular analysis. *Eur J Endocrinol* 2013; **170**: 1-12 [PMID: 24096523 DOI: 10.1530/EJE-13-0623]

14 **Nasser T**, Qari F. Pheochromocytoma, papillary thyroid carcinoma. *Saudi Med J* 2009; **30**: 1087-1090 [PMID: 19668893]

15 **Zbuk KM**, Patocs A, Shealy A, Sylvester H, Miesfeldt S, Eng C. Germline mutations in PTEN and SDHC in a woman with epithelial thyroid cancer and carotid paraganglioma. *Nat Clin Pract Oncol* 2007; **4**: 608-612 [PMID: 17898811 DOI: 10.1038/ncponc0935]

16 **Yang JH**, Bae SJ, Park S, Park HK, Jung HS, Chung JH, Min YK, Lee MS, Kim KW, Lee MK. Bilateral pheochromocytoma associated with paraganglioma and papillary thyroid carcinoma: report of an unusual case. *Endocr J* 2007; **54**: 227-231 [PMID: 17264467 DOI: 10.1507/endocrj.K06-068]

17 **Hashiba T**, Maruno M, Fujimoto Y, Suzuki T, Wada K, Isaka T, Izumoto S, Yoshimine T. Skull metastasis from papillary thyroid carcinoma accompanied by neurofibromatosis type 1 and pheochromocytoma: report of a case. *Brain Tumor Pathol* 2006; **23**: 97-100 [PMID: 18095126 DOI: 10.1007/s10014-006-0203-z]

18 **Neumann HP**, Pawlu C, Peczkowska M, Bausch B, McWhinney SR, Muresan M, Buchta M, Franke G, Klisch J, Bley TA, Hoegerle S, Boedeker CC, Opocher G, Schipper J, Januszewicz A, Eng C; European-American Paraganglioma Study Group. Distinct clinical features of paraganglioma syndromes associated with SDHB and SDHD gene mutations. *JAMA* 2004; **292**: 943-951 [PMID: 15328326 DOI: 10.1001/jama.292.8.943]

P- Reviewer: Mogulkoc R, Coskun A
S- Editor: Dou Y **L- Editor:** Wang TQ **E- Editor:** Bian YN

World Journal of Clinical Cases

Submit a Manuscript: https://www.f6publishing.com

World J Clin Cases 2019 March 6; 7(5): 663-667

DOI: 10.12998/wjcc.v7.i5.663

ISSN 2307-8960 (online)

CASE REPORT

Rare empty sella syndrome found after postoperative hypotension and respiratory failure: A case report

Peng Guo, Zeng-Jun Xu, Chang-En Hu, Yue-Ying Zheng, Dan-Feng Xu

ORCID number: Peng Guo (0000-0003-2449-5629); Zeng-Jun Xu (0000-0002-5500-3271); Chang-En Hu (0000-0003-4548-6641); Yue-Ying Zheng (0000-0001-9610-7133); Dan-Feng Xu (0000-0002-4764-5282).

Author contributions: Xu DF and Zheng YY designed the report; Xu ZJ and Hu CE collected the patient's clinical data; Guo P wrote the paper.

Supported by the Zhejiang Clinical Funding, No. 2016YC-A86.

Informed consent statement: The patient gave informed consent. Consent was obtained from the patient for publication of this report and any accompanying images.

Conflict-of-interest statement: The authors declare that they have no conflicts of interest.

CARE Checklist (2016) statement: The guidelines of the CARE Checklist (2016) have been adopted.

Open-Access: This article is an open-access article which was selected by an in-house editor and fully peer-reviewed by external reviewers. It is distributed in accordance with the Creative Commons Attribution Non Commercial (CC BY-NC 4.0) license, which permits others to distribute, remix, adapt, build upon this work non-commercially, and license their derivative works on different terms, provided the original work is properly cited and the use is non-commercial. See: http://creativecommons.org/licen

Peng Guo, Zeng-Jun Xu, Chang-En Hu, Dan-Feng Xu, Department of Anesthesiology, Shaoxing Central Hospital, Shaoxing 312000, Zhejiang Province, China

Yue-Ying Zheng, Department of Anesthesiology, the First Affiliated Hospital of Zhejiang University, Hangzhou310000, Zhejiang Province, China

Corresponding author: Dan-Feng Xu, MD, Doctor, Department of Anesthesiology, Shaoxing Central Hospital, 1 Huayu Road, Keqiao, Shaoxing 312000, Zhejiang Province, China.
xdf@zju.edu.cn
Telephone: +86-575-85580896

Abstract

BACKGROUND

Empty sella syndrome is a condition in which the pituitary gland shrinks or flattens. Patients with empty sella syndrome often present with headache, hypertension, obesity, visual disturbances, cerebrospinal fluid (CSF) rhinorrhoea, or endocrine dysfunction. Herein, we report a rare case of empty sella syndrome discovered after the patient experienced postoperative hypotension and respiratory failure.

CASE SUMMARY

A 60-year-old man was admitted for further workup of left shoulder pain. He was assessed by the orthopaedics team and booked for internal fixation of the left clavicle. General anaesthesia with a nerve block was administered. His blood pressure continued to decrease post-operation. Endocrine tests were performed, with the results supporting a diagnosis of hypopituitarism with hypocortisolism and hypothyroidism. Brain magnetic resonance imaging demonstrated that the sella was enlarged and filled with CSF, confirming a diagnosis of empty sella syndrome. The patient was started on endocrine replacement therapy. The patient regained consciousness and spontaneous breath finally.

CONCLUSION

This case highlights the importance of considering pituitary hormone insufficiency in the context of respiratory and hemodynamic failure during the perioperative period.

Key words: Empty sella; Hypotension; Respiratory failure; Case report

©The Author(s) 2019. Published by Baishideng Publishing Group Inc. All rights reserved.

ses/by-nc/4.0/

Manuscript source: Unsolicited manuscript

Received: January 9, 2019
Peer-review started: January 10, 2019
First decision: January 19, 2019
Revised: February 4, 2019
Accepted: February 18, 2019
Article in press: February 18, 2019
Published online: March 6, 2019

Core tip: A 60-year-old man was admitted for internal fixation of the left clavicle. General anaesthesia with a nerve block was administered. His blood pressure continued to decrease post-operation. Endocrine tests were performed, with the results supporting a diagnosis of hypopituitarism. Brain magnetic resonance imaging demonstrated that the sella was enlarged and filled with cerebrospinal fluid, confirming a diagnosis of empty sella syndrome. The patient was started on endocrine replacement therapy. The patient regained consciousness and spontaneous breath finally. This case highlights the importance of considering pituitary hormone insufficiency in the context of respiratory and hemodynamic failure during the perioperative period.

Citation: Guo P, Xu ZJ, Hu CE, Zheng YY, Xu DF. Rare empty sella syndrome found after postoperative hypotension and respiratory failure: A case report. *World J Clin Cases* 2019; 7(5): 663-667
URL: https://www.wjgnet.com/2307-8960/full/v7/i5/663.htm
DOI: https://dx.doi.org/10.12998/wjcc.v7.i5.663

INTRODUCTION

The pituitary gland is a pea-sized gland located within the sella turcica[1,2]. Empty sella syndrome is a condition in which the pituitary gland shrinks or flattens, and thus the pituitary cannot be visualised by magnetic resonance imaging (MRI). In this condition, the sella turcica also becomes partially or completely filled with cerebrospinal fluid (CSF). Primary empty sella syndrome occurs when there is a defect in the diaphragma sellae accompanied by an increase in CSF pressure[3]. Secondary empty sella syndrome occurs when the pituitary gland has been damaged or injured; common causes include malignancy, trans-sphenoidal surgery, radiotherapy, and medications[4]. Patients with empty sella syndrome often suffer from headaches, hypertension, obesity, visual disturbances, CSF rhinorrhoea, or endocrine dysfunction. Postoperatively, our patient presented with hypotension and respiratory failure, and was subsequently diagnosed with empty sella syndrome.

CASE PRESENTATION

Chief complaints

Left shoulder pain and activity restriction for 3 h.

History of present illness

A 60-year-old man was admitted for further workup of left shoulder pain. X-ray demonstrated a left distal clavicle and shoulder blade fracture. He was assessed by the orthopaedics team and booked for internal fixation of the left clavicle. General anaesthesia with a nerve block was administered. Pre-operative vitals included a blood pressure (BP) of 120/63 mmHg, heart rate (HR) of 65 bpm, and SpO_2 of 95% in room air. After induction, BP and HR decreased to 90/52 mmHg and 50 bpm, respectively. A 6 mg dose of ephedrine was given intravenously. A total of 24 mg ephedrine was given over the whole operation. No further muscle relaxants were required. The surgery was uneventful and lasted for 1 h. Total blood loss was 100 mL and a total of 1000 mL of crystalloid was given. After surgery, he was transferred to the post-anaesthesia care unit to continue machine ventilation. The patient began spontaneously breathing at 40 min postoperatively, at which point the laryngeal mask was removed and an oxygen mask provided. However, SpO_2 remained below 92% without the use of the oxygen mask. The patient was subsequently admitted to the orthopaedics ward. Vitals at that time were BP 115/76 mmHg, HR 72 bpm, SPO_2 99%, and temperature (T) 37.2°C.

Unfortunately, his BP continued to decrease over the next 6 hours, to 80/50 mmHg. The next morning, the patient appeared confused and was not cognisant to person, place, or time. Arterial blood gas indicated respiratory acidosis without any evidence of electrolyte imbalance. Due to increasing respiratory distress, emergent intubation was performed and the patient was transferred to the intensive care unit for machine-assisted ventilation and vasopressor medications. Over the next 2 d, there was minimal improvement in the patient's condition despite ongoing treatment.

Careful review of the patient's history, as provided by his family, revealed that over the last year, he began demonstrating signs of progressive indifference, lack of communication, and lethargy. Further physical examination revealed a diffuse loss of body hair and dry skin. This new information, combined with the current episode of hypotension and respiratory distress, strongly suggested a possible aetiology of hormonal dysfunction. As such, endocrine tests were performed, with the results supporting a diagnosis of hypopituitarism with hypocortisolism and hypothyroidism. Then, he underwent brain MRI.

History of past illness

He denied any other medical conditions.

Personal and family history

He worked as a manual labourer. He neither smokes nor drinks.

Physical examination upon admission

The left shoulder joint is tender, the snoring pain is positive, and the activity is limited.

Laboratory examinations

Haemoglobin concentration was 108 g/dL. The results of endocrine tests are listed in Table 1.

Imaging examinations

X-ray of the shoulder demonstrated a left distal clavicle. Brain computed tomography revealed a low density shadow in the saddle region of the brain. Brain MRI (Figure 1) demonstrated that the sella was enlarged and filled with CSF.

FINAL DIAGNOSIS

Empty sella syndrome.

TREATMENT

The patient was started on replacement therapy with once-daily intravenous hydrocortisone 100 mg. After 3 d, levothyroxine was added.

OUTCOME AND FOLLOW-UP

The patient's consciousness and breathing improved progressively and the endotracheal catheter was removed after 5 d of treatment. He continued oral medication after he was discharged and was followed regularly to the department of endocrinology.

DISCUSSION

The pituitary gland is composed of an anterior and posterior lobe. The anterior lobe secretes hormones that regulate target glands, including the gonads, thyroid, and adrenal cortex. These hormones serve to regulate growth, sex organ function, pregnancy and nursing, metabolism, and BP. When all or most of the pituitary gland is destroyed, hypopituitarism occurs and a series of characteristic symptoms will manifest depending on the specific hormone deficiency. Common causes of hypopituitarism in adults include pituitary tumours or surgery, cerebral trauma, radiation, or Sheehan syndrome caused by postpartum ischemia. Clinical outcomes vary with the type and degree of hormone deficiency, and with the rapidity of onset, age, and sex. Pituitary crisis occurs if the hypopituitarism is further exacerbated by fatigue, hunger, cold, anaesthetic sedation, trauma, surgery, or infection. The diagnosis and management of the condition are based on history, physical examination and, occasionally, laboratory findings.

In a study by Ghatnatti *et al*[5], hyperprolactinemia was found to be the most common endocrine abnormality. Thwin *et al*[6] reported a patient who initially developed meningeal irritation with long-term galactorrhoea. Based on elevated serum prolactin and MRI findings, the patient was subsequently diagnosed with

Table 1 Laboratory investigations

Analyte	Measured value	Normal value
Na^+	132 mmol/L	137-148 mmol/L
Ca^{2+}	2.17 mmol/L	2-2.52 mmol/L
TSH	2.4 μIU/mL	0.27-4.2 μIU/mL
FT4	0.24 ng/dL	0.93-1.7 ng/dL
FT3	0.93 pg/dL	2.0-4.4 pg/dL
Cortisol (8:00 am)	13.73 μg/L	52.7-224.5 μg/L
ACTH 9:00	10.5 ng/L	7.5-63.3 pg/L
ACTH 16:00	3.43 ng/L	< 46 ng/L
ACTH 24:00	< 1 ng/L	< 46 ng/L
Testosterone	0.03 ng/mL	2.8-8.0 ng/mL
Growth hormone	0.10	< 3.0

The results supporting a diagnosis of hypopituitarism with hypocortisolism and hypothyroidism. TSH: Thyroid stimulating hormone; FT3: Free triiodothyronine 3; FT4: Free triiodothyronine 4; ACTH: Adrenocorticotropic hormone.

empty sella syndrome. Taieb *et al*[7] described a 47-year-old woman with bilateral galactorrhoea and spaniomenorrhea since the age of 31 years. Investigation revealed an elevated serum prolactin level of 635 mIU/L and an empty sella turcica on MRI.

Aijazi *et al*[8] reported a 41-year man with a history of osteogenesis imperfecta, who presented with vomiting, decreased oral intake, and confusion. In treating his hyponatremia, the treatment team was prompted to look for other pituitary hormone deficiencies. Various hormonal defects were found, and the patient was subsequently diagnosed with primary empty sella syndrome. Yang *et al*[9] described a 69-year-old woman with hyponatremia, who presented with manic symptoms that resolved after plasma sodium was normalised.

Xu *et al*[10] reported a 41-year-old man with persistent epiphyses and severe osteoporosis. He initially presented with high levels of serum phosphorus and prolactin, and low levels of free triiodothyronine, free thyroxine, and testosterone. Imaging of the brain revealed an empty sella.

Dange *et al*[11] reported a 16-year-old girl with a history of stunted growth and primary amenorrhea, presenting with headache and vomiting. Endocrine testing showed reduced levels of growth hormone, luteinising hormone, and follicular stimulating hormone. MRI of the brain showed an empty sella.

The most common cause for postoperative respiratory and hemodynamic failure is the residual effect of anaesthesia[12]. Our patient was administered both general and regional anaesthesia. All anaesthetic types had a short duration of action, except the small dose of sufentanyl given at time of induction. Marked dysfunctions in SpO_2, BP, and consciousness emerged in the immediate postoperative period. After careful review of the patient's history and further physical examination, it was felt that the respiratory distress and impaired consciousness could be secondary to hormonal dysfunction. This hypothesis was supported by further endocrine testing and MRI, with a subsequent diagnosis of empty sella syndrome causing the hypopituitarism with typical hypocortisolism and hypothyroidism. Effective treatment was achieved through hormone replacement therapy.

CONCLUSION

We report a case of empty sella syndrome discovered in the workup of postoperative hypotension and respiratory failure. We believe that the patient's pituitary crisis was induced by surgery. This case highlights the importance of considering pituitary hormone insufficiency in the context of respiratory and hemodynamic failure during the perioperative period. We recommend that in the preoperative examination, a thyroid function test can be added. If there is any abnormality, the examination can be further improved to exclude related diseases.

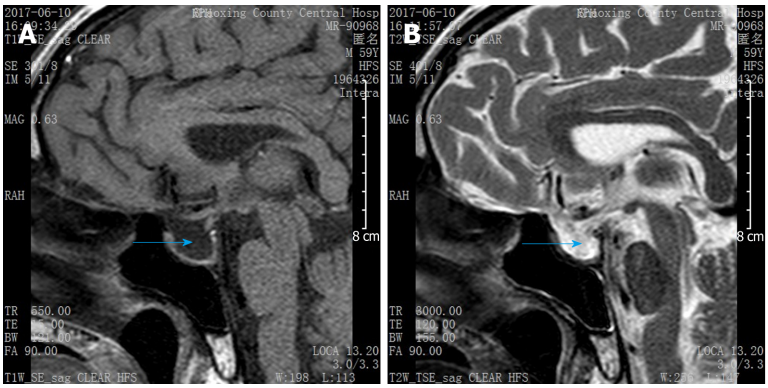

Figure 1 Saggital view of T1 and T2 weighted magnetic resonance images. A: Saggital view of T1 weighted magnetic resonance (MR) image; B: Saggital view of T2 weighted MR image. Arrow showing empty sella turcica filled with cerebrospinal fluid.

REFERENCES

1 **McLachlan MSF**, Williams ED, Doyle FH. Applied anatomy of the pituitary gland and fossa: a radiological and histopathological study based on 50 necropsies. *Br J Radiol* 1968; **41**: 782-788 [DOI: 10.1259/0007-1285-41-490-782]

2 **Bergland RM**, Ray BS, Torack RM. Anatomical variations in the pituitary gland and adjacent structures in 225 human autopsy cases. *J Neurosurg* 1968; **28**: 93-99 [PMID: 5638016 DOI: 10.3171/jns.1968.28.2.0093]

3 **Maira G**, Anile C, Mangiola A. Primary empty sella syndrome in a series of 142 patients. *J Neurosurg* 2005; **103**: 831-836 [PMID: 16304986 DOI: 10.3171/jns.2005.103.5.0831]

4 **Kim JH**, Ko JH, Kim HW, Ha HG, Jung CK. Analysis of empty sella secondary to the brain tumors. *J Korean Neurosurg Soc* 2009; **46**: 355-359 [PMID: 19893726 DOI: 10.3340/jkns.2009.46.4.355]

5 **Ghatnatti V**, Sarma D, Saikia U. Empty sella syndrome - beyond being an incidental finding. *Indian J Endocrinol Metab* 2012; **16**: S321-S323 [PMID: 23565413]

6 **Thwin M**, Brophy BP. Hyperprolactinaemia and the empty sella. *J Clin Neurosci* 2012; **19**: 605-606 [PMID: 22245276 DOI: 10.1016/j.jocn.2011.06.025]

7 **Taieb A**, Maha KN, El Abed YH, Beizig AM, Chadli MC, Ach K. Macroprolactinemia and Empty Sella Syndrome. *Pan Afr Med J* 2017; **27**: 278 [PMID: 29187947 DOI: 10.11604/pamj.2017.27.278.11361]

8 **Aijazi I**, Abdullah Al Shama FM, Adam Mukhtar SH. Primary Empty Sella Syndrome Presenting With Severe Hyponatremia And Minimal Salt Wasting. *J Ayub Med Coll Abbottabad* 2016; **28**: 605-608 [PMID: 28712246]

9 **Yang CH**, Lin YC, Chou PH, Chen HC, Chan CH. A Case Report of Late Onset Mania Caused by Hyponatremia in a Patient With Empty Sella Syndrome. *Medicine (Baltimore)* 2016; **95**: e2629 [PMID: 26871784 DOI: 10.1097/MD.0000000000002629]

10 **Xu P**, He H, Chen Y, Wang C, Zhu Y, Ye X. Osteoporotic fractures and persistent non-fusion of the hand epiphyses caused by empty sella syndrome in an adult: a case report. *J Int Med Res* 2013; **41**: 1768-1772 [PMID: 24029021 DOI: 10.1177/0300060513490609]

11 **Dange N**, Redhu R, Kawale J, Mahore A. Primary amenorrhea due to empty sella: an underestimated entity. *Turk Neurosurg* 2012; **22**: 499-501 [PMID: 22843475 DOI: 10.5137/1019-5149.JTN.3901-10.0]

12 **Frost EA**. Differential diagnosis of delayed awakening from general anesthesia: a review. *Middle East J Anaesthesiol* 2014; **22**: 537-548 [PMID: 25668997]

P- Reviewer: Caceres-Loriga FM, Omboni S
S- Editor: Ji FF **L- Editor:** Wang TQ **E- Editor:** Bian YN

World Journal of Clinical Cases

Submit a Manuscript: https://www.f6publishing.com

World J Clin Cases 2019 March 6; 7(5): 668-675

DOI: 10.12998/wjcc.v7.i5.668

ISSN 2307-8960 (online)

CASE REPORT

Use of tunnel endoscopy for diagnosis of obscure submucosal esophageal adenocarcinoma: A case report and review of the literature with emphasis on causes of esophageal stenosis

Song Liu, Nian Wang, Jian Yang, Jia-Yao Yang, Zhao-Hong Shi

ORCID number: Song Liu (0000-0001-8832-3100); Nian Wang (0000-0001-7790-1956); Jian Yang (0000-0003-2530-373X); Jia-Yao Yang (0000-0002-7528-7347); Zhao-Hong Shi (0000-0003-1615-1359).

Author contributions: Liu S and Wang N contributed to study conception and design, data collection, assembly, and analysis, manuscript writing, and literature search, and they contributed equally to this work; Yang J contributed to the collection and assembly of data; Yang JY contributed to data analysis and study conception; Shi ZH contributed to valuable suggestions; all authors reviewed and approved the manuscript.

Informed consent statement: Informed consent was obtained from the patient.

Conflict-of-interest statement: The authors declare that they have no conflicts of interest.

CARE Checklist (2016) statement: The manuscript was revised according to the CARE Checklist guidelines.

Open-Access: This article is an open-access article which was selected by an in-house editor and fully peer-reviewed by external reviewers. It is distributed in accordance with the Creative Commons Attribution Non Commercial (CC BY-NC 4.0) license, which permits others to distribute, remix, adapt, build upon this work non-commercially,

Song Liu, Nian Wang, Jian Yang, Jia-Yao Yang, Zhao-Hong Shi, Department of Gastroenterology, The First Hospital of Wuhan, Wuhan 430000, Hubei Province, China

Corresponding author: Zhao-Hong Shi, PhD, Chief Doctor, Department of Gastroenterology, The First Hospital of Wuhan, No. 215, Zhongshan Road, Qiaokou District, Wuhan 430000, Hubei Province, China. wuhandyyy@126.com
Telephone: +86-27-85332309

Abstract

BACKGROUND

The tunnel endoscopic technique is the treatment of choice for submucosal tumors. However, the use of tunnel endoscopy to diagnose adenocarcinoma of the esophagus originating from the submucosa has not been well studied.

CASE SUMMARY

A 74-year-old man who presented with dysphagia for half a year underwent a series of checks, such as gastroendoscopy, X-ray contrast examination of the upper digestive tract, endoscopic ultrasonography, high-resolution esophageal manometry, and positron emission computed tomography. It should be noted that the stenosis of the esophagus was too narrow for endoscopic ultrasound-guided fine needle aspiration. The cause remained undiagnosed. Eventually, the tunnel endoscopic technique was perform for the pathological examination in the submucosa and the final diagnosis was adenocarcinoma of the esophagus. The patient and family members chose expectant treatment due to the patient's age and the high costs of surgical treatment.

CONCLUSION

Tunnel endoscopy could be used to diagnose tumors. Moreover, we review the literature to provide guidance regarding the causes of esophagostenosis.

Key words: Esophageal stenosis; Adenocarcinoma of the esophagus; Tunnel endoscopic technique; Case report

©The Author(s) 2019. Published by Baishideng Publishing Group Inc. All rights reserved.

Core tip: Tunnel endoscopy is not only effective as a treatment for submucosal tumors, but also as a means of performing pathological examination for diagnosing tumors.

and license their derivative works on different terms, provided the original work is properly cited and the use is non-commercial. See: http://creativecommons.org/licenses/by-nc/4.0/

Manuscript source: Unsolicited manuscript

Received: November 12, 2018
Peer-review started: November 12, 2018
First decision: December 20, 2018
Revised: January 13, 2019
Accepted: January 30, 2019
Article in press: January 29, 2019
Published online: March 6, 2019

Moreover, we review the literature to provide guidance regarding the causes of esophageal stenosis.

Citation: Liu S, Wang N, Yang J, Yang JY, Shi ZH. Use of tunnel endoscopy for diagnosis of obscure submucosal esophageal adenocarcinoma: A case report and review of the literature with emphasis on causes of esophageal stenosis. *World J Clin Cases* 2019; 7(5): 668-675
URL: https://www.wjgnet.com/2307-8960/full/v7/i5/668.htm
DOI: https://dx.doi.org/10.12998/wjcc.v7.i5.668

INTRODUCTION

Tumors of the esophagus are a severe health problem worldwide with crypticity and high mortality. According to the different pathologic types, tumors of the esophagus have been divided into esophageal squamous cell carcinoma and esophageal adenocarcinoma[1]. Esophageal squamous cell carcinoma is the predominant histologic type while esophageal adenocarcinoma remains rare[2]. It is generally accepted that pathological examination is the "gold standard" for the diagnosis of esophageal tumors. Moreover, imaging modalities such as endoscopy, endoscopic ultrasonography (EUS), and computed tomography (CT) have been applied to measure the depth of the invasion of the esophageal wall, tumor size, the presence of invasion into adjacent organs, lymph node metastasis, and distant metastasis[3]. The high mortality rate has been attributed to the fact that half of patients have a locally-advanced form of the disease at diagnosis[4]. Therefore, early pathological diagnosis can effectively improve patient prognosis.

The tunnel endoscopic technique is an innovative and minimally-invasive endoscopic surgical procedure. The first submucosal tunnel endoscopic resection in the world was conducted in China, when it was used to remove submucosal tumors (SMTs) originating from the muscularis propria of the esophagus[5]. Nevertheless, biopsy in a submucosal tunnel has not been well studied. We report herein an unusual case involving diagnosis of esophageal stenosis caused by adenocarcinoma through the tunnel endoscopic technique, and review the causes of esophageal stenosis. The patient has signed an informed consent form and data had been anonymized and unidentified.

CASE PRESENTATION

Chief complaints

A 74-year-old male patient visited our hospital complaining of dysphagia which he had experienced for half a year with no clear trigger.

History of present illness

He vomited after eating, bringing up the contents of the stomach. There was no obvious chest pain, hematemesis, or weight loss. He was in good physical condition.

Personal and family history

There were no special circumstances in personal and family history.

Physical examination upon admission

On physical examination, he showed no evident positive characteristics.

Laboratory examinations

With regard to laboratory values, only the serum tumor marker CA199 (47.85 U/mL; normal reference range: < 39 U/mL), albumin (35.6 g/L; normal reference range: 40-50 g/L), and hemoglobin (124 g/L; normal reference range: 130-175 g/L) were moderately changed. Renal function, electrolytes, blood sugar, cholesterol, erythrocyte sedimentation rate, blood coagulation, humoral immune function, antiphospholipid antibody, anti-autoantibody, antineutrophil cytoplasmic antibody, urine, and conventional stool concentration were all within normal limits.

Imaging examinations

Color Doppler ultrasonography revealed chronic cholecystolithiasis. A chest CT scan

revealed thickening of the esophageal wall (Figure 1A and B). Barium meal X-ray showed that the lower esophagus presented the beak sign, suggesting achalasia (Figure 1C and D). Regarding condition, no ulceration, prominence lesions, or Barrett's esophagus manifestation was found by endoscopy (Figure 2A-D). In addition, routine gastroscopy was performed at a local hospital, and no tumor cell was detected by pathological examination at esophageal stenosis. EUS was performed to clarify the cause of the narrow esophageal structure. On EUS, esophageal cavity stenosis was visible at a distance of 37 cm from the incisors, along with obvious thickening of the intrinsic muscularis which reached 0.8 cm, and the first to third layer structure was not clear (Figure 2E and F). High-resolution esophageal manometry suggested lower esophageal outflow obstruction (Figure 3). Based on these findings, a tumor that originated from the tunica muscularis esophagi was highly suspected. Therefore, we recommended the patient to undergo a positron emission CT (PET-CT) examination. The PET-CT results from Wuhan Tongji Hospital indicated dilatation of the entire esophagus, stenosis of the esophagus and cardia junction, and increased local metabolism. However, it was difficult to obtain pathological evidence as the esophageal mucosa was only roughened, with no ulceration, erosion, or bleeding. We invited a general thoracic vascular surgeon and a gastrointestinal surgeon to assist in the diagnosis and treatment. Eventually, a multidisciplinary consultation recommended that tunnel endoscopy was performed for biopsy. Therefore, the tunnel endoscopic technique was chose for pathological examination. We created a submucosal tunnel, advanced towards the stenosis of the esophagus, and obtained muscularis tissues (Figure 4).

FINAL DIAGNOSIS

The final diagnosis was adenocarcinoma of the esophagus (Figure 5).

TREATMENT

Regretfully, the patient and family members chose expectant treatment due to the patient's age and the high costs of surgical treatment. The flow chart of disease diagnosis can be referred to Figure 6.

DISCUSSION

Adenocarcinoma of the esophagus is a malignant tumor arising from the submucosal tissue of the esophagus or from the glands of the cardia. However, because early disease is asymptomatic in most patients, timely diagnosis of esophageal adenocarcinoma (especially arising from the submucosa) is relatively difficult. Even when treated by radical surgery combined with radiotherapy and chemotherapy, the 5-year survival rate remains low[6,7]. Thus, early diagnosis and treatment of esophageal tumors are of great significance.

Esophageal strictures can result from a wide variety of benign and malignant conditions. Meanwhile, dysphagia is the most common symptom which urges patients to seek medical treatment. Benign esophageal strictures can occur following peptic strictures[8], eosinophilic esophagitis[9], achalasia[10], pill-injury esophageal strictures[11], caustic strictures[12], anastomotic strictures[13], Crohn's disease-associated esophageal stricture[14], IgG4-related esophagitis[15], radiation-induced esophageal strictures[16], esophageal intramural pseudodiverticulosis[17], or epidermolysis bullosa[18] (Table 1). It is generally known that a malignant esophageal stricture refers to esophageal cancer. Some esophageal strictures can be treated by drug therapy such as with proton pump inhibitors or steroids[9,11,15,17], while others can be refractory to most optical endoscopic therapies such as dilation[15,16,18], stent placement[13], or peroral endoscopic myotomy.

In the present case, the mucosa of the esophageal stenosis was only rough, with no obvious ulceration or erosion. It could well be that mucosal biopsies failed to achieve real results. Meanwhile, the stenosis of the esophagus was too narrow for a conventional endoscope to pass, l*et a*lone the large probe required for EUS. Therefore, it could not perform EUS guided fine needle aspiration for biopsy and we chose to use small probe endoscopic ultrasonography to clarify the cause of the esophageal stricture.

Subcutaneous emphysema, pneumothorax, and secondary infection are common complications of endoscopic resection[19-21]. As there was no serous layer of the

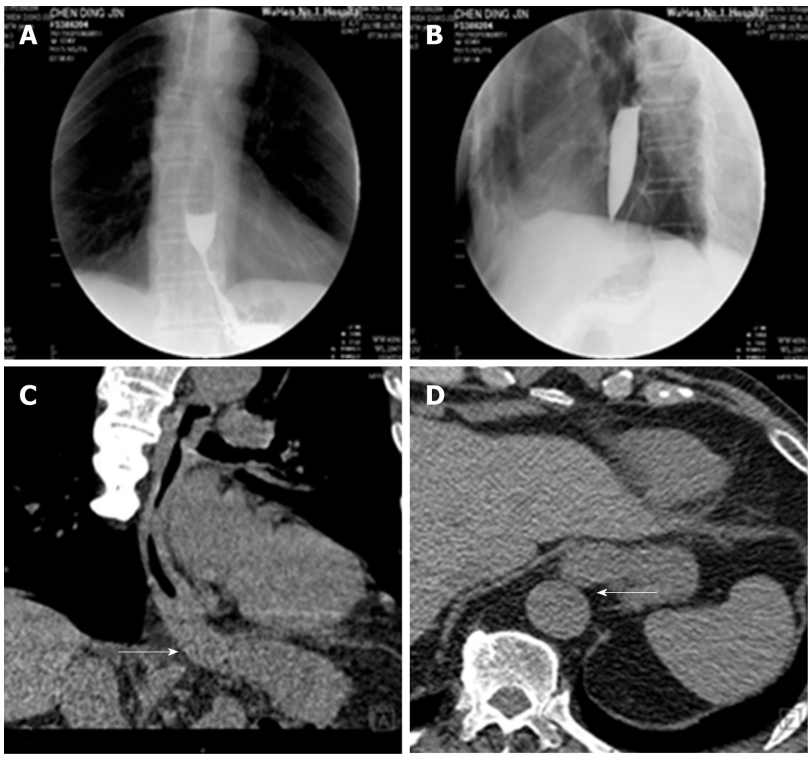

Figure 1 X-ray and thoracic computed tomography imaging of the patient. A and B: A barium meal X-ray revealed poor relaxation of the distal sphincter, dilatation of middle esophageal and stenosis of lower esophagus, weakened esophageal peristalsis, and ultimately stricture of the esophageal lumen with a beak-like appearance; C and D: Thoracic computed tomography imaging revealed thickening of the esophageal wall and antrum stricture (arrows), with a regular mucosal pattern.

esophagus, resection of the muscularis propria of the esophagus would be more prone to concurrent subcutaneous emphysema, pneumothorax, and secondary infection than the gastric muscularis propria. When the tunnel endoscopic technique is used to excise SMTs, the lesion mucosal surface remains intact and the mucosa of the tunnel opening is closed with a titanium clip, avoiding leakage of gas and digestive fluid into the chest and abdominal cavity, thus reducing the risk of secondary infection. Moreover, the tunnel endoscopic technique allows clear visualization of bleeding foci in the tunnel, reducing bleeding during the operation and postoperative delayed bleeding.

CONCLUSION

In conclusion, this was an unusual case of esophageal stenosis caused by adenocarcinoma and diagnosed by the tunnel endoscopic technique. As a method of diagnosis and treatment, the tunnel endoscopic technique would be a less complicated and less risky choice. We would like to emphasize the role of tunnel endoscopy in diagnostic treatment. Further, we analyzed the common causes of esophageal stenosis, hoping to provide some information which will help with clinical work.

Table 1 Analysis of causes of esophageal stenosis

Ref.	Years	Cause analysis of stenosis	Clinical manifestation
Ramage Jr *et al*[8]	2005	Peptic strictures	Acid reflux, dysphagia
Moonen *et al*[10]	2014	Achalasia	Dysphagia, regurgitation aspiration, chest pain, and weight loss
Muir *et al*[9]	2018	Eosinophilic esophagitis	Dysphagia
Yeoh *et al*[11]	2017	Pill-injury esophageal strictures	Regurgitation, retrosternal pain
He *et al*[12]	2018	Caustic strictures	Dysphagia, hematemesis
Siddiqui *et al*[13]	2012	Anastomotic strictures	Dysphagia, when a standard endoscope could not pass through the post-ESD scar
Nandy *et al*[14]	2017	Crohn's disease induced esophageal strictures	Dysphagia and odynophagia
Obiorah *et al*[15]	2017	IgG4-related esophagitis	Dysphagia
Agarwalla *et al*[16]	2015	Radiation-induced esophageal strictures	Dysphagia
Abbes *et al*[17]	2017	Esophageal intramural pseudodiverticulosis	Dysphagia and weight loss
Michalak *et al*[18]	2018	Epidermolysis bullosa	Dysphagia, skin blistering, joint contractures and missing nails

ESD: Endoscopic submucosal dissection.

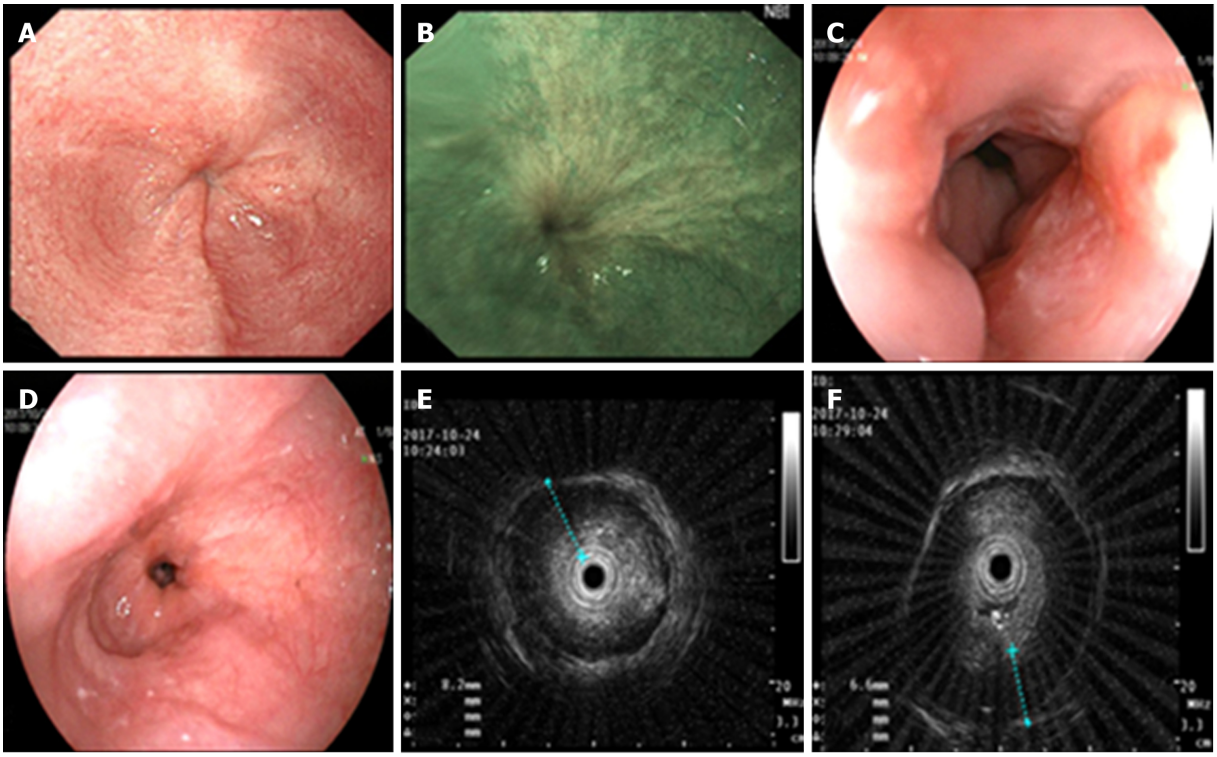

Figure 2 Upper gastrointestinal endoscopy and endoscopic ultrasonography of the patient. A-D: Upper gastrointestinal endoscopy revealed esophageal stenosis 37 cm from the incisors, along with mucosal surface asperities; E and F: Endoscopic ultrasonography revealed that the esophageal ring cavity was in the stenosis and the muscularis propria markedly thickened, together with an unclear structure of the first to third layers.

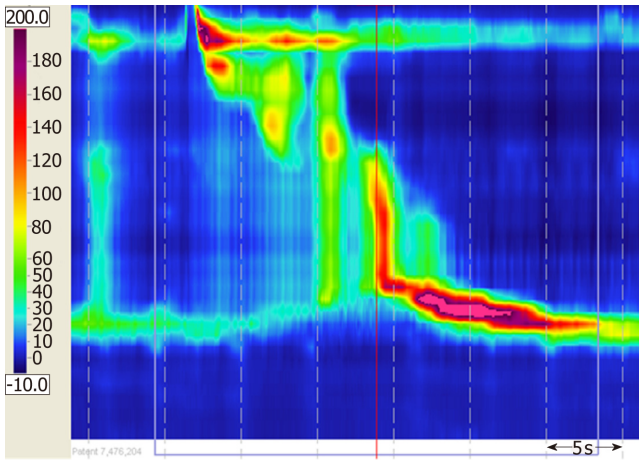

Figure 3 High-resolution esophageal manometry. The integrated relaxation pressure (4s integrated relaxation pressure; normal reference value: 15 mm Hg) was 26.6 mm Hg which suggested relaxation dysfunction of the lower esophageal sphincter.

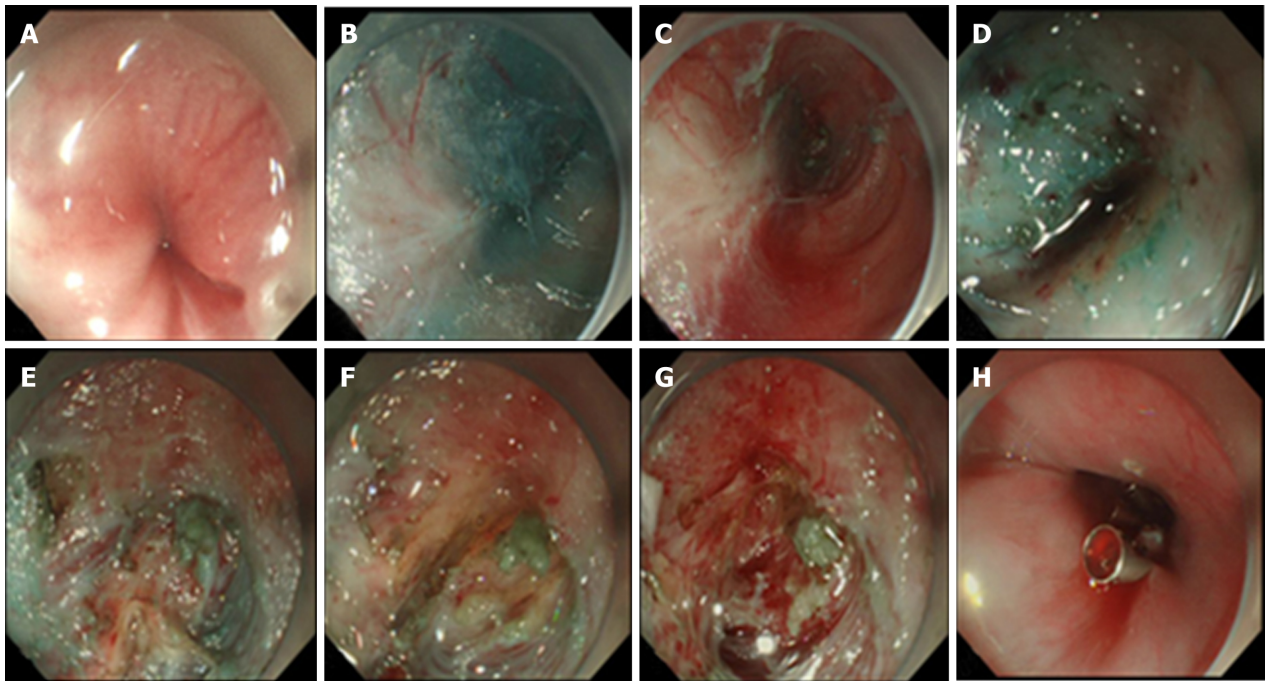

Figure 4 Case illustration of endoscopic biopsy through a tunnel. A: The narrow place in the lower esophagus (37 cm from the incisors); B: The submucosal tunnel was established; C: White fibrotic adhesions can be seen in the tunnel; D: The submucous structure was disorganized; E and F: It was difficult to distinguish yellow tissue and white tissue from the muscular layer in the tunnel; G: Tissue biopsy in the tunnel; H: The mucosal entry incision was sealed with several clips.

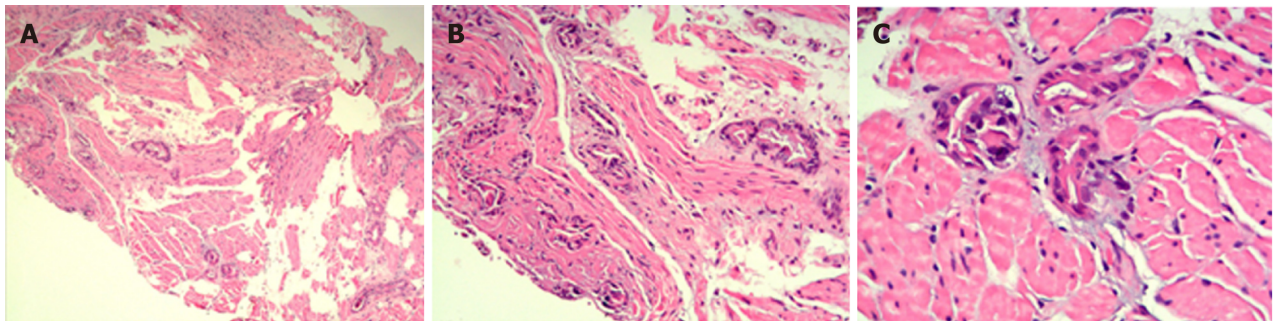

Figure 5 Microscopic images. In smooth muscle cells, abnormal glands, dense nuclei of glandular epithelial cells, irregular glandular cavities, and fibrous hyperplasia were seen (hematoxylin and eosin staining; A, B, and C, magnification × 40, × 100, and × 200, respectively).

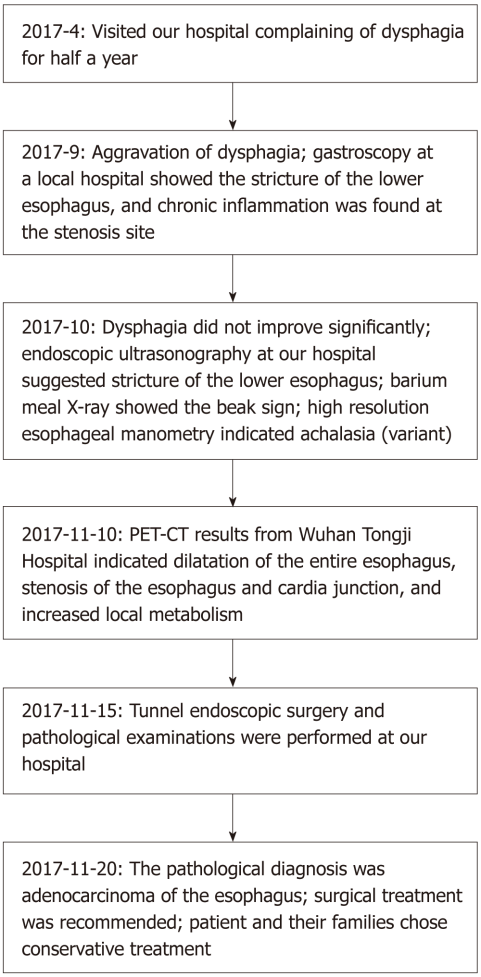

Figure 6 Information schedule. PET-CT: Positron emission computed tomography.

REFERENCES

1 **Rustgi AK**, El-Serag HB. Esophageal carcinoma. *N Engl J Med* 2014; **371**: 2499-2509 [PMID: 25539106 DOI: 10.1056/NEJMra1314530]
2 **Shibata A**, Matsuda T, Ajiki W, Sobue T. Trend in incidence of adenocarcinoma of the esophagus in Japan, 1993-2001. *Jpn J Clin Oncol* 2008; **38**: 464-468 [PMID: 18664481 DOI: 10.1093/jjco/hyn064]
3 **Ajani JA**, D'Amico TA, Almhanna K, Bentrem DJ, Besh S, Chao J, Das P, Denlinger C, Fanta P, Fuchs CS, Gerdes H, Glasgow RE, Hayman JA, Hochwald S, Hofstetter WL, Ilson DH, Jaroszewski D, Jasperson K, Keswani RN, Kleinberg LR, Korn WM, Leong S, Lockhart AC, Mulcahy MF, Orringer MB, Posey JA, Poultsides GA, Sasson AR, Scott WJ, Strong VE, Varghese TK, Washington MK, Willett CG, Wright CD, Zelman D, McMillian N, Sundar H; National comprehensive cancer network. Esophageal and esophagogastric junction cancers, version 1.2015. *J Natl Compr Canc Netw* 2015; **13**: 194-227 [PMID: 25691612 DOI: 10.6004/jnccn.2015.0028]
4 **Enzinger PC**, Mayer RJ. Esophageal cancer. *N Engl J Med* 2003; **349**: 2241-2252 [PMID: 14657432 DOI: 10.1056/NEJMra035010]
5 **Xu MD**, Cai MY, Zhou PH, Qin XY, Zhong YS, Chen WF, Hu JW, Zhang YQ, Ma LL, Qin WZ, Yao LQ. Submucosal tunneling endoscopic resection: a new technique for treating upper GI submucosal tumors originating from the muscularis propria layer (with videos). *Gastrointest Endosc* 2012; **75**: 195-199 [PMID: 22056087 DOI: 10.1016/j.gie.2011.08.018]
6 **Fan YJ**, Song X, Li JL, Li XM, Liu B, Wang R, Fan ZM, Wang LD. Esophageal and gastric cardia cancers on 4238 Chinese patients residing in municipal and rural regions: a histopathological comparison during 24-year period. *World J Surg* 2008; **32**: 1980-1988 [PMID: 18566857 DOI: 10.1007/s00268-008-9674-x]
7 **Borghesi S**, Hawkins MA, Tait D. Oesophagectomy after definitive chemoradiation in patients with locally advanced oesophageal cancer. *Clin Oncol (R Coll Radiol)* 2008; **20**: 221-226 [PMID: 18248970 DOI: 10.1016/j.clon.2007.12.001]
8 **Ramage JI**, Rumalla A, Baron TH, Pochron NL, Zinsmeister AR, Murray JA, Norton ID, Diehl N, Romero Y. A prospective, randomized, double-blind, placebo-controlled trial of endoscopic steroid injection therapy for recalcitrant esophageal peptic strictures. *Am J Gastroenterol* 2005; **100**: 2419-2425 [PMID: 16279894 DOI: 10.1111/j.1572-0241.2005.00331.x]
9 **Muir AB**, Wang JX, Nakagawa H. Epithelial-stromal crosstalk and fibrosis in eosinophilic esophagitis. *J Gastroenterol* 2019; **54**: 10-18 [PMID: 30101408 DOI: 10.1007/s00535-018-1498-3]
10 **Moonen A**, Boeckxstaens G. Current diagnosis and management of achalasia. *J Clin Gastroenterol* 2014;

48: 484-490 [PMID: 24926623 DOI: 10.1097/MCG.0000000000000137]
11 **Yeoh SW**. Esophageal bezoar due to karaya gum granules used as a laxative. *Clin J Gastroenterol* 2017; **10**: 437-441 [PMID: 28730320 DOI: 10.1007/s12328-017-0764-x]
12 **He K**, Zhao L, Bu S, Liu L, Wang X, Wang M, Fan Z. Endoscopic mucosal autograft for treating esophageal caustic strictures: preliminary human experience. *Endoscopy* 2018; **50**: 1017-1021 [PMID: 29890517 DOI: 10.1055/a-0622-8019]
13 **Siddiqui AA**, Sarkar A, Beltz S, Lewis J, Loren D, Kowalski T, Fang J, Hilden K, Adler DG. Placement of fully covered self-expandable metal stents in patients with locally advanced esophageal cancer before neoadjuvant therapy. *Gastrointest Endosc* 2012; **76**: 44-51 [PMID: 22726465 DOI: 10.1016/j.gie.2012.02.036]
14 **Nandy N**, Gavin M, Martin D, McCarthy D. Crohn's Disease: Hard to Swallow! *Dig Dis Sci* 2017; **62**: 2690-2693 [PMID: 28884257 DOI: 10.1007/s10620-017-4751-3]
15 **Obiorah I**, Hussain A, Palese C, Azumi N, Benjamin S, Ozdemirli M. IgG4-related disease involving the esophagus: a clinicopathological study. *Dis Esophagus* 2017; **30**: 1-7 [PMID: 28881885 DOI: 10.1093/dote/dox091]
16 **Agarwalla A**, Small AJ, Mendelson AH, Scott FI, Kochman ML. Risk of recurrent or refractory strictures and outcome of endoscopic dilation for radiation-induced esophageal strictures. *Surg Endosc* 2015; **29**: 1903-1912 [PMID: 25277484 DOI: 10.1007/s00464-014-3883-1]
17 **Abbes L**, Perrod G, Rahmi G, Cellier C. Esophageal intramural pseudodiverticulosis, a rare cause of stenosis. *Clin Res Hepatol Gastroenterol* 2017; **41**: 505-506 [PMID: 28506454 DOI: 10.1016/j.clinre.2017.04.001]
18 **Michalak A**, Cichoż-Lach H, Prozorow-Król B, Buk L, Dzida M. A rare case of skin blistering and esophageal stenosis in the course of epidermolysis bullosa - case report and literature review. *BMC Gastroenterol* 2018; **18**: 47 [PMID: 29653516 DOI: 10.1186/s12876-018-0771-5]
19 **Soh JS**, Kim JK, Lim H, Kang HS, Park JW, Kim SE, Moon SH, Kim JH, Park CK, Cho JW, Lim MS, Kim KO. Comparison of endoscopic submucosal dissection and surgical resection for treating gastric subepithelial tumours. *Scand J Gastroenterol* 2016; **51**: 633-638 [PMID: 26673033 DOI: 10.3109/00365521.2015.1124451]
20 **He G**, Wang J, Chen B, Xing X, Wang J, Chen J, He Y, Cui Y, Chen M. Feasibility of endoscopic submucosal dissection for upper gastrointestinal submucosal tumors treatment and value of endoscopic ultrasonography in pre-operation assess and post-operation follow-up: a prospective study of 224 cases in a single medical center. *Surg Endosc* 2016; **30**: 4206-4213 [PMID: 26823060 DOI: 10.1007/s00464-015-4729-1]
21 **Shen C**, Chen H, Yin Y, Chen J, Han L, Zhang B, Chen Z, Chen J. Endoscopic versus open resection for small gastric gastrointestinal stromal tumors: safety and outcomes. *Medicine (Baltimore)* 2015; **94**: e376 [PMID: 25569663 DOI: 10.1097/MD.0000000000000376]

P- Reviewer: Ananthakrishnan N, Lee JI, Lim SC
S- Editor: Wang JL **L- Editor:** Wang TQ **E- Editor:** Bian YN

World Journal of Clinical Cases

Submit a Manuscript: https://www.f6publishing.com

World J Clin Cases 2019 March 6; 7(5): 676-683

DOI: 10.12998/wjcc.v7.i5.676

ISSN 2307-8960 (online)

CASE REPORT

Intrauterine cystic adenomyosis: Report of two cases

Yan-Yan Fan, Yi-Nan Liu, Jia Li, Yan Fu

ORCID number: Yan-Yan Fan (0000-0002-0008-094X); Yi-Nan Liu (0000-0003-0881-9056); Jia Li (0000-0001-8456-3182); Yan Fu (0000-0003-1653-9249).

Author contributions: Fan YY, Liu YN, Li J, and Fu Y participated in the diagnosis and management of this case; Fan YY wrote the manuscript; Fu Y revised the manuscript; all authors read and approved the final manuscript.

Informed consent statement: All study participants, or their legal guardian, provided informed written consent prior to study enrollment.

Conflict-of-interest statement: The authors declare no conflict of interest.

CARE Checklist (2016) statement: The authors have read the CARE Checklist (2016), and the manuscript was prepared according to CARE checklist (2016).

Open-Access: This article is an open-access article which was selected by an in-house editor and fully peer-reviewed by external reviewers. It is distributed in accordance with the Creative Commons Attribution Non Commercial (CC BY-NC 4.0) license, which permits others to distribute, remix, adapt, build upon this work non-commercially, and license their derivative works on different terms, provided the original work is properly cited and the use is non-commercial. See: http://creativecommons.org/licenses/by-nc/4.0/

Manuscript source: Unsolicited manuscript

Yan-Yan Fan, Jia Li, Yan Fu, Department of Obstetrics and Gynecology, the First Hospital of Jilin University, Changchun 130021, Jilin Province, China

Yi-Nan Liu, Department of Otorhinolaryngology, Jilin Province FAW General Hospital, Changchun 130011, Jilin Province, China

Corresponding author: Yan Fu, MD, Chief Doctor, Department of Obstetrics and Gynecology, the First Hospital of Jilin University, No. 71, Xinmin Street, Changchun 130021, Jilin Province, China. yanfudoc@163.com
Telephone: +86-431-81875228
Fax: +86-431-81875228

Abstract

BACKGROUND

Cystic adenomyosis is a special type of adenomyosis. Its clinical manifestations lack specificity. Pelvic ultrasound and nuclear magnetic resonance imaging can help clarify the diagnosis. Because cystic uterine adenomyosis is rare in clinical work, it can be easily misdiagnosed or its diagnosis can be missed. Early surgical treatment and postoperative drug treatment can alleviate dysmenorrhea, menorrhagia, anemia, and other symptoms.

CASE SUMMARY

Two cases complained about abnormal vaginal bleeding and were diagnosed with intrauterine cystic adenomyosis by gynecological ultrasound and pathological examination. The clinical manifestations included dysmenorrhea, hypermenorrhea, and a history of cesarean section. Both cases underwent a surgery, and chocolate-like liquid was released from the cystic mass in the uterus and the manifestations were relieved.

CONCLUSION

Intrauterine cystic adenomyosis could be diagnosed by pathological examination and treated by hysterectomy or hystscopy to release the liquid inside.

Key words: Cystic adenomyosis; Adenomyosis; Junctional zone; Intrauterine; Case report

©The Author(s) 2019. Published by Baishideng Publishing Group Inc. All rights reserved.

Core tip: Because cystic uterine adenomyosis is rare in clinical work, it is easy to misdiagnose it or miss its diagnosis. We present two cases of intrauterine cystic adenomyosis that were recently treated at our department to explore its clinical features and treatment options so as to provide a reference for the early diagnosis and rational treatment of the disease.

Received: June 20, 2018
Peer-review started: June 20, 2018
First decision: July 8, 2018
Revised: February 6, 2019
Accepted: February 18, 2019
Article in press: February 18, 2019
Published online: March 6, 2019

Citation: Fan YY, Liu YN, Li J, Fu Y. Intrauterine cystic adenomyosis: Report of two cases. *World J Clin Cases* 2019; 7(5): 676-683
URL: https://www.wjgnet.com/2307-8960/full/v7/i5/676.htm
DOI: https://dx.doi.org/10.12998/wjcc.v7.i5.676

INTRODUCTION

Adenomyosis refers to a common gynecological disease wherein the endometrial gland or stroma appears in the myometrium and is accompanied by compensatory hypertrophy and proliferation of peripheral smooth muscle cells. The etiology and pathogenesis remain unclear. Currently, studies suggest that adenomyosis belongs to the junctional zone (JZ) lesions, also known as subintimal muscle, located between the endometrium and extrauterine myometrium, which shows cyclical variation owing to the effect of estrogen and progesterone. When the endometrial zona basalis is damaged, the endometrium directly invades the adjacent JZ, resulting in diffuse or limited thickening of JZ and adenomyosis formation. Imaging changes of JZ lesions detected by ultrasound and magnetic resonance imaging (MRI) have become reliable indicators for clinically diagnosing adenomyosis[1,2]. Cystic adenomyosis, also known as cystic adenomyoma or adenomyotic cyst, is a special type of adenomyosis, which is a cystic structure lining the endometrium and covered with the uterine smooth muscle, containing old blood cyst fluid. Most of the case reports of cystic adenomyosis revealed that the lesions are located in the uterine muscular wall or subserosa.

CASE PRESENTATION

This study was conducted in accordance with the Declaration of Helsinki and approved by the Ethics Committee of Jilin University. Written informed consent was obtained from all participants. We reviewed two cases of intrauterine cystic adenomyosis recently treated at our department and explored the clinical features and treatment options to provide a reference for the early diagnosis and rational treatment of the disease. The study was reviewed and approved by the First Hospital of Jilin University Institutional Review Board. All study participants, or their legal guardian, provided informed written consent prior to study enrollment.

Case 1: Chief complaints

A 36-year-old woman was admitted to the hospital owing to an increase in menstrual blood volume and abnormal echo in the uterine cavity for 7 months.

History of present illness

Since September 2016, the patient's menstrual period was extended to 6 d without any significant cause, and the menstrual blood volume was increased two-fold of the previous amount. She was admitted to a local county hospital. Doppler ultrasound examination revealed an abnormal intrauterine echo; thus, the physician suggested a dilation and curettage of the uterus, which she rejected. In October 2016, she found that the increase in menstrual blood volume was obviously aggravated, reaching about three times of the ordinary volume; then, she underwent Doppler ultrasound examination at the local hospital again. The results showed an intrauterine mildly strong echo (21 mm × 13 mm). The pathological results after curettage revealed the endometrium at the proliferative phase. After her menstrual period, she obtained a recheck of gynecological ultrasound, which showed the endometrial thickness to be 12 mm. Then, she was asked to be followed. Two months before hospitalization, her dysmenorrhea was progressively aggravated, and the bleeding was not changed, presenting as hypogastrium cramps at the menstrual period.

History of past illness

Her previous history included undergoing a cesarean section at a local hospital 15 years ago with three induced abortions thereafter.

Physical examination upon admission

She had smooth vagina and soft mucous membrane, normal and smooth cervix, and anterior uterine body with a size of about 7.0 cm × 6.0 cm × 6.0 cm, which was hard and tough with normal uterine mobility but without tenderness. No abnormality or tenderness was noted in the double appendage area; vaginal secretions were white

and less, without abnormal flavor.

Laboratory examinations

Routine blood test (October 25, 2016) showed a WBC count of 6.32 × 10^9/L, percentage of neutrophils of 73%, RBC count of 3.57 × 10^{12}/L, hemoglobin concentration of 125 g/L, and platelet count of 261 × 10^9/L. Gynecological ultrasound revealed an endometrial thickness of 20 mm and a mixed partially strong echo of 31 mm × 24 mm × 24 mm in the uterus. The pathological report after the uterine curettage at a local hospital (Pathology No. 39869) on October 28, 2016 showed a broken uterine endometrium at the proliferative phase.

Imaging examinations

The gynecological ultrasound examination on April 6, 2017 at our hospital revealed the following: the uterine body was anterior, measuring 61 mm × 55 mm × 54 mm, the shape of the uterus was symmetrical, and the velamen was smooth; two low echogenic areas were detected in the smooth muscle wall; and the larger one with clear border was located in the back wall, measuring 11 mm × 8 mm, although the uterine cavity line was unclear. The endometrial thickness was 20 mm, with an uneven echo. A mixed partially strong echogenic area of 31 mm × 24 mm × 24 mm in the uterus with blood flow was found, in which there was an irregular liquid anechoic area with a size of 20 mm × 18 mm × 16 mm and the liquid content was not clear. The size and echo of the ovaries were normal. She was clinically diagnosed with an intrauterine lesion (endometrial polyp or cystic adenomyosis), adenomyosis combined with small myoma, and scarred uterus after caesarean section.

After admission, she underwent hysteroscopy under the guidance of ultrasound with general anesthesia. During the operation, a neoplasm measuring about 4.0 cm × 3.0 cm × 4.0 cm was found, which was located in the anterior wall from the base of the uterus to near the isthmus with a length of 3.0 cm and had mulberry-like surface and thick pedicle. The endometrium was pink and white and diffusely proliferated. The opening of the bilateral fallopian tubes could be seen. The neoplasm was opened using an annular electrode; then, chocolate-like liquid flowing out from it was observed. The neoplasm was resected from the pedicle using the annular electrode, and a Mirena ring was placed in the uterus at the same time. Postoperative pathological examination (Pathology No. 614984C) revealed that the endometrium had secretory changes and adenomyosis in the uterine cavity. Postoperatively, intramuscular injections of 3.75 mg diphereline once every 28 days for a total of three times were administered to the patient. Two months after the operation, the patient's return visit showed obviously alleviated dysmenorrhea. Gynecological Doppler ultrasound examination revealed that the uterus had notably shrunk compared with its previous size and the intrauterine Mirena ring was in normal position.

Case 2: Chief complaints

A 39-year-old woman was admitted to the hospital owing to relapse of uterine fibroids after undergoing hysteromyomectomy twice.

History of present illness

On February 19, 2017, the patient found continuous heavy vaginal bleeding in dark red color. Thus, on March 5, 2017, she visited a physician at a hospital in Changchun City. Gynecological Doppler ultrasound examination revealed relapse of uterine fibroids. To confirm the result, she visited physicians at our hospital and other hospitals in Changchun and obtained the same diagnosis of recurrent uterine fibroids and possible degeneration. Surgery was suggested. Then, she was admitted to our hospital due to the uterine fibroids with a moderate amount of bloody secretions without abnormal flavor.

History of past illness

The patient underwent hysteromyomectomy at a hospital in Changchun, China in 2007. She self-reported that three uterine fibroids, measuring 2 cm in diameter, were removed, but no follow-up was conducted after the operation. In 2012, a physical examination at a hospital in Changchun showed relapse of uterine fibroids, but pregnancy was also noted. Hence, in 2013, she underwent a cesarean section and intraoperative hysteromyomectomy at the same time at a hospital in Changchun City. She self-reported that two uterine fibroids were resected, and no postoperative review was conducted.

Physical examination upon admission

Smooth vagina and soft mucous membrane; normal and smooth cervix.

Laboratory examinations

Routine blood test (March 11, 2017) showed a WBC count of 13.12 × 10^9/L, percentage of neutrophils of 0.89, RBC count of 4.20 × 10^{12}/L, hemoglobin concentration of 97 g/L, and platelet count of 482 × 10^9/L. Serum human chorionic gonadotropin level (March 11, 2017) was 2.39 mIU/mL. The rechecked routine blood test on admission showed a WBC count of 6.14 × 10^9/L, percentage of neutrophils of 0.81, RBC count of 4.19 × 10^{12}/L, hemoglobin concentration of 97 g/L, and platelet count of 453/10^9/L. The D-dimer level on admission was 3597.00 μg/L. Screening of female tumor markers revealed a carbohydrate antigen (CA)-125 level of 1212.00 U/mL and CA-72 level of 416.51 U/mL; the remaining items were normal. After 3 days of anti-infective treatment, the blood test was reviewed, showing a normal WBC count, hemoglobin concentration of 86 g/L, D-dimer level of 3172.00 ug/L, and CA-125 level of 775.90 U/mL.

Imaging examinations

Gynecological examination revealed normal vulva development, smooth vagina and soft mucous membrane, normal and smooth cervix with a small amount of blood flowing out, and the uterine body at the anterior position larger than fist and round shaped; the right posterior wall of the uterus was convex, hard, and tough, but the mobility was not normal, without tenderness. Neither abnormality nor tenderness was noted in the bilateral appendage area. Gynecological Doppler ultrasound examination performed on March 11, 2017 revealed the anterior uterus, which had a symmetrical shape and smooth contours with a size of 65 mm × 60 mm × 59 mm. The muscle wall echo was rough and uneven. One low echogenic area of 56 mm × 44 mm at the right posterior wall was found, with an uneven internal echo and peripheral blood flow, in which there were two irregular liquid anechoic areas, with the larger being 40 mm × 29 mm × 22 mm and protruding to the uterine cavity. The uterine cavity line was not clear, and the endometrium was 17 mm thick, with an uneven echo. The size and echo of the ovaries were normal. Pelvis routine scan + enhancement + diffusion by 3.0 T MRI revealed the presence of occupying lesions at the base and posterior wall of the uterus, suggesting possible uterine fibroids with degeneration, multiple small cysts in the cervix, and small amount of fluids in the pelvic cavity. A clinical diagnosis of recurrent uterine fibroids (with the possibility of degeneration), adenomyosis, postoperation of two hysteromyomectomies, postoperative scarred uterus of cesarean section, pelvic adhesion, and mild anemia was made. After appropriately communicating with the patient, hysterectomy, bilateral salpingectomy, and lysis of pelvic adhesions were performed on March 17, 2017. Intraoperative findings were partial intestinal canal adhering to the abdominal wall, mesosigmoid adhering to the left appendage and lateral pelvic wall, and anterior rectal wall mesenterium extensively adhering to the posterior wall of uterine body; there was a small amount of pink ascites in the pelvic cavity; the uterine body was spherically enlarged (about 8 cm × 8 cm × 6 cm) and hard, and the posterior wall of the uterus was evaginated; fibrinoid inflammatory exudation was found on the surface of the uterine body. Cyst with a diameter of about 2 cm could be seen in the bilateral ovaries. The appearance of the bilateral oviducts was normal. After the uterus was opened, a cystic mass with a size of about 5 cm × 4 cm × 4 cm was found in the uterus, attached to the posterior wall with a pedicle. The cystic wall thickness was about 0.8 cm, with a smooth and yellow surface, containing chocolate-like liquid. Intraoperative pathology (Pathology No. 611231C) revealed adenomyosis. Postoperative pathology (Pathology No. 611231C) revealed adenomyosis, endometrium at the proliferative phase, chronic cervicitis, and no obvious lesions in the bilateral oviducts. Cytological examination of ascites revealed no cancer cells. Five days after the operation, routine blood test showed a WBC count of 3.41 × 10^9/L, percentage of neutrophils of 0.54, RBC count of 4.37 × 10^{12}/L, hemoglobin concentration of 10^6 g/L, platelet count of 359 × 10^9/L, and CA-125 level of 356.50 U/mL. Two months after the surgery, the review showed the vaginal cuff healing well and a normal CA-125 level.

FINAL DIAGNOSIS

Intrauterine cystic adenomyosis.

TREATMENT

Operation (hysteroscopy and hysterectomy, bilateral salpingectomy).

OUTCOME AND FOLLOW-UP

Both of them were cured.

DISCUSSION

Clinical manifestations of cystic adenomyosis

In 1908, Cullen[3] first described the formation of capsular space in the submucosa of patients with adenomyosis, and the cysts were lined with normal endometrial glands, filled with chocolate-like fluid. In 1990, Parulekar[4] reported the first case of cystic adenomyosis, and in 1996, Tamura *et al*[5] reported the first case of cystic uterine adenomyosis in an adolescent. Current clinical data show that the age span of the patients with cystic adenomyosis is broad, ranging from 13 to 54 years, although it is common in adolescent and adult women aged < 30 years. Its clinical manifestation is similar to that of typical uterine adenomyosis, mainly presenting as severe dysmenorrhea, menorrhagia, and chronic pelvic pain. A small number of patients have no clinical symptoms. According to the onset age, cystic adenomyosis can be divided into the adolescent and adult types[6,7]. There are two sets of diagnostic criteria for the adolescent type. The diagnostic criteria include the following: (1) the age is < 30 years; (2) the cyst is > 1 cm in diameter, and the capsular space is independent of the uterine cavity and surrounded by hyperplastic smooth muscle tissue; and (3) severe dysmenorrhea develops early. The diagnostic criteria proposed by Chun[8] in 2011 are as follows: (1) the onset age is < 18 years, or severe dysmenorrhea develops within 5 years after the onset of menarche; (2) there is no history of operation in the uterus; and (3) the diameter of the cystic cavity is > 5 mm. Both sets of diagnostic criteria have their own advantages and disadvantages, and the former is more consistent with the clinical practice in terms of the standard of histopathology, while the latter is more accurate in the definition of age. The diagnostic criteria for adult type are more obscure, generally referring to those with the onset age of > 30 years and most with a history of uterine operation.

In this study, both patients presented with dysmenorrhea, hypermenorrhea, and a history of cesarean section, and the second patient had a history of hysteromyomectomy twice, suggesting that the clinical manifestations and pathogenesis of intrauterine cystic adenomyosis are similar to those which originate from other parts.

Diagnostic methods and differential diagnosis of intrauterine cystic adenomyosis

In this study, both cases showed an intrauterine mass with a diameter of 3–5 cm (Figure 1). The surface of the mass was red mulberry shaped or yellowish-white and smooth. As the mass was opened, chocolate-like liquid flowed out. The inner wall of the cyst was smooth, with a thickness of 0.5–0.8 cm. The pathological examination revealed that the cystic wall was composed of arranged endometrial glands and stroma and covered with hyperplastic muscular tissues.

Transvaginal color Doppler ultrasound examination is convenient and economical for screening intrauterine cystic adenomyosis (Figure 2). In this study, ultrasound showed low echo masses in the uterine cavity or muscle wall intruding into the uterine cavity, with irregular liquid echopattern inside. There were dense strong echo spots in the liquid echopattern and dotted distribution of blood flow signals. The typical sonographic findings of endometrial polyps are as follows: regularly shaped lesions with a high-level echo and strong echo halo around the lesions can be seen in the uterine cavity, and cysts can be seen in the polyp. Color Doppler can display the typical single blood flow signal supplying the endometrial polyps.

Nuclear MRI is a commonly used method for the clinical diagnosis of uterine adenomyosis. The T2W1 characteristics of adenomyosis include the broadening JZ and ill-defined shadows mixed by hypointensity and hyperintensity[9]. In this study, an intrauterine thick-walled cyst was displayed in the MRI scan, which showed hyperintensity in T1 weighted image, moderate to high intensity in T2 weighted image, and low intensity in the edge (Figure 3). MRI plays a vital role in the differential diagnosis between adenomyosis and uterine fibroid degeneration[10]. The characteristics of uterine fibroid hyalinosis in MRI are moderate intensity in TIW1 and low intensity in T2W1, while uterine fibroids mucinous degeneration has a characteristic of high intensity in T2W1, sometimes characterized by multiple patches, without reinforcement in the enhanced scan. MRI can not only reflect the characteristic signal of the tumor to identify the position and size but also identify the complex uterine malformations, which is the best diagnostic method for the disease[11].

The specificity and sensitivity of serum CA-125 level in the diagnosis of cystic

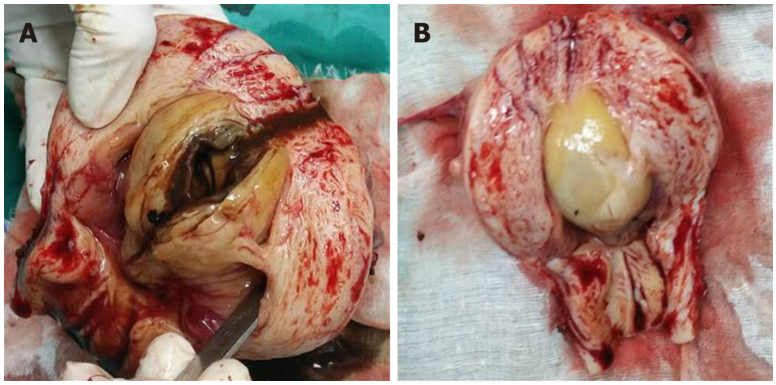

Figure 1 Gross display of intrauterine cystic adenomyosis. A: The cyst contained chocolate-like liquid; B: After the uterus was opened, a cystic mass with a size of about 5 cm × 4 cm × 4 cm was found in the uterus, attached to the posterior wall with a pedicle with a smooth and yellow surface.

uterine adenomyosis are low, but an increased CA-125 level is helpful in the differential diagnosis of the disease from endometrial polyps and uterine myoma degeneration. Takeuchi *et al*[12] reported that the CA-125 level can be from normal to > 500 U/mL in patients. In this study, CA-125 level was normal in one case and as high as 1212.00 U/mL in the other case. The reasons may be as follows: first, since the intrauterine lesion was huge, and a large amount of CA-125 produced by the lining endometrial epithelium and interstitial cells in the lesion was released into the blood, the diffuse type of uterine adenomyosis had an elevated CA-125 level; second, during the operation, a large area of inflammatory cellulosic exudation was found on the surface of the uterus, which was considered as complicated with pelvic inflammatory disease, leading to a significant increase in CA-125 level.

The therapeutic principle for cystic adenomyosis is radical resection of the lesions, promoting fertility and preventing recurrence. The therapeutic modality can vary according to the onset age, request of fertility, location and size of the lesion, and symptoms[13].

Hysteroscopic resection of lesions is preferred for the treatment of intrauterine cystic adenomyosis[14]. In this study, one patient underwent hysteroscopic resection and intrauterine Mirena ring placement at the same time. It not only effectively alleviated her symptoms of dysmenorrhea and increased menstrual volume but also led to endometrial atrophy by local release of efficient progestin in the uterine cavity, so as to effectively prevent disease recurrence. However, if the cyst is too large to perform hysteroscopic surgery, total hysterectomy can be considered if the patient has no fertility request[15]

Although cystic adenomyosis is common, the location of cystic adenomyosis in the uterine cavity is rare. The case report would bring more attention on the diagnosis. However, these two cases were of different phases and not comparable, which needs more cases to be collected to gain evidenced value.

In conclusion, cystic adenomyosis is a rare type of adenomyosis of the uterus, and intrauterine cystic adenomyosis has even been less reported. Owing to the clinicians' low understanding of the disease, it is easy to be misdiagnosed or missed in the diagnosis. At present, there is no clinical data with large samples to confirm its prognosis, influence on fertility, and whether postoperative medication can effectively prevent its recurrence. How to detect and treat intrauterine cystic adenomyosis effectively and develop effective methods to prevent its recurrence is an urgent problem that needs to be resolved.

CONCLUSION

Intrauterine cystic adenomyosis could be treated by hysterectomy or by hystscopy.

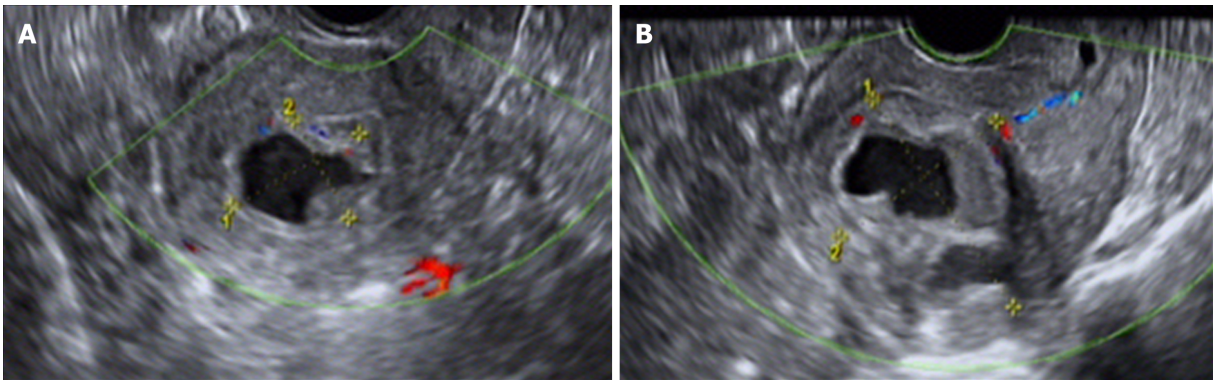

Figure 2 Ultrasonic images of intrauterine cystic adenomyosis. Regularly shaped lesions with a high-level echo and strong echo halo around the lesions can be seen in the uterine cavity, and cysts can be seen in the polyp. Color Doppler can display the typical single blood flow signal supplying the endometrial polyps. A: Case 1; B: Case 2.

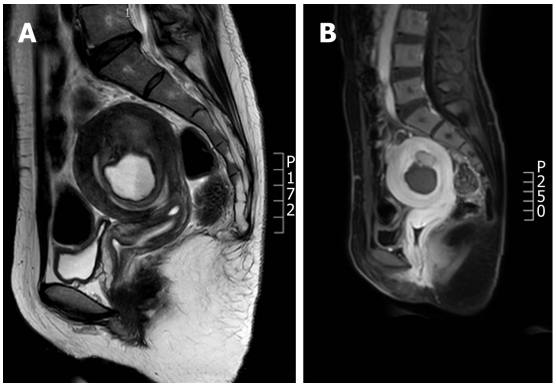

Figure 3 Magnetic resonance images of cystic adenomyosis (hyperintensity in T1 weighted image, moderate to high intensity in T2 weighted image, and low intensity in the edge). A: Case 1; B: Case 2.

REFERENCES

1 **Porpora MG**, Vinci V, De Vito C, Migliara G, Anastasi E, Ticino A, Resta S, Catalano C, Benedetti Panici P, Manganaro L. The Role of Magnetic Resonance Imaging-Diffusion Tensor Imaging in Predicting Pain Related to Endometriosis: A Preliminary Study. *J Minim Invasive Gynecol* 2018; **25**: 661-669 [PMID: 29126882 DOI: 10.1016/j.jmig.2017.10.033]

2 **Tsui KH**, Lee WL, Chen CY, Sheu BC, Yen MS, Chang TC, Wang PH. Medical treatment for adenomyosis and/or adenomyoma. *Taiwan J Obstet Gynecol* 2014; **53**: 459-465 [PMID: 25510683 DOI: 10.1016/j.tjog.2014.04.024]

3 **Cullen TS**. *Adenomyoma of the uterus*. Philadelphia: Saunders 1908; 128-149

4 **Parulekar SV**. Cystic degeneration in an adenomyoma (a case report). *J Postgrad Med* 1990; **36**: 46-47 [PMID: 2097356]

5 **Tamura M**, Fukaya T, Takaya R, Ip CW, Yajima A. Juvenile adenomyotic cyst of the corpus uteri with dysmenorrhea. *Tohoku J Exp Med* 1996; **178**: 339-344 [PMID: 8727716 DOI: 10.1620/tjem.178.339]

6 **Manchanda R**, Manchanda P, Meena J. Cystic Adenomyosis. *Hysteroscopy* 2018; 479-492

7 **Brosens I**, Gordts S, Habiba M, Benagiano G. Uterine Cystic Adenomyosis: A Disease of Younger Women. *J Pediatr Adolesc Gynecol* 2015; **28**: 420-426 [PMID: 26049940 DOI: 10.1016/j.jpag.2014.05.008]

8 **Chun SS**, Hong DG, Seong WJ, Choi MH, Lee TH. Juvenile cystic adenomyoma in a 19-year-old woman: a case report with a proposal for new diagnostic criteria. *J Laparoendosc Adv Surg Tech A* 2011; **21**: 771-774 [PMID: 21561337 DOI: 10.1089/lap.2011.0014]

9 **Stoelinga B**, Hehenkamp WJK, Nieuwenhuis LL, Conijn MMA, van Waesberghe JHTM, Brölmann HAM, Huirne JAF. Accuracy and Reproducibility of Sonoelastography for the Assessment of Fibroids and Adenomyosis, with Magnetic Resonance Imaging as Reference Standard. *Ultrasound Med Biol* 2018; **44**: 1654-1663 [PMID: 29784438 DOI: 10.1016/j.ultrasmedbio.2018.03.027]

10 **Agostinho L**, Cruz R, Osório F, Alves J, Setúbal A, Guerra A. MRI for adenomyosis: a pictorial review. *Insights Imaging* 2017; **8**: 549-556 [PMID: 28980163 DOI: 10.1007/s13244-017-0576-z]

11 **Krentel H**, Cezar C, Becker S, Di Spiezio Sardo A, Tanos V, Wallwiener M, De Wilde RL. From Clinical Symptoms to MR Imaging: Diagnostic Steps in Adenomyosis. *Biomed Res Int* 2017; **2017**: 1514029 [PMID: 29349064 DOI: 10.1155/2017/1514029]

12 **Takeuchi H**, Kitade M, Kikuchi I, Kumakiri J, Kuroda K, Jinushi M. Diagnosis, laparoscopic management, and histopathologic findings of juvenile cystic adenomyoma: a review of nine cases. *Fertil Steril* 2010; **94**: 862-868 [PMID: 19539912 DOI: 10.1016/j.fertnstert.2009.05.010]

13 **Oliveira MAP**, Crispi CP, Brollo LC, Crispi CP, De Wilde RL. Surgery in adenomyosis. *Arch Gynecol Obstet* 2018; **297**: 581-589 [PMID: 29197987 DOI: 10.1007/s00404-017-4603-6]
14 **Levgur M**. Therapeutic options for adenomyosis: a review. *Arch Gynecol Obstet* 2007; **276**: 1-15 [PMID: 17186255 DOI: 10.1007/s00404-006-0299-8]
15 **Ascher-Walsh CJ**, Tu JL, Du Y, Blanco JS. Location of adenomyosis in total hysterectomy specimens. *J Am Assoc Gynecol Laparosc* 2003; **10**: 360-362 [PMID: 14567812 DOI: 10.1016/S1074-3804(05)60262-9]

P- Reviewer: Cosmi E, Khajehei M, Zhang XQ
S- Editor: Ji FF **L- Editor:** Wang TQ **E- Editor:** Bian YN

World Journal of Clinical Cases

Submit a Manuscript: https://www.f6publishing.com

World J Clin Cases 2019 March 6; 7(5): 684-690

DOI: 10.12998/wjcc.v7.i5.684

ISSN 2307-8960 (online)

CASE REPORT

Melanotic Xp11-associated tumor of the sigmoid colon: A case report

Gang Wang, Gang-Gang Li, Sheng-Mao Zhu, Bao-Jia Cai, Peng-Jie Yu, Cheng-Wu Zhang

ORCID number: Gang Wang (0000-0002-8111-0118); Gang-Gang Li (0000-0001-5465-7284); Sheng-Mao Zhu (0000-0002-1329-5026); Bao-Jia Cai (0000-0002-7970-2667); Peng-Jie Yu (0000-0001-7372-6919); Cheng-Wu Zhang (0000-0003-4078-2767).

Author contributions: Li GG and Zhu SM designed the study; Zhang CW, Cai BJ, and Yu PJ performed the operation; Wang G wrote the paper; all authors read and approved the final manuscript.

Supported by The Key Research & Development and Transformation Project of Qinghai Province for 2018 (No. 2018-SF-113).

Informed consent statement: Informed consent was obtained from the patient for this publication.

Conflict-of-interest statement: The authors declare that they have no competing interests.

CARE Checklist (2016) statement: The guidelines of the "CARE Checklist - 2016: Information for writing a case report" have been adopted.

Open-Access: This article is an open-access article which was selected by an in-house editor and fully peer-reviewed by external reviewers. It is distributed in accordance with the Creative Commons Attribution Non Commercial (CC BY-NC 4.0) license, which permits others to distribute, remix, adapt, build upon this work non-commercially, and license their derivative works

Gang Wang, the Graduate School of Qinghai University, Xining 810016, Qinghai Province, China

Gang-Gang Li, Sheng-Mao Zhu, Bao-Jia Cai, Peng-Jie Yu, Cheng-Wu Zhang, Department of Gastrointestinal Surgery, Affiliated Hospital of Qinghai University, Xining 810000, Qinghai Province, China

Corresponding author: Cheng-Wu Zhang, MD, Chief Doctor, Professor, Department of Gastrointestinal Surgery, Affiliated Hospital of Qinghai University, No. 29, Tongren Road, Xining 810000, Qinghai Province, China. 861072284@qq.com
Telephone: +86-153-4973630

Abstract

BACKGROUND

Melanotic Xp11-associated tumors are rare mesenchymal-derived tumors. So far, most primary melanotic Xp11-associated tumors have been reported in the kidney, and reports of this tumor in the gastrointestinal tract are rare.

CASE SUMMARY

Here we describe the case of a 25-year-old woman who presented with a melanotic Xp11-associated tumor in the sigmoid colon. Colonoscopy revealed a large mucosal bulge in the sigmoid colon, approximately 32cm inside the anus. The surface was rough with local erosion. The tumor was brittle on biopsy and bled easily. Computed tomography revealed thickening of the rectal wall with edema. Postoperative pathology indicated the likelihood of a perivascular epithelioid cell tumor. Histologically, the tumor comprised plump epithelioid cells with abundant clear to lightly eosinophilic cytoplasm and round nuclei arranged in an alveolar or trabecular pattern. The tumor cells were strongly positive for HMB-45, Melan-A, Cathepsin K, and TFE3 but negative for vimentin, smooth muscle actin, S100 protein, CD10, CK20, and desmin. The tumor cells had a low Ki-67 labeling index (approximately 2%). Fluorescence *in situ* hybridization revealed TFE3 fracture. Based on these histologic and immunohistochemical features, a diagnosis of melanotic Xp11-associated tumor of the sigmoid colon was made.

CONCLUSION

In summary, we report the clinicopathological features of a primary tumor that is extremely rare in the sigmoid colon and review the clinicopathological characteristics of melanotic Xp11-associated tumors, compatible with the very rare tumor termed "melanotic Xp11 translocation renal cancer" in all aspects.

on different terms, provided the original work is properly cited and the use is non-commercial. See: http://creativecommons.org/licenses/by-nc/4.0/

Manuscript source: Unsolicited manuscript

Received: November 16, 2018
Peer-review started: November 16, 2018
First decision: December 9, 2018
Revised: December 30, 2018
Accepted: January 30, 2019
Article in press: January 30, 2019
Published online: March 6, 2019

Key words: Melanotic Xp11-associated tumor; Perivascular epithelioid cell tumor; Melan-A; Sigmoid colon; Case report

©The Author(s) 2019. Published by Baishideng Publishing Group Inc. All rights reserved.

Core tip: Melanotic Xp11-associated tumors can occur at all ages; children and young adults are particularly prone whereas it is rare in middle-aged and elderly individuals. So far, most primary melanotic Xp11-associated tumors have been reported in the kidney, and reports of this tumor in the gastrointestinal tract are rare. Therefore, data regarding the clinical features and biologic behavior of melanotic Xp11-associated tumors are limited.

Citation: Wang G, Li GG, Zhu SM, Cai BJ, Yu PJ, Zhang CW. Melanotic Xp11-associated tumor of the sigmoid colon: A case report. *World J Clin Cases* 2019; 7(5): 684-690
URL: https://www.wjgnet.com/2307-8960/full/v7/i5/684.htm
DOI: https://dx.doi.org/10.12998/wjcc.v7.i5.684

INTRODUCTION

Melanotic Xp11-associated tumors are rare mesenchymal-derived tumors. In 2009, Argani *et al*[1] reported the clinicopathological features of a distinctive renal cell cancer (RCC) termed "melanotic Xp11 translocation renal cancer". In 2012, LeGallo *et al*[2] reported the first case of primary melanotic Xp11-associated tumor in the ovary, for which the immunohistochemical markers were very similar to those of RCC. Melanotic Xp11-associated tumors can occur at all ages; children and young adults are particularly prone whereas it is rare in middle-aged and elderly individuals. The common pathological features are: (1) the pigments are visible; (2) the tumor cells are nested, have highly developed capillary vessels, are rich in cytoplasm, and can coexpress melanocyte markers HMB45 and Melan-A but not epithelial markers; and (3) there are *TFE3* gene rearrangement and Xp11 translocation. So far, most primary melanotic Xp11-associated tumors have been reported in the kidney, and reports of this tumor in the gastrointestinal tract are rare. Therefore, data regarding the clinical features and biologic behavior of melanotic Xp11-associated tumors are limited. Here we report the clinicopathologic features of a sigmoid colon tumor in a 25-year-old woman showing morphologic, immunohistochemical, and molecular genetic features identical to those of melanotic Xp11 translocation renal cancer, and performed a review of the published literature.

CASE PRESENTATION

Chief complaints

A 25-year-old woman presented with a 4-d history of abdominal pain, melena, and nausea that were aggravated 1 d prior to admission. She had diarrhea approximately four times a day.

History of present illness

The patient presented to a local Chinese Medicine Hospital and was diagnosed with hemorrhoids. Her condition did not improve after the medical treatment, so she presented to our hospital for further evaluation.

History of past illness

There was no obvious abnormality in the past illness.

Personal and family history

She denied any family history of related diseases.

Physical examination upon admission

No obvious positive signs were found in the abdomen.

Laboratory examinations

The laboratory findings revealed normal routine blood parameters, coagulation

function, tumor markers, and biochemistry results. Blood pressure was 90/70mmHg, heart rate was 90 beats/min, and the heart rhythm was normal. Immunohisto-chemically, the tumor cells were strongly positive for HMB45, CD34 (vascular+), CD117, CD163, CD68, and Melan-A and negative for CK, Vimentin, S100, CK7, CK20, CD10, Dog-1, Des, CgA, SYN, LCA, EMA, smooth muscle actin (SMA), and SOX-10. Mitotic figures were approximately ≥ 2/5 per high power field, Ki-67 labeling index was approximately 2%, and there was a partially invasive boundary. The initial diagnosis was a gastrointestinal tract malignancy with perivascular epithelioid cell tumor (PEComa). However, we excluded primary melanoma and primary clear-cell sarcoma of the gastrointestinal tract. The patient was advised to have a genetic test or pathological consultation. Pathological consultation and a fluorescence *in situ* hybridization (FISH) test were subsequently performed at Xijing Hospital, Fourth Military Medical University; immunohisto-chemistry showed that the tumor cells expressed a melanin marker and TFE3, accompanied by *TFE3* gene translocation (Figure 1). FISH for *TFE3* rearrangement showed that the *TFE3* gene was fractured (Figure 1). The tumor showed an abnormal signal pattern consistent with rearrangement of the *TFE3* locus in 52% of the cells. Taking into account all these immunohistochemistry and FISH tests, the final diagnosis was a melanotic Xp11-associated tumor. There was no intraoperative evidence of metastasis or involvement of other abdominal organs. Moreover, subsequent staging studies showed no evidence of metastatic disease.

Imaging examinations

Colonoscopy revealed a large mucosal bulge in the sigmoid colon, approximately 32cm inside the anus. The surface was rough with local erosion. The tumor was brittle on biopsy and bled easily. Computed tomography revealed thickening of the rectal wall with edema. Gastroenterography revealed a filling defect at the junction of the sigmoid and the descending colon. Sputum passed through, the local wall was stiff, and the mucosal destruction was interrupted. Barium sulfate passed through, the local wall was stiff, and the mucosal destruction was interrupted. A malignant tumor was suspected after we completed the relevant examinations. Laparoscopic-assisted resection of the large sigmoid colon mass (about 10 cm × 2.1 cm) was performed. Postoperative pathology indicated the likelihood of a PEComa.

FINAL DIAGNOSIS

Melanotic Xp11-associated tumor of the sigmoid colon.

TREATMENT

Laparoscopic-assisted resection of the large sigmoid colon.

OUTCOME AND FOLLOW-UP

She was followed by imaging studies of the chest, abdomen, and pelvis as well as colonoscopy every 3 mo. At 6 mo after the initial diagnosis, she was disease-free.

DISCUSSION

Since Argan *et al*[1] first reported Xp11 translocation RCC in 2009, increasing numbers of melanotic tumors have been reported. In 2012, LeGallo *et al*[2] first reported melanotic Xp11-associated tumor originating in the ovary. The common pathological feature are that the tumor cells are nested, have highly developed capillary vessels, and are rich in cytoplasm, and the pigments are visible, which makes it very similar to PEComa, and tumor cells can coexpress melanocyte markers HMB45 and Melan-A[3,4]. Melanotic Xp11-associated tumors originating in the digestive system are rare. Therefore, most previous reports on this disease misdiagnosed it as a PEComa. So far, no relevant clinical data can predict the prognosis of these rare postoperative melanotic Xp11-associated tumors[2]. Due to the fact that melanotic Xp11-associated tumors are extremely rare and their histologic features vary, a differential diagnosis to exclude other tumors is important. The differential diagnosis of melanotic Xp11-associated tumors includes various types of epithelial and mesenchymal tumors, including PEComa, malignant melanoma, clear-cell sarcoma, gastrointestinal stromal

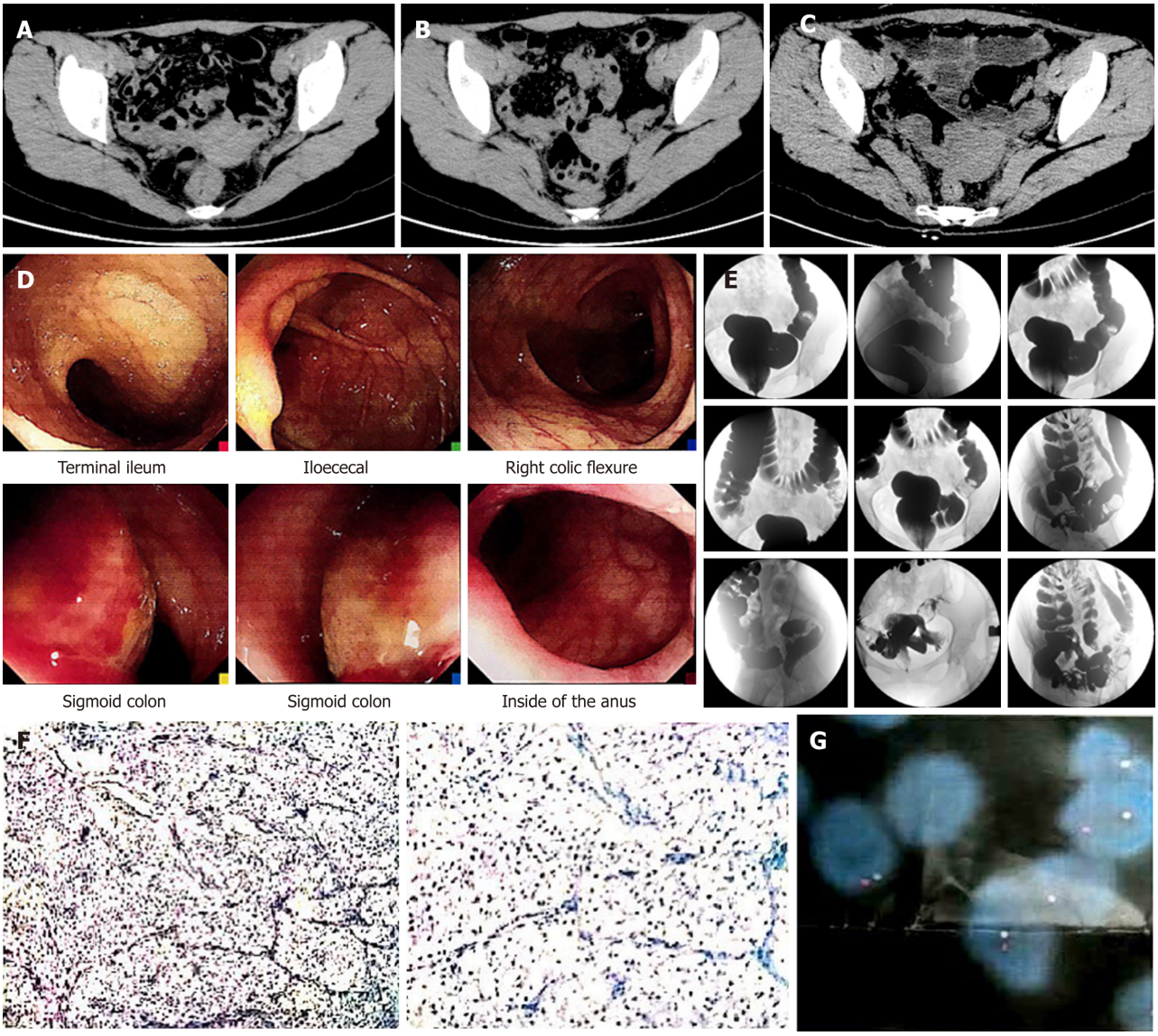

Figure 1 The examination results of the patient. A and B: Preoperative computed tomography (CT) showing thickening of the rectal wall with edema; C: Postoperative CT showing a high-density suture shadow in the operation area; D: Approximately 32cm inside the anus, a large mucosal bulge can be seen in the sigmoid colon. The surface was rough with local erosion. The tumor was brittle on biopsy and bled easily; E: Preoperative gastrointestinal angiography showing a filling defect at the junction of the sigmoid and the descending colon. The barium sulfate passed through, the local wall was stiff, and the mucosal destruction was interrupted; F: Pathological consultation at Xijing Hospital. The tumor cells in the muscle layer of the sigmoid colon were scattered in the nest, and capillaries were separated. The cytoplasm of tumor cells was rich and lightly stained. The nucleus was medium-sized and round or oval (note the nucleolus). The nuclear division was rare, and a small amount of pigment was visible. Immunohistochemistry showed that the tumor cells expressed a melanin marker and TFE3, accompanied by *TFE3* gene translocation, consistent with pigmented Xp11-related tumors. Tumor cells were positive for TFE3 and Cathepsin, and fluorescence *in situ* hybridization (FISH) results showed *TFE3* gene fragmentation (see the FISH report). Original immunohistochemistry results showed HMB45 (+), Melan-A (+), Ki-67 (+, approximately 5%), smooth muscle actin (-), CK (-), and EMA (-); G: Results of FISH test at Xijing Hospital shown that the *TFE3* is fractured.

tumor (GIST), metastatic RCC, and epithelioid leiomyosarcoma. It is well known that the morphology and immunohistochemical features of these unique melanotic Xp11-associated tumors overlap with the morphologic and immunohistochemical features of PEComa. Although the distinction of melanotic Xp11-associated tumors from PEComas is difficult, we believe that the overall morphologic features of the current tumor, particularly the presence of large amounts of melanin, the absence of SMA expression, the lack of the tuberous sclerosis complex gene mutation, and the presence of *SFPQ/TFE3* fusion[3,5-8], encouraged us to interpret this lesion as a melanotic Xp11-associated tumor (Table 1), thereby making it less difficult to differentiate. The detailed differences are shown in Table 1. FISH is the most commonly used method for gene detection[9]. Malignant melanoma and clear-cell sarcoma have a high positive rate of S100 protein and *TFE3* recombination but a lack of expression of myogenic markers[10,11]. Therefore, the melanin and myogenic immune markers can be used for identification. GIST is the most common tumor of the gastrointestinal mesenchymal tissue, which has a morphology very similar to that of

gastrointestinal PEComa, and can also coexpress the CD117 tumor marker, which increases the difficulty in differentiation of this disease. However, GIST does not have the characteristic of expressing the melanin marker; hence, we can use the melanin marker to distinguish it[12-15].

CONCLUSION

In summary, we report the clinicopathological features of a primary tumor that is extremely rare in the sigmoid colon and review the clinicopathological characteristics of melanotic Xp11-associated tumors, compatible with the very rare tumor termed "melanotic Xp11 translocation renal cancer" in all aspects. Xp11 melanoma should be considered in the differential diagnosis of abnormal melanomas, particularly in cases involving PEComas or unusual primary melanoma tumors. Melanotic Xp11-associated tumors are a special type of tumor with a low incidence, especially for tumors originating in the gastrointestinal tract. The etiology, pathogenesis, and related biological behaviors of this disease remain unclear. Postoperative management, including adjuvant chemotherapy, has not been established yet. A further study of these particularly rare tumors is necessary to understand their biological behavior and pathogenesis. Therefore, patients with postoperative melanotic Xp11-associated tumors should be carefully followed.

Table 1 Comparative features of melanotic Xp11 tumors and perivascular epithelioid cell tumors

	Melanotic Xp11 tumors	PEComas
Sex predilection	Females > males	Females > males
Age	Children and young adults, but may affect older adults	Middle age, but may affect children and older adults
Family history		Tuberous sclerosis
Site	Kidneys, uterus, ovaries, cervix, colon, pancreas, bladder, and pelvis	Genitourinary tract, viscera, skin, soft tissue, and bone
Histology	Epithelioid with clear cytoplasm	Spindled, epithelioid, or sclerosing
Melanin pigment	Usually present	Usually absent
Muscle marker expression	Usually absent	Usually present
Melanocytic marker expression	Present	Present
Epithelial marker expression	Absent	Absent
Molecular genetic alteration	Xp11 translocation; *PSF-TFE3* fusion	Loss of *TSC1* (9q34) or *TSC2* (16p13.3) gene

PEComa: Perivascular epithelioid cell tumor.

REFERENCES

1 **Argani P**, Aulmann S, Karanjawala Z, Fraser RB, Ladanyi M, Rodriguez MM. Melanotic Xp11 translocation renal cancers: a distinctive neoplasm with overlapping features of PEComa, carcinoma, and melanoma. *Am J Surg Pathol* 2009; **33**: 609-619 [PMID: 19065101 DOI: 10.1097/PAS.0b013e31818fbdfl]

2 **LeGallo RD**, Stelow EB, Sukov WR, Duska LR, Alisanski SB, Folpe AL. Melanotic xp11.2 neoplasm of the ovary: report of a unique case. *Am J Surg Pathol* 2012; **36**: 1410-1414 [PMID: 22895274 DOI: 10.1097/PAS.0b013e31826277a9]

3 **Wang XT**, Xia QY, Ni H, Ye SB, Li R, Wang X, Shi SS, Zhou XJ, Rao Q. SFPQ/PSF-TFE3 renal cell carcinoma: a clinicopathologic study emphasizing extended morphology and reviewing the differences between SFPQ-TFE3 RCC and the corresponding mesenchymal neoplasm despite an identical gene fusion. *Hum Pathol* 2017; **63**: 190-200 [PMID: 28315422 DOI: 10.1016/j.humpath.2017.02.022]

4 **Saleeb RM**, Srigley JR, Sweet J, Doucet C, Royal V, Chen YB, Brimo F, Evans A. Melanotic MiT family translocation neoplasms: Expanding the clinical and molecular spectrum of this unique entity of tumors. *Pathol Res Pract* 2017; **213**: 1412-1418 [PMID: 28969862 DOI: 10.1016/j.prp.2017.08.004]

5 **Rao Q**, Shen Q, Xia QY, Wang ZY, Liu B, Shi SS, Shi QL, Yin HL, Wu B, Ye SB, Li L, Chen JY, Pan MH, Li Q, Li R, Wang X, Zhang RS, Yu B, Ma HH, Lu ZF, Zhou XJ. PSF/SFPQ is a very common gene fusion partner in TFE3 rearrangement-associated perivascular epithelioid cell tumors (PEComas) and melanotic Xp11 translocation renal cancers: clinicopathologic, immunohistochemical, and molecular characteristics suggesting classification as a distinct entity. *Am J Surg Pathol* 2015; **39**: 1181-1196 [PMID: 26274027 DOI: 10.1097/PAS.0000000000000502]

6 **Argani P**, Zhong M, Reuter VE, Fallon JT, Epstein JI, Netto GJ, Antonescu CR. TFE3-Fusion Variant Analysis Defines Specific Clinicopathologic Associations Among Xp11 Translocation Cancers. *Am J Surg Pathol* 2016; **40**: 723-737 [PMID: 26975036 DOI: 10.1097/PAS.0000000000000631]

7 **Zhan HQ**, Chen H, Wang CF, Zhu XZ. A case of PSF-TFE3 gene fusion in Xp11.2 renal cell carcinoma with melanotic features. *Hum Pathol* 2015; **46**: 476-481 [PMID: 25582502 DOI: 10.1016/j.humpath.2014.11.013]

8 **Rao Q**, Williamson SR, Zhang S, Eble JN, Grignon DJ, Wang M, Zhou XJ, Huang W, Tan PH, Maclennan GT, Cheng L. TFE3 break-apart FISH has a higher sensitivity for Xp11.2 translocation-associated renal cell carcinoma compared with TFE3 or cathepsin K immunohistochemical staining alone: expanding the morphologic spectrum. *Am J Surg Pathol* 2013; **37**: 804-815 [PMID: 23598965 DOI: 10.1097/PAS.0b013e31827e17cb]

9 **Manucha V**, Sessums MT, Lewin J, Akhtar I. Cyto-histological correlation of Xp11.2 translocation/TFE3 gene fusion associated renal cell carcinoma: Report of a case with review of literature. *Diagn Cytopathol* 2018; **46**: 267-270 [PMID: 29024535 DOI: 10.1002/dc.23839]

10 **Wang XT**, Xia QY, Ni H, Wang ZY, Ye SB, Li R, Wang X, Lv JH, Shi SS, Ma HH, Lu ZF, Shen Q, Zhou XJ, Rao Q. Xp11 neoplasm with melanocytic differentiation of the prostate harbouring the novel NONO-TFE3 gene fusion: report of a unique case expanding the gene fusion spectrum. *Histopathology* 2016; **69**: 450-458 [PMID: 26844676 DOI: 10.1111/his.12949]

11 **Dickson BC**, Brooks JS, Pasha TL, Zhang PJ. TFE3 expression in tumors of the microphthalmia-associated transcription factor (MiTF) family. *Int J Surg Pathol* 2011; **19**: 26-30 [PMID: 20164056 DOI: 10.1177/1066896909352861]

12 **Kanazawa A**, Fujii S, Godai TI, Ishibe A, Oshima T, Fukushima T, Ota M, Yukawa N, Rino Y, Imada T, Ito J, Nozawa A, Masuda M, Kunisaki C. Perivascular epithelioid cell tumor of the rectum: report of a case and review of the literature. *World J Surg Oncol* 2014; **12**: 12 [PMID: 24410788 DOI: 10.1186/1477-7819-12-12]

13 **Alvarado-Cabrero I**, Vázquez G, Sierra Santiesteban FI, Hernández-Hernández DM, Pompa AZ. Clinicopathologic study of 275 cases of gastrointestinal stromal tumors: the experience at 3 large medical centers in Mexico. *Ann Diagn Pathol* 2007; **11**: 39-45 [PMID: 17240306 DOI: 10.1016/j.anndiagpath.2006.03.014]

14 **Torii I**, Kondo N, Takuwa T, Matsumoto S, Okumura Y, Sato A, Tanaka F, Nishigami T, Hasegawa S, Tsujimura T. Perivascular epithelioid cell tumor of the rib. *Virchows Arch* 2008; **452**: 697-702 [PMID: 18437415 DOI: 10.1007/s00428-008-0612-y]

15 **Lee M**, Cho KJ, Yu C, Park Y, Kim JC, Kim J, Yu E, Kim MJ. Perivascular epithelioid cell tumor of the sigmoid colon with transcription factor E3 expression. *Ann Diagn Pathol* 2012; **16**: 306-311 [PMID: 21546294 DOI: 10.1016/j.anndiagpath.2011.01.007]

P- Reviewer: Parellada CM, Rubbini M, Fukuda S
S- Editor: Dou Y **L- Editor:** Wang TQ **E- Editor:** Bian YN

Published By Baishideng Publishing Group Inc
7041 Koll Center Parkway, Suite 160, Pleasanton, CA 94566, USA
Telephone: +1-925-2238242
Fax: +1-925-2238243
E-mail: bpgoffice@wjgnet.com
Help Desk:https://www.f6publishing.com/helpdesk
https://www.wjgnet.com

© 2019 Baishideng Publishing Group Inc. All rights reserved.